OCULAR COUNTERROLLING INDUCED IN HUMANS BY HORIZONTAL ACCELERATIONS

by

BYRON KURT LICHTENBERG

Sc.B., Brown University, 1969

S.M., Massachusetts Institute of Technology, 1975

SUBMITTED IN PARTIAL FULFILLMENT

OF THE REQUIREMENTS FOR THE

DEGREE OF DOCTOR OF SCIENCE

IN

BIOMEDICAL ENGINEERING

at the

MASSACHUSETTS INSTITUTE OF TECHNOLOGY

June 1979

Signature of Author_____
Department of Aeronautics and Astronautics, May , 1979

Certified by_____
Thesis Supervisor

Certified by_____
Thesis Supervisor

Certified by_____
Thesis Supervisor

Accepted by_____
Chairman, Departmental Graduate Committee

OCULAR COUNTERROLLING INDUCED IN HUMANS BY HORIZONTAL ACCELERATIONS

by

Byron Kurt Lichtenberg

Submitted to the Department of Aeronautics and Astronautics
on May 18, 1979 in partial fulfillment of the requirements
for the degree of Doctor of Science in Biomedical Engineering.

ABSTRACT

The response of the otolith-ocular counterrolling (OCR) system to horizontal lateral linear step and sinusoidal accelerations has been measured. A linear acceleration cart capable of providing step and sinusoidal acceleration profiles of up to 0.3 g, 0.02 to 1.0 Hz was designed and built. Photographic data recording analysis procedures were developed that did not require fixation of the head with a rigid bite board yet yielded measurement repeatability on the order of 0-30 minutes of arc.

The results indicate that the OCR response to sinusoidal horizontal linear accelerations is similar to the response obtained by constant velocity rotation (roll) around the line of sight (producing a sinusoidal modulation of the direction of the gravitoinertial force). A Bode plot of the data is in good agreement with other investigations. The step response of the system, however, appears to be slightly underdamped which is predicted by a dynamic model of the otolith-perception system.

Thesis Supervisors:

Laurence R. Young
Professor of Aeronautics and Astronautics

Charles M. Oman
Associate Professor of Aeronautics and Astronautics

Richard M. Held
Professor of Experimental Psychology

ACKNOWLEDGEMENTS

I would like to first thank my wife, Lee Lichtenberg, who has been extremely understanding through the many hours and years leading to the completion of this thesis.

Professor Laurence R. Young, my Thesis Committee Chairman, deserves a special note of thanks for his support and encouragement along the way. His experience in these matters was extremely helpful. Professor Charles M. Oman provided many stimulating discussions on the problems which cropped up during this thesis. Professor Richard Held was able to shed a psychologist's light on the subject. For all their help I am grateful.

During the early days of the thesis, I was particularly dependent on Dr. John Tole for equipment design and selection. His knowledge saved me many, many hours. Bob Renshaw, Bill Morrison, and Earl Wassemouth were totally indispensible to the completion of the equipment, without which, no thesis would have been possible.

My fellow students Howard Zucker for his work on the equipment construction, Jonah Garbus for the seat design and construction, and Richard Jennings for assistance with the initial data analysis development, deserve a hearty thank you. They were not nearly so emotionally attached but at least as well motivated as I. To E.R. Edelman, one who is as deeply involved in ocular counterrolling as I am, my thanks and best wishes.

I would like to acknowledge the much more than generous help that

was extended me in the later stages of data collection and analysis by Anthony Arrott. He spent many hours and days slaving with me on the computer to make the data analysis possible.

Finally, I gratefully acknowledge the help of Sherry Modestino, with assistance from Kerry Campbell, who was able to deciper my handwriting and turn this into a polished thesis.

I would like to express my heartfelt gratitude to the Fannie and John Hertz Foundation who provided ample financial assistance to me through the years of this thesis. For equipment and administrative support, I would like to acknowledge two NASA contracts, NASA Ames Research Center Contract NSG 2032 on basic vestibular research which generously funded the sled, and the NASA Spacelab 1 contract, NAS9-15343, which provided much financial assistance for other equipment and administration.

TABLE OF CONTENTS

TABLE OF FIGURES

TABLE OF TABLES

CHAPTER 1

INTRODUCTION

1.1 Objectives and Scientific Justification

The objective of these experiments is to investigate the response of the otolith-ocular counterrolling (OCR) system to purely linear horizontal accelerations. A linear acceleration cart was built to provide step and sinusoidal acceleration profiles. The transient OCR response to step acceleration was measured as well as the frequency response to sinusoidal inputs. Although several types of rotary eye movements and stimuli for these movements exist, this thesis will use the term ocular counterrolling (OCR) to indicate torsional movements (either slow phase or saccadic) induced by changes of the gravitoinertial vector with respect to the subject's head (see Figure 1.1). This system is believed to be primarily reflexive; however, the possibility exists that changes in perception of orientation (gravitoinertial force with respect to head position) could influence the OCR movements. Briefly, OCR has been shown to be dependent primarily upon otolith organ (seismic linear accelerometer) function and only slightly dependent upon semicircular canal (angular accelerometer) function.*

Most previous OCR experiments have used steady state lateral

*See Chapter 2

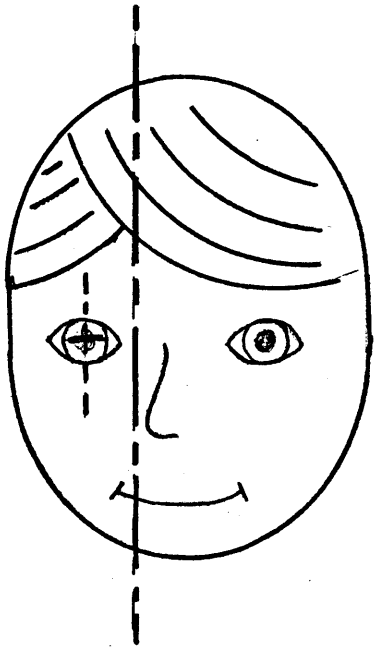

head erect :

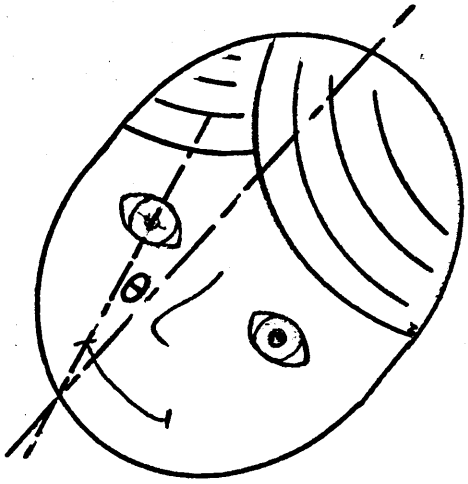

head tilted :

Figure 1.1 This sketch shows the definition of ocular counterrolling (θ) due to a change in the gravitoinertial force (GIF) with respect to the subject's head.

head/body tilt as the stimulus and measured OCR magnitude as the response. A few studies have utilized sinusoidally varying gravito-inertial force (GIF) inputs generated by a constant angular velocity around the line of sight (roll axis). These studies recorded OCR magnitude as a function of stimulus frequency and attempted to describe the OCR system in terms of a linear second-order system. Most studies have recorded data only after the transients had disappeared (approximately 60 seconds). Any transient data that have been recorded using roll axis motion included semicircular canal inputs by nature of the angular acceleration involved in the start-up of roll velocity. The second characteristic of these studies is that the magnitude of the GIF has always been 1.0 'g'. Since the axis of rotation has been very near the otolith organs, any centripetal accelerations were neglected.

The equipment and experiments described in this thesis were designed to record original ground-based OCR data using purely linear horizontal acceleration stimuli (step and sinusoid). The specifications and performance criteria of the equipment for these experiments exceeded those for the Space Sled scheduled to fly in the NASA/ESA Spacelab-1. Because of the short track length of the equipment (about 15 feet), the recording of OCR data was limited to less than 10 seconds per run for step acceleration stimuli in the 0.05 to 0.3 g range. Sinusoidal stimuli could be produced from 0.01 to 1.0 Hz and from 0.01 to 0.2 g. In these experiments, sinusoidal stimulation from 0.2 Hz to 1.0 Hz at 0.2 g was used.

Since virtually no data is available in the literature on the response of OCR (both transient and sinusoidal) to purely linear horizontal accelerations, it was decided to pursue a program to collect ground-based data that could be compared with spaceflight data and to propose a model relating transient step accelerations to OCR in 1 'g'.

1.2 Hypothesis

The hypothesis of this thesis is that the OCR reflex is essentially linear over a range of inputs normally found in a 1 'g' environment, and that the transient response to step lateral linear acceleration is consistent with previous studies that recorded steady state static and sinusoidal OCR. Because the stimuli of this investigation (lateral horizontal acceleration) modulate the "shear force" on the utricular macula, yet maintain the 1 g compressive force (unlike the stimuli in normal lateral tilt), the data recorded during these experiments will yield a new set of data points.

1.3 Related Spacelab I Experiments

In addition to the inherent scientific interest in studying the otolith-OCR system in 1 g, an experiment has been proposed to study the otolithic system including OCR during space flight. This experiment, known as INS102 "Vestibular Experiments in Spacelab I",

actually consists of seven "functional objectives" (FOs) or subexperiments. All the FOs are designed to be performed pre-flight and post-flight, and at least twice during the flight to record any changes in vestibular function that occur over a seven day period of weightlessness. The objective is to compare pre- and post-flight data with ground-based data and also to compare in-flight data between the beginning and end of the mission. The experiments on-board are divided into two groups: three are Space Sled (hereafter called sled) experiments and three are non-sled experiments. The sled FOs (1, 2a, 2b, 6a) will use lateral (left-right, also known as y-axis) acceleration profiles. FO1 investigates the detection of step linear acceleration as well as the ability of the subject to track perceived velocity during suprathreshold sinusoidal stimuli. FO2a investigates lateral eye movements in response to the same stimuli used in FO1. FO2b investigates the OCR response to these same stimuli and is the functional objective most closely related to this thesis.

1.5 Review of Conclusions

The results of this thesis show that the OCR response (transient and sinusoidal) to linear accelerations is consistent with previous sinusoidal response studies and that it is linear over a range of horizontal accelerations up to at least 0.3 g. The transient response of the system can be modelled with a second order linear system first proposed by Young and Meiry (1968). The sinusoidal transfer function derived from the data of this thesis agrees with a model proposed by Hannen et al (1966) with the exception of a somewhat larger time delay in the system.

1.6 Organization of the Thesis

Chapter 2 reviews previous ocular counterrolling studies and attempts to relate these studies to several models that have been developed to describe not only the OCR system, but also the otolith end-organ and otolith perception systems. Some background on eye movements induced by stimulation of the otoliths and related vestibular areas of the brainstem is also provided.

Chapter 3 describes the methods employed in this thesis including a description of the experimental equipment which was built, the data recording and analysis techniques which were finally chosen and the protocol of the experiments.

Chapter 4 presents the results including corrections necessary due to small head movements. Static, step and sinusoidal results are presented. Not all the data is presented here, some reduced data and representative plots are included. Appendix D is a complete set of all the data recorded.

Chapter 5 is a discussion of the results with emphasis placed on the agreement of the data of this work with other investigations and the first of several models discussed in Chpater 2. In addition, there is a discussion of the possible effects of perception upon OCR with no definite conclusion yet.

Chapter 6 attempts to reiterate the main conclusions of the thesis and provide suggestions for future work.

Appendix A is a detailed design study of the equipment that was built including the rationale for various decisions and a set of working engineering drawings.

Appendix B explores the depths of the computer program and hardware interfaces which control the sled. Due to the continuing evolution of the equipment however, the information in this appendix reflects the state of the software and hardware at the time these experiments were conducted.

Appendix C describes how to use the data analysis equipment.

Appendix D is a collection of all the data recorded during these experiments. The first section is static OCR induced by head tilt, the second section is step acceleration data and the third section is sinusoidal data.

CHAPTER 2

OTOLITH-OCR SYSTEM

2.1 Introduction

A comprehensive review of all aspects of the otolith organ is beyond the scope of this work. This chapter will present previous ocular counterrolling and related studies including several models relating accelerations to otolith dependent phenomena (linear acceleration perception, otolith organ afferent nerve output, ocular counterrolling). For review of the otolith organ and vestibulo-ocular relations, one should see Goldberg and Fernandez (1975), Jongkees (1967) and Cohen (1971).

2.2 Otolith Organs

The otolith organs have been shown to be primarily sensitive to linear accelerations. The work of Fernandez and Goldberg (1976a, b, c) has shown (most recently) that shear force directed parallel to the surface of the macula is a necessary and sufficient stimulus for saccular and utricular afferents in the anesthetized squirrel monkey.

2.3 Ocular Counterrolling

Ocular counterrolling (OCR) is defined as the counterrotation of the eyes induced by a lateral head tilt, or, equivalently, by rotation

or the gravitoinertial vector in the frontal plane. The existence of OCR has been debated for at least one hundred years, but newer, more sophisticated measuring techniques have unequivocally measured this phenomenon. The apparent effective stimulus for OCR is the direction and magnitude of the gravitoinertial vector in the frontal plane with respect to the longitudinal axis of the head (z axis). Many studies have been conducted to determine the sense organ(s) responsible for this transduction. It appears that the major responsible end-organ is the otolith (although somatoreceptors cannot be completely ruled out). The semicircular canals appear to have some dynamic affect on OCR (at least the neural pathways are present), but the long-term static or DC component rules out the semicircular canal as the prime end-organ. The studies that showed only a small residual OCR in labyrinthine defective subjects are most convincing in their implication of the otolith organs. This section will extensively discuss the OCR phenomenon.

Many techniques have been devised to measure OCR. Most of these techniques make use of artificial landmarks on the eye. Experiments have made use of a pellicle from a hard-boiled egg placed on the cornea with inscribed indentification markers, sutures in the conjunctiva, tatoo marks on the cornea, contact lens sewn into the sclera, contact lens affixed to the cornea by suction, iris landmarks, blood vessels and retinal after-images. As is readily apparent some of these techniques are unsuitable for human use. Others leave doubt as to their accuracy; for example, the conjunctiva is firmly attached to the sclera at the limbus, but tends to be tenuously attached near the periphery. Retinal after-images are easy to use, but

only have an accuracy of about one degree.

The first definitive study on human OCR was done by Miller (1962). He perfected a repeatable (average standard deviation of 5.3 minutes of arc) photographic technique using all available iris landmarks to measure OCR. He investigated static OCR throughout 360 degrees of body roll. In addition, he carefully controlled the subject's fixation to avoid errors due to voluntary eye movements. His results indicated that OCR follows the gravitoinertial vector, but tends to reach peak values at about 60 to 70 degrees of tilt -- the static gain of the system in this range is about 0.1. Miller's findings indicate that the maximum value of OCR is about 6 or 7 degrees. This particular study used only one subject, but subsequent studies have confirmed his major finding.

In agreement with other investigations (Fender, 1955; Robinson, 1963), Miller found that there are many variations in OCR. There appears to be some small rotary jitter that is about 8 to 10 minutes of arc. Miller recorded variations in OCR of up to one degree at a given tilt position over a period of several minutes. In addition, the magnitude of OCR varied among individuals and also between test sessions for one individual, although the qualitative shape of the curve remained the same.

Miller found no difference between clockwise (CW) and counterclockwise (CCW) tilt (i.e., the system is memoryless), but did find that there was usually a directional preponderance (i.e., a larger maximum value of OCR for right ear down head tilt, see Figure 2.1).

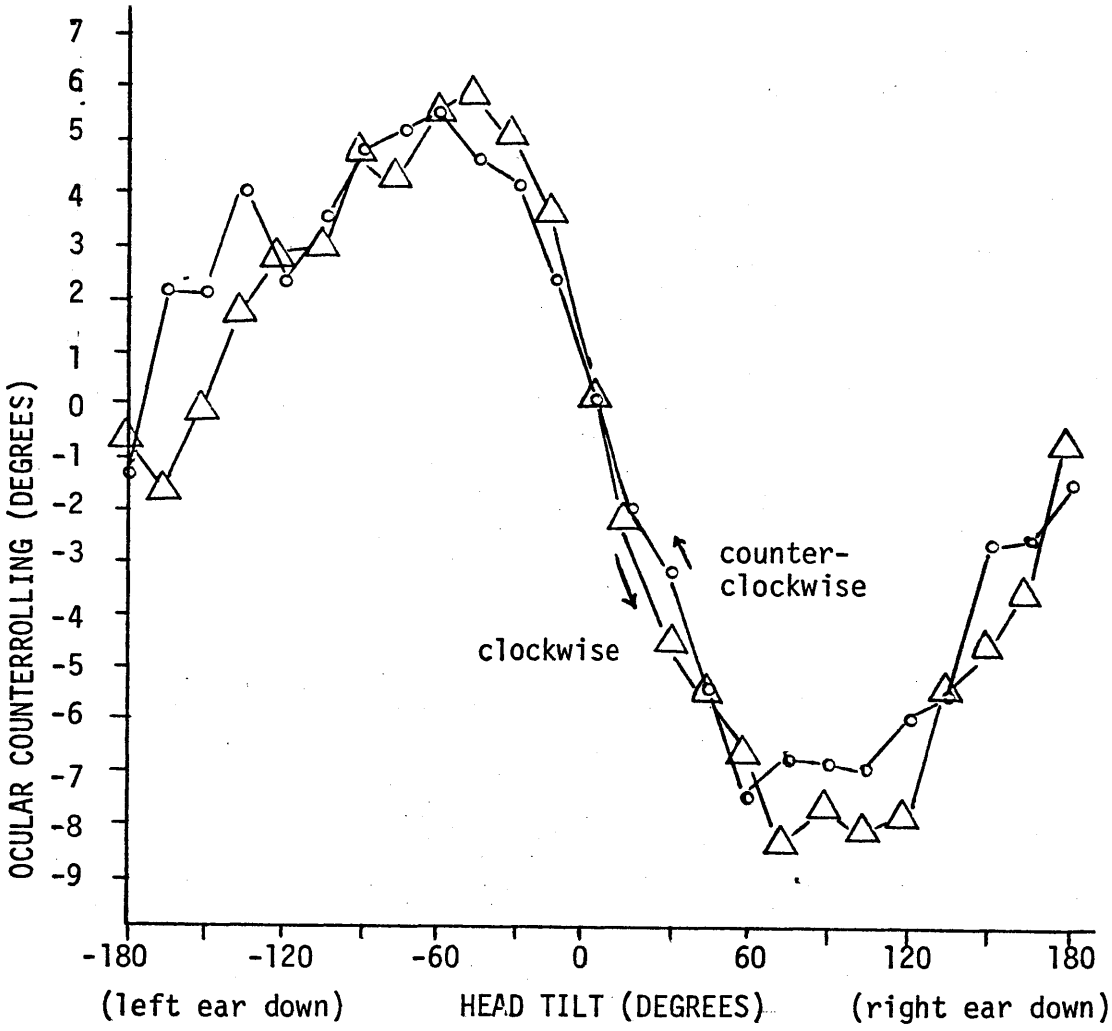

Figure 2.1 Static clockwise and counterclockwise ocular counterrolling data from one subject averaged over three complete rotations. From Miller (1962).

Fore and aft tilt did not induce OCR, but tilt in oblique planes resulted in OCR with reduced gain.

Diamond et al (1979) measured OCR in a manner similar to Miller. They fixed subjects in a seat that could be rotated around the horizontal axis of the line of sight. They rotated seven subjects very slowly (3°/second) and took binocular pictures every 10°. They used a slight variation of Miller's method of measuring OCR by aligning projections of eye pictures. Their results indicate two asymmetries. First, right ear down appeared to produce slightly more OCR than left ear down and second, the downward eye (i.e., the right eye for right ear down tilt) showed more OCR than the other eye. In addition, they found a statistically significant inverse correlation between subjects' age and peak-to-peak OCR (sum of 90° right and left head tilt) with values in the range of 8° to 35° peak-to-peak. (See Figure 2.2).

In order to fully explore the role of the otoliths in OCR, many other investigations have been done. Cohen et al (1970) showed in the monkey (1) that neck receptors play no role in OCR and (2) that OCR was not influenced by cervical dorsal root section. Miller and Graybiel (1965), Hannen et al (1966), and Smiles et al (1975) have shown that OCR is almost absent in labyrinthine defective humans. Several studies have shown a relationship between OCR in humans and the magnitude of the gravitoinertial force acting on the otoliths. Figure 2.3 shows the data obtained by Woellner and Graybiel (1959) and their attempt to connect the points. Their experiment protocol consisted of seating a human subject upright in a centrifuge facing either in or opposite

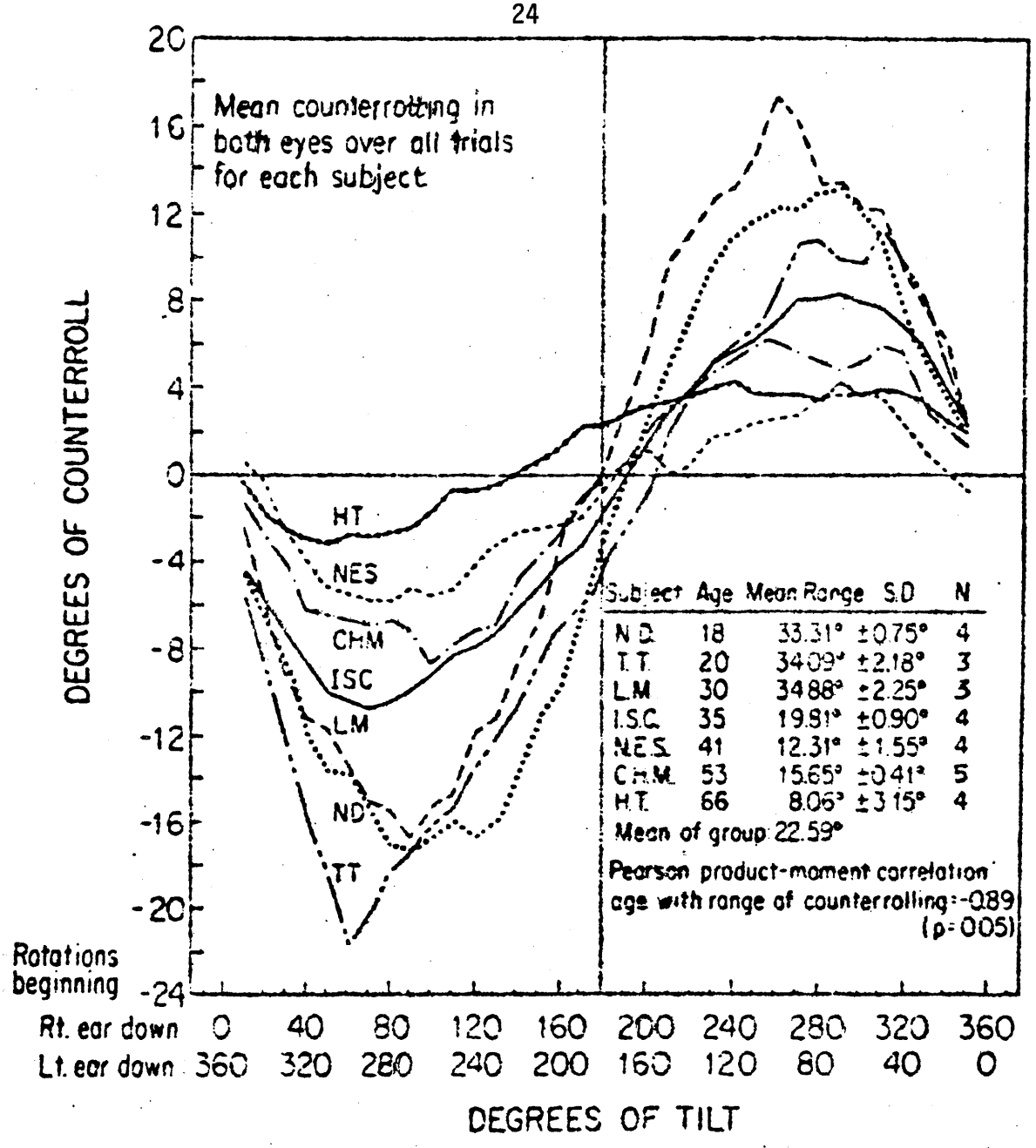

Fig. 2.2 Counterrolling profiles of all 7 subjects. The mean for each subject includes both eyes and both directions for each point in the rotations. Abscissa is labeled with both directional designations. Table inset in figure shows mean range of counterrolling by age of subject. Magnitude of response is inversely correlated with age ($p=0.05$).
(from Diamond et al, 1979)

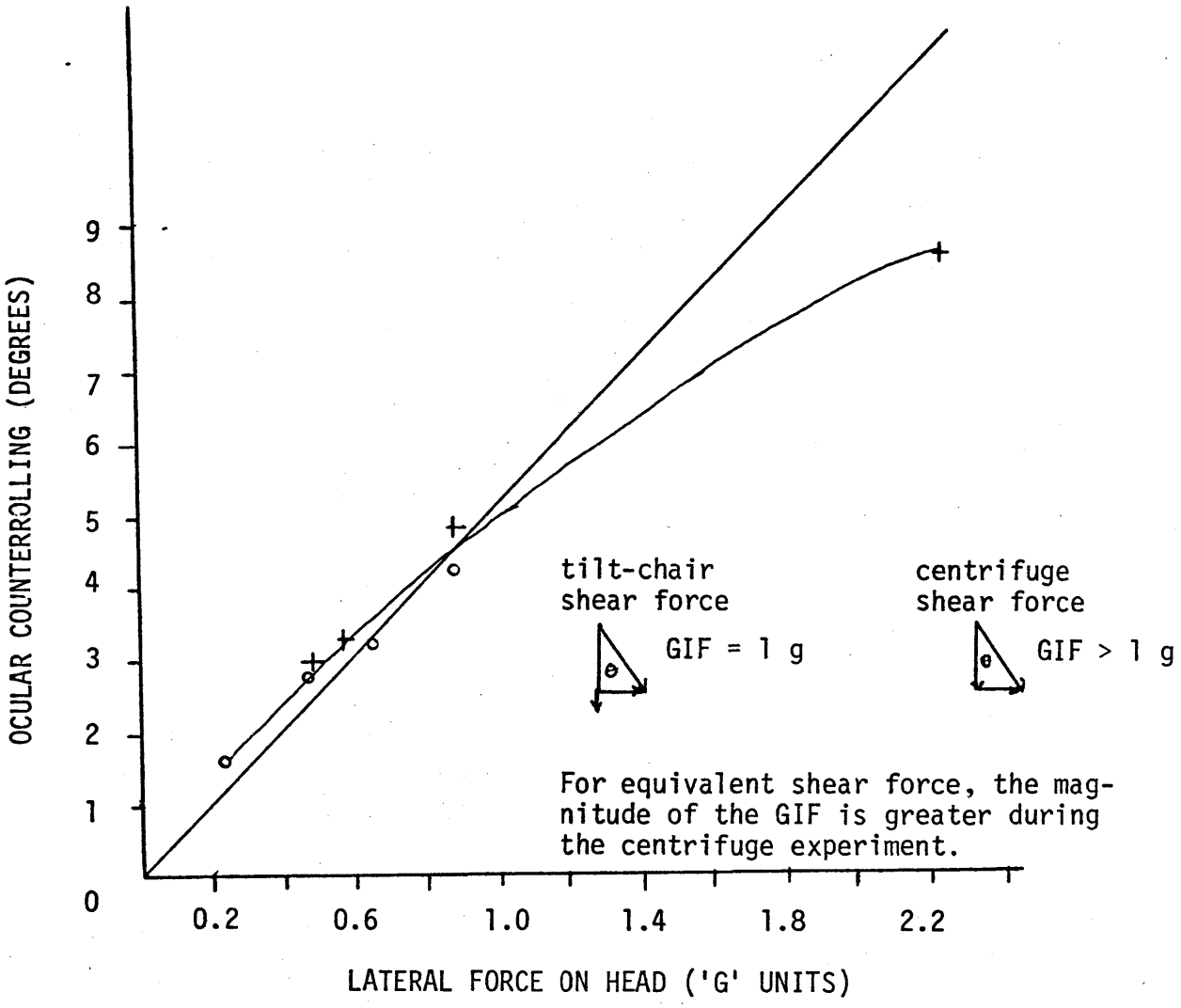

Figure 2.3 Magnitude of ocular counterrolling as a function of the magnitude of lateral force acting on the head in a tilt-chair (o) and a centrifuge (+). The curved is their attempt to connect the points. The 45° inclined line is put there to shcw the deviation from linearity at high shear force levels. From Woellner and Graybiel (1959).

to the direction of rotation. In that manner, as the centrifuge rotated a shear force was produced on the utricular maculae as well as a compressive/tractive force on the saccular maculae. They also tilted the subjects with no centrifugation. Thus they were able to create two situations where the direction of the gravitoinertial force (GIF) could remain the same but two different shear forces could be applied to the utricles. They were able to use 4 different values of "tilt-angle". They then plotted the ocular counterrolling against lateral shear force. They claim that the OCR is a linearly related function to shear force over a limited range. The 45° inclined line was drawn by them to indicate the non-linearity at high 'g'-levels. It appears that all the data points obtained during centrifugation lie above (i.e., greater counterrolling for a given "tilt-angle") the points obtained from pure tilt. This observation would indicate that not only shear force but total magnitude of the GIF is an important stimulus for OCR. The use of sutures on the conjunctiva as landmarks could have induced some error into their values (slippage of the conjunctiva with respect to the sclera could have occurred). In fact, the values of OCR that they report appear in the low range, about a maximum of 4.2° at 66° of tilt. In a more recent study, Miller and Graybiel (1971) performed additional experiments used the same protocol as the Woellner and Graybiel study but used Miller's photographic techniques. During these experiments, they observed OCR values of about 6 - 7° for 63° of body tilt. Figure 2.4 shows Miller and Graybiel's data. They used a centrifuge to change the direction of the gravitoinertial force and measured OCR. By appropriately manipulating the centrifugal force

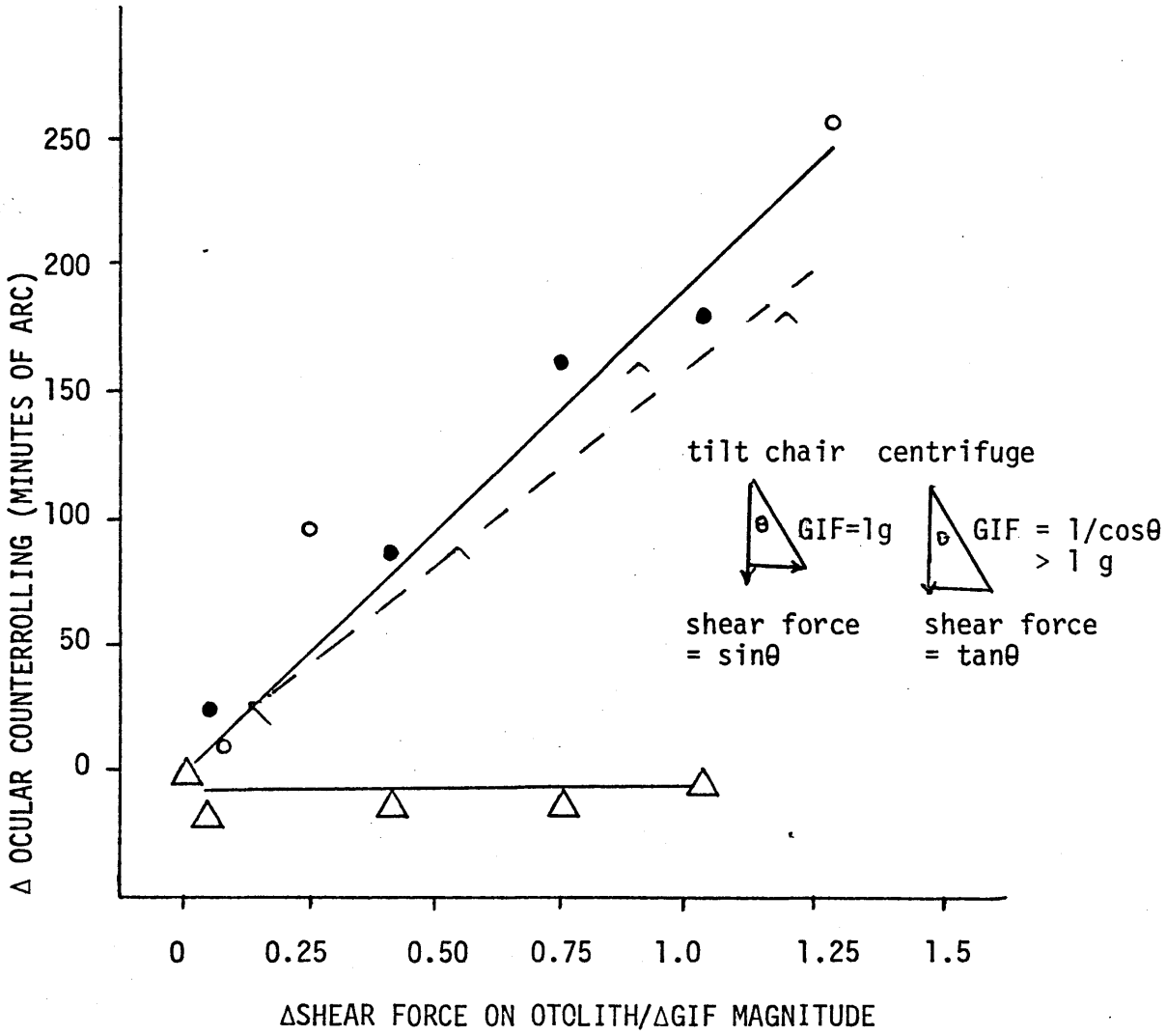

Figure 2.4 Average change in ocular counterrolling as a function of change in otolithic shear force and magnitude of GIF. Data in solid circles (normals) and triangles (labyrinthine defective) from Miller and Graybiel (1971). Data in open circles from Woellner and Graybiel (1959) recalculated for this format. The dashed line is the plot of OCR against change in magnitude of GIF. The inserts detail the two experimental protocols. Adapted from Miller and Graybiel (1971).

they were able to establish various directions of the GIF with respect to vertical. They then compared the change in ocular counterrolling (OCR(centrifuge) - OCR(tilt chair) at a given angle θ with the change in shear force ($\tan\theta - \sin\theta$) at that angle. They were able to vary θ from about 30° to 63°. They claim that the results show a linear relationship of ΔOCR to Δshear force. It is also possible to plot ΔOCR against ΔGIF which takes into account not only the shear force but the additional compressive force on the utricle (which is shear force on the saccule). This plot also gives a straight line. The point that should be considered is that under these two hypergravic experiments, the change in shear force is directly coupled to a change in magnitude of the GIF. They also demonstrated no appreciable ΔOCR in labyrinthine defective (LD) subjects.

In a related experiment, Miller and Graybiel (1965) investigated OCR under hypogravic conditions. They used a tilt chair mounted on a C-131 aircraft. By flying certain trajectories, the airplane is able (for short periods of time) to obtain relatively constant acceleration levels varying from 0 g up to hyper g (greater than 1 g). For this set of experiments, varying g levels (less than 1.0) were flown and the tilt chair was tilted to either 25° or 50° with respect to the vertical. In this manner many different shear force magnitudes could be produced. Miller and Graybiel plotted their data (Figure 2.5) on a semi-log scale, plotting normalized OCR (with respect to 50° of tilt in a 1 g environment) against the $\log_{10}$ of the acceleration level of the airplane. Their results indicate an assymptotic trend at low acceleration levels

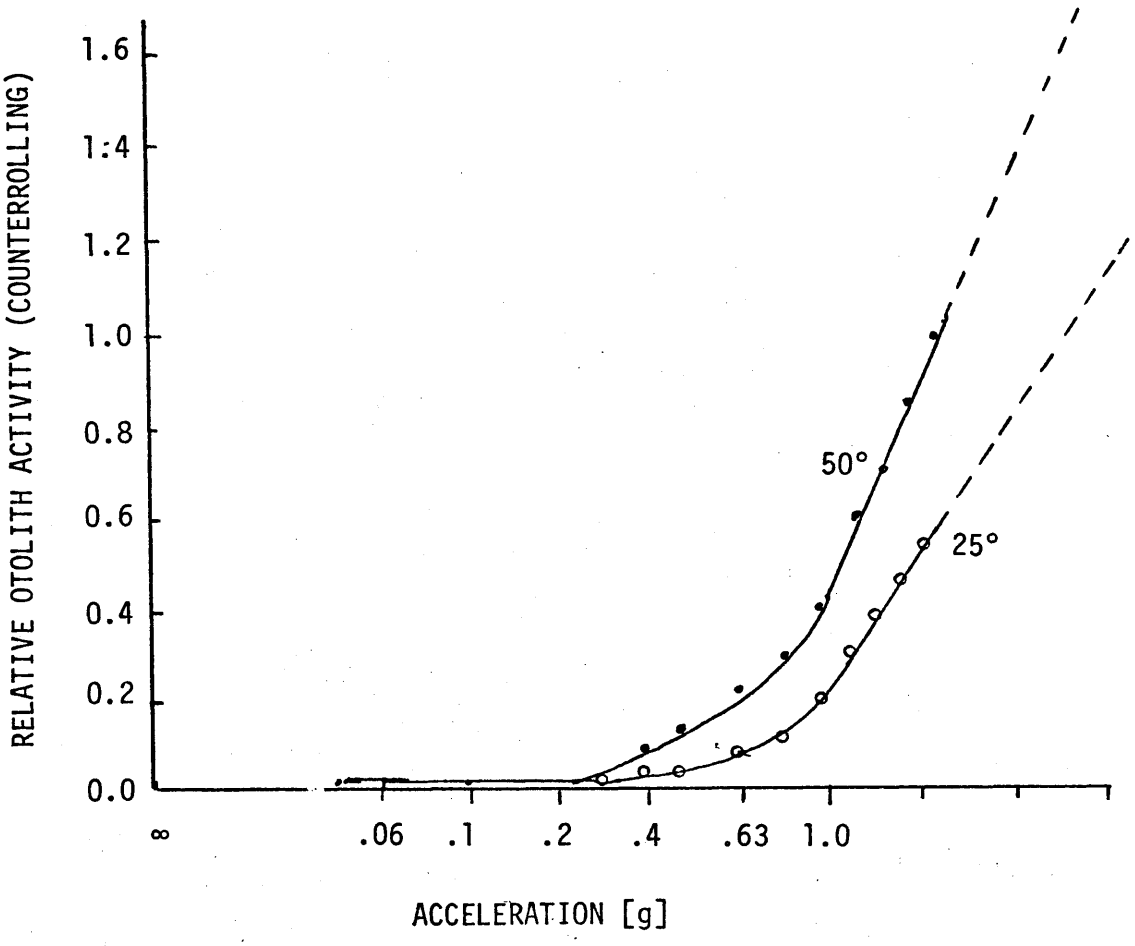

Figure 2.5 Relative otolith activity (mean counterrolling response of three subjects) as a function of the logarithm of the gravitational force. From Miller and Graybiel (1965).

consistent with a Fechnarian Law.

Miller and Graybiel (1968) also investigated the effects of drugs on OCR. They found that drugs such as scopolamine and dexadrine (used for motion sickness) did not affect OCR. Of the drugs tested, only alcohol had an affect; it acted to reduce the magnitude of OCR. Alcohol reduces all nystagmus levels - and the ability to inhibit it with vision.

During eight hours of steady tilt, Miller and Graybiel (1972) saw essentially no change in OCR. As in other investigations, there were inter- and intra-subject variations in the magnitude of OCR exhibited throughout the test. LD subjects exhibited low magnitude OCR (less than 100 minutes of arc). Therefore, it appears that for an eight hour period at least, there is no or minimal adaptation taking place throughout the otolith-OCR system.

Several studies have been undertaken to investigate the dynamic properties of OCR. In the monkey, Chassen et al (1967) applied constant angular velocity roll around the visual axis (in the frontal plane) to stimulate OCR. This stimulus provides a sinusoidal change in the gravito-inertial vector, but no apparent semicircular canal stimulation after the initial start-up transient. Around the same axis, they also used sinusoidal pendular motions and band-limited Gaussian noise position changes (both of which included angular accelerations). Chassen et al had no control over the monkey's fixation and voluntary eye movements apparently made static OCR unrecordable. Their OCR recording technique was to sew a contact lens into the sclera and use a flexible coupling attached to a potentiometer to continuously record OCR. They report that during their

constant angular velocity roll tests, the peak-to-peak amplitude of OCR decreased as the constant angular velocity increased. The response appeared to become more sinusoidal at high frequencies. Their pendular motion tests indicated that the OCR amplitude increased as stimulus frequency increased; they attribute this increase to the influence of angular acceleration on the semicircular canals.

They also found that the monkeys could "suppress" the OCR response (i.e., there were periods of stimulation during which no OCR was present). They thought the monkey was using the predictability of the sinusoidal stimulus in order to turn down the "gain". They introduced band-limited Gaussian, white noise position inputs to attempt to eliminate this suppression because of the stimulus unpredictability. However, the OCR response was at times still "suppressed" indicating that the monkey can somehow lower the gain of the OCR system even to unpredictable stimuli.

They attempted to characterize the OCR system as a linear system, but when they analyzed the response to a Gaussian input, they found the output (OCR) was not Gaussian. They point out that the angular acceleration has a radial acceleration component that is not Gaussian, since it depends on the square of the angular velocity. Therefore, they could not draw any conclusion as to the linearity of the system.

Baarsma and Collewijn (1975) measured eye movements in the rabbit induced by linear accelerations. They used a search coil implanted in a contact lens, a system which is relatively non-intrusive. They used both sinusoidal and step acceleration stimuli in the ranges 0.068 and 1.22 Hz and amplitudes 0.02 to 0.11 g. Their equipment was crude, a cart with a falling weight for step accelerations and two springs for the sinusoidal

accelerations. It must be realized that the rabbits eyes are located on the side of the head and that they have no fovea, so that any comparisons or extrapolations between this data and human/primate data are tenuous at best. They found the gain of the system (eye rotation/rotation of specific force vector) was low, "about 0.1 for 0.3 Hz and smaller than 0.01 for frequencies above 1.0 Hz". They also determined that step accelerations resulted in an overdamped type response with the gain approaching 0.65 after 5 seconds. Figure 2.6 shows the Bode plot which they fit with a slightly underdamped second-order system.

Because the work of Hannen et al (1966) was in the human, fixation and alertness of subjects was more easily controlled. Hannen used equipment and stimulus techniques similar to Miller, Diamond and Chassen. The subject was strapped into a chair which could be rotated around the line of sight at constant angular velocity. The rotation axis was closely aligned to the position of the otolith organs. Their data analysis was based on Miller's (1962) technique of matching pictures of the complete iris. Their results indicated that peak-to-peak OCR was fairly constant up to 0.25 Hz, but attenuated as frequency increased above 0.25 Hz. They saw an increasing lag at higher frequencies and occasional rotary nystagmus. The LD subjects showed very little OCR, about 10 minutes of arc. They note a directional preponderance in both normal and LD subjects which they attribute to a lack of eyeball position sense. During one experimental series, they took pictures of both eyes and noted some differences and asymmetry but were not able to

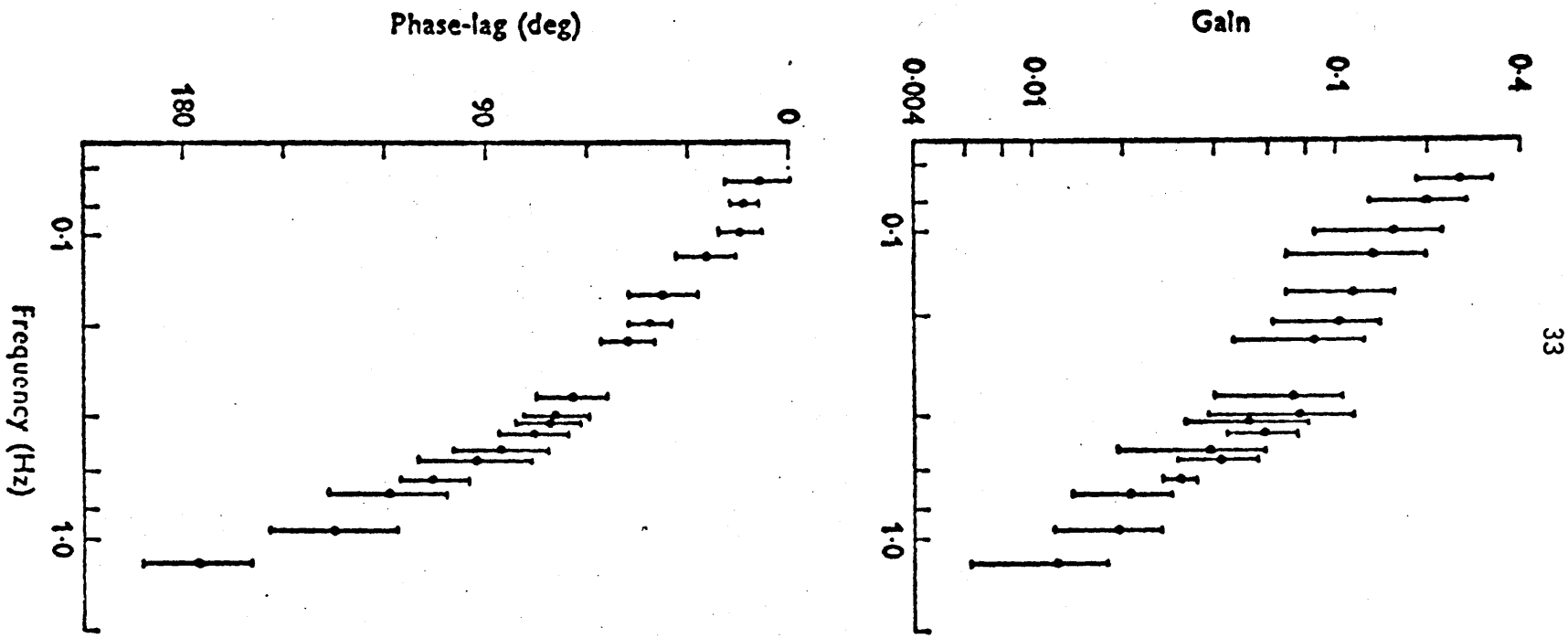

Figure 2.6 This figure shows the Bode plot of torsional eye movements in the rabbit. Note the large phase lag of almost 180° at 1.0 Hz. This Bode plot can be fitted with a second order system with natural frequency of 2.2 rad/sec and damping constant 2.0, although the large variation of data makes the accuracy of such model parameters questionable. From Baarsma and Collewijn (1975).

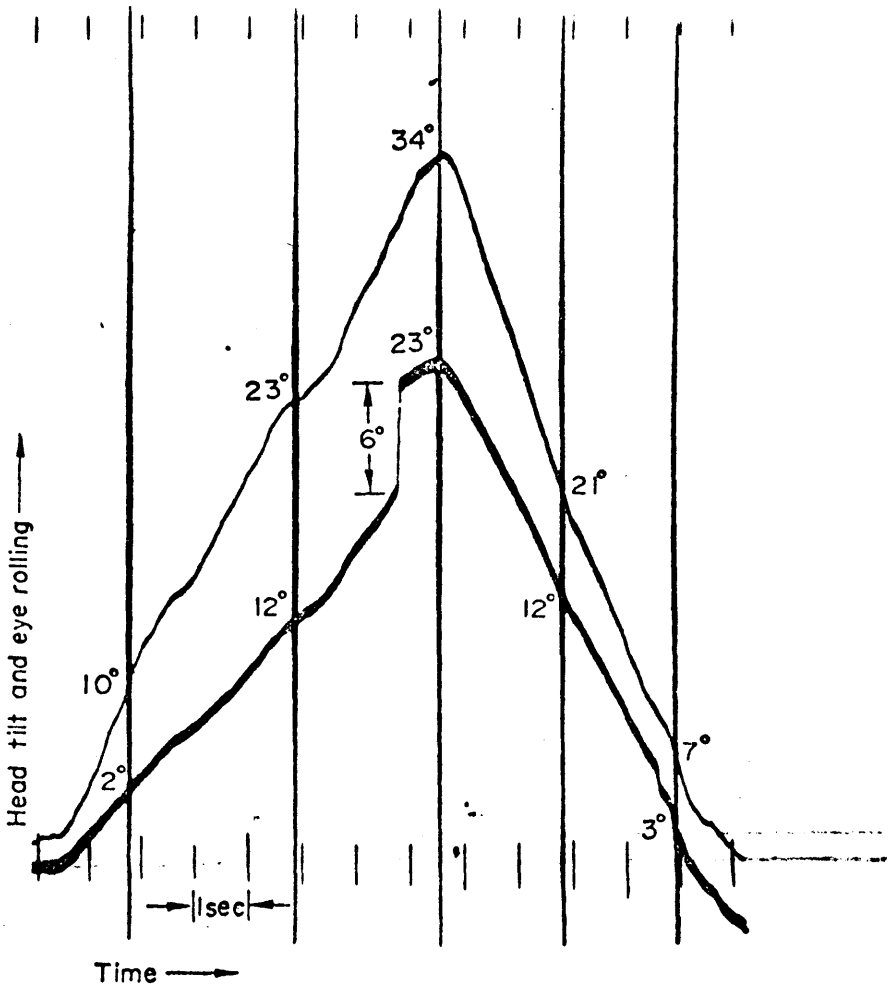

Record of the head and eye (below) movement in the dark. The head has been tilted towards the left shoulder and brought back to the normal position. The vertical lines mark the times of taking the photographs. The figures given at some places of the curves show that under such conditions the eye changes its orientation in space smoothly following the head (torsion drift). Residual torsion is accumulated gradually up to 11°.

Figure 2.7 (from Petrov and Zenkin (197

make as definitive a statement as Diamond et al (1979). They also used Fourier analysis to derive a model of the otolith-OCR system. This model will be discussed later.

Petrov and Zenkin (1973) studied dynamic human OCR in response to pendular motion (similar to the pendular motion stimulus that Chassen et al used). Petrov and Zenkin used an apparatus affixed to the eyeball by a suction cup which rotated with the eyeball and which projected light onto a slit photokymograph as it moved. They measured rotary eye movements during uncontrolled head tilt (the subject slowly but voluntarily tilted his head from side to side) with room lights on and off. Their results show slow velocity rotational motion interspersed with roll saccades (0.5 - 8.0° in amplitude, 100 - 200°/sec in velocity). Their results also show a "residual torsion" which is equivalent to OCR. However, the values of OCR that they recorded are in the range of 12 - 15° for 45° of head tilt. They note that "these figures are outside the limits known from the literature"[1]. However, their values are obtained in the dynamic state and as such will include a semicircular canal input since the roll rates were on the order of 5 - 10°/second.

For the experiments that were conducted in the dark, Petrov and

[1] Petrov and Zenkin, p. 2467. To put these figures into perspective, Chassen et al (1967) indicate that, in the monkey, pendular motion produces up to 14° peak-to-peak OCR for tilts of ±60 - 80° or about one-half the OCR values recorded by Petrov and Zenkin. Melvill Jones (1958), however, reports OCR of up to 20° in humans during rapid rolling movements in airplanes. Diamond et al (1979) also recorded OCR of up to 25-30° peak-to-peak.

Zenkin found very few saccades and mostly slow rotary eye movements (Figure 2.7). It appears from the limited data in the paper that the OCR increases in the dark. Analysis of Petrov and Zenkin's data indicates that the velocity gain (slow phase rotary eye movement velocity/head velocity) of the system is larger in the light (about 0.8) than in the dark (about 0.5). These results appear to be consistent with other experiments performed in the yaw axis (however the velocity gain here in the light is almost 1.0 with the gain decreasing in the dark).

In their discussion, Petrov and Zenkin attribute slow eye movements and torsional saccades to a system for maintaining visual constancy during tilt. They feel that the "residual torsion" or OCR might just be an "artifact".

Under the dynamic conditions of the previously discussed protocols it appears that two effects may be contributing to OCR. One is the input from the semicircular canals which is known to produce OCR movements. The second effect could be a dynamic otolith response which would initially overshoot the final value obtained during a steady state tilt. In fact, the results of Petrov and Zenkin (dynamic head tilts), Melvill Jones (rolls in an airplane), Diamond et al and Baarsma and Collewijn tend to cooroborate the existence of these effects. Because most studies have allowed the transients to die out, this behavior of the OCR system under transient conditions has not been well documented.

Section 2.5 will discuss models of the OCR system and will go into more detail about the relationship of utricular and saccular (shear force

versus total magnitude of GIF acting on the otoliths) influence on OCR.

2.4 Comparison of Unilateral LD Studies and Gross Electrical Stimulation

The data from unilateral LD studies (Benjamins and Nienhuis, 1927; Owada and Shizu, 1960; Jonkees, 1966) is consistent with electrical stimulation studies (Suzuki et al, 1969; Westheimer and Blair, 1975). The LD studies have shown that OCR only occurs when the intact side is on the top (contralateral tilt). The electrical stimulation studies have shown that stimulation of the left utricle or left side of the brainstem elicits OCR that compensates for rightward head tilt (Contralateral tilt).

The next section discusses several models of the otolithic sytem and attempts to relate previous experimental data on the OCR system to the various models.

2.5 Models of the Otoliths

De Vries (1950) did some early measurements on the otoliths. He stimulated fish otoliths with step and sinusoidal linear acceleration stimuli (actually used a centrifuge) and measured the deflection of the otoconia using x-rays. The otolith was assumed to function as a standard second order mass-spring-dashpot system with the following equation of motion:

$$m_e\ddot{x} + b\dot{x} + kx = F \qquad (2.1)$$

where m_e is the effective mass, b, is the viscous damping, K is the elastic spring constant, and F is the input force. From static measurements of otoconial displacement under 1 and -1 g acceleration and an estimate of m_e based on the density and volume, the spring constant, K, was found to have a value in the range of 1300 dyne/cm. De Vries estimated the damping, b, by measuring the otoconia displacement at various sinusoidal input frequencies, then choosing two values of b, one corresponding to just critical damping, the other to one half of this friction value. He then calculated the predicted displacement using these values of damping. Finally, he compared the predicted to the observed displacements and concluded that the best fit was obtained by assuming a value of b needed to give just critical damping (c = 1). He argued that this value seemed reasonable because it gave the fastest rise time with no overshoot. He concluded that a value of b = 15 $\pm$ 3 dynes-sec/cm was reasonable. Two factors determine the value of the mass that should be used in the calculations. The first factor is bouyancy, i.e. the otoconial membrane lies within an endolymph fluid filled chamber. The density of the otoconia imbedded in the membrane is about 2.9 while the endolymph fluid has a density of about 1.02 (Jongkees, 1967). The second factor is a virtual mass effect which is the additional mass of endolymph accelerated when the otoconial membrane moves. To attempt to calculate natural frequencies and/or parameters of the system one must distinguish between the effects of these two masses. If one uses a constant acceleration, say gravity and measures the final displacement of the otoconial membrane, as De Vries did; then to determine the spring constant using the final value theorem, one uses only the bouyancy effects or effective mass $m_e = (\rho_o - \rho_e)V$

where:

ρ_o = average density of otoconia plus otoconial membrane

ρ_e = density of endolymph

V = volume of otoconia and otoconial membrane

In this case, using estimates of V, ρ_o, ρ_e and measuring the steady state displacement, one can calculate a value of K, which is what De Vries did.

To calculate natural frequency, however, one must use as a mass value the actual mass of the otoconia and otoconial membrane. For a representative calculation, a displacement of 100 μm (average for De Vries fish) yields a natural frequency of about 50 Hz. Vilstrup and Vilstrup (1952) x-rayed the otoliths of sharks and estimated a displacement of 15 to 30 μm for a 1 g stimulus. This displacement indicates a natural frequency in the range of 100 Hz. Hudspeth and Corey (1977) looked at single unit afferent firing in the bullfrog. By gently removing the otoconial membrane (if in fact this can be done gently), they were able to mechanically stimulate individual kinocilia (hairs protruding from the sensory cells). Their data show a saturation of firing rate at about 2-3 μm of displacement. This displacement figure, assuming it was valid for 1 g acceleration (which is probably too low) would yield a natural frequency in the range of 300 Hz or higher. As can be seen, the range of values for the natural frequency of the otolith organ is large and still not completely understood.

Using electrophysiological data from the barbiturate anesthetized squirrel monkey, Fernandez and Goldberg (1976c) derived a transfer

function of the otolith organ relating afferent firing rate to input acceleration. Their model for the end organ includes a velocity sensitive, fractional exponent element, adaptation element, and first order lag element associated with the mechanics of the otolith. Different dynamic responses from individual neurons can be accounted for by changes in the adaptation (subscript A) and velocity-sensitive elements (subscript V). The transfer function of the model (relating shear force to firing rate) is

$$H(s) = \frac{1 + k_A\tau_A s}{1 + \tau_A s} \; \frac{1 + k_V(\tau_V s)^{k_V}}{1 + \tau_V s} \qquad (2.2)$$

By assuming an overdamped system, and disregarding the shortest time constant, Fernandez and Goldberg model the otolith dynamics with a first order lag. τ_V is set equal to 40 seconds, but they state that large changes in τ_V can be cancelled out by small changes in k_V.

The parameters of the model were obtained by fitting the model to the Bode plots. Sinusoidal acceleration stimuli were superimposed on steady state excitatory and inhibitory accelerations. For units responding to excitatory stimuli, the following average (n = 16 regular units, 14 irregular) parameters were obtained:

Regular	Irregular
$k_V = 0.188$	$k_V = 0.440$
$k_A = 1.12$	$k_V = 1.90$

Regular	Irregular
τ_A = 69 sec	τ_N = 101 sec
τ_m = 16 msec	τ_m = 9 msec

The regular units were characterized by little adaptation over time, relatively constant gains over a frequency range of 0.006 Hz to 2.0 Hz and phase lead/lag around 0°. The irregular units however were classed as tonic (i.e., adapting over time) and showed up to a 20-fold gain increase as the frequency of stimulation increased, and uniformly larger phase leads (around 30 - 40°) than the regular units.

Another interesting result of the work of Fernandez and Goldberg (1976b) is a static force-firing rate plot. Figure 2.8 shows the relationship between force and afferent neuron discharge rate for various regular units. One notices a distinct sigmoid shape that is very similar to Hudspeth and Corey's (1977) sigmoidal curve relating cilia deflection to receptor potential.

The final model of the otolith end-organ to be discussed is a variation of the De Vries' model. Benson and Barnes (1970) postulated a mechanical model of the otolith that incorporated both shear and compressive forces. The model is shown in Figure 2.9.

The model works as follows. During pure compressive force stimuli, there is no cilia bending and no receptor potential. However, when a shear force shifts the otoconial membrane with respect to the hair cells, a compressive force can then generate an

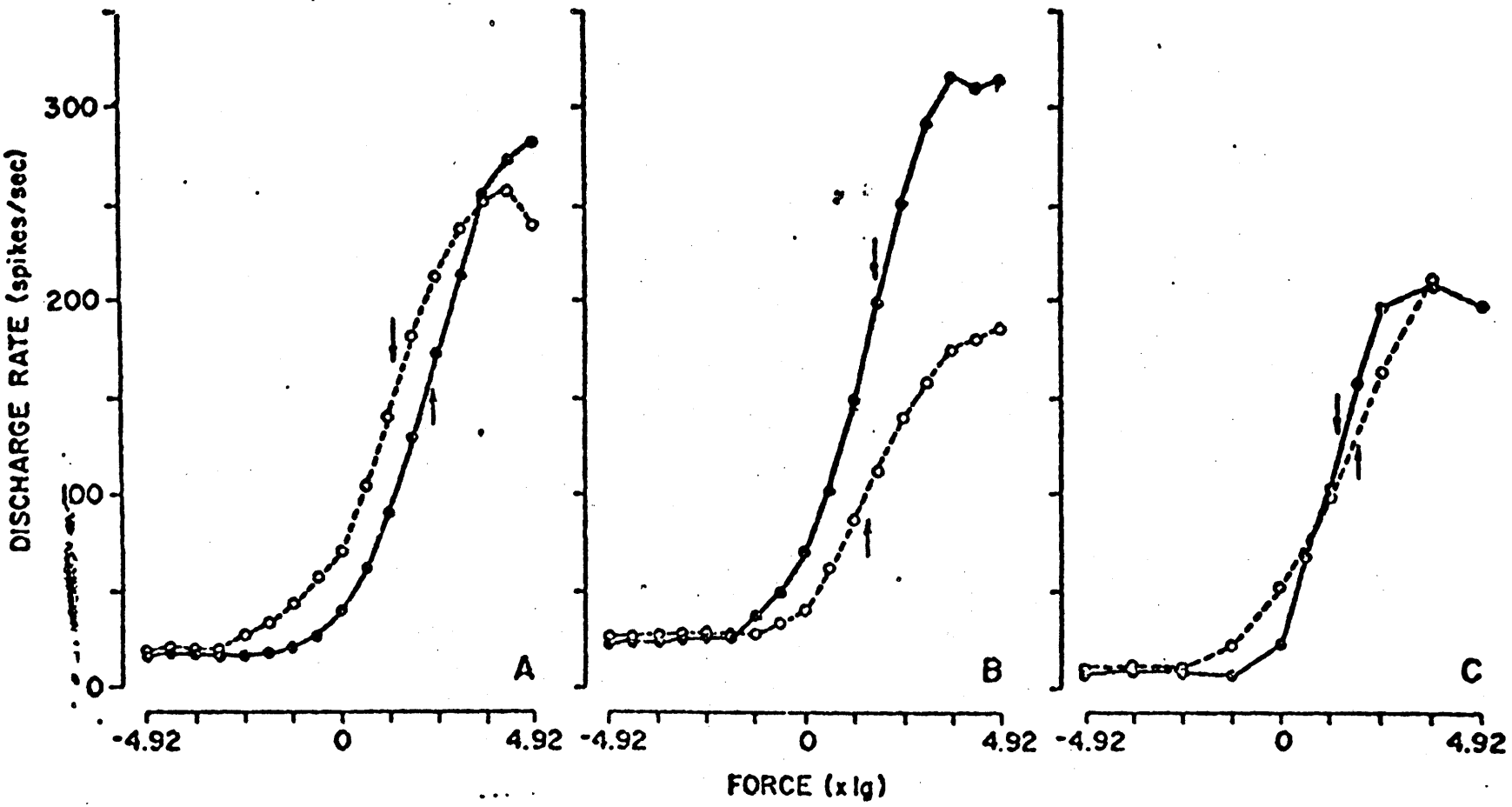

Figure 2.8 Force-firing rate curves for three first order otolithic afferents in the squirrel monkey. Note the saturation near 5.0 g. From Fernandez and Goldberg (1976b).

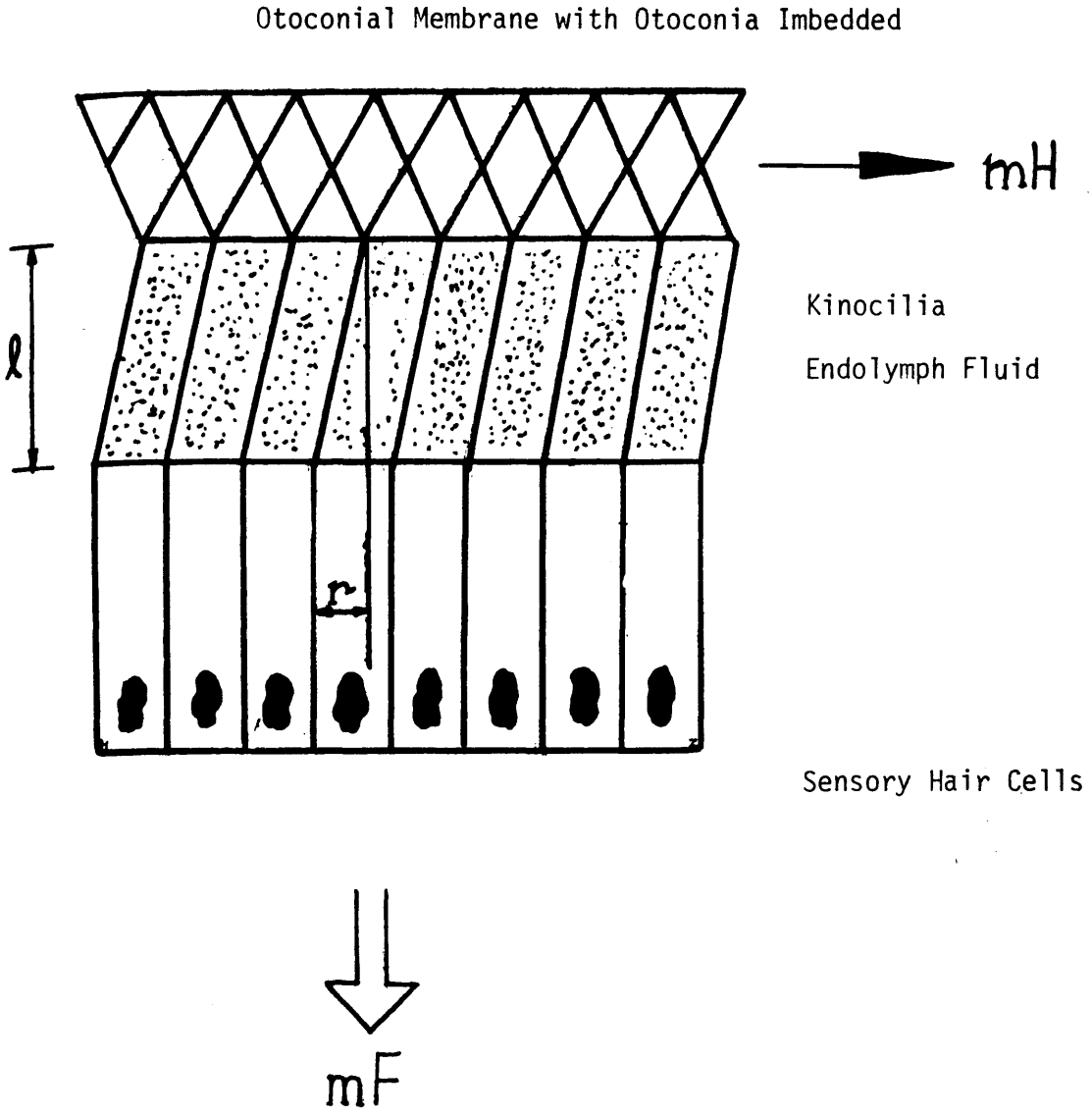

Figure 2.9 A depiction of the mechanical model of the otolith proposed by Benson and Barnes. The model acts in the following way. During no shear force (MH), the displacement of the otoconial membrane (r) is 0 and consequently the moment produced by MF is 0. When a shear force is applied, r differs from 0 and MF then has a moment arm which produces additional bending of the cilia.

additional moment about the base of the cilia. This model is somewhat simplistic and in fact the data of Fernandez and Goldberg (1976b) which showed no modulation of utricular afferent firing rate (at a given shear force) when the compressive acceleration was changed from +1 g to -1 g) tend to refute this interpretation of the model. However, sufficient evidence exists (as initally discussed in the section on hypergravic OCR studies), so that the effects of the magnitude of GIF on OCR and perception of down etc, must be investigated. The role of the magnitude of GIF in stimulating these sensory systems will be discussed fully later but it is sufficient to say for now that the Benson and Barnes model produces some convincing predictions concerning OCR in a 1 g field.

2.6 Models of the Otolith-OCR System

2.6.1 Static Models

Many investigators have investigated OCR as a function of normal lateral head tilt. Close inspection of the data shows that the maximum OCR occurs at about 60 to 70° of head tilt in all reports. Miller's (1962) data was carefully measured and appears typical of all the reports; it will, therefore, be used as the typical OCR versus head tilt curve. Miller's protocol consisted of restraining a subject in a tilt chair and photographing one eye at various lateral tilt angles from 0° to 360°. He examined clockwise and counterclockwise rotation and found no significant difference. However, he did note that the right eye showed more OCR during right ear down

head tilt than during left ear down tilt and also more OCR than the left eye for right ear down tilt. To avoid transient effects or semi-circular canal interactions, he waited for 60 seconds after the tilt chair had stopped prior to taking the data. Miller postulated a model that related OCR to a cosine square law. He argued that the saccules, as well as the utricles, contribute to OCR, but that the saccules only have an influence when the tilt angle is between about 44° and about 134°. His model is:

$$\psi_T^{(\alpha)} = \psi_u + \psi_s = U_R\cos^2(84 - \alpha) - U_L\cos^2(276 - \alpha) \qquad (2.3)$$
$$+ SA_R\cos^2(134 - \alpha) - SA_L\cos^2(226 - \alpha)$$
$$+ SP_R\cos^2(158 - \alpha) - SP_L\cos^2(202 - \alpha)$$

where

α = head tilt angle

ψ = total OCR

ψ_u, ψ_s = OCR due to utricle and saccule

$U_{R,L}$, $SP_{R,L}$, $SA_{R,L}$ = maximum contribution of right and left utricles and right and left sacculus posterior and anterior (gains which are subject dependent)

Fluur and Mellstrom (1970a + b) electrically stimulated the utricles and saccules of cats, some of which were decerebrated and some under light anesthesia. They noted eye movements by visual inspection. Stimulation of both macculae produced varying eye movements depending on the area simulated; stimulation of the utricle in the decerebrated cat usually resulted in eye movements that could be related to specific muscles

of the eye. In fact, stimulation of most areas of the utricle produced rotary eye movements consistent with those obtained during the OCR studies. Rotary eye movements that would be compensatory for left ear down tilt were obtained from stimulation of the left saccular macula. In decerebrated cats the effect was only observable on one eye with superior macula stimulation yielding rotary movements of the right eye while inferior macula stimulation caused rotation of the left eye but in the same direction. In spinalized, lightly anesthesized cats the rotary motion was coordinated.

2.6.2 Dynamic Models

Several investigators have reported dynamic OCR results in primates and humans. Chassen et al (1967), Smiles et al (1975) and Junker et al (1971) have reported primate results, while Hannen et al (1966) Petrov and Zenkin (1973), Goloyan, Zenkinand Petrov (1976) have reported results in humans. The primate studies confirm the otolith organs as the primary transducer for the OCR system. They also indicate a system that has either a slight reduction (Chassen's data) or no change (Junker's data) in amplitude ratio over a frequency range of about 0.1 to 0.9 Hz. The phase angle decreases steadily with increasing frequency; this decrease is explained by a time lag in the system of about 200 msec (See Figure 2.10 for Junker's data).

Hannen et al (1966) were able to derive an approximate transfer function relating lateral head tilt to OCR in the human. They also

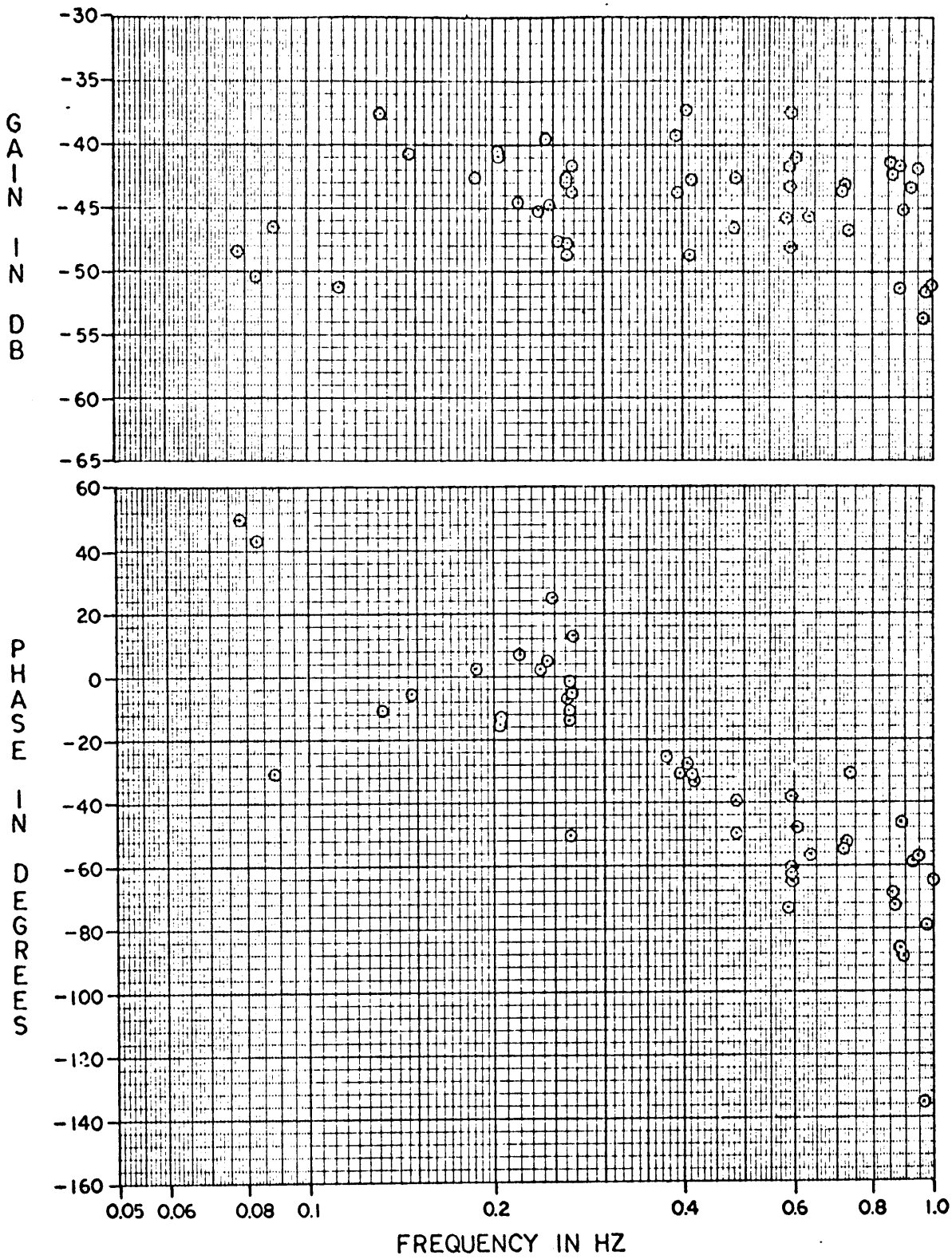

Figure 2.10 Bode plot of ocular counterrolling in the monkey. At very low frequencies, there is some phase lead, at higher frequencies, the phase data appear similar to Kellogg's. The amplitude ratio, however, is almost flat to 1.0 Hz. From Junker et al (1971).

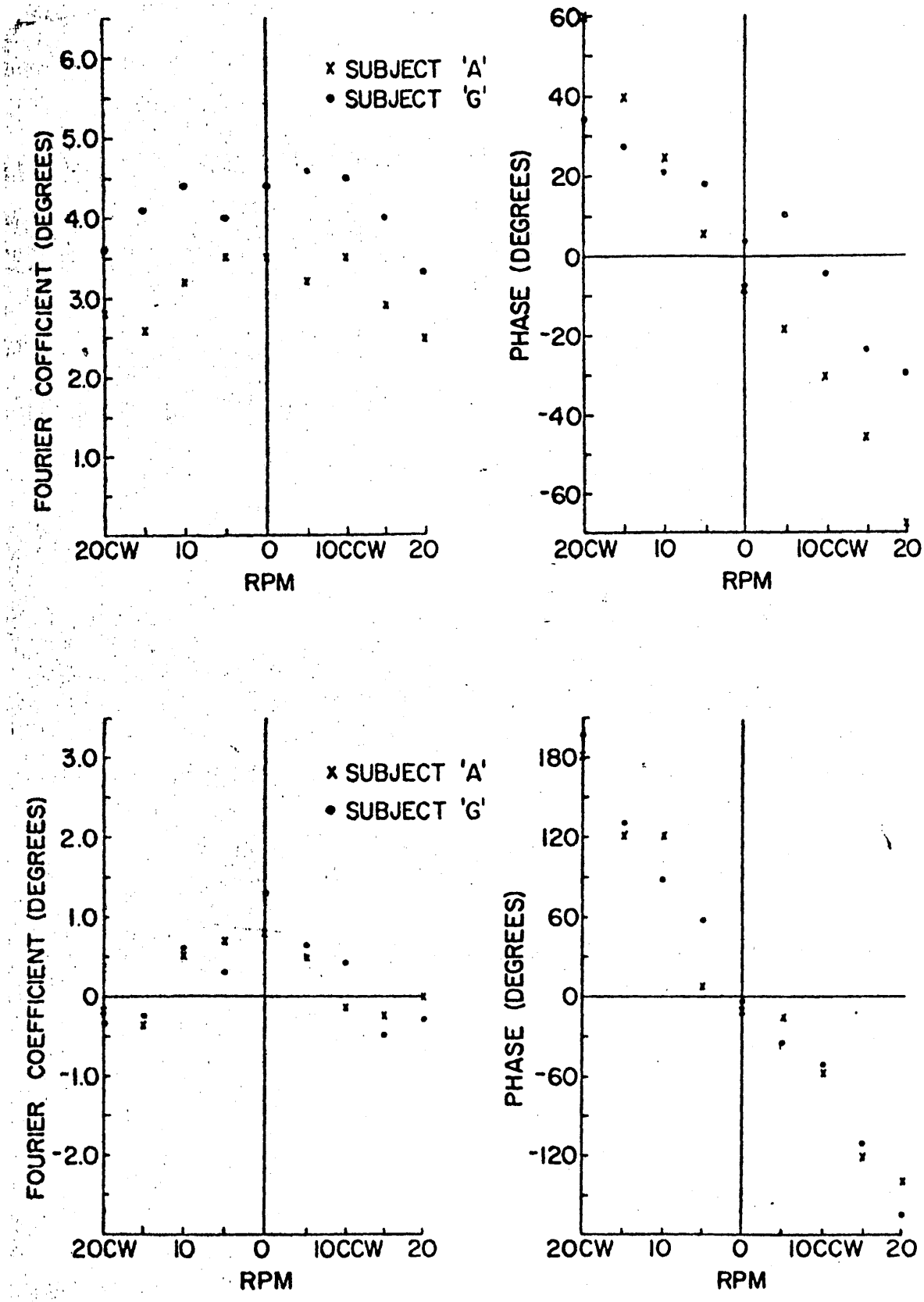

Figure 2.11 FFT data from Hannen et al (1966) showing gain and phase of lower harmonics.

showed a large reduction in static and dynamic OCR in labyrinthine defective subjects. Their transfer function has the form:

$$R(s) = ke^{-\alpha s}/(s + \beta) \qquad (2.4)$$

where α varies from 0 to 400 msec, k = 0.02 and β = 3.14. In contrast to the data of Junker et al (1971) (Figure 2.10) which indicates a phase lag caused only by a time delay, Hannen's data (Figure 2.11) and model indicate a first order lag and a time delay. The species involved are different, of course, and the data from different primate studies appears to be somewhat conflicting. Petrov and Zenkin have also investigated human dynamic OCR induced by lateral head tilt. While they did not formulate a mathematical model, they did attempt to formulate a psychophysical model for the justification and cause of OCR. Their data, the only human transient OCR data, are complicated by the effects of angular acceleration acting on the semicircular canals.

2.7 Psychophysical Experiments Related to Otolith Function

All of the experiments discussed so far have recorded objective data (either eye movements or neural firing rates). This section of the thesis is devoted to several psychophysical experiments that recorded subjective sensation of movement or body position.

Young and Meiry (1968) used psychophysical linear acceleration detection experiments to formulate a model of the entire system relating specific force to perceived tilt or linear velocity.

The linear model is described below:

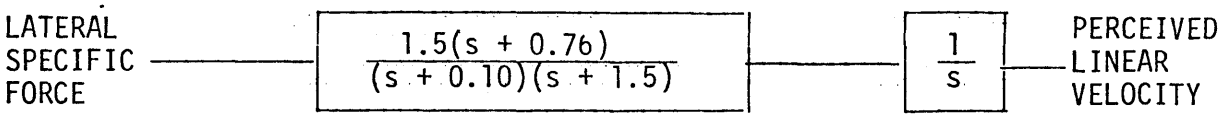

The response of the linear model to a step acceleration is slightly underdamped (see Figure 2.12). The predictions of the model, which is based primarily on perception of linear accelerations, are in agreement with the OCR frequency response data of Hannen et al (1966) and Kellogg (1967) (these are two different papers that used the same data; see Figure 2.13). The response of Young and Meiry's model to a step acceleration is very similar to Baarsma and Collewijn's (1975) data on OCR response to step accelerations in the rabbit.

Corriea, Hixson and Niven (1965) investigated human perception of the vertical when subjects were placed on a centrifuge in various orientations. The experimenters were able to manipulate the shear and compressive force components acting on the otolith. Schöne (1964) proposed a linear relationship between the shear force on the otoliths due to tilt in the saggital plane (sin α) and the perception of the horizontal.*

*Schöne also included data on the perception of the vertical with tilt in the frontal plane (that is, roll).

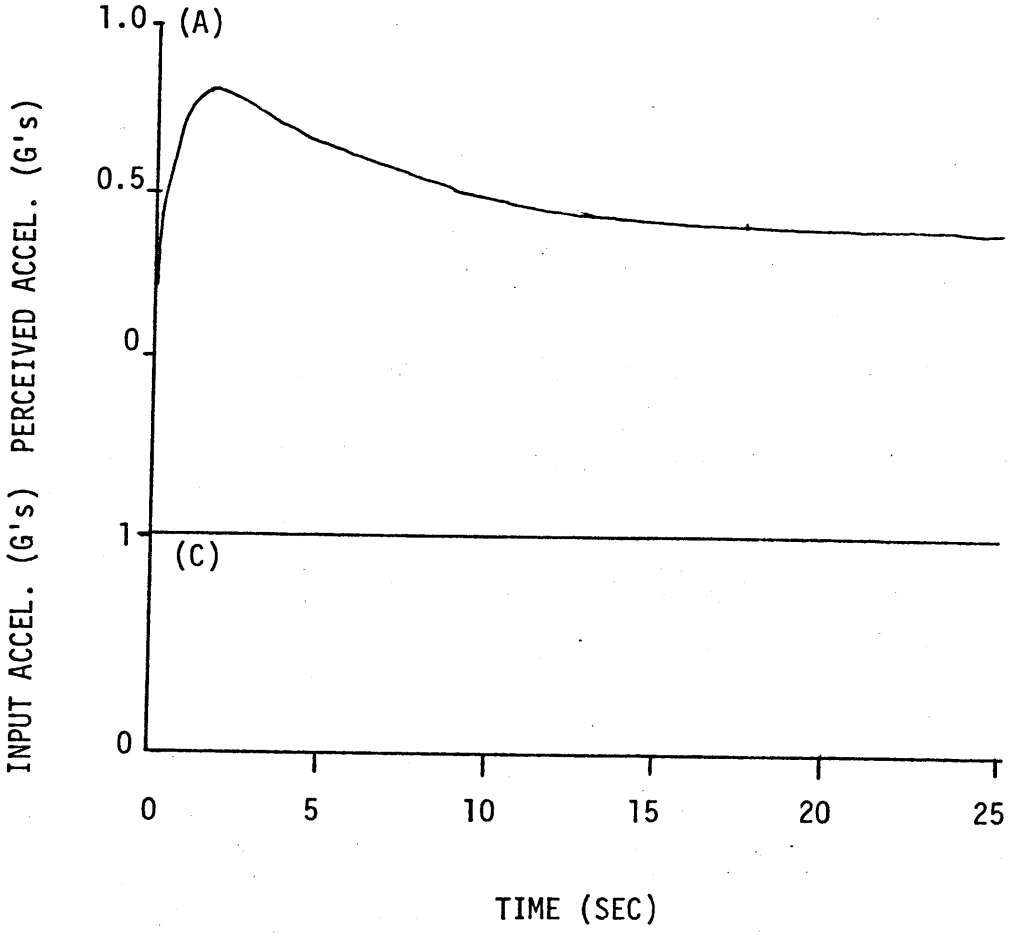

Figure 2.12 Step response of linear model

(A) Perceived Acceleration or Tilt

(B) Acceleration or Tilt Step Input

From Young and Meiry (1968).

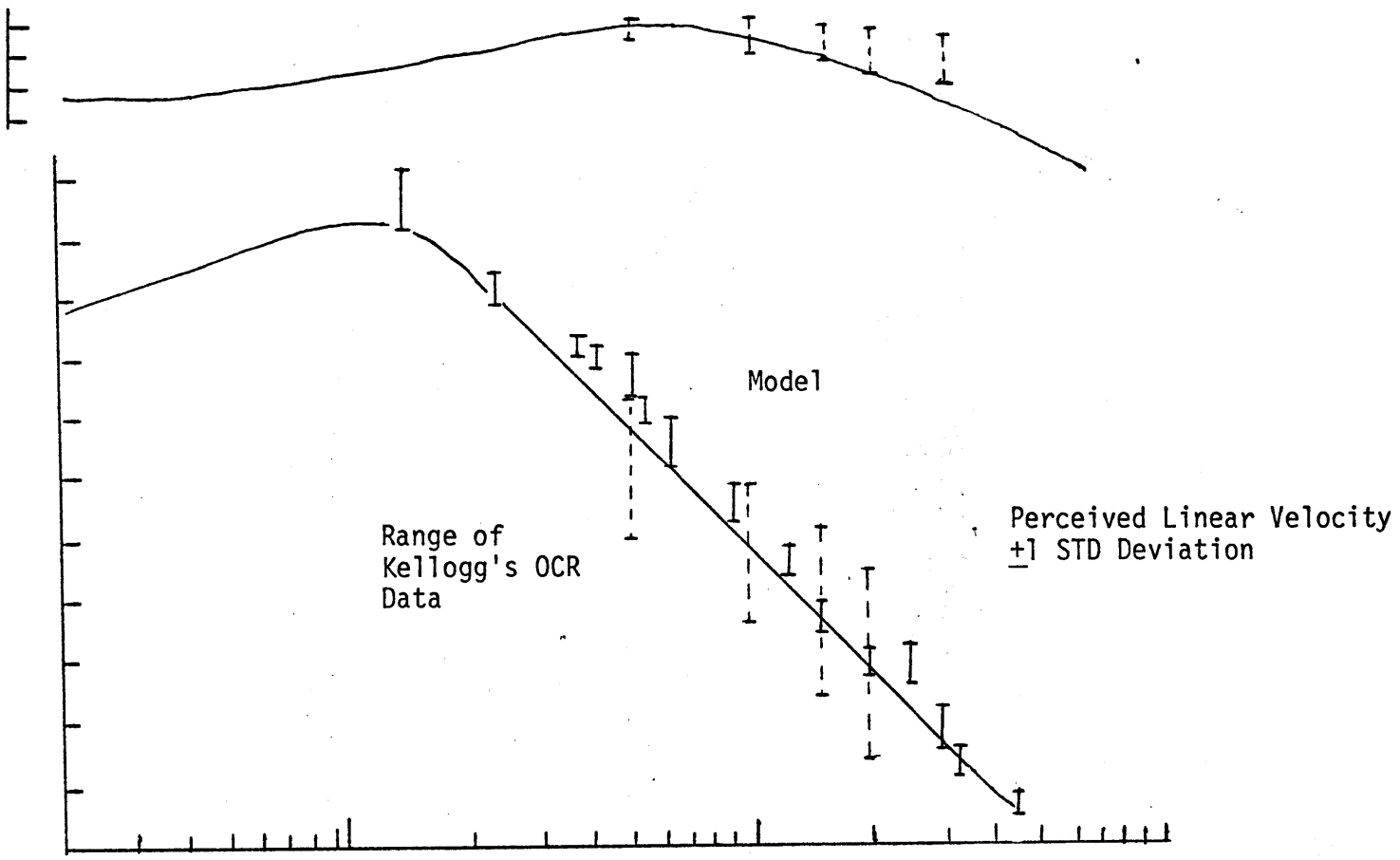

Figure 2.13 Bode plot of Young-Meiry model including their data on perceived linear velocity (solid vertical lines) and Kellogg's OCR data (range indicated by dashed vertical line). From Young and Meiry (1968).

Correia, Hixson and Niven showed that Schöne's relationship did not hold under a wider range of conditions. They formulated a more accurate model by using the tangent of the angle (instead of the sine) and the magnitude of the specific force. This model shows a linear relationship between perceived horizontal and/or vertical and a combination of shear and compressive forces. In the case of otolith stimulation to the frontal plane, the planes relevant to OCR experiments, they conclude that (1) when the specific force is aligned with the z-axis of the head, no change in perception of vertical occurs with changes in magnitude of the force. This situation produces primarily compressive force acting on the utricles and primarily shear force on the saccules; and (2) when the specific force vector is not aligned with the z-axis, a utricular shear force model alone would not predict the observed results. In fact, they held the utricular shear force constant, manipulated the compressive force, and noted changes in the perceived direction of the vertical. Finally, they reviewed several ocular counterrolling experiments (Miller, 1962; Woellner and Graybiel, 1959; and Colenbrander, 1963) and concluded that for the most part, OCR was not a linear function of shear force for values of shear force exceeding about 0.5 g. After they fit the tangent model to a majority of the data, they include a disclaimer to the effect that "it is not denied that the displacement of the otolith membrane from its null position may be linearly related to $A\sin\psi$, the shear directed component of the static linear acceleration stimulus". Benson and Barnes (1970) postulated that, in fact, for both shear and compressive forces, the transduction site was in the otolith.

Correia, Hixson and Niven never address the question of what happens to the model as the angle approaches 90° - at that point $\tan\psi$ approaches infinity. Benson and Barnes' model eliminates this problem by assuming that the compression acts in addition to the shear force (and so does not use a ratio of the forces).

Bischof (1974) critically reviewed many psychophysical studies of orientation and revised von Holst's (1950) concept of an optic-vestibular weight ratio.* This ratio describes the relative dominance of the visual system versus the vestibular system in the determination of body orientation with respect to gravity. Figure 2.14 shows the correlation of this optic-vestibular weight ratio with objectively determined OCR as a function of body tilt. They also observed a maximum of both curves at about 60° of roll. These data were recorded from only three subjects and while they cannot be taken as general results, they offer more evidence for the good correlation between perceptual studies and objective measurement of OCR studies.

Finke and Held (1978) investigated the relationship between steady state OCR and perception of roll vection. They used an afterimage technique to measure OCR and a rotating visual field to induce roll vection with the subject's head immobilized by a bite board. Their results indicate that steady state OCR is reduced when the subject has a sensation that the visual world is stationary and that the subject

*Bischof and Sheerer (1971) used the mean oscillation of the position of a line set to the vertical while a subject was observing a constantly rotating visual field. They took this measurement at various body tilts.

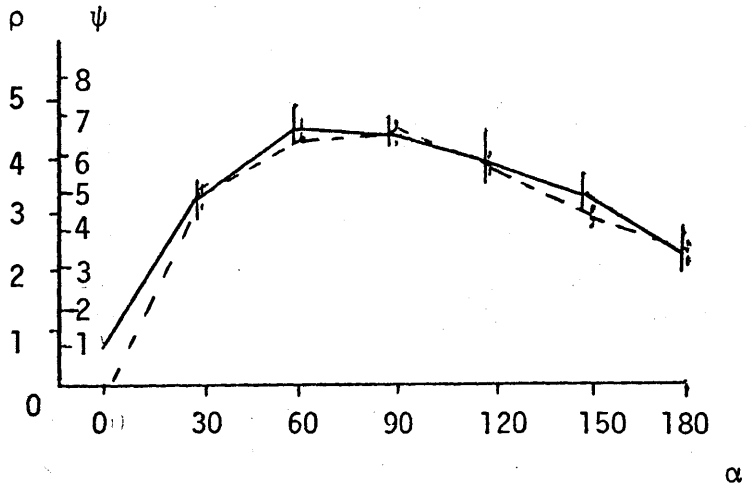

Figure 2.14 Mean range of oscillation of luminous beam setting (ψ, solid line) and ocular counterroll (ρ, dashed line) plotted against body tilt (α). Notice the good correlation of the perceptual results versus the OCR results. Data from three subjects from Bischof (1974).

is moving. With the subject in an upright position, the complete sensation is called paradoxical vection because even though the visual system signals constant rotation, the otoliths contradict this sensation and the final result is a combination of constant rotation and at the same time a steady state tilt. This data indicates that perception of tilt does not increase but rather decreases OCR since the maximum tilt experienced by the subjects is during the states when the OCR is reduced. This study is complicated by the results of another, less formal study done by the author while wearing a helmet specially designed to induce OCR movements with a video monitor visible to one eye and an IR imaging device recording the movements of the other eye. In this situation, the amount of rotary nystagmus was clearly influenced by the subject's perception of self motion and orientation. During periods of compelling roll vection, the amount and magnitude of rotary saccades increased markedly. It was not possible to measure steady state OCR during this study just as it was not possible to measure rotary saccades during the Finke and Held study. Only a comprehensive investigation can settle the question of the influence of self motion upon OCR.

CHAPTER 3

METHODS

3.1 Equipment

The equipment built to conduct this study comprises a ground version of the Space Sled. The various parts consist of the drive mechanism, guide rails, seat, head fixation device, and data recording apparatus. In addition, substantial software had to be developed to control the sled and acquire data. The basic description of the sled including its design, capabilities and performance will be discussed in this section. For a detailed discussion of design philosophy, rationale for equipment selection, and actual design parameters including engineering drawings, the reader is referred to Appendix A. The software description is contained in Appendix B.

The sled (Figure 3.1 and 3.2) consists of a cart and seat constructed from aluminum angle stock, supported by four ball-bushings which ride on two round guide rails anchored to the top of a two foot high cement block structure. The seat is independent of the cart and can be positioned to allow x-axis (fore and aft), z-axis (head or feet first) or y-axis (lateral, left-right) accelerations. The y axis position can be accomplished with the subject on his back, or as in this study, upright.

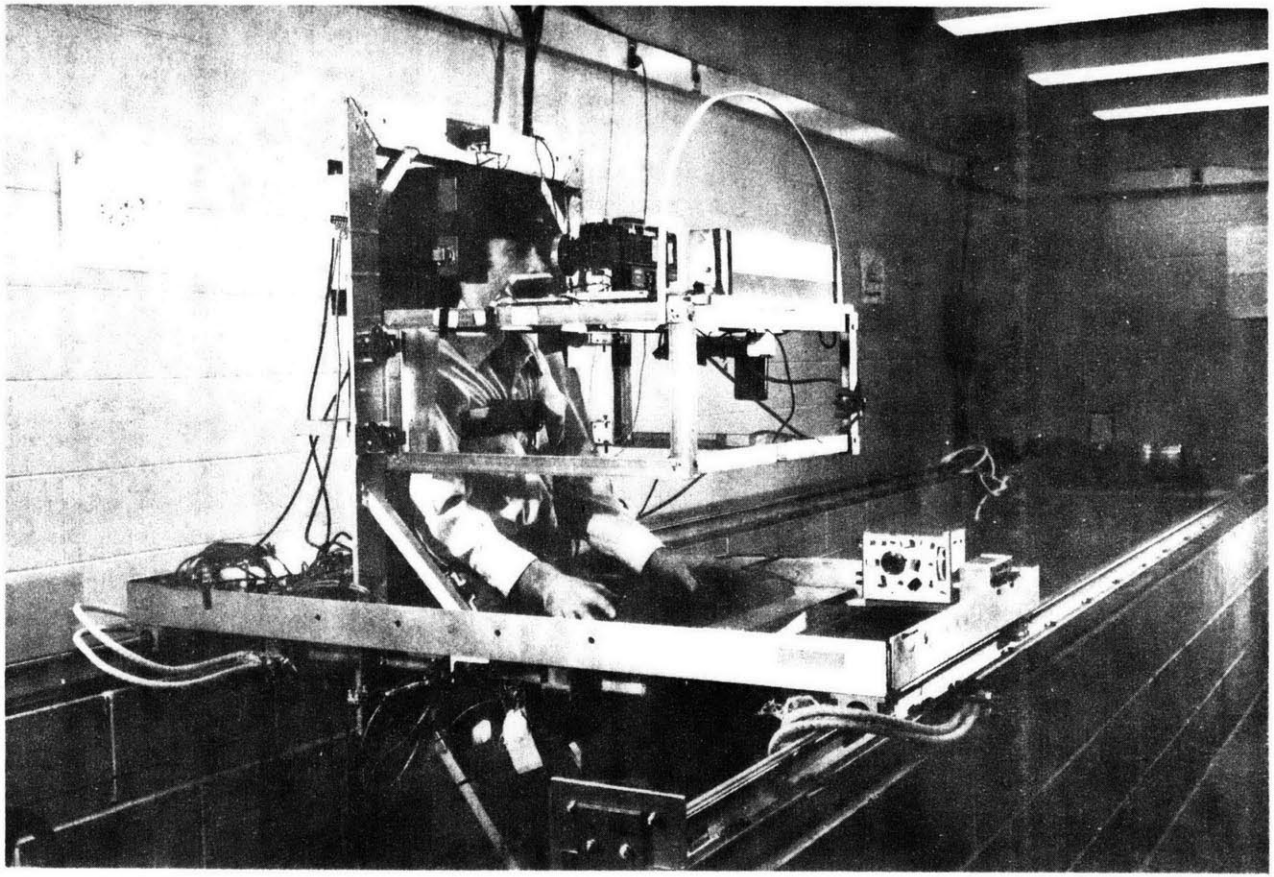

Figure 3.1 This Figure shows the sled equipment designed and built for this thesis.

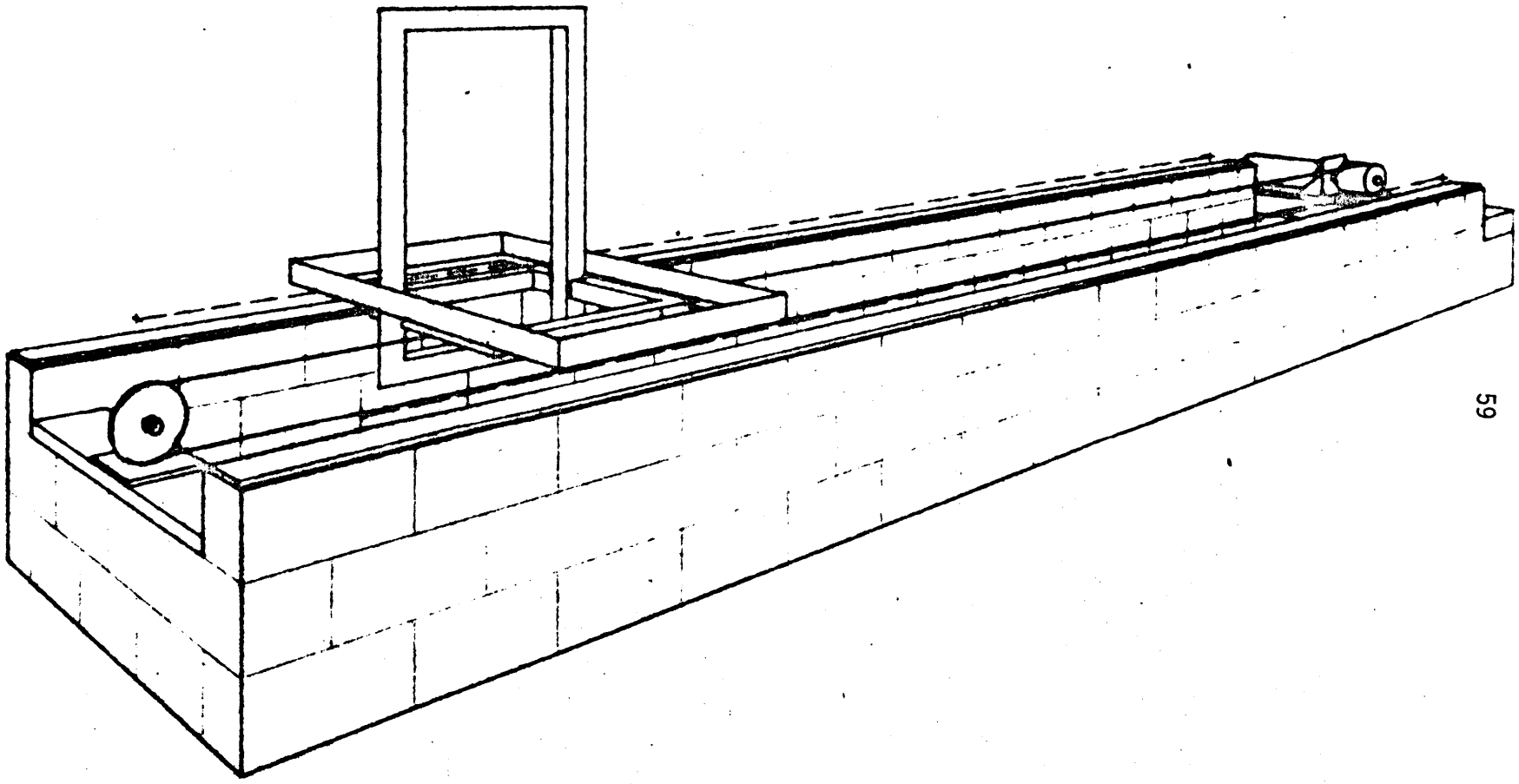

Figure 3.2 Sketch of sled without seat

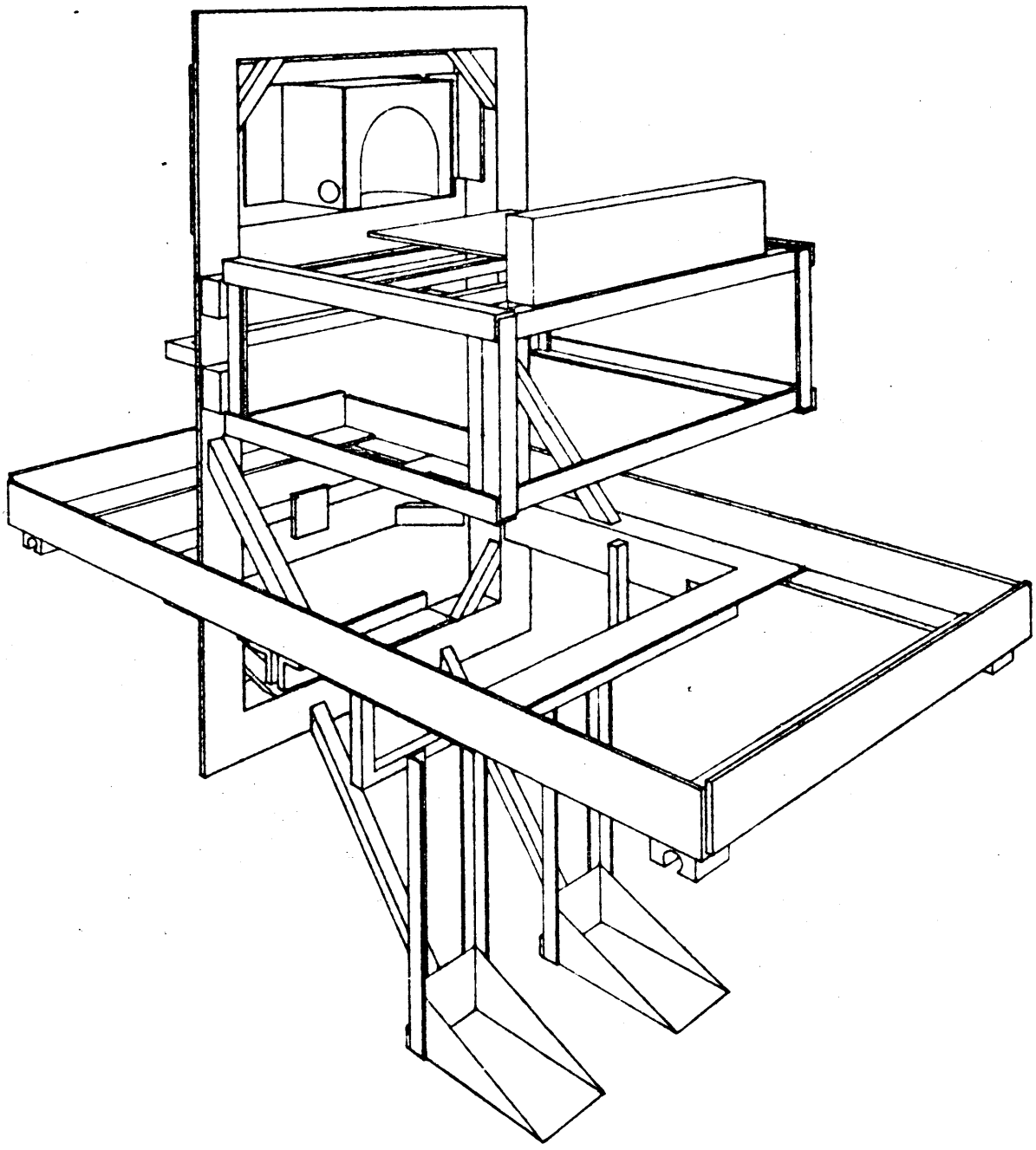

Figure 3.3 Sketch of sled seat showing camera mount and head holder.

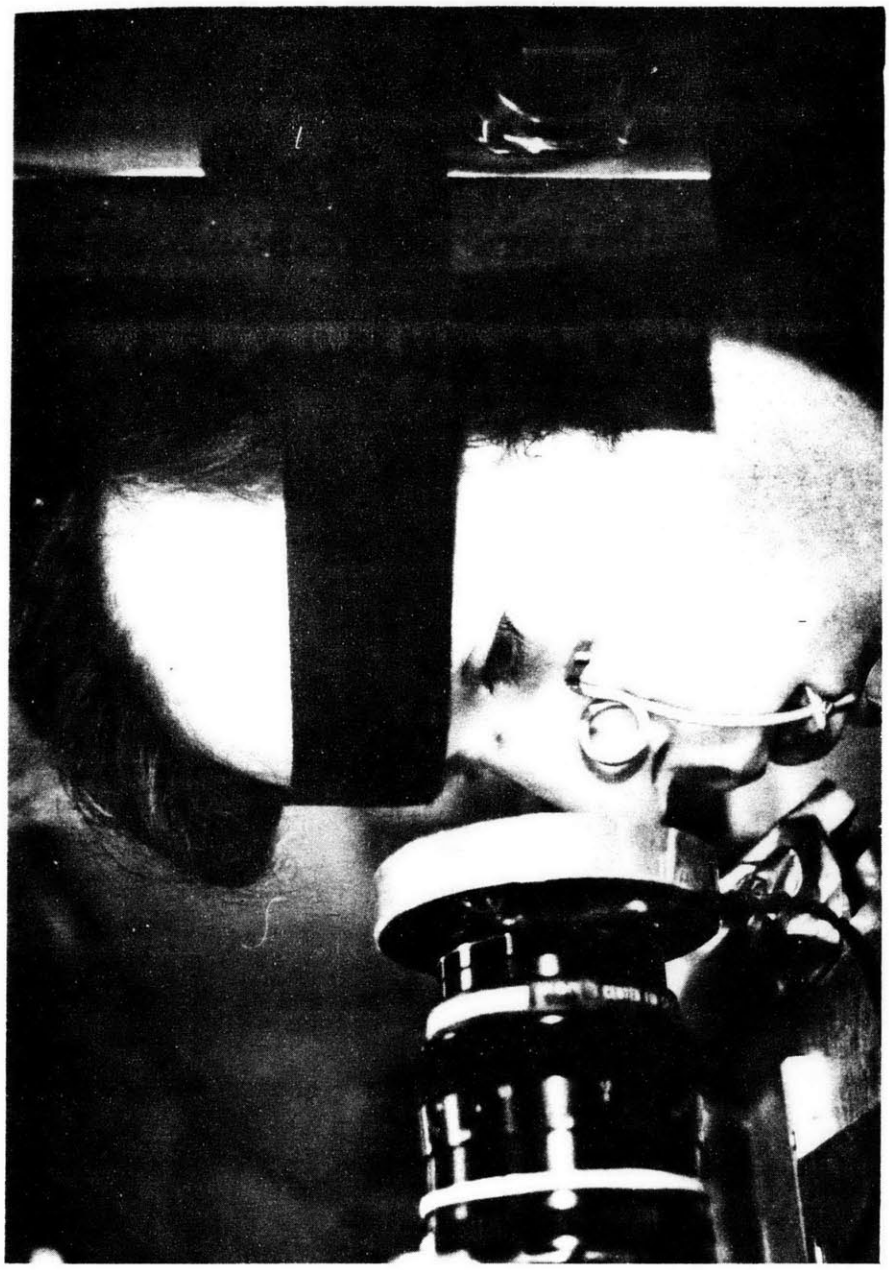

Figure 3.4 This figure shows a close-up of the camera head holder and bite stick with Fiducials attached.

The drive system is a commercially available DC permanent magnet motor and silicon controlled rectifier (SCR) controller. The motor drives the cart through a direct drive, cable and winch drum system.

The control of the motor is accomplished through software; a PDP-11/34 computer acquires the position and velocity of the cart and selects various control logic algorithms.

The performance specifications prescribe step accelerations of up to 0.3 g and periodic (sinusoidal and square-wave) acceleration profiles of 0.02 to 1.0 Hz and up to 0.3 g amplitude. In addition, the capability now exists to produce pseudo-random (sum of sines) acceleration profiles.

The motor uses a tachometer feedback for accuracy and stability. The input to the controller is a velocity command, so the software control was initially designed to provide a velocity output command. In this way, a ramp velocity command would generate a step acceleration and sinusoidal velocity commands would generate sinusoidal acceleration profiles (except that they are phase advanced 90 degrees). After the system was built, Bode plot analysis showed that, indeed, over a 0.03 to 1.0 Hz range, the amplitude ratio was flat to within 1.5 dB. The phase data showed a maximum of 18° of phase lag at 1.0 Hz. Further testing has indicated that the system reaches a resonance peak near 5.0 Hz.

The sled software control operates as follows. If a ramp velocity is desired, the sled is positioned to the closest end of the

track. When the interrupt is hit, the sled velocity increases rampwise until a point is reached along the track at which the sled must decelerate at 0.35 g in order to avoid running over the normal track limits. This decision point is determined in real time by the computer by monitoring the position and velocity.

The subject is fixed in the seat (Figure 3.3) with a four point aircraft type lap belt and shoulder harness and an additional chest strap to reduce left-right movement. In addition, stiff foam blocks are wedged between the subject's shoulder and the seat frame to further reduce torso motion. The head is supported with a foam rubber appliance which completely encases the head up to the frontal plane of the face (Figure 3.4). The head support is adjustable vertically and has an aluminum plate on each side which hold the earphones and provide additional lateral support when they are pushed tightly against the foam. The subject also has a microphone to insure communication to and from the seat.

3.2 Data Recording

There are several techniques available for measuring OCR; Chapter 2 describes several of them and the pros and cons of each. After a review of the techniques, it appeared that Miller (1962) has developed the most repeatable and accurate non-invasive photographic technique. For routine laboratory or spaceflight conditions, contact lenses, although providing an excellent means of measuring

OCR, are, at this time, unacceptable. Miller's technique aligns two photographs - the control and the frame to be measured, then measures the rotation of the film strip. This technique requires that the head be held immobile with respect to the camera and also requires a topical drug such as pilocarpine to constrict the pupil to provide a constant iris diameter. Both of these constraints cannot be met by the space sled system; therefore, a new technique was developed to allow precision analysis of the OCR data.

Rather than attempt to hold the head rigidly fixed with respect to the camera, it was decided to employ fiducial marks near the eye that were attached to a bitestick held in the subject's mouth. In this manner, a head reference was available in each frame. The analysis consisted of measuring the coordinates of the fiducial marks and the coordinates of selected iris landmarks on each frame. The angle between lines drawn through the fiducial and eye landmarks was then calculated - this angle in the control frame (upright, no horizontal linear acceleration) is then subtracted from the angles in the frames recorded during stimulation to produce the OCR angle.

The measurement of vernier protractors or microscope stages is very time consuming and error prone. A film analysis machine (Hermes Senior) was discovered in the Laboratory for Nuclear Science. This machine projects a 35 mm film strip on a ground glass cover screen that has a cursor in the field of view. The stage holding the film can be moved with a joystick to place various landmarks on the film

under the cursor. The coordinates of this point can then be read by a minicomputer and recorded in digitized format. The resolution of the machine is one micron on the film plane and the repeatability is about 2 microns.

3.2.1 Selection of Camera, Lens and Film

The ideal OCR measurement device would be a non-invasive, continuous device with a real time readout. Unfortunately, such a device is not yet known to exist. 35 mm photography was chosen as the best method currently available. When one tries to photograph close-up objects or get a large image size on the film, two problems immediately arise. The first problem is the very shallow depth of field. In other words, focussing is critical. The second problem is to get enough light on the subject. To achieve a 1:1 reproduction ratio (the image size on the film is the actual object size), the film plane and object must be equidistant from either side of the lens. This distance is equal to the focal length of the lens. The increased light path inside the camera (necessitated by the use of an extension tube or bellows to get the 1:1 reproduction ratio) cuts down on the intensity of the light at the film surface. The solution to the light problem is to use a stronger light source and to "open" the lens aperture, that is, a small f-stop number such as f/4.0 or f/5.6. This procedure of opening the lens aperture unfortunately reduces the depth of field. Therefore, a trade-off between depth of field and available light must be made.

The camera and lens selected was the Nikon F2 photomic with a 105 mm micro-Nikkor lens and extension tube. This combination allows a 1:1 reproduction ratio and keeps the front of the lens about 15 to 17 cm from the subject. The flash chosen was the Vivatar 283 Thyristor controlled flash. At distances close to the subject, the full flash intensity is not needed and the thyristor circuit enables a reduction in light thus allowing a fast (about 3 Hz) firing rate.

This combination appeared to be very good; however, when the space sled dimensions became available, it was obvious that the combination would not fit in the available space. Another search of lenses was done and the 55 mm micro-Nikkor lens with extension tube was purchased. This combination places the front of the camera about 5 cm from the subject. At this distance, it is difficult if not impossible to use a rectangular flash like the 283 without producing lens shadows on the eye. A focussed flash was tried, but the problem of alignment was severe. The final solution was a ring flash mounted on the camera lens. The flash that was purchased, a Honeywell Prox-O-Lite, was very intense, but had a recycle time of about 16 seconds. The power supply was reworked by the Laboratory for Space Experiments to produce a 3 Hz firing rate with an acceptable intensity.

Many films were evaluated. The majority of past analysis techniques used slide film projected to a 40-fold enlargement. The following slide films were evaluated: Kodachrome 25, Kodachrome 64, Ektachrome 64, 160, 200, 400, Ektachrome IR, and photomicrography

film. In addition, color negative film, Kodacolor 400, monochromatic (black and white), visible light and IR sensitive films were evaluated. The negative films were deemed too difficult to analyze and the use of a reversal process to make positive images was deemed impractical. The black and white film did not yield enough information about the iris, which is usually multicolored. The black and white IR film was very difficult to focus properly, and very slow (equivalent ASA of about 64). Of the color slide films, the photomicrography and other low speed (25 and 64) films were too slow. An f-stop of f/4.5 was needed to obtain much color detail and at that f-stop, the depth of field was so narrow that usually the iris was not completely in focus and the fiduciary marks were very blurred. Ektachrome IR film was very promising as the film is very sensitive to brown iris pigments. However, with the required use of a Wratten #12 filter, the effective speed was too low even when "pushed" one extra stop during development. The film finally decided upon was Ektachrome 200. However, to get the required depth of field f-stop of f/8.0, it is necessary to "push" the film one stop which effectively doubles the ASA rating. Just prior to the start of experiments, an Ektachrome 400 film was released by Kodak, but unfortunately was only available in 36 frame cassettes and not in the 100 foot rolls that are needed for the 250 frame cassettes. This film, pushed to 800 ASA, might be a good choice for the future, as it will allow an f-stop of f/11.0, thereby increasing the depth of field.

3.3 General Protocol

The detailed procedure involved in running a subject is as follows. The subject was first examined by an otoneurologist for any obvious labyrinth/auditory/neurological disorder. The subject was then informed about the experiment and asked to sign an informed consent statement. Two biteboards (a full-mouth biteboard and a one-sided bite stick) were made using Kerr Dental impression sticks. The sticks soften at 132°F when placed in a jar of hot water. The compound is formed to the biteboard, which is then positioned in the mouth with the fiduciary marks close to the right eye. The subject is instructed to bite into the compound enough to leave a good impression, but not hard enough to touch the underlying metal. After the impression is taken, small adjustments are made to the fiducial marks to place them under the eye, close to but not touching the skin, and roughly in the plane of the iris.

Three different stimuli were used to generate OCR: (1) static head tilt, (2) lateral step acceleration, and (3) lateral sinusoidal acceleration. Assuming that the static OCR was recorded first (the order of the three events were varied, see Section 3.3.1 Experimental Design), the following procedure was followed. The static measurements were taken at seven different positions: Head upright, ±10°, ± 20°, and ± 30° of head tilt. To do this, the camera baseplate was modified to hold the full mouth biteboard rigidly. The subject was restrained loosely in the cart seat with an eyepatch over the

left eye and the camera plate was positioned to the desired tilt angle using a wedge. The subject bit on the biteboard and two pictures were taken after a period of stabilization (30 seconds to one minute to allow the semicircular canal effects to die down). This procedure was repeated for all seven positions.

The subject was then strapped into the cart with the lap belt, chest strap and head strap. The eye patch was replaced over the non-measured (left) eye and the bite stick inserted into the subject's mouth. The camera mount was positioned and the camera focused on the iris. A communication check was made and the cover placed around the cart. A small light in the camera mount maintained some light adaptation (so that the camera flash was not too uncomfortable). Prior to acceleration tests, an audio masking signal (approximately white noise) was sent to the headset. The subject was then exposed to step acceleration stimuli of 0.1, 0.2, and 0.3 g magnitudes. The deceleration was constant at 0.35 g. The camera took two pictures before the run and fired at the rate of 3.3 frames per second during the acceleration, deceleration and for four seconds after the cart stopped. After each run, a marker was photographed to facilitate later data analysis.

For the periodic stimuli, three frequencies (0.2, 0.4 and 1.0 Hz) were used with an acceleration magnitude of 0.2 Hz. Five cycles of 0.2 Hz and 0.4 Hz and ten cycles of 1.0 Hz stimulus were used. Two control pictures were taken, then the stimulus was applied for two

cycles without picture taking to allow any transients to die out. Pictures were then taken for the rest of the run and for two stimulus periods after the cart was stopped. The camera firing rate for the 0.2 Hz sinusoids was reduced to 2.2 frames per second because of the low stimulus frequency.

In addition to the normal procedure, one subject was exposed to 80 seconds of 0.2 Hz, 0.2 g stimulus, so that the stationarity of the system could be observed. A second subject was exposed to three ramps of 0.15 g acceleration to check for habituation, and three sinusoidal runs at 0.3 Hz and 0.1, 0.2 and 0.3 g to investigate amplitude non-linearities of the system.

3.3.1 Experimental Design

The sequence of the experimental runs was varied to reduce any possible order effects. No effects were anticipated between step acceleration profiles and sinusoidal profiles, so the sequence of step profiles before sinusoidal profiles was preserved throughout the experiments. The static OCR tests were performed before the dynamic runs for half the subjects and after the runs for the other half. Within each category, static, step and sinusoid, the presentation of the stimuli were varied in an incomplete Latin-square design. No OCR study known to the author has shown any conclusive order effects, so the above procedures were merely a precaution and not an attempt to quantify any order effects.

3.4 Data Collection

A total of nine subjects were used to obtain OCR data. Seven subjects were exposed to the complete protocol, one subject was used for the stationarity check (stimulated for 80 seconds continuously at 0.3 g, 1.0 Hz), and the last subject (14) was used for a linearity and habituation test (stimulated with three identical 0.15 g step acceleration profiles and three (0.1, 0.2, 0.3 g) 0.3 Hz sinusoidal acceleration profiles. The data (photographic film) for one subject was not analyzable because the iris was completely out of focus.

The data file abbreviations used in the computer and also on the graphs describe the type of stimulus, subject number and acceleration (for sinusoids).

Ramp		Sine	
Code	Acceleration level	Code	Frequency
0	0.05	1	1.0 Hz
1	0.1	2	0.2 Hz
2	0.2	4	0.4 Hz
3	0.3		

For example, RAMP 72 would indicate a ramp velcocity stimulus on subject 7 with a 0.2 g acceleration. SIN 121 would indicate a 1.0 Hz (0.2g for all sines except subject 14) sinusoid on subject 12.

All subjects were asked to report any unusual sensations during the tests. Specifically, two effects were of interest. First, is a

lateral acceleration judged subjectively as tilt or lateral motion, and second, does the sensation of motion persist after the motion is stopped. The answers were negative from all but one subject, who stated that during the sinusoidal oscillations, it felt as though the cart were tilting to a small extent as well as translating. In another series of experiments, several subjects reported a sensation of linear acceleration with an "outward tilt" at either end of the track.

3.5 Analysis Method

Figure 3.5 shows a functional diagram of the data analysis. The developed but unmounted, uncut rolls of film were taken to the Laboratory for Nuclear Science (contact Marianne von Randow, 3-6068), fourth floor of 575 Tech Square. The machine used is a Hermes Senior, machine #9. The film is spliced into a leader roll and a take up roll. The machines are designed to take 100-200 foot rolls of film and, unless proper leader roll size is used, the torque motors used to advance the film will tear it. The left hand reel should be almost fully loaded with a leader film (large reel). The right hand reel should also be a large one, but almost empty. The film to be analyzed should be placed upside down, emulsion side up, on the film stage. This means that the film advances from left reel to right reel which is opposite from the signs on the machine. In other words, the bulk of the film will be on the left hand reel prior to starting the analysis. It might be necessary to rewind the film first because different photoprocessing companies wind it differently. Once the film is installed in view #2, the middle of the three film holders, the machine is set up according to Appendix C. The machine readout is in

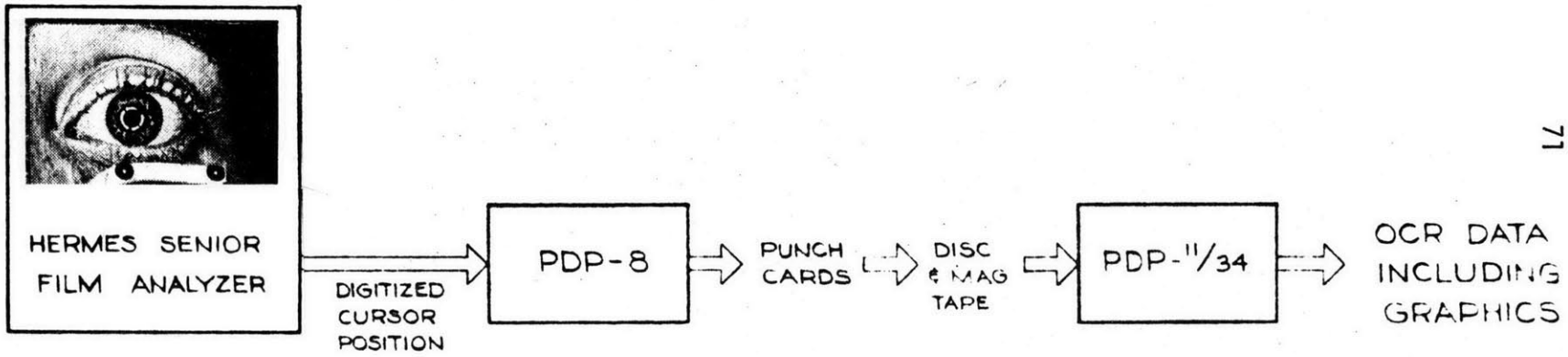

Figure 3.5 Block diagram of data analysis procedures. Includeg is a picture of an actual data slide.

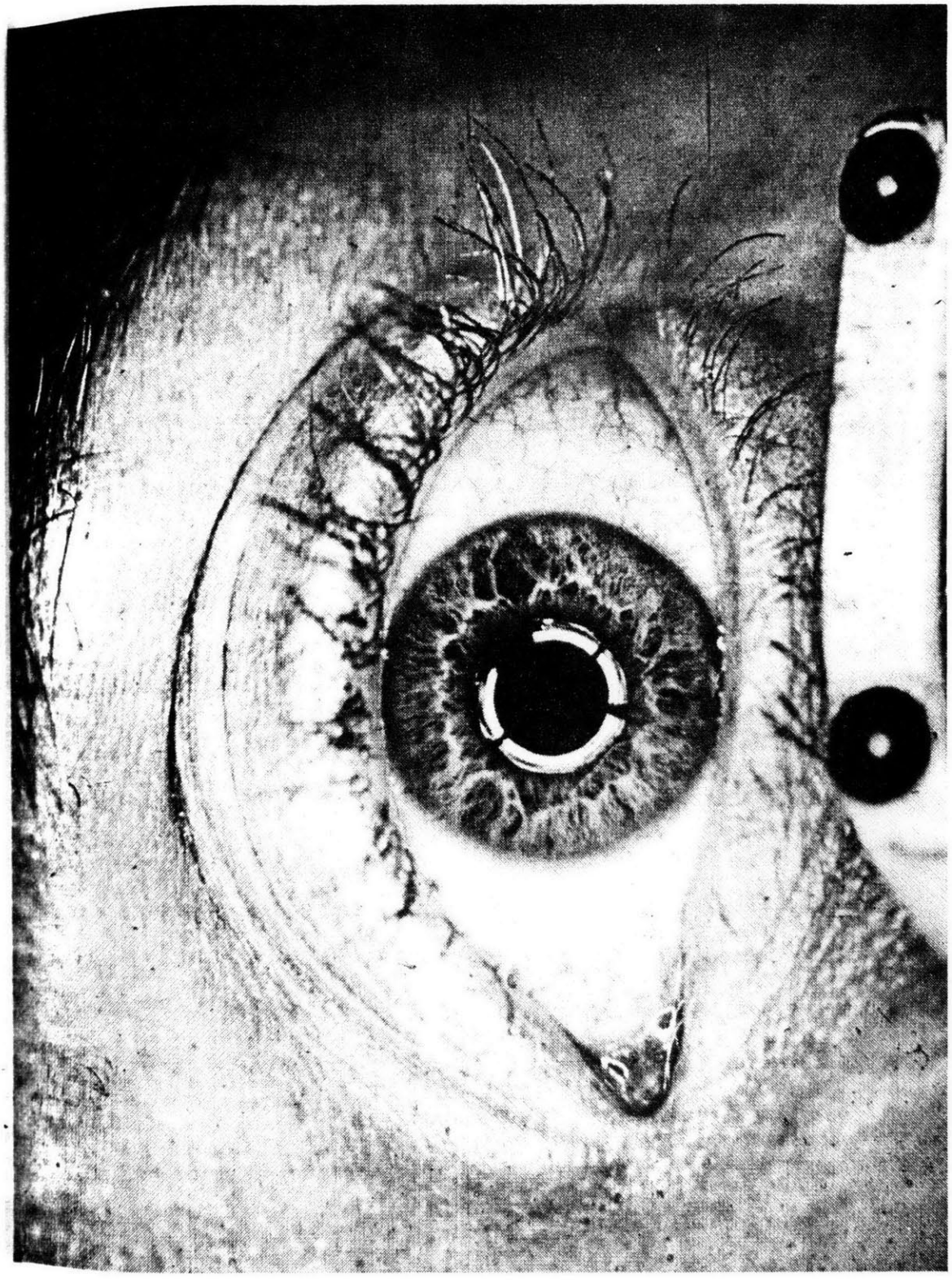

Figure 3.6 An eye

microns on the film plane. Because the numbers can be and usually are larger than 32,767 (the largest integer accepted by FORTRAN IV), it was necessary to modify the zero procedure so that the readings lie in the range 0 to 65,534 to prevent any ambiguousness in the number being processed by the PDP-11 computer. The technique was to use a new zero location which is 10 inches to the right of the normal zero location of the machine and 10 inches above the top of the film. By placing the cursor at this point for zero (this doesn't have to be extremely accurate), and using the left most portion of the stage for film analysis, the x coordinates should be between 5,000 and 50,000. The current procedure is to place the cursor with the left edge of the horizontal cross-hair aligned with the right edge of the previously analyzed frame with the vertical cross-hair (see Figure 3.7). To avoid slack in the film (which might cause it to tear during motor start), it is a good idea to leave the film in the move film position. A control experiment was done to assure that the motors have no drift that would cause errors in the data recorded from a frame. No movement of the film was detected with the motors left on for 1 1/2 hours. Since the time needed to analyze one frame is on the order of one minute, no errors should occur. The current data analysis programs take the data points in the following order: (1) left fiducial; (2) right fiducial; (3-10) four repetitions of two eye landmarks, with the left landmark first in each repetition.

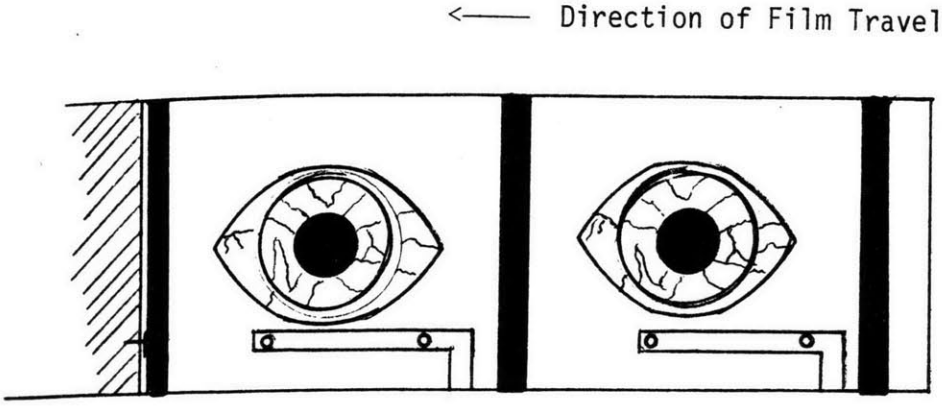

Figure 3.7 Alignment of the film for analysis

The procedure is to log into the PDP-8I monitoring system following the instructions in Appendix C, using the scanner number that is assigned by Marianna. To avoid excess charges be sure to log off when done or when changing film. Three options for data recovery are available: magnetic tape, paper tape and hard copy teletype print out. The magnetic tape is transformed into punched cards, but the procedure takes a while. The paper tape/teletype data is available in real time. To record data points, follow the instructions in Appendix C.

Once the data is recorded, it is transferred to and stored on RK05 discs. The format of the data is indicated in Appendix C in the general operating procedures of the machine. If the data is received on punched cards, the information available besides the data points includes the frame number, measurement number and event number. The frame number is self explanatory. The measurement number is used as the subject identification and the event number corresponds to the type of stimulus used. The event numbers are limited to integers between 0 and 7. The event number and the stimuli they represent for this thesis are listed below.

Event Number	Stimulus profile
0	0.05 g ramp
1	0.1 g ramp
2	0.2 g ramp
3	0.3 g ramp
4	0.2 Hz - 0.2 g sine
5	0.4 Hz - 0.2 g sine
6	1.0 Hz - 0.2 g sine
7	Static head tilt

The hard copy printout can be entered onto the disc through the program DATAIN. This program allows a variable number of frames of data and is currently set up to record 6 data points (12 x, y coordinates) per frame. The data is analyzed with program FILM. If the punched cards are used and transferred to an RK05 disc, the information is read in as ASCII characters (*.RAW). A program to convert this data to floating format (*.OCR) was written and is called CNVRT. The data is then analyzed by the family of programs called FILM, FILM25, FILM20 and FILM10. FILM25 was used to analyze the early sets of data which consisted of 5 repetitions of 5 points per frame. The five points were the lower right corner of the camera frame, the left, then right fiducial marks, and then the left and right iris landmarks. The data recorded in this format is RAMP73.RAW, STAT71.RAW and SINE72.RAW. The data of SINE74.RAW and SINE71.RAW was generated in the 20 point format (using FILM20 for analysis). This format consisted of the left, right fiducials, then left, right and extra iris landmark. The amount of data generated and the time needed to analyze the film was overwhelming, so the repeatibility of the fiducial measurements was determined by taking nine repetitions of fiducial marks that were out of focus on one slide. The resulting standard deviation was 0.08° which is well below the expected deviation of landmark measurements. Therefore, the fiducials were only measured once in each frame and four repetitions of the two iris landmarks brought the total number of points to 10 per frame. The majority of the data is in this format and was analyzed using the FILM10 computer program.

Because the film frames are positioned in a set manner, it is possible to calculate the translation of the head with respect to the camera by comparing the coordinates of the fiducial marks of the measurement frame with the coordinates of the fiducials in the control (no stimulation) frames. The rotation of the head with respect to the camera can be calculated by comparing the angle (arc tan (slope)) of the line determined by the fiducials in the measurement frame to the control frame. Similarly, the ocular counterrolling can be determined from the angle between the eye landmark points and the fiducial points with 0° OCR being the angle measured in the control frames.

There are two output files from the FILM10 program. The first file (*.ANG) contains the head translation and rotation data, four individual eye angles (angle of eye landmarks with respect to fiducials), average eye angle and standard deviation. The second output file (*.PLT) is used for the plotter and contains only the frame number, averaged eye angles, and standard deviation.

The program BYPLOT is used to take *.PLT data and plot the average OCR data obtained by subtracting the average of the two control frame eye angles from all subsequent data. This program also needs to know the number of frames in the data file (for axis scaling) which can be obtained from the CNVRT program by dividing the number of lines converted by two.

The sinusoidal data was analyzed by an FFT program in SPARTA. This program dakes a data file consisting solely of OCR values. The program PLTOFT takes the *.PLT file and returns a TEMP2.DAT file which has only OCR angles. One must be careful because some data frames were not analyzable due to momentary flash failure, eye blink or momentary shifts of gaze fixation. The FFT program will not recognize this anomaly. After taking the FFT of the OCR data, the phase and magnitude plots were obtained using SPARTA. FFTanalysis of the acceleration data during the dynamic sled testing showed an essentially flat frequency response (less than 1.5 dB change in amplitude ratio from 0.1 to 1.0 Hz). The camera was started at a predetermined point in the acceleration profile for every run. For these reasons, FFTs of the acceleration data were not performed. The amplitude ratio of the Bode plot was determined by first scaling the OCR up by a factor of 1,000 before taking the FFT. The Fourier Gain (of the fundamental frequency) was then compared to a reference OCR value. This reference value was computed by using 1000 x the average value of OCR for each subject at the appropriate static tilt angle. For example, $\pm$ 0.2 g of lateral acceleration rotates the GIF about 2 x arctan(0.2) = 22.6°. So for most of the sinusoidal runs, the static OCR at 20° left and right tilt were averaged. For subject 14 who was stimulated at 0.1, 0.2, and 0.3 g, the reference values were taken from the 10, 20, and 30° average static OCR values.

The nonlinearities were investigated by analyzing amplitude dependence of the sinusoidal response function (at one frequency) and the step response. Also for the sinusoidal data, the low harmonics of the

fundamental frequency were computed in terms of the percent of the fundamental frequency.

CHAPTER 4

RESULTS

4.1 Data Precision

To interpret and evaluate the significance of the OCR results , it is necessary to have some feeling for the general resolution of the results.

The standard deviation of the mean of four repetitions of the measurements of each frame was used as a measure of the resolution of the data. Most investigators have published data with a resolution of about 1°. Miller (1962) achieved a resolution of between 5 and 15 minutes of arc (mean standard deviation, 9.2 minutes of arc). Diamond et al (1979) published practical accuracies of 15 to 30 minutes of arc. Both of these studies employed biteboards to fix subject's heads and used superposition and alignment of two photographic frames. The mean value of the standard deviation of the measurements done in this study was 12 minutes of arc with a range of 1 to 30 minutes of arc. Occasionally, a data point mean would have an excessive standard deviation. In these few cases (3), examination of the raw data indicated one "wild" point. This point was discarded and only three repetitions were used to calculate these means.

The fiducial marks were very easy to detect. After a trial experiment using very out of focus marks, the standard deviation of nine

measurements was about 5 minutes of arc. This is a worst case and consequently only one measurement/frame of each fiducial mark was made.

4.2 Analysis of Head Motion

The data analysis yielded not only OCR values, but also head translation and rotation with respect to the camera mount. Average values of head translation were in the range of 0 - 5 mm with the maximum head translation being about 1.2 mm for the lateral (y-axis) and about 0.8 mm for the vertical (z-axis). Average head rotations were on the order of 0.5° with a maximum of up to 1.0° during peak jerk periods.

A double analytical differentiation was done on the head rotation data to approximate the roll angular acceleration of the head. The process is noisy at best, so the results must be interpreted with caution. At times, the roll acceleration was above semicircular canal threshold, occasionally reaching values of up to 15 to 20°/s^2. It must be remembered, however, that the maximum roll was less than 1°, so that the duration of the acceleration was very short and occurred during the deceleration phase of the step stimulus.

Analysis of the data showed that the rotation was produced by torso movement with the top of the head acting as a pivot, instead of by pure inertial forces acting on the head. Thus, it might be possible that the OCR observed (usually 2 to 4°) during the step

acceleration profiles might be due solely or in part to semicircular canal stimulation by the slight head rotation. That this is not the case is shown by the following argument. As the subject is accelerated from left to right, the inertial force on the otolith will approximate a left ear down tilt. However, the actual head rotation (of about 1°) is right ear down, because of the effective pivot at the top of the head, so that the net effect of semicircular canal induced compensatory OCR is to subtract from the OCR produced by the otoliths in response to the change in gravitoinertial force.

Melvill Jones (personal communication) observed almost fully compensatory OCR for small, high frequency (greater than 0.25 Hz) oscillations around the vertical. Petrov and Zenkin (1973) also observed compensatory OCR during smooth head tilts of about ±40° both with and without visual cues. In the dark, with only a dim light to fixate, the OCR movements were smooth with a position gain (eye roll/head roll) of about 0.5 (see Figure 2.7). In the light, the gain was larger and roll saccades were present.

Results similar to these have been reported for humans undergoing yaw rotation. In the light, the gain (slow phase eye velocity/head velocity) is about unity. In the dark, the gain drops to about 0.6.

The above discussion was presented in an attempt to justify a correction factor for slight head rotation. From Petrov and Zenkin's data, it appears that a correction of one half of the head rotation

(added algebraically) is reasonable. This correction has been added to all the OCR data. The subject's head rotation was determined by using the rotation of fiducial marks attached to the bite board with respect to the camera.

STATIC OCR GAINS

SUBJECT	AGE	GAIN
0	24	0.13
3	34	0.14
6	27	0.17
7	42	
left ear down		0.28
right ear down		0.01
8	35	0.26
12	30	0.20
14	29	
left ear down		0.17
right ear down		0.08

Table 4.1. This table lists the static OCR gains of the seven subjects and their ages. The gains were calculated by eye roll/head roll at 30° of tilt (left and right). Two subjects (7 and 14) showed large asymmetries. For these cases, two gain figures are listed.

4.3 OCR Data

The entire collection of graphs of OCR data is available in Appendix D. Selected samples are reproduced in Chapters 4 and 5.

4.3.1 Static OCR

Figures D.1 to D.7 are the plots of static OCR versus left and right head tilt. Table 4.1 lists the static OCR gains (eye roll/head roll) which were calculated by taking the slope of the best fit lines through the data of figures D.1 to D.7. The data of subjects 7 and 14 show a large asymmetry. In both cases, the OCR recorded during right ear down is substantially less than that recorded during left ear down. In fact, there appears to be a saturation at about 20° of tilt. One other intersting aspect of these data is that in both cases, the amount of OCR elicited by a left ear down tilt of 30° is much greater than would be expected of a system with a gain of about 0.1. Subject 7 reached 8° of OCR for 30° of left ear down tilt. Two apparently normal subjects (8 and 12) recorded up to 7° of OCR for 30° of tilt. The other subjects' OCR values were lower, reaching about 4-5° or OCR for 30° of head tilt.

The static OCR data of subject 3 indicated some anomaly during right ear down tilt. For 10° and 20° of right ear down tilt, virtually no OCR or OCR in the inappropriate direction was recorded. However, at 30° of tilt, the OCR appeared to be "normal", i.e. about the same amplitude as that observed during 30° left ear down.

The results of the otoneurology examination indicated some loss of left ear auditory function in subject 7. Caloric testing on both subjects 3 and 7 indicated reduced nystagmus during left ear stimulation. The results of the examination on subject 14 showed nothing abnormal. However, caloric testing was not done on this subject.

The asymmetries in the data of subjects 7 and 14 will be important in analyzing the dynamic data and will be discussed in more detail in Chapter 5.

Diamond et al (1979) have indicated a greater amount of OCR during right ear down tilt, although they discuss earler papers that sometimes contradict this statement. The data of this study, while testing OCR for a maximum of 30° of tilt, show generally symmetric or possibly greater OCR (in the right eye) induced by left ear down. In fact, only one of seven subjects (subject 0) showed a greater OCR due to right ear down tilt.

4.3.2 Step Acceleration Response

Figures D.8 to D.34 are the plots of OCR (corrected for semicircular canal effects due to head rotation) versus time induced by step accelerations of various amplitudes. Figures 4.1 and 4.2 show typical responses to acceleration profiles. These figures also show the OCR data before correction (O) to indicate the generally small effect of head roll. The mean of four measurements on one film frame is

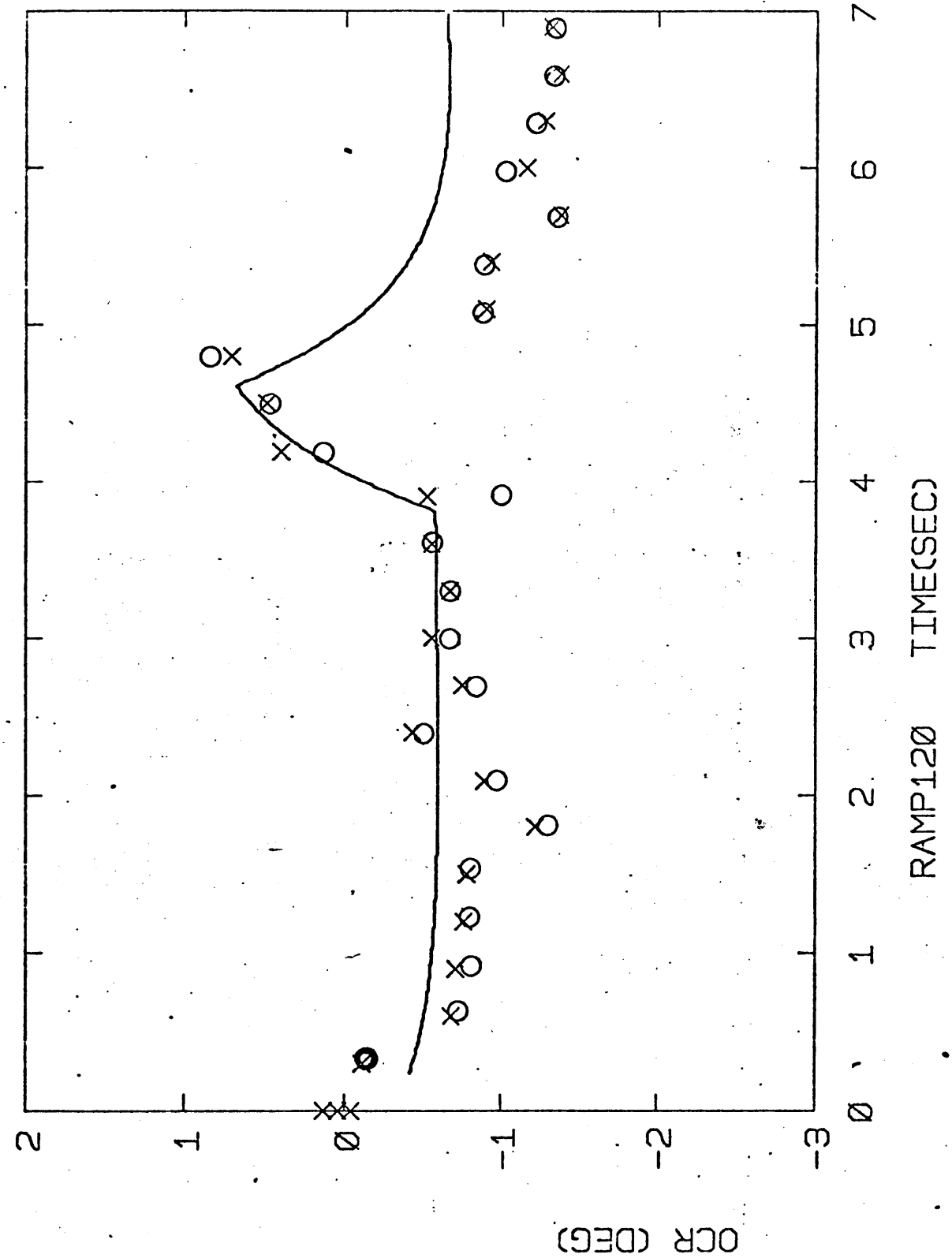

Figure 4.1 OCR step response of subject 12, 0.05g

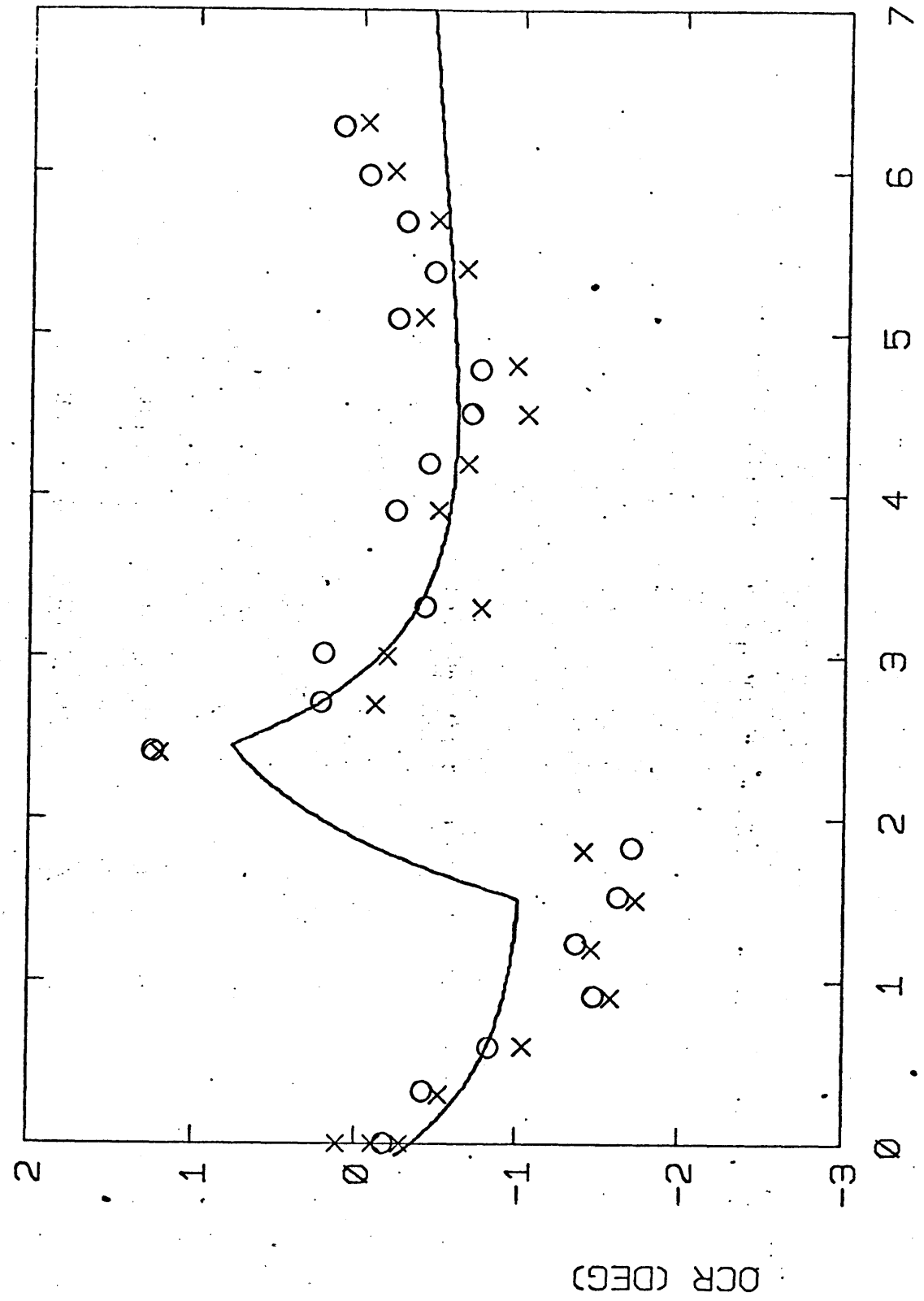

Figure 4.2 OCR step response of subject 12, 0.2g

plotted as an (0) for raw data and an (x) for corrected data. Because the standard deviations were low (12 minutes of arc average), they are not shown. The data in Appendix D indicates only the mean values of corrected OCR. The convention used in this thesis is that positive OCR is compensatory OCR produced by left ear down tilt.

The predictions of the Young-Meiry dynamic otolith model for the appropriate acceleration profile is overlaid on the OCR data. This prediction was scaled to fit one subject's OCR response and that scale factor was used in all plots.

Several observations can be made concerning the OCR induced by step accelerations. During subject O's runs, there appeared to be an initial lag of OCR, followed by a rapid build-up; however, the decline of OCR after the subject stopped appears to follow the model predictions. One interesting anomaly was noted; during the 0.1 g run, the OCR started out in the wrong direction, but soon reversed direction and appeared to react normally to the deceleration phase. The return of the OCR to the initial baseline looked quite good in this subject's data.

Subject 3 showed some very puzzling results. The OCR data from the 0.05 and 0.2 g runs look very similar and reasonable, but apparently are in the wrong direction. The two other runs show correct OCR direction,

but very poor fits with the model predictions. During the 0.3 g run, the camera moved, so that interpretation of the data is impossible.

Subject 6 showed about the best correlation between the data and the model, with one exception: the OCR produced by the 0.3 g acceleration was approximately twice as large as that predicted by the model.

Subject 7 showed a large reduction in OCR induced by right ear down as compared to left ear down tilt. The results of the step accelerations are somewhat difficult to interpret. For 0.05 g acceleration (initially right ear down), one sees about 1° of peak OCR, but no large change during deceleration, which would be as expected. With a 0.1 g left ear down stimulus, there is only slight OCR, but with a 0.35 g right ear down deceleration, there is no return to baseline (consistent with static OCR data). The most puzzling observation is that the 0.2 g stimulus (initially right ear down) produces a "normal" OCR response. One possible explanation is that there is residual left otolith function (corroborated by a reduced but non-zero gain during right ear down tilt). Both accelerations producing initial left ear down stimuli (0.1 and 0.3 g) show the effect of diminished left otolith function, because the OCR data doesn't show the characteristic return to baseline. There is no indication how long this elevated OCR lasts; if it were to continue for 30 seconds (time between runs), this might help explain the 0.2 g data. Since the runs alternate in direction and the 0.2 g run followed the 0.1 g run, it might be that the decrease in OCR seen at the begining of the 0.2 g run was due primarily to a return to baseline effect with the subsequent deceleration producing the appropriate response.

Subject 8's OCR data show a fast rise during acceleration with a slower then predicted return to baseline after deceleration. However, the peak amplitudes correlated well with the predicted amplitudes.

Subject 12's OCR data also show reasonable correlation with the model. However, there is a predominant negative DC bias at the end of several runs in different directions. The static OCR indicates a slight asymmetry favoring positive OCR (left ear down tilt), so the observation is difficult to explain.

Subject 14 was used to examine any habituation or time dependent non-linearities. Three runs were made, all at 0.15 g, with one minute waiting periods between runs. No statistically significant difference was seen between the peak to peak amplitudes of the three runs. This shows that no habituation is apparent.

4.3.3 Sinusoidal OCR Response

The sinusoidal data is presented in two forms. All the data is shown in Figures D.35 to D.55. In these plots, the raw data (corrected for semicircular canal effects induced by head roll) is presented. The idealized sinusoidal input acceleration (phase shifted approximately) was overlaid on the data. No amplitude scaling was done. Selected plots are shown in Figures 4.3 to 4.5. These plots show both the raw and corrected OCR data and again indicate the small effects of head movement. In a few cases (SINE 141, 142, 143, 02, 82), there was a noticeable DC drift associated with the sinusoidal OCR response. In these cases, the average drift was clearly

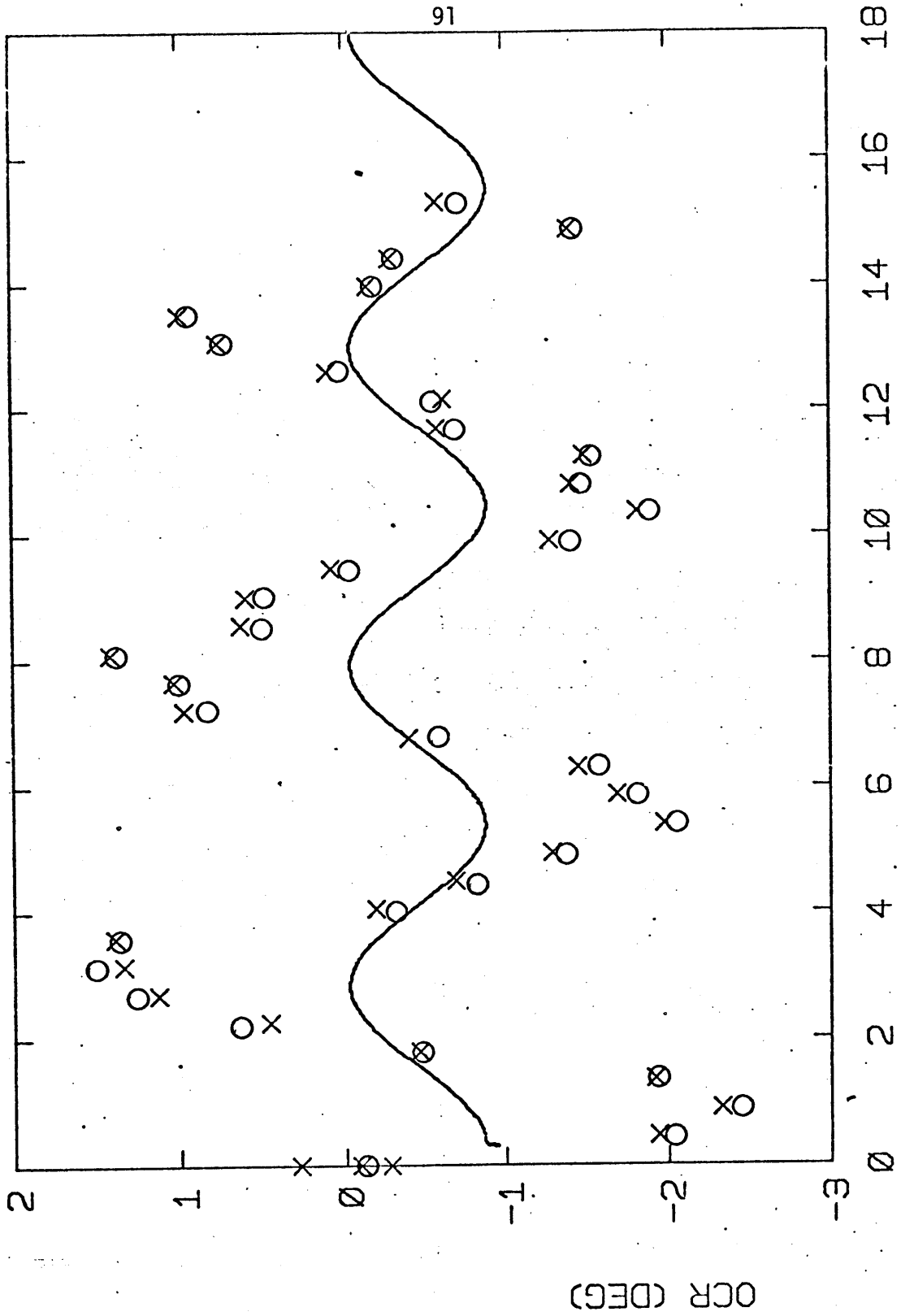

Figure 4.3 Sinusoidal response at 0.2 Hz

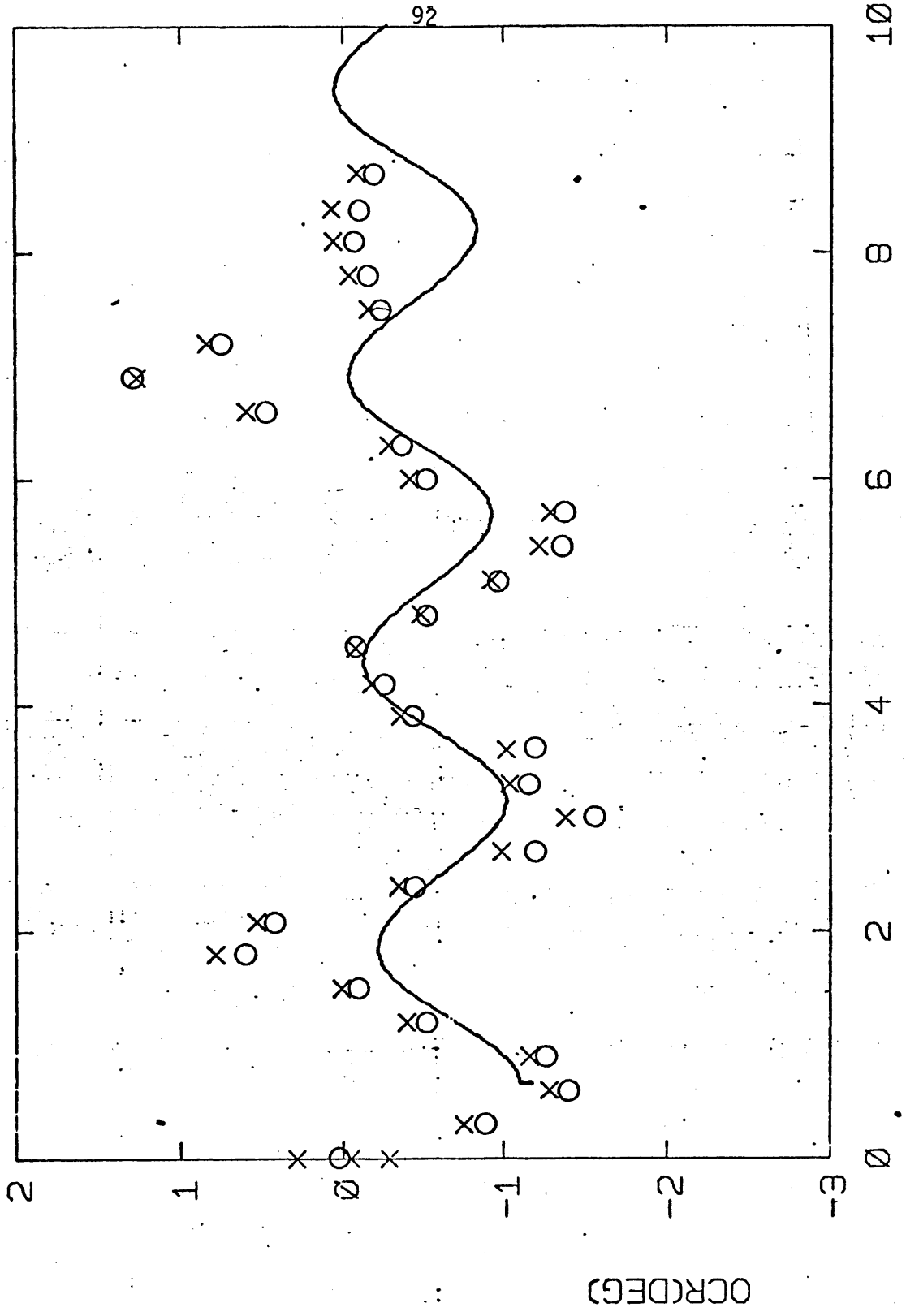

Figure 4.4 Sinusoidal Response at 0.4 Hz

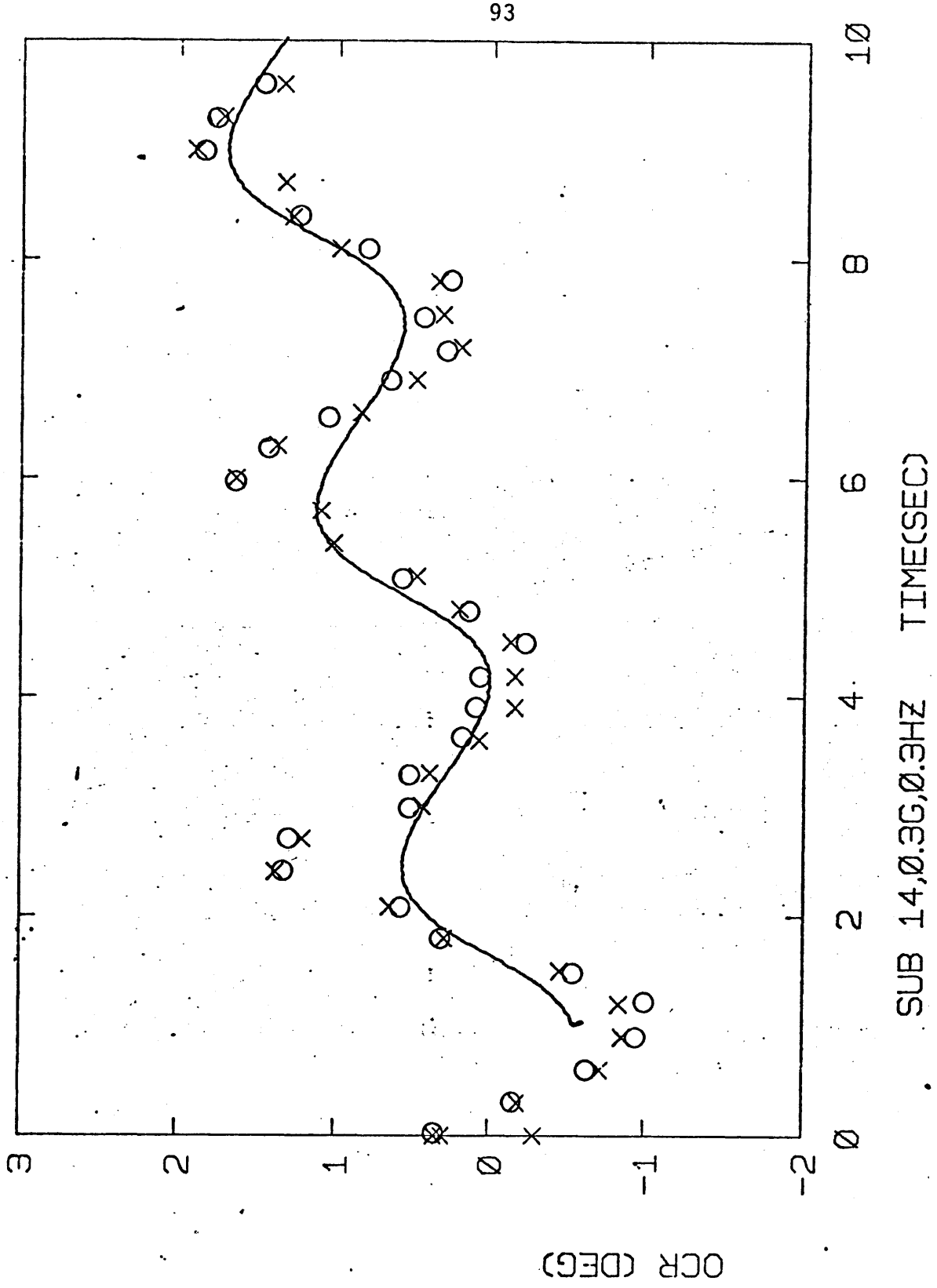

Figure 4.5 Sinusoidal response at 0.3 Hz

seen with the help of the overlay. In the case of subject 14, the bias is positive which is supported by the static OCR data indicating higher gain for positive OCR than for negative OCR. The data of subject 0 (0.2 Hz) show a negative OCR offset, but a positive slope of this offset; the data of subject 8 (0.2 Hz) shows a slight positive bias, neither of which are indicated in the static gains. Subject 7's data is somewhat puzzling again because there is a slight negative bias (for the 0.4 and 1.0 Hz stimulation) not in agreement with a reduced static gain for negative OCR. Subject 3 showed very erratic sinusoidal OCR which is difficult to explain, but this erratic behavior was also seen in the step acceleration data as well as the static data. The rest of the data looked very good. However, all the data at 1.0 Hz was somewhat more difficult to analyze subjectively because of the low (3 Hz) sampling rate and relatively high frequency. The stimulus overlay provided much help in recognizing the sinusoidal nature of the data in all subjects except SIN121.

4.3.3.1 Bode Plot, Linearity and Stationarity Data

Figure 4.6 shows the Bode plot obtained from the sinusoidal data. The circles with vertical bars ($\pm$ one S.D.) correspond to the data obtained in this study. The vertical bars indicate the range of data from Kellogg (1967) (both gain and phase). The solid line indicates the predictions of the Hannen model (which was based on the Kellogg data). For the phase portion, two lines are drawn, one corresponds to zero time delay (top line) and the second corresponds to 400 msec of time delay.

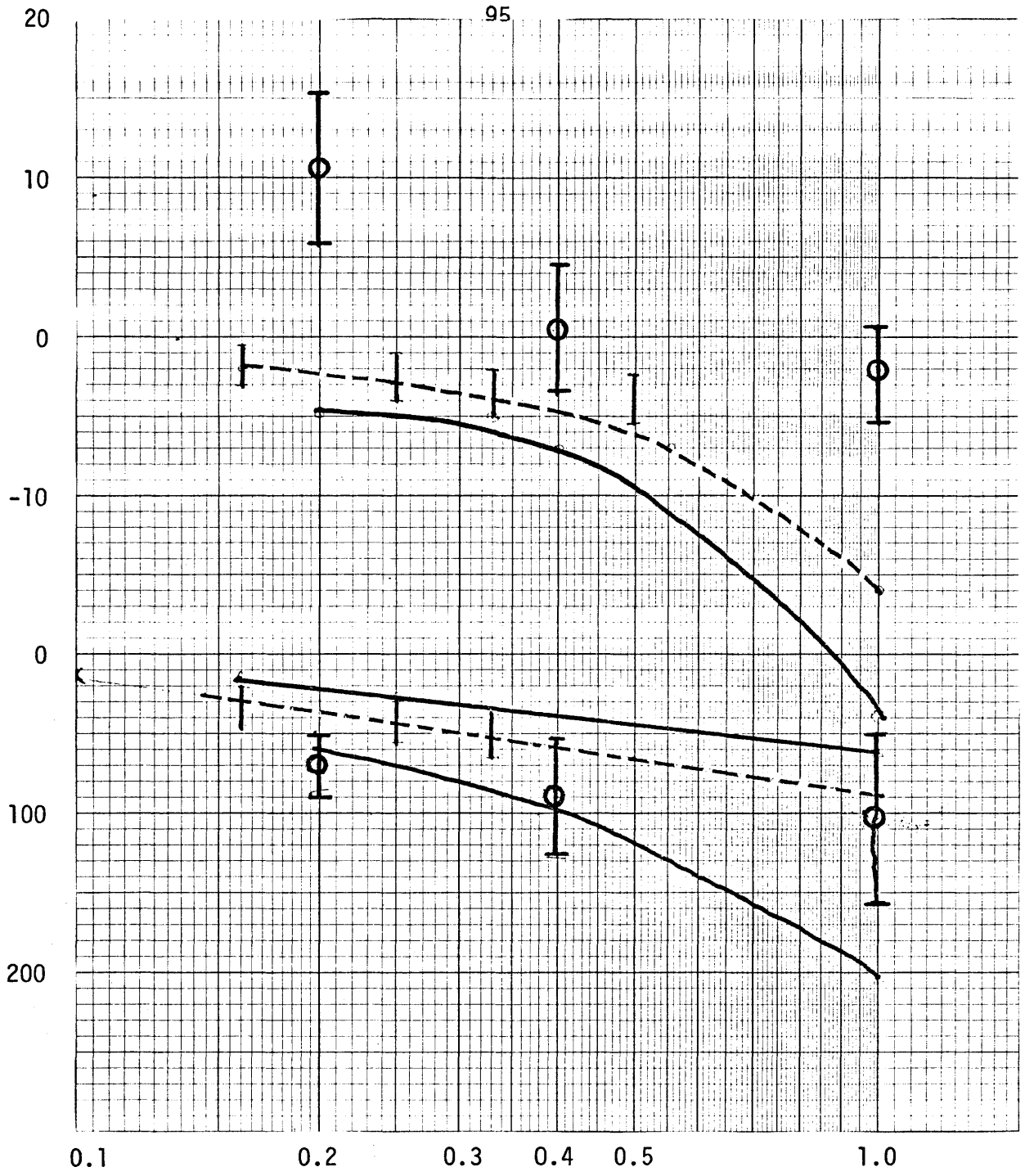

Figure 4.6 Bode plot of OCR data and models. The circles with vertical lines indicate the data of this thesis (mean ± S.D.). The vertical lines with no circles or end caps indicate the range of data from Kellogg. The dashed lines are the results of the Young-Meiry model and the solid lines are the results of the Hannen model. The upper line of the two phase lag predictions was computed with zero time delay; the lower line incorporates a 400 msec time delay.

The dashed lines are the predictions of the Young-Meiry model. As discussed earlier, it is impossible to formulate a model based on three data points, but the degree of correlation between the model and the data can be shown.

Table 4.2 lists the second and third harmonic components of the FFT gain values in terms of percent of the fundamental frequency.

Table 4.2 Non-linearities in OCR sinusoidal response, indicated by the relative contribution of the second and third harmonics in percent of the fundamental harmonic

	0.2 Hz		0.4 Hz	
SUBJECT	SECOND	THIRD	SECOND	THIRD
0	32	46	15	32
3	8	31	3	19
6	45	18	66	45
7	12	5	29	16
8	19	13	25	48
12	9	7	22	6

Table 4.3 shows the non-linearity properties of the sinusoidal OCR response as a function of amplitude for one subject. The acceleration profiles were 0.1, 0.2 and 0.3 g, all at 0.3 Hz.

Table 4.3 Non-linearity properties of the sinusoidal OCR response

ACCEL.	AR (dB)	PHASE (°)	HARMONICS (% OF FUNDAMENTAL) SECOND	THIRD
0.1 g	15.35	-106.72	25	21
0.2 g	10.96	- 92.66	12	17
0.3 g	13.33	- 92.83	6	9

The final check of non-linearity was done by recording 80 seconds of sinusoidal data at 0.2 g, 0.2 Hz and then comparing the FFT's of the first 14 seconds and the last 14 seconds. The phases of the two records are identical and the gain change amounted to -0.23 dB from beginning to end.

CHAPTER 5

DISCUSSION

5.1 Step Response

The OCR response to a step input of acceleration was analyzed in several ways. First, an overlay of the Young-Meiry dynamic otolith model (solid line in step acceleration plots) was made with no attempt to "tune" the model. These predictions, in most cases, follow the form of the OCR data, but there were only a few graphs where the fit could be called good. To attempt to fit models to the observed data, a simpler model developed by Hannen et al (1966) incorporating a first order lag and pure time delay was used. The largest step change in acceleration occurred during the transition from acceleration to deceleration. This section of the OCR data most approximated an exponential and so was used to get the individual time constants of each subject at each acceleration level. There were several cases where the OCR response did not come close to approximating an exponential function. In these cases, no analysis was done.

Hannen's model is

$$G(s) = ke^{-as}/(s + \beta) \qquad (5.1)$$

with a, the time delay, ranging from 0 to 400 msec, and $\beta = 3.14$. Table 5.1 shows the values of $1/\tau$ for all analyzable data with the mean and 95% confidence limits for each subject and the value obtained

TABLE 5.1

The reciprocals of the mean (of each subject) experimentally determined time constants are listed with 95% confidence limits. Also included is the mean of the means and its 95% confidence limit.

Subject	$1/\tau$ ± 95% confidence
0	4.68 ± 2.78 sec^{-1}
3	5.54 ± 7.01
6	1.76 ± 0.14
8	4.22 ± 2.89
12	0.49 ± 0.72
14	1.68 (only value obtained)
Grand mean	3.25 ± 2.66

by averaging the averages. The value of the overall average is 3.25 which is surprisingly close to Hannen's value of 3.14, although the confidence limits are wide. From the data, it is obvious that there is an inherent variability among subjects as well as variability within each subject.

The step response data had several other features of interest. The peak to peak OCR that was observed in the data was well fit by a scaled version of the Young-Meiry model. At times, the experimental data differed from the predictions, but, over a range of subjects and amplitudes, the peak values of the OCR data due to the differing step acceleration levels were linearly related to the acceleration level.

A linear regression program was used to relate the maximum amplitude of OCR during acceleration to the stimulus amplitude. The average maximum values of OCR (over the subjects that showed no anomalies in OCR) at each acceleration level was related to the predicted OCR by

$$\text{predicted OCR} = 0.56\ (\text{actual OCR}) = 0.22 \qquad (5.2)$$

with a regression coefficient of 0.93. The predicted OCR (from the Young and Meiry model) was used instead of g level because of the transient nature of the investigation. In other words, the predicted value of OCR due to 0.2 g step acceleration was 1.2°, while the predicted value of OCR due to 0.3 g step acceleration was 1.3°. These values differ only slightly (although there is a 50 percent change in stimulus

level) because the time duration of the 0.2 g stimulus was substantially longer than the 0.3 g stimulus. Therefore, the OCR response had more time to develop for the 0.2g run. This observation has practical importance for the Space Sled experiments because the sled can only generate 0.2 g maximum. The predicted OCR at this acceleration, however, is only 10 percent lower than that predicted at 0.3 g. One must also remember that the Young-Meiry model was scaled for one subject and that scale factor was then used for all other subjects. If one were to rescale the model for each subject, the results would be even better.

The model of Young and Meiry predicts an overshoot of both perceived acceleration with a long time constant of about 5 seconds (Figure 2.12). This result appears compatible with the data of this thesis and also observations by Diamond et al (1979), in the sense that there appears to be an initially increased OCR response due to a step acceleration input. The data of this thesis cannot fully confirm the notion of an overshoot, but the problem lies in track length and amount of stimulus time, not in data contradictions. For the 0.05 g stimulus (lowest amplitude and longest duration), the duration was about 3.5 seconds, which is just on the edge of detecting the overshoot. In fact, observation of the 0.05 g data indicates a slight overshoot, but due to the low amplitude it is difficult to make any strong statements. Diamond et al (1979) reported that the OCR in response to a step change in tilt appeared to reach a peak before declining to a steady state value, but gave no figures. All other OCR investigators have usually waited 30 seconds to one minute before recording

OCR after a step change in head tilt to allow semicircular canal effects to die out.

The return of OCR to the before-stimulus levels appeared to be erratic. Some subjects indicated an overshoot (subject 12), others showed an undershoot (subject 8). Sometimes the data from a subject (for example, subject 12 (0.05, 0.2, 0.3 g)) showed a DC bias (in the same direction) after stimuli of different polarity, indicating a possible directional preponderance although no substantiating evidence was available from the static OCR data. Subject 0 showed initial anti-compensatory OCR during one run (0.05 g), but then showed a large jump to the appropriate direction. Subject 3's data indicated several anomalies (irregular OCR, inappropriate direction), which is also indicated in the static OCR curves. For this subject, there is the possibility of a stiction effect during right head tilt, i.e. the OCR produced by 10° and 20° of head tilt was minimal, but 30° of tilt produced a normal OCR response (symmetric to left head tilt at 30°). Both the step and sinusoidal OCR data of subject 3 is erratic. Subject 7 showed a marked asymmetry in static OCR and an erratic step response. One possible explanation for the dynamic behavior (especially the apparently correct response during 0.2 g step stimulus) is a slow return to baseline. In this case, if the control baseline for the 0.2 g run were elevated, the effect of the initial acceleration would be to return it to about zero. Then, during deceleration (equivalent to left head tilt), a 'normal' response would be obtained. In general, however, subject 7's data did not show the large OCR changes during accelerations equivalent

to right ear down tilt. The data from Subject 8 indicated a faster than predicted rise in OCR during acceleration, but a slower than predicted decline to zero at the end of the stimulus. If indeed OCR is partly influenced by perception of orientation, a relatively long lasting acceleration could be interpreted as a change of tilt whereas a very short deceleration could be interpreted as a jolt around a tilted position (models from Ormsby (1974) also predict this effect). If this were the situation, then one could predict a slower than average return to zero, but the quicker than average rise time is hard to reconcile.

The data of Diamond et al (1979) indicate two types of directional preponderance. First, right ear down tilt seems to produce larger OCR values (either eye) than the comparable amount of left ear down tilt. In addition, the downward eye appears to indicate slightly more OCR than the upward eye for a given tilt condition (left or right). Miller (1962) and Hannen (1966) both noticed some asymmetry between eyes and the direction of tilt, but did not quantify it. The data of this thesis was taken solely on the right eye. For this case, one would expect to see a directional preponderance for right ear down tilt (both above-mentioned effects would be cumulative). It is difficult to make a conclusive statement from the present study. However, one subject (14) was tested three times at 0.15 g step acceleration . After analysis of the static OCR response, a reduced gain was seen in this subject for right ear down tilt. For this reason it is impossible to draw any conclusions from this data on the subject of directional

preponderance. In contrast, the majority of the sinusoidal OCR. runs indicate some negative offset (equivalent to a predominant right ear down OCR) which would tend to support Diamond's data.

5.2 Sinusoidal Response

The sinusoidal data was analyzed through an FFT routine which produced Fourier coefficients and phases of the fundamental and higher frequencies. The reference values used to determine the gains were obtained from the mean of the appropriate left and right head tilt static OCR. All runs, except those for subject 14, were made at 0.2 g, so that the peak to peak amplitude of the OCR should correspond closely to the OCR recorded at 20° of head tilt. For subject 14, 0.1, 0.2, and 0.3 g runs were made, all at 0.3 Hz; these peak to peak OCR values should correspond approximately to static OCR values recorded at 10, 20 and 30° Of head tilt. The OCR values that were entered into the FFT program had to be integers, so a scale factor of 1000 was used. The static OCR values (in degrees) were also multiplied by 1000, so that they could be compared with the Fourier coefficients. In this manner, if the peak to peak amplitude of dynamic OCR was the same as the static OCR corresponding to the appropriate tilt angle, the amplitude ratio (AR) should be 0 db. The gains and phases were used to produce the Bode plot shown in Figure 4.6. This figure shows the data of this thesis indicated by a circle (mean) and vertical bar ($\pm$ one S.D.). The data of Hannen et al (1966) is also plotted as a vertical bar (indicating the range of their data). In addition, the Hannen

model prediction is shown as one solid line for gain and two solid lines for the phase prediction - the upper line indicates 0 time delay and the lower line indicates a time delay of 400 msec. The Young and Meiry model is also shown using dashed lines to denote the values produced by this model. Inspection of the Bode plot indicates that the amplitude ratio for many of the subjects is greater than zero, especially at the lower frequencies (0.2 and 0.4 Hz). This indicates that there might be some additional dynamic otolith component to OCR. As discussed in Chapter 2, several investigators (Diamond et al, 1979; Baarsma and Collewijn, 1975) have reported a possible overshoot of OCR during a step change in linear acceleration.

The expected variability among subjects is evident in both gain and phase. The amplitude ratios do not appear to drop off at higher frequencies as fast as the models. This observation was also noted by Young and Meiry (1968) when they compared their model with the dynamic OCR data recorded by Kellogg (1967). In fact, Kellogg's data appears to show a 3-6 db rolloff between 0.05 and 0.5. The Hannen model (based on Kellogg's data) predicts about 21 dB rolloff over 0.2 to 1.0 Hz. The Benson and Barnes model (1970) discussed in section 5.5, predicts about 13 dB rolloff between 0.2 and 1.0 Hz . The data of this study show rolloffs of from 9 to 18 dB over this frequency range which tends to support the models. Also, the data of this study generally show greater phase lag than the Kellogg data when compared at the same frequency. Several authors have reported some gravity dependent effects on the semicircular canals. If this phenomenon were indeed

present, it could well explain the smaller phase lag and slower rolloff of the Kellogg data, since a constant horizontal rotation about the line of sight was used by Kellogg to generate a sinusoidal input to the otoliths. The phase data show substantially more phase lag at 1.0 Hz than would be predicted by the Young-Meiry model. The Hannen model, however, with bounds on the time delay of 0 and 400 msec, brackets this data.

As discussed earlier, the results of Diamond et al (1979) showed a directional preponderance for right ear down tilt. The results of the Fourier analysis of this thesis show farily large (6-48%) contributions of the third harmonic which would be evidence for a directional preponderance. In addition, the data of Hannen et al (1966) also showed a large (about 20%) contribution of the second and third harmonics to the total dynamic OCR data. The presence of a second harmonic would tend to make the OCR peak more rapidly than a pure sinusoid which is certainly evidenced in the static OCR data (peaks usually occur between 60-75° of head tilt).

5.3 Amplitude Linearity and Stationarity

The investigation of amplitude linearity showed that for at least one subject, the amplitude ratio of the OCR system varied only 4.5 dB during a range of 0.1 to 0.3 g with the peak AR occurring at 0.1 g, but no obvious trend. The results of the step response also showed a linear relationship between actual and predicted OCR as a function of acceleration level.

The stationarity of the OCR data was investigated by examining the amplitude ratio and phase of the signal at the beginning and end of an 80 second record length. The amplitude ratio changed by -0.23 dB and there was no change in phase. From this result, it can be concluded that there is very little change between the beginning and the end of a record.

5.4 Influence of Perception on OCR

Until recently, most eye movements were thought to be reflexive in nature. Current results indicate that a subject's eye movements can be correlated with sensation of self motion. The results of Petrov and Zenkin (1973) (indicating reduced OCR velocity gain and greater OCR magnitude in the dark) tend to support the notion that perception also plays a part in OCR movements. The results of yet unpublished experiments with the author as subject have demonstrated that (1) the OCR system is "plastic" and (2) that OCR can depend on a subject's perception of motion. In the first case, after four hours of wearing dove prism glasses which reverse left-right, and also produce, for example, a 90° right visual roll for 45° of right head roll, the OCR gain had actually changed sign (although the magnitude of the final gain was small). In the second case, the subject was viewing a rotating disc designed to induce roll vection. OCR was being observed simultaneously. During periods of roll vection, both with the subject seated upright and prone on the floor, large OCR nystagmus was detectable, but during periods of "drop out" (which can be controlled to an

extent by the subject), no OCR nystagmus was detected. These experiment are preliminary, but do lend support to the notion that perception can influence eye movements. On the other hand, the data of Finke and Held (1978) suggest that the static component of OCR is reduced when the subject experiences a state of self rotation. The problems of OCR nystagmus and the difficulty in recording high frequency OCR movements have kept this subject from being fully explored experimentally.

5.5 Influence of Magnitude of Gravitoinertial Force on OCR

Several varied experimental results indicate that the utricles and saccules are an integral unit. Miller (1962) has proposed a model to relate static OCR to head tilt which incorporates both the utricles and saccules. Corriea et al (1965) have examined much data on perception of body orientation and OCR along with their own data, and have shown that shear force alone on the utricle is not sufficient to predict the experimental results. They showed that modulation of the "compressive" z-axis force without changing the y-axis component can indeed alter a subject's perceived vertical when that subject is tilted. They claim, however, that when the subject is upright, changes in the z axis component of force do not alter the perception of vertical. Since the utricles and saccules are to a first approximation roughly perpendicular, shear force on the utricles is compressive (or tractive) force on the saccules and vice versa. It is therefore difficult to separate these two components when attempting to relate these forces to OCR. The hypergravic data of several

investigations (Woellner and Graybiel, 1959; Miller and Graybiel, 1971) indicate that the OCR can be linearly related not only to shear force on the utricle but also to total magnitude of applied force. An early attempt to incorporate "compressive" as well as shear forces into a model was made by Benson and Barnes (1973).

This model is discussed in Chapter 2, but for a reminder, they postulated that compressive forces on the utricle could be a stimulus when coupled with a shear force. They formulated a mathematical model and went on to show that the model predictions of otoconial displacement correlated reasonably well with observed eye movements for several different experimental protocols. They did not address OCR movements in their paper. After calculating the predicted otoconial displacement from their model for a head tilt of 90°, a striking similarity was found to the static OCR curves (Figure 5.1). Both model and data reach peak values at tilt angles between 60-75° and not 90° as would be predicted by a purely utricular shear force model. Using the physical values assumed by Barnes and Benson, it is possible to calculate a predicted Bode plot. As discussed earlier, their model predicts about 13 dB of rolloff between 0.2 and 1.0 Hz, while the phase lag goes from 63° to 84° over the same frequency range. This AR change is very close to that observed experimentally although the predicted phase lag increase is much less than that seen experimentally. These predictions, however, depend heavily on some assumptions one makes about the physical parameters of the system. This point will be discussed shortly.

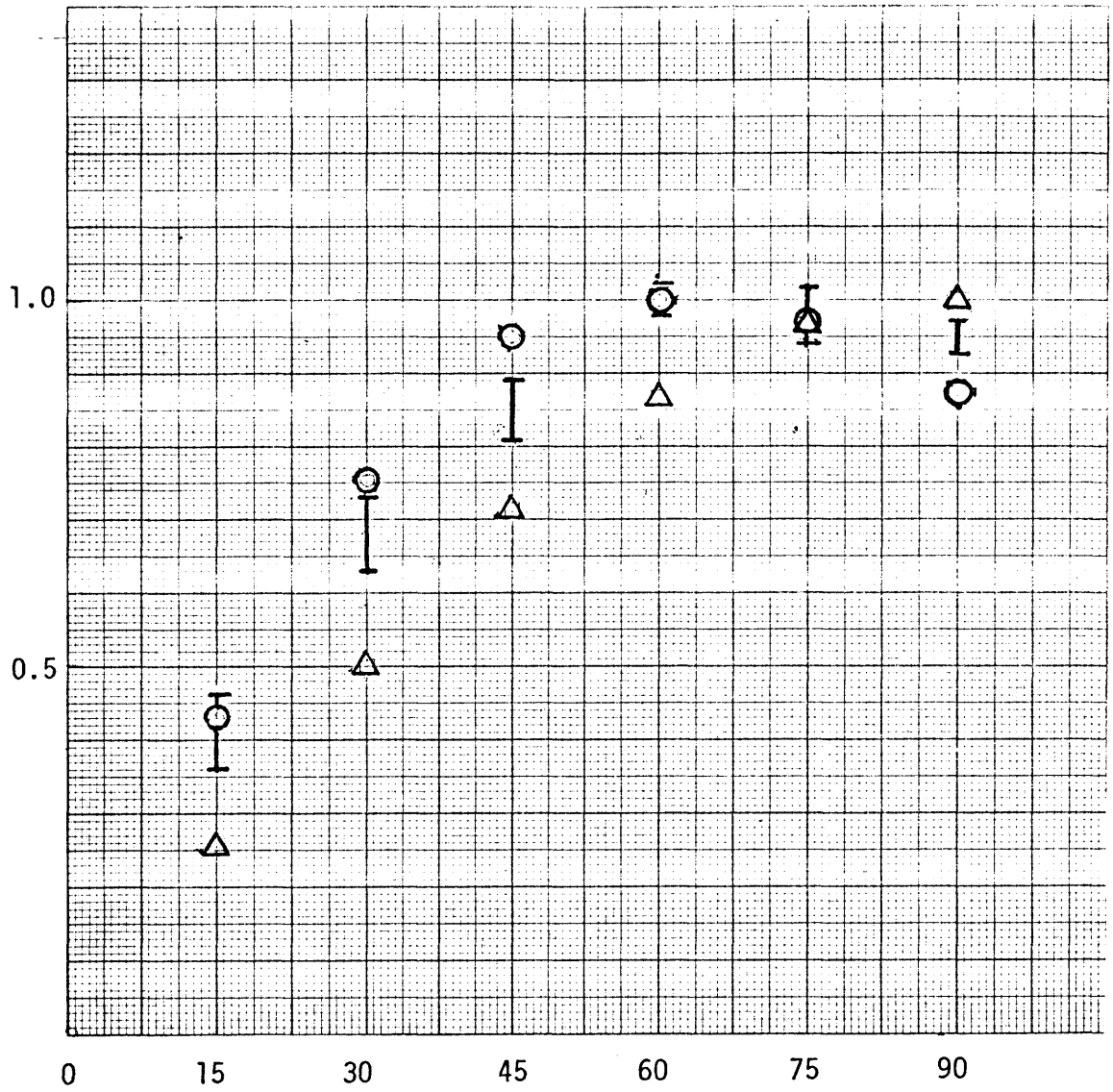

Figure 5.1 Plot of normalized OCR data from Miller (1962), sin (tilt) and normalized otoconial deflection from model of Barnes and Benson. The OCR data is plotted as a vertical line indicating ±1 S.D. The round circles indicate otoconial deflection and the triangles indicate the sin (tilt).

Further analysis of the Barnes and Benson model shows that the predictions for hypergravic and hypogravic (Miller and Graybiel, 1965) stimuli diverge substantially from the experimental data. In these cases, the model predicts a steeper slope of otoconial deflection versus applied force than is shown in the experimental curves of OCR versus applied force. The response curves of first order otolithic afferents of several investigators have shown a saturation effect at high levels of force (Fernandez and Goldberg, 1976c) and at large cilia displacements (Hudspeth and Corey, 1977) (see Figure 2.8).

The model of Benson and Barnes has many problems associated with it, the first and foremost being the experimental evidence of Fernandez and Goldberg (1976b). They show that for single unit recording in the barbiturate anesthetized squirrel monkey, changes in the compressive force at a given shear force do not modulate the firing of first order afferents. Second, several assumptions by Benson and Barnes about the values of physical parameters (mass of otoconia, length of cilia, expected displacement of the otoconial membrane under a 1 g force field) of the otolith organs and derived quantities (natural frequency and damping coefficient) must be treated with caution. For instance, they argue that their predicted damping coefficient of 200 (highly overdamped) is high but not unreasonable. They do not say why it is not unreasonable when in fact deVries argued albeit teleologically that the system should be just critically damped to give the fastes rise tiem with no overshoot. The Young-Meiry model, however, argues for a

lead term which could produce some overshoot even though the mechanical portion might be critically or overdamped.

CHAPTER 6

CONCLUSIONS AND SUGGESTIONS FOR FUTURE WORK

The main conclusion is that transient linear accelerations produce OCR similar to that produced by sinusoidal or static head tilt. However, preliminary evidence suggests that the transient OCR response includes a lead term similar to that proposed in Young and Meiry's dynamic model of the otoliths. This lead produces an initial overshoot of OCR before it reaches steady state. Only the 0.05 g step acceleration profile provided enough stimulus time duration to see the effect. The amplitude of the OCR response however is small at this stimulus level and it is difficult to make a strong statement about the dynamics at this time. Additional evidence for this conclusion is supported by the sinusoidal response data which shows amplitude ratio values (relating sinusoidally stimulated OCR to static OCR for an equivalent change in direction of the gravitoinertial force (GIF) of up to about 12 dB. This result indicates that some enhancement of dynamic OCR is taking place. At least one other investigator (Diamond et al, 1979) has also observed this transient effect although they have not described or quantified it and semicircular canal effects may be a factor in their study.

The step response of OCR was measured and quantified in terms of a first order exponential because of the short stimulus times. The results indicate a large spread between individuals but the grand mean of the individual averages of values of $1/\tau$ (3.25) is very close to the value of

that Hannen et al (1966) calculated. His model is $H(s) = ke^{-\alpha s}/(s + 1/3.14)$

Two models have been proposed for the dynamic otolith-OCR system. Hannen's (1966) model was based on OCR while the Young-Meiry (1968) model was based on subjective perception of acceleration. Hannen's model is a first order exponential with a pure time delay. The Young'Meiry model is a second order otolith dynamics system cascaded with a lead term. Both models fit the OCR data (Bode plot phase values) of Hannen. The experimental data of this thesis shows greater phase lag than the Young-Meiry model at the 3 frequencies (0.2 Hz, 0.4 Hz, and 1.0 Hz) tested. The data of Hannen was recorded while the subject was undergoing steady state roll (thus producing a sinusoidal modulation of the direction of the GIF) which could have included some tonic semicircular canal input. The semicircular canal response, if present, could have acted to reduce the phase lag. Hannen's model incorporated a time delay of between 0 and 400 msec (depending on the subject). The range of phase lags measured during this thesis were consistent with this range of time delays.

The amplitude ratios calculated from the data of this thesis show rolloffs of from 9 to 18 dB over a frequency range of 0.2 Hz to 1.0 Hz. The Young-Meiry model predicts about 12 dB rolloff and the Hannen model about 21 dB rolloff over the same frequency range. The data so far imply that the Young-Meiry model more aptly fits both the OCR system as well as the perception of motion system.

Although the presence of higher order harmonics (obtained by FFT analysis of the sinusoidal response) implies system nonlinearities,

the data suggest that there is amplitude linearity over a range of at least 0.1 to 0.3 g of lateral acceleration. One subject was sinusoidally stimulated at 0.1 to 0.3 g; to determine amplitude linearity. Analysis was done of all subject's step responses (over 0.1 to 0.3 g range) and the fit of the OCR magnitude to the magnitude predicted by an appropriately scaled Young-Meiry model was established by linear regression (regression coefficient = 0.93). Finally, one subject was sinusoidally stimulated for 80 seconds to investigate stationarity. No change in phase and only a -0.23 dB change in amplitude was noted from the first 14 seconds to the last 14 seconds of the record.

6.1 Suggestions for Future Work

The major suggestion for future investigations into the OCR system is to develop a non-invasive, real-time OCR measuring system with a resolution of about 30 minutes of arc. The sampling rate of 3 Hz used during this study was a major drawback for the precision analysis of the OCR step response. The preliminary finding of enhanced transient response should be further investigated. Hopefully, a real time OCR recording device will help in this study but a major change in equipment will be needed to provide the track length necessary to obtain 5 or more seconds of higher (0.3 to 0.5 g) acceleration so that this effect can be better studied.

The effects of perception upon OCR are still not very clear. Conflicting evidence now exists. Some studies (in other axes) indicate that perception of motion can influence eye movements. The only study done so far in OCR indicates that the magnitude of OCR reduced when the

subject perceives self roll vection. This coupling of OCR and roll vection should be more closely investigated. The use of a high resolution, high sampling rate OCR recording devide will be essential due to the presence of roll nystagmus while undergoing roll vection stimulation.

APPENDIX A

Sled Design, Construction and Performance

A-1 Specifications

The sled specifications were taken from the ESA Space Sled specifications wherever possible so that the sled would be a good simulation for the space sled. The "Space Sled System Specification Appendix I" dated October 1977 (ESA, 1977) was used as the guiding document. Briefly, this document sets the sled specifications as follows:

(1) Weight = cart: 100 lb; subject: 200 lb

(2) Vibration: During measurement phases, the superimposed vibration level will be below the following limit curve

Frequency (Hz)	Level (g)
0.5	9.3×10^{-4}
1.0	2.6×10^{-3}
2.0	7.4×10^{-3}
3.0	1.4×10^{-2}
5.0	2.9×10^{-2}
10.0	8.3×10^{-2}
15.0	1.5×10^{-1}
30.0	4.3×10^{-1}

In addition, the settling time will be less than 250 msec and overshoot less than 10%.

(3) Motion Profiles

(a) step acceleration - up to 0.2 g

(b) sinusoidal acceleration - 0.02 to 1.0 Hz up to 0.2 g amplitude

The MIT sled is also capable of producing pseudo-random (sum of sines) stimulus

(4) Track length - The space sled track is about 15 feet long. The MIT track is 21 feet long, so that lower frequencies and higher accelerations may be produced.

A-2 Experimental Justifcation for Specifications

The specifications for the space sled were based both on scientific rationale and physical constraints imposed by the Spacelab module. The normally accepted step acceleration threshold is about 0.005 'g' for the horizontal linear acceleration. For this reason, low frequency vibrations are restricted to less than about 5×10^{-3} g.

Threshold detection experiments have shown that there is a latency time in the detection of acceleration. This latency is a function of the magnitude of the step acceleration, with longer latencies occurring with lower magnitudes until threshold is reached. Melvill Jones and Young (1978) quantified this "detection curve" for vertical acceleration profiles and related it to previous horizontal acceleration studies (Meiry, 1965). The data were fitted with the equation

$$T = B/A + T_{min} \qquad \text{(for } A > 0.005 \text{ g)}$$

where T = mean measured response latency (sec)

A = step acceleration magnitude (g)

T_{min} = reaction time independent of A = 0.37 sec

B = slope of the regression line when plotting T against $1/A$ = 0.022 g-sec = 0.71 ft/sec

(from Melvill Jones and Young, 1978).

Table A.1 shows the time, velocity, and distance traversed prior to detection. This table uses the parameters associated with Meiry's (1965) data; the only change is that the reaction time is increased to 0.76 sec. It is obvious that only short distances are required to successfully detect the acceleration steps.

Table A.1

A(g)	T(sec)	V(ft/sec)	S(ft)
0.005	5.16	0.83	2.14
0.01	2.96	0.95	1.41
0.02	1.86	1.49	1.11
0.03	1.49	1.44	1.07
0.04	1.31	1.69	1.10
0.05	1.20	1.93	1.15
0.10	0.98	3.15	1.54

This table shows the time, velocity and distance travelled prior to detection of various step acceleration magnitudes. (Based on Melvill Jones and Young, 1978.)

A-3 Design Justification

A-3.1 Motor

Several designs were considered. Schulte and Vreeland (1964) designed and built an acceleration cart used in Meiry's (1965) thesis work. They did a detailed design study of various options such as hydraulic or electrical power, and cable, linear actuator, or lead screw drive. This design evaluation was again done, in more detail, by ESA and ERNO in the report Space Sled Design (ESA, 1978). Before the equipment for this thesis was constructed, several designs were evaluated including designs of various carts used for driving cameras on model boards to provide high quality video displays for flight simulators. The final space sled design uses an electric motor to drive the sled by a cable and winch drum. A hydraulic piston actuator was seriously considered for use in the MIT sled design, but finally discarded because of physical constraints (a large volume of fluid would have been necessary) and the desire to faithfully simulate the space sled; it was decided to use an electric motor and cable/winch drum on the MIT sled. After much discussion and advice from designers of the above-mentioned model boards, a 3.5 HP DC permanent magnet servo motor and SCR controller (bandwidth 0-30 Hz) manufactured by Inland Motors (Radford, VA) were selected.

To avoid the backlash and power dissipation inherent in most gear reducers, a direct drive system was chosen. After selecting a winch drum

diameter of 8 inches, the torque-speed curves required to achieve a 0.3 g acceleration for a track length of 15 feet were defined. All design criteria were based on a 1.5 safety factor. The Inland Motors TTB-5302-C motor has the low speed (645 rpm maximum) and high torque (35 ft-lb continous) that satisfy the design specifications. The choice of controllers was somewhat limited; most transistor switching controllers are low power, low voltages devices incapable of utilizing the motor's capabilities. Motor generator sets are expensive and would require some custom-built electronics. The Inland Company sells silicon controlled rectifier (SCR) and pulse width modulated (PWM) controllers that are compensated for the individual motors. The PWM system, according to the factory, would only result in a larger bandwidth (up to about 50 Hz). Therefore, an SCR controller was chosen. After the entire system had been installed, it was obvious that the motor had a large vibration at 0 rpm. The cause was found to be the cycling of the SCRs at 180 Hz (three phase power supply). Unfortunately, this vibration is quite noticeable and audible. Fortunately, the fundamental vibration frequency (although not waveform) is independent of motor speed, so that these vibrations do not provide motion cues during the threshold determination experiments. A possible solution might be to use the motor generator set that once was used for the NE-2 trainer, although the power lines would be long and some additional electronics would be necessary.

A.3.2 Guide Rails

Several methods of guiding and suspending the cart were investigated.

Most carts use rubber wheels with ball bearings and vibration isolation mountings along with some sort of guide rail. To achieve very low vibration levels, it is necessary to have very smooth tracks upon which the wheels slide. Probably the best solution is the use of an air bearing type suspension which is practically frictionless. This solution poses problems of noise and air supply to the cart. In addition, some sort of guide system is necessary. As a compromise, ball bushings riding on high precision ground rails were chosen. The guide rails were manufactured by Thomson Ball Bushing Company (Manhasset, NY). These rails are supported continuously and accommodate ball-bushing pillow blocks. These ball bushings have very low friction and, though noisy, have essentially no low frequency vibrations. These bushings can handle speeds up to 15 feet/sec and acceleration loads up to 0.3 g, as verified by the factory. The rails are specially machined and hardened and are straight to within 0.0005 inch/foot of rail. They are overdesigned with resepct to the weight supported on the bushings. A 1-inch diameter rail was chosen on the advice of the factory.

Proper construction of the track was crucial to ensure rail straightness. The foundation consisted of two parallel walls, 2 feet high and 64 inches apart with poured concrete mounting pads on either end to accommodate the motor and dummy pulley (see the engineering drawings at the end of this Appendix). A masonry contractor was hired to lay the foundation. The top course of blocks had anchor bolts cemented into the cells at about 16 inch intervals. These anchor bolts were positioned using a template and the template was then used to mark the holes on

the 1/2" x 6" steel bar stock. The steel bars were bolted into position on top of the blocks and the master guide rail (nearest the outside wall) was positioned using a theodolite to ensure straightness. The mounting holes for the rails were then spotted, drilled and tapped in the steel bar. The rail was finally optically aligned in both the horizontal and vertical planes (shimmed where necessary) to within 68 arc seconds of straightness over the entire length. After the master rail was aligned, the second rail was aligned by running the cart up and down the track, and mounted. Even after careful alignment, it was found that the cart would tend to bind at various positions along the track. This problem occurred because four pillow blocks were used to support the cart instead of three. The problem was anticipated, but it was decided that the added support and symmetry of four pillow blocks was desirable. The solution to the problem was to let the second rail "float". It is loosely held by bolts, but free to conform to the master rail. After the entire system was installed, a final check of alignment was made by using an auto-collimator and a first-surface optically flat mirror attached to the accelerometer block. This check revealed a total deviation from straightness of 5.5 arc-minutes as measured very near the subject's head position.

After plotting the deviation as a function of track length an approximately sinusoidal shape was obtained. Using an equation from Schulte and Vreeland (1964), the maximum accelerations due to the deviation were calculated for several stimulus acceleration levels. The equation is:

$$a_{max} = v_{max}^2 \omega^2 \underline{Y}$$

where a_{max} = the maximum acceleration due to the "bump"

v_{max} = maximum cart velocity at the "bump"

ω = spatial frequency of the bump in units of rad/in, for example

$\underline{Y}$ = maximum amplitude of the "bump"

For the worst case, $\underline{Y}$ - 0.38 inches and ω = 0.06 rad/in. These values were obtained from the plots of rail straightness.

Assuming a step acceleration of 0.01 'g' starting at the end near the "bump", an out-of-plane acceleration of 6.0×10^{-4}g is produced, which is an order of magnitude below threshold. For 0.05 'g', the out-of-plane acceleration is calculated to be 5.32×10^{-2}g which is suprathreshold; however, at that point, the velocity is 2.54 ft/sec and t - 1.58 sec. These values are substantially above threshold (see previous section), so detection should be made prior to reaching the bump.

A-3.3 Cart

The cart was designed to provide flexibility in subject orientation, and to be light-weight and rigid. Substantial work in the design and construction of the cart was done by Johan Garbus under the auspicies of a design course at MIT. The final design consisted of a rigid cart attached to the rails and a movable chair that could be

repositioned inside the cart to provide x or y axis stimulation with the subject seated upright and y or z stimulation when the subject is positioned on his/her back (see engineering drawings). The cart was required to have a natural frequency above 20 Hz to avoid any resonance peaks due to the input stimuli. In addition, the cable mass structure and cable were required to have natural frequencies above 20 Hz to avoid any low-frequency vibration problems. With a 300 lb cart, 18 foot cable length and 3/16" steel cable, the natural frequency of the cable with the cart at one end of the track is about 25 Hz with a 625 lb preload in the cable.

To minimize out-of-plane torques, it was decided to align as closely as possible the center of gravity of the cart and cable attachment point with the plane of the guide rails. The diameter of the winch drum that was selected (8") dictated part of the design of the chair and unavoidably raised the center of gravity of the cart slightly out of the drive plane. The chair frame and cart were constructed of 3" x 3" aluminum angles for ease of construction and rigidity Although a detailed load and vibration analysis was not done, basic structural and safety calculations showed that the lowest natural frequency of any member was about 22 Hz and that the chair was capable of sustaining at least three times the crash loads imposed by a 3.0 g deceleration.

After construction, the presence of 180 Hz vibration due to the zero-speed bias current in the motor was felt not only through the cable but also through the cement blocks and steel rails. Therefore, Lord

(BH-80) vibration dampers were installed between the cart and chair frame. The characteristics of these isolation devices approximate a second order system, slightly underdamped with a natural frequency of about 10 Hz depending on the load. These dampers subjectively appeared to reduce the vibration level in the chair frame with respect to the cart, although some vibration is still present.

The chair frame not only holds the subject but also provides support for the camera mount, blackout shroud and electronics. The camera mount has quick-release latches and hinges that allow it to be swung open or be removed if the nature of the experiment does not require photographs. The camera mount has two positions for the plate used to secure the camera. The forward (closest to the subject) position is used in conjunction with a 55 mm Micro-Nikkor lens and extension tube mounted on the Nikkon camera. This position allows a maximum reproduction ratio of 1:1.5. The other position is used with the 105 Micro-Nikkor lens and extension tube attached to the camera. This combination allows a 1:1 maximum reproduction ratio and keeps the camera and lens farther away from the subject. Also attached to the camera mount is the power unit for the ring shaped strobe flash. This power unit has been specially reworked by the Laboratory for Space Experiments to allow flash firing rates of three frames per second. The 110 volt plug of the power unit is plugged into an extension cord on the chair frame behind the seat.

The seat is a commercially available (PV Performance Centers, Malden, MA) automobile racing seat picked for its strength, comfort, support and

lightness. The subject is held in the seat with an aircraft lap safety belt, a chest strap and head restraint. Styrofoam pads are wedged between the subject's shoulders and chair frame to reduce torso movement. The head restraint is a contoured foam rubber appliance with a wide velcro strap that passes around the forehead. Under large accelerations, the maximum movement of the head and chest is about equal (1 to 2 cm); therefore, no potentially dangerous shearing forces are applied to the neck during emergency decelerations. One current problem with the head restraint is that the foam rubber behaves like a linear spring with increasing force generated by increasing head displacement, but no "breakout" force. The ideal concept is to have the head rigidly immobilized during normal operating accelerations, but to allow the head to move in concert with the chest during an emergency stop. One possible solution to this problem is a rubber bladder filled with small plastic particles. When the air in the bladder is evaculated, the bladder conforms to the head, but is very rigid. This bladder could be supported on a surface that has a high breakout force and could be supported on either side with foam rubber to provide a restraining force if the head is displaced.

A-4 Safety Interlocks

Because of the large torque capability of the motor and distinct physical limits on the track length (thus cart travel), an elaborate and multiply redundant safety system was necessary. The motor and

controller have several built-in safety features that protect the motor from overheating, drawing too much current, and from momentary power surges. The controller has a regenerative braking feature that allows the back EMF of the motor to be used for braking if the primary power fails. Also, a fail-safe disc brake option was ordered on the motor so that if prime power was lost, the brake (normally held open by 110 V AC power) would engage, thus providing positive braking. In addition to these interlocks, it was deemed necessary to have panic switches for both the observer and subject as well as limit switches on the track. The block diagram of this interlock system is shown in Figure A.1.

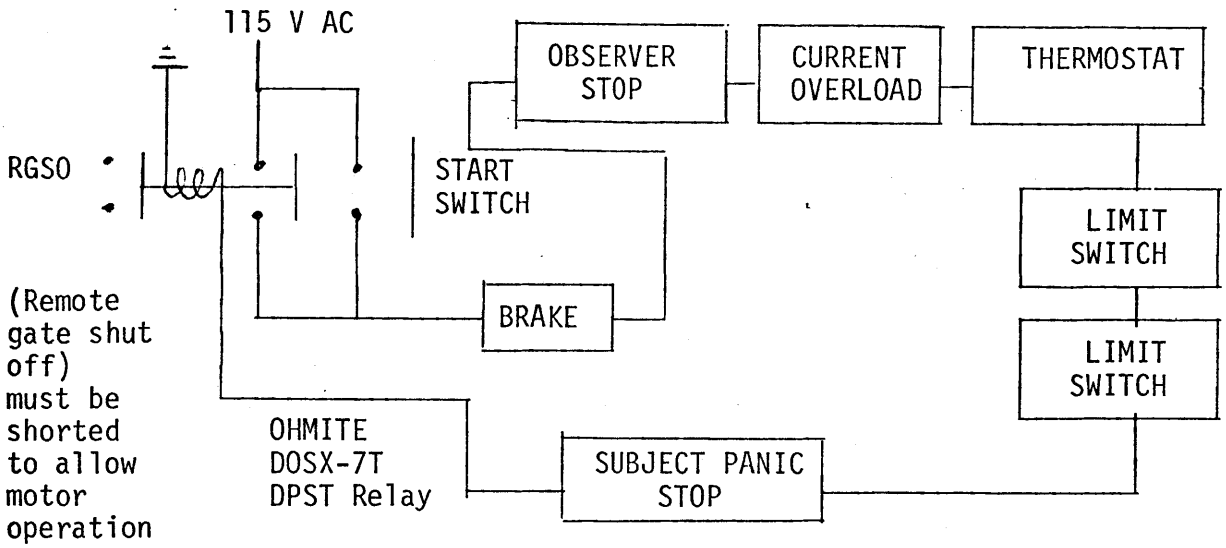

Figure A.1 Schematic of mechanical safety interlock circuit. All elements are normally closed except for brake and start switch. Brake is held disengaged by 115 V AC in a fail-safe mode.

The system operates in the following manner. All switches are normally closed and wired in series. The start switch is a momentary ON type. If all safety switches are closed, pushing the start button energizes the brake and relay. The relay is wired to be self-latching until one of the safety switches is open. A momentary opening of any safety switch will disconnect power to the motor and activate the brake until the start button is pushed again. If the cart reaches the limit switches, a computer program failure is the most likely cause. In this case, it is possible for the cart to be travelling at a high velocity and the disc brake alone would not be sufficient to stop it in the allocated 16 inches. For this reason, additional energy absorbers were placed at the ends of the track. At the present time, shock cords (essentially springs) are bolted to the steel bar stock on top of the concrete blocks and catch the cart if exceeds the normal track limits. For the future, hydraulic bumpers have been procured, but have not yet been installed. These bumpers will be purely energy absorbing and will not produce the recoil against the brake that is associated with the shock cords (energy storing devices). The shock cords that are used are 1/2 and 3/4 inch in diameter and are rated by the force produced for a given percent extension over original length. For example, a 14 inch length of 1/2" diameter cord that is stretched to 28 inches (100% elongation) will produce about 250 lbs of force. To stop a 300 lb cart moving at 17 feet per second (the maximum velocity with a full scale computer output) in a distance of 14 inches requires a 3 g deceleration or 900 lbs of force. It can be seen that four shock cords each

fourteen inches long will provide more than enough force. At one end of the track four 3/4 inch diameter cords are used, but are slightly longer than the 1/2 inch cords, so that approximately the same deceleration is obtained at either end.

A-5 Performance Data

Preliminary analysis of the cart and chair frame was done by mounting two linear accelerometers, one at the cable attachment point on the cart and the other at a position near the subject's head and analysing the data via Fourier transforms. At this point, the motor and controller had not yet arrived so a falling weight was used to provide a "step" acceleration. Due to friction, the acceleration was not constant, but the end result of a transmission Bode plot could be obtained. The Bode plot was obtained by dividing the Fourier coefficient (at various frequencies) of the head mounted accelerometer by the coefficient of the cable attachment point mounted accelerometer. The frequency range of interest was 0.1 Hz to 50 Hz or about 2.5 decades. A peak in the amplitude ratio at about 22 Hz indicated the approximate value of the cart/chair frame natural frequency. Due to the limited availability of the accelerometer, a Bode plot using sine wave inputs was not obtained, but the preliminary results appeared satisfactory.

Due to the complexity and non-linearity of the SCR phase controller and motor combinations, very little modelling of this system has been done. Extensive consultation with the manufacturer (Inland) indicated that the motor-controller loop was very tight and would most certainly

meet the needs of this project, but other than the stated figures of 120 dB forward loop gain and a bandwidth of 0 to 30 Hz, no quantitative data were available. The continuous torque of the motor is 35 ft-lb which yields a force (through a 1/3 foot radius winch drum) of 105 lbs at the cable. This force is enough to provide a 0.3 g acceleration to a 300 lb cart, but the peak torque charactersitics of the motor are somewhat nebulous.

Because the otoliths respond to linear acceleration, it is only natural to study the system by controlling the input acceleration. It was first decided to place a precise servo accelerometer in the feedback loop to measure and regulate the acceleration. The controller however is a closed loop velocity servo. After much discussion, it was decided to first control the cart through an open loop velocity command (ramp to approximate a step acceleration input; and sine wave to approximate sine wave acceleration (with 90° of phase lead)). The accelerometer in this situation would only be used for measurement. If the system appeared sloppy, a portion of the accelerometer signal could be fed into the velocity input to improve the performance. However, since the controller itself comes with a lead filter in the tachometer feedback loop, the use of acceleration feedback was not anticipated. In fact, the system is very smooth and responsive with no noticeable backlash when going through zero velocity and closely approximates the desired acceleration input over the required bandwidth.

One perplexing interaction of electronic equipment on the sled

was noted. The Sundstrand Q-flex 1000 servo accelerometer operates well except when the camera and flash are operating, at which time spurious spikes are noted in the accelerometer output. Some sleuthing showed that the trouble was not with the vibrations associated with the motor drive, shutter and mirror movement, but rather with an electrical interaction between the high voltage flash tube and the accelerometer. The "noise" in the accelerometer would make feedback of the signal to the controller very difficult. Two solutions could be proposed. One is to make a matched filter receiver that has an impulse response which is the inverse of the noise, if one wanted to use acceleration feedback. If one merely wanted the data for analysis, the Fourier transform of the acceleration could be used to regain the amplitude of the fundamental input sine frequency or the DC component of the step acceleration record. If less accurate methods would suffice, visual inspection of the data could be done.

A-6 Sled Bode Plot Analysis

The Bode plot analysis of the sled was derived from the sine wave velocity command whose frequency was specified and whose amplitude was a function of frequency and track length. Assuming a position function of the form $x = A \sin \omega t$, then $\dot{x} = A\omega \cos \omega t$ and $\ddot{x} = -A\omega^2 \sin \omega t$. Therefore, if one knows frequency and track length (2 x A) the maximum acceleration is determined. The sled has a specified frequency range of 0.02 Hz to 1.0 Hz. Figure A.2 shows the Bode plot (Amplitude ratio (dB) and phase lead (deg)) as a function of frequency from

0.03 Hz to 1.0 Hz. At frequencies below 0.2 Hz, the acceleration was set as high as the track length would permit, above 0.2 Hz, the acceleration level was 0.2 g. Because the input is a velocity command and the output an acceleration, the phase lead should ideally be 90°. The input velocity command (ft/sec) was converted to a desired acceleration command:

$$\text{Accel}_{\text{desired}} = V \times \omega/32.17 \quad \text{(g units)}$$

Therefore, the amplitude ratio (AR) in decibels should ideally be 0. Figure A.2 shows that the phase lead approaches 90° at low frequency and drops to about 72° at the maximum frequency. Conversely, the AR increases slightly over the frequency range indicating a resonance somewhere above 1 Hz. The Bode plot of the loaded cart (subject weight 185 lb) indicates a slightly lower resonance frequency which is to be expected. Subjective impressions while viewing the subject at 1.0 Hz stimulation indicated that this frequency was near the resonant frequency of the human body which is supported by the Bode plot data. The values of the AR were about 1.0 over the range rather than zero as would be expected. This difference is only slight and is probably due to a slight misadjustment of transducer gains through the system.

Other Performance Criteria

The Space Sled was specified to have a rise time of 250 msec.

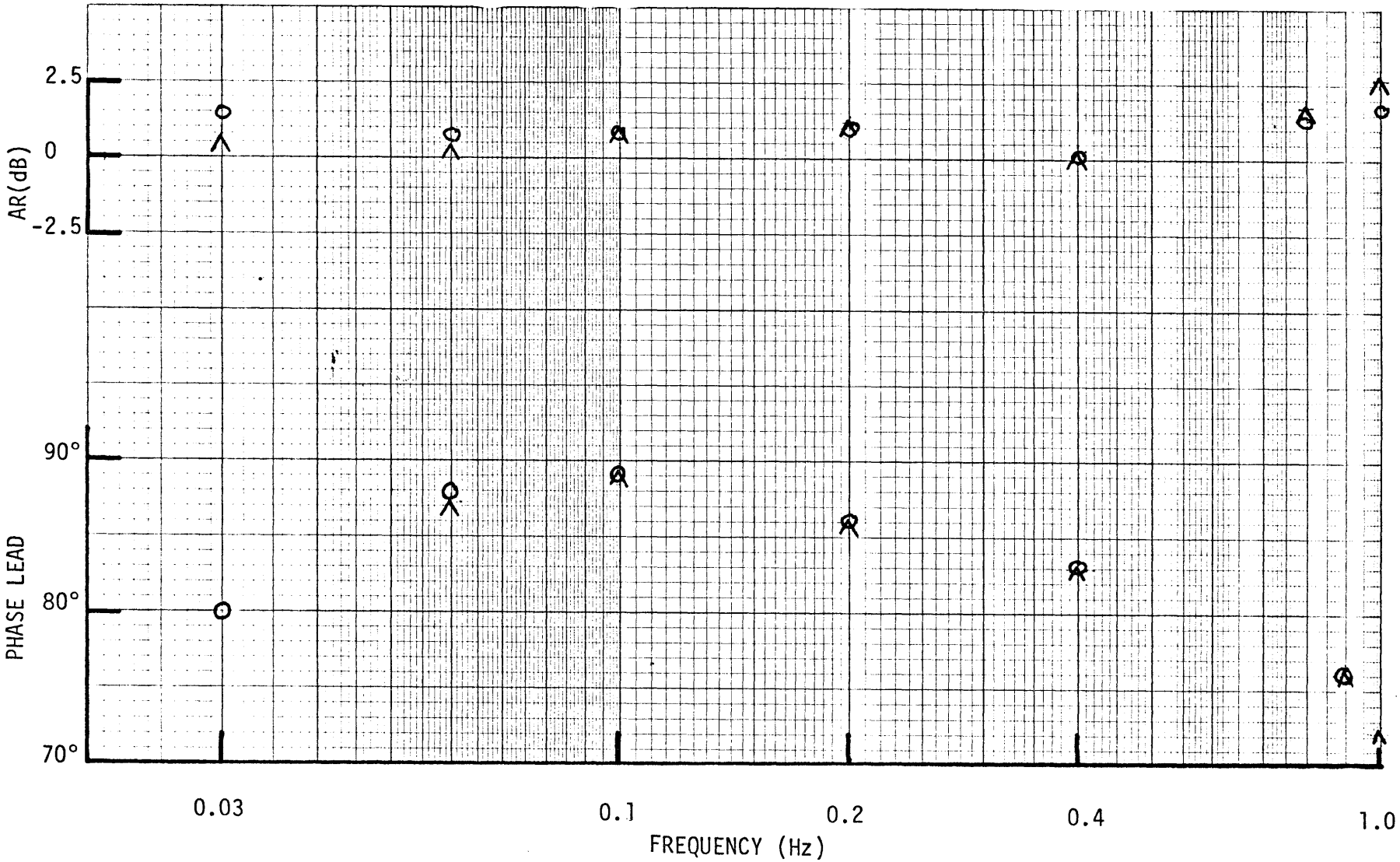

Figure A.2 Sled Bode Plot of unloaded sled (O) and sled with 180 16 test subject (^)

Examination of strip chart printouts (see Figure A.3) of the sled with a ramp velocity input show that indeed the rise time of the sled is about 160 to 180 msec. It appears as though the sled with a quasi-open loop control system will meet the specifications.

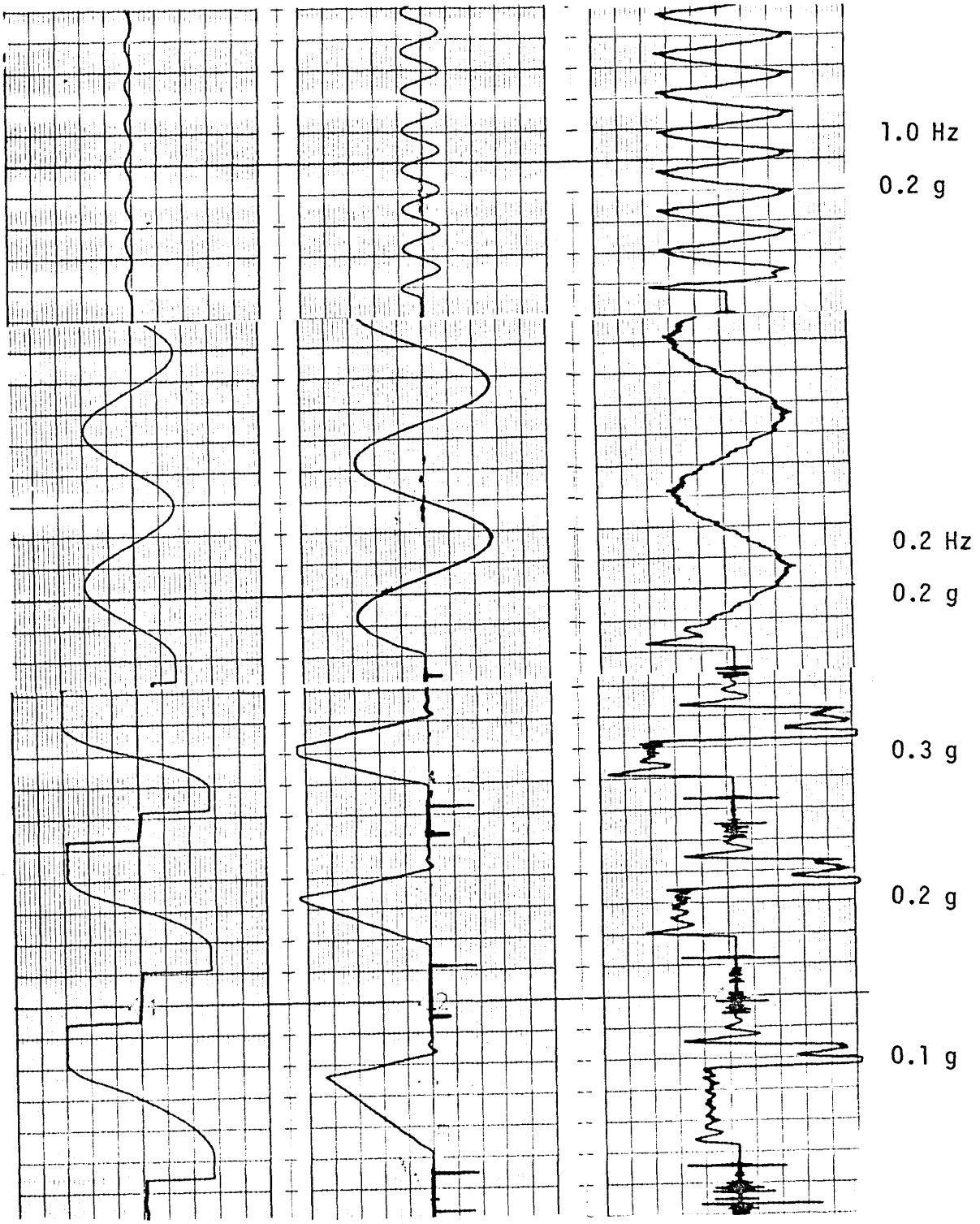

Figure A.3 Sled Performance

Figure A.4

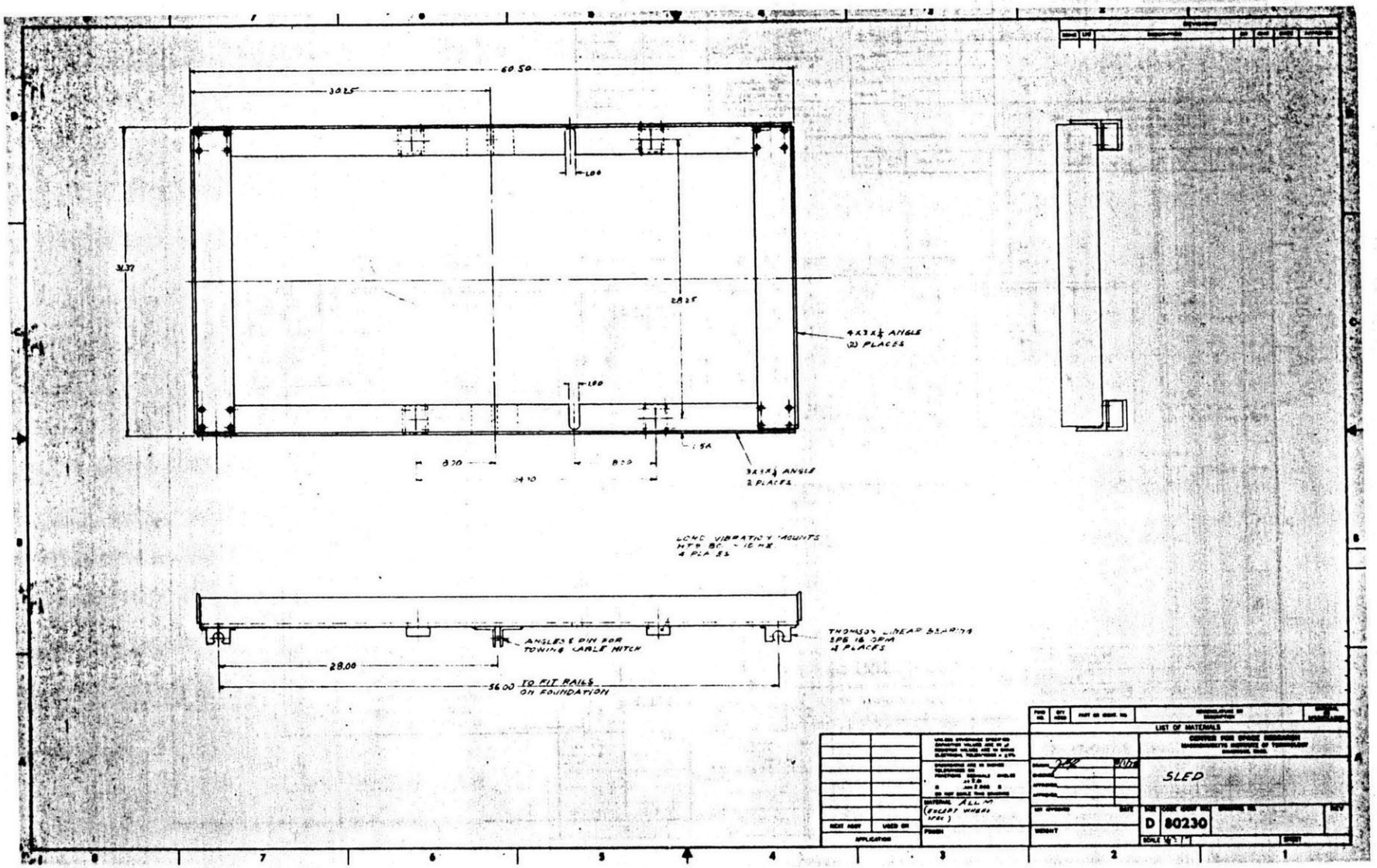
60.50
30.25
34.37
28.25
4x3x1/4 ANGLE
(2) PLACES
3x3x1/4 ANGLE
2 PLACES
28.00
56.00 TO FIT RAILS ON FOUNDATION
THOMSON LINEAR BEARING
SPB 16 ORM
4 PLACES
LIST OF MATERIALS
SLED
D 80230

Figure A.5

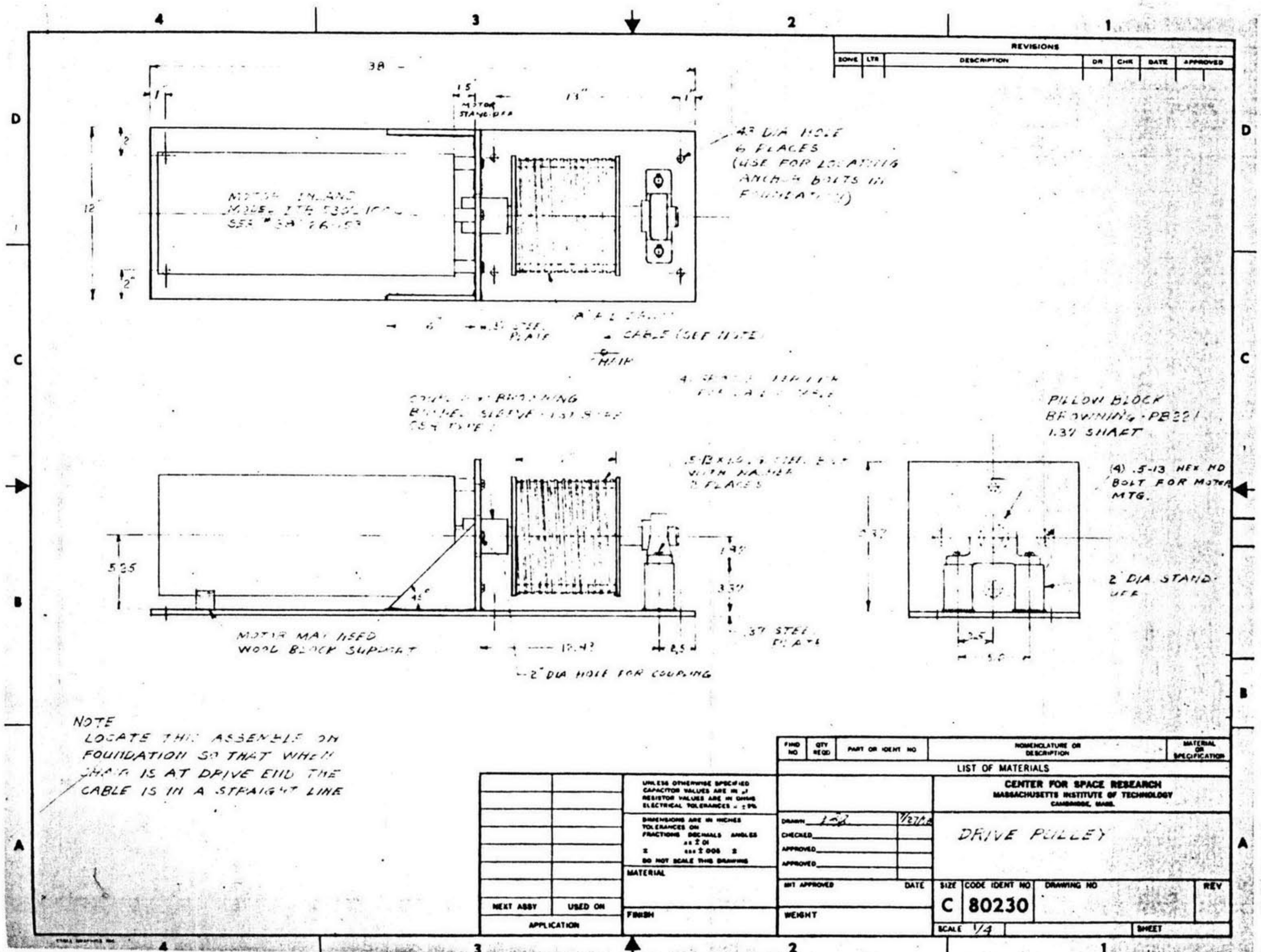
38
13"
.43 DIA HOLE
6 PLACES
PILLOW BLOCK
1.37 SHAFT
(4) .5-13 HEX HD
BOLT FOR MOTOR
MTG.
2 DIA STAND-
5.35
12.43
2" DIA HOLE FOR COUPLING
NOTE
LOCATE THIS ASSEMBLY ON
FOUNDATION SO THAT WHEN
IS AT DRIVE END THE
CABLE IS IN A STRAIGHT LINE
REVISIONS
LIST OF MATERIALS
CENTER FOR SPACE RESEARCH
MASSACHUSETTS INSTITUTE OF TECHNOLOGY
CAMBRIDGE, MASS.
DRIVE PULLEY
C
80230
SCALE 1/4
NEXT ASSY
USED ON
APPLICATION
MATERIAL
FINISH
WEIGHT

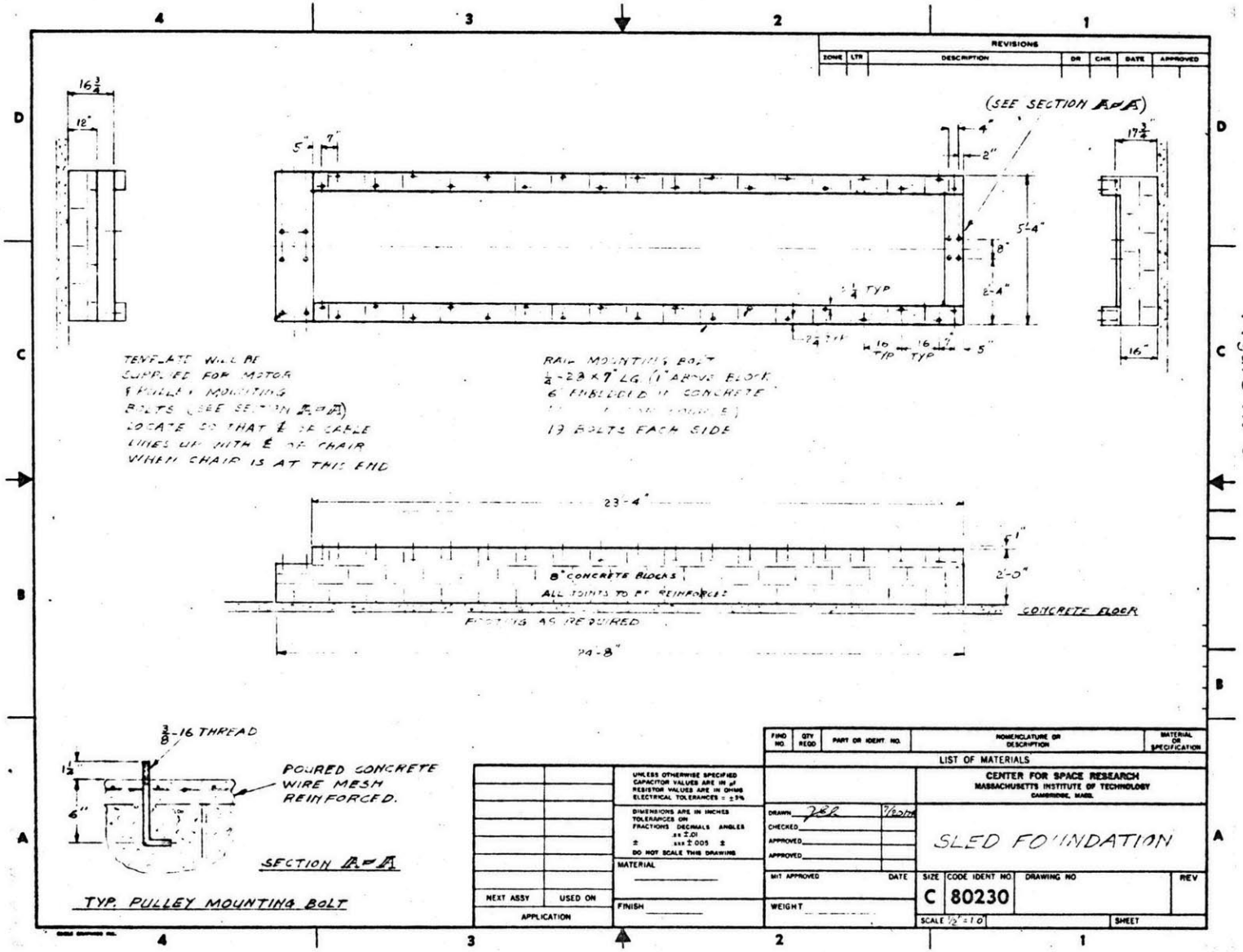
REVISIONS
ZONE LTR DESCRIPTION DR CHK DATE APPROVED
(SEE SECTION A-A)
16¾"
12"
5"
7"
4"
2"
17¾"
5'-4"
8"
2'-4"
1¼ TYP
2¾"
10" TYP
16" TYP
5"
16"
TEMPLATE WILL BE SUPPLIED FOR MOTOR & PULLEY MOUNTING BOLTS (SEE SECTION A-A) LOCATE SO THAT ℄ OF CABLE LINES UP WITH ℄ OF CHAIR WHEN CHAIR IS AT THIS END
RAIL MOUNTING BOLT ¼-28 X 7" LG. (1" ABOVE BLOCK & EMBEDDED IN CONCRETE
19 BOLTS EACH SIDE
23'-4"
8" CONCRETE BLOCKS
ALL JOINTS TO BE REINFORCED
FOOTING AS REQUIRED
24'-8"
1'-1"
2'-0"
CONCRETE FLOOR
⅜-16 THREAD
1½"
6"
POURED CONCRETE WIRE MESH REINFORCED.
SECTION A-A
TYP. PULLEY MOUNTING BOLT
FIND NO. QTY REQD PART OR IDENT NO. NOMENCLATURE OR DESCRIPTION MATERIAL OR SPECIFICATION
LIST OF MATERIALS
UNLESS OTHERWISE SPECIFIED CAPACITOR VALUES ARE IN μf RESISTOR VALUES ARE IN OHMS ELECTRICAL TOLERANCES = ±5%
DIMENSIONS ARE IN INCHES TOLERANCES ON FRACTIONS DECIMALS ANGLES .xx ±.01 .xxx ±.005 ±
DO NOT SCALE THIS DRAWING
MATERIAL
FINISH
NEXT ASSY USED ON
APPLICATION
DRAWN JRL 7/20/74
CHECKED
APPROVED
APPROVED
MFT APPROVED DATE
WEIGHT
CENTER FOR SPACE RESEARCH
MASSACHUSETTS INSTITUTE OF TECHNOLOGY
CAMBRIDGE, MASS.
SLED FOUNDATION
SIZE C CODE IDENT NO 80230 DRAWING NO REV
SCALE ½"=1'0 SHEET

Figure A. 6

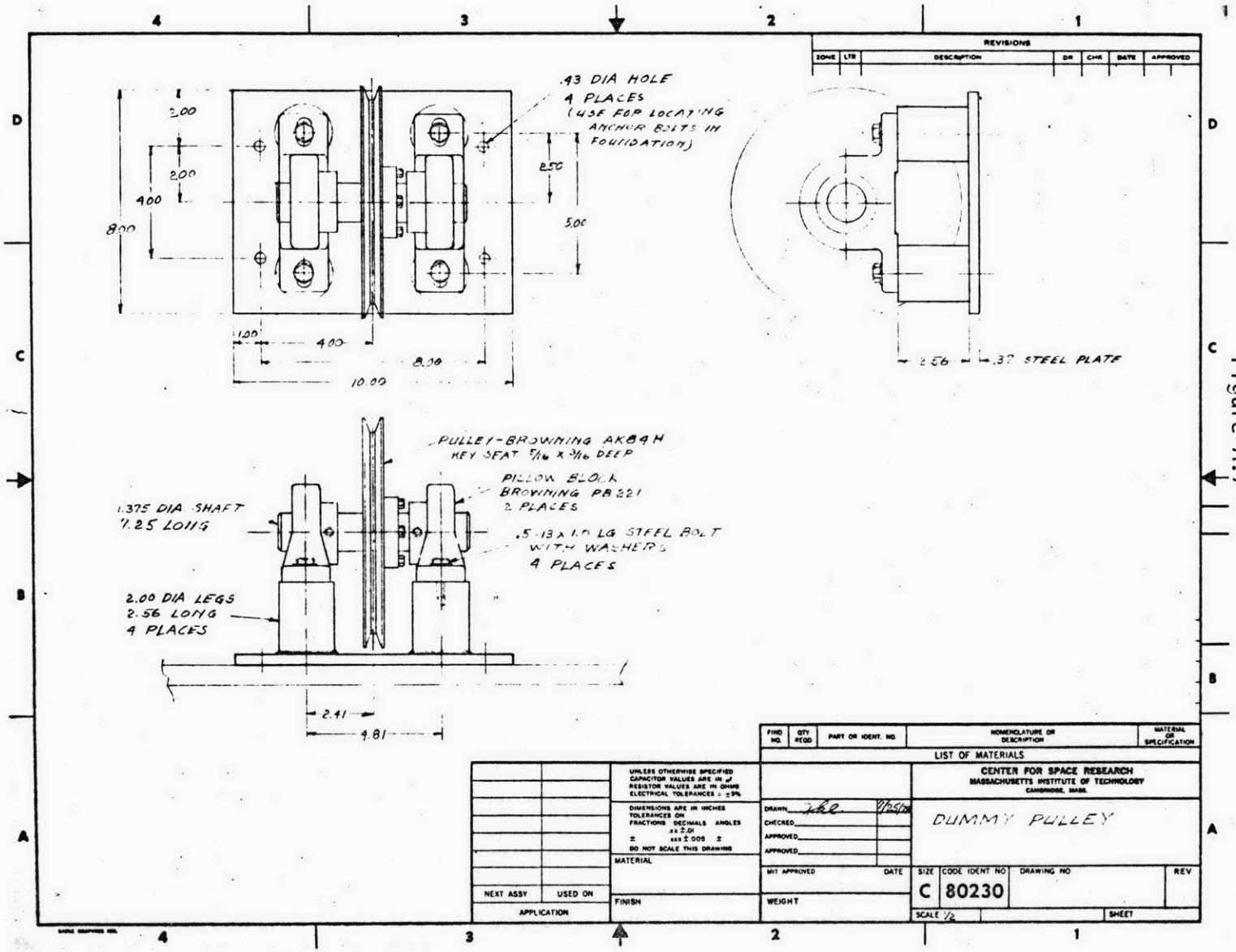
.43 DIA HOLE
4 PLACES
(USE FOR LOCATING ANCHOR BOLTS IN FOUNDATION)
2.00
2.00
4.00
8.00
2.50
5.00
1.00
4.00
8.00
10.00
2.56
.37 STEEL PLATE
PULLEY-BROWNING AK84H
KEY SEAT 5/16 X 3/16 DEEP
PILLOW BLOCK
BROWNING PB221
2 PLACES
.5-13 x 1.0 LG STEEL BOLT
WITH WASHERS
4 PLACES
1.375 DIA SHAFT
1.25 LONG
2.00 DIA LEGS
2.56 LONG
4 PLACES
2.41
4.81
REVISIONS
ZONE
LTR
DESCRIPTION
DR
CHK
DATE
APPROVED
FIND NO.
QTY REQD
PART OR IDENT. NO.
NOMENCLATURE OR DESCRIPTION
MATERIAL OR SPECIFICATION
LIST OF MATERIALS
UNLESS OTHERWISE SPECIFIED
CAPACITOR VALUES ARE IN μf
RESISTOR VALUES ARE IN OHMS
ELECTRICAL TOLERANCES ± ±5%
DIMENSIONS ARE IN INCHES
TOLERANCES ON
FRACTIONS DECIMALS ANGLES
.xx ± .01
± .xxx ± .005 ±
DO NOT SCALE THIS DRAWING
MATERIAL
FINISH
NEXT ASSY
USED ON
APPLICATION
DRAWN
CHECKED
APPROVED
APPROVED
MIT APPROVED
DATE
WEIGHT
CENTER FOR SPACE RESEARCH
MASSACHUSETTS INSTITUTE OF TECHNOLOGY
CAMBRIDGE, MASS.
DUMMY PULLEY
SIZE
CODE IDENT NO
DRAWING NO
REV
C
80230
SCALE 1/2
SHEET

Figure A.7

Figure A.8

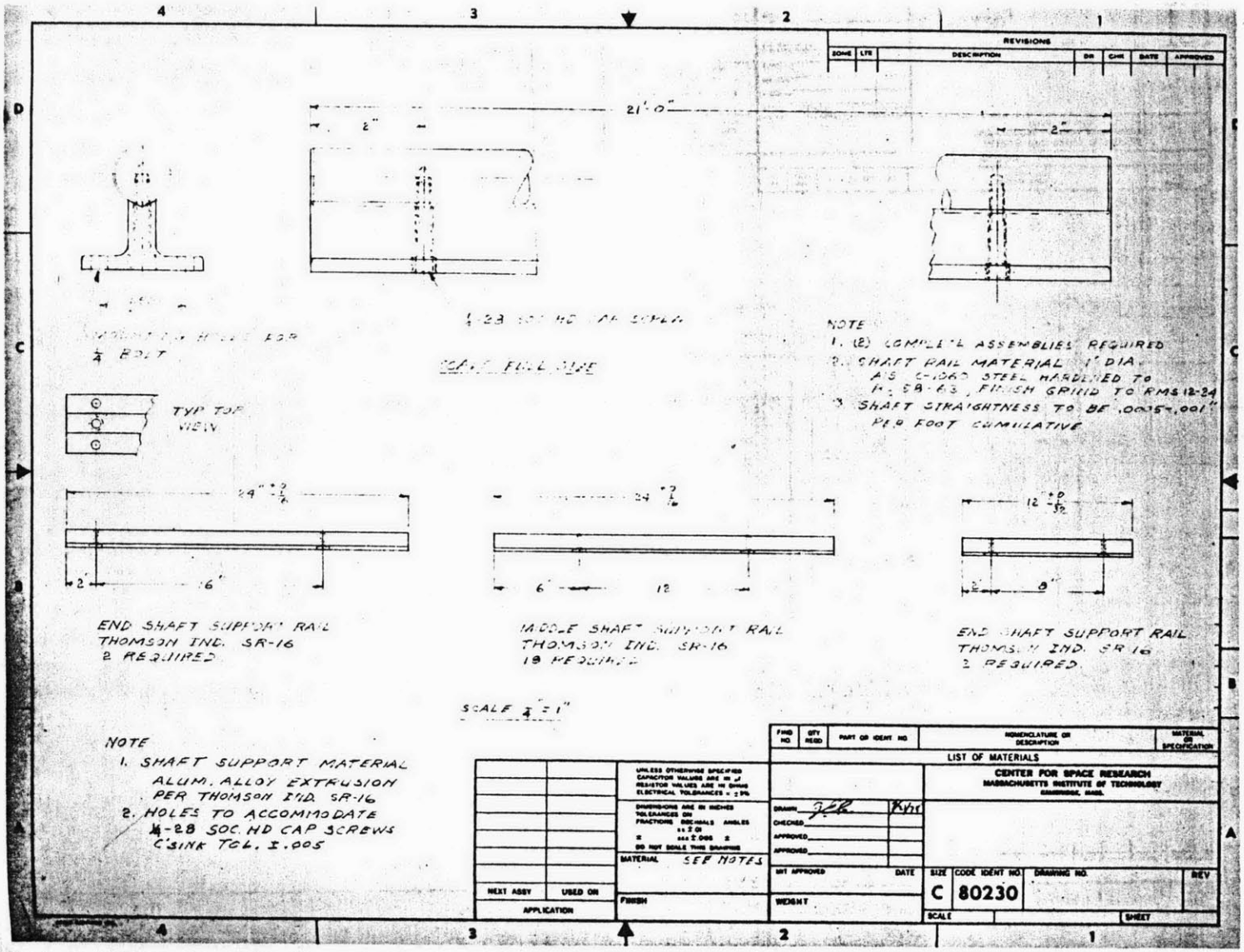
REVISIONS
ZONE LTR DESCRIPTION DR CHK DATE APPROVED
21'-0"
2"
2"
MOUNTING HOLE FOR 1/4 BOLT
TYP TOP VIEW
NOTE
1. (2) COMPLETE ASSEMBLIES REQUIRED
2. SHAFT RAIL MATERIAL 1" DIA. AIS C-1040 STEEL HARDENED TO Rc 58-63, FINISH GRIND TO RMS 12-24
3. SHAFT STRAIGHTNESS TO BE .0015-.001" PER FOOT CUMULATIVE
24" +1/2 -0
2"
16"
END SHAFT SUPPORT RAIL
THOMSON IND. SR-16
2 REQUIRED
24" +1/2 -0
6"
12
MIDDLE SHAFT SUPPORT RAIL
THOMSON IND. SR-16
18 REQUIRED
12" +0 -1/2
2"
8"
END SHAFT SUPPORT RAIL
THOMSON IND. SR-16
2 REQUIRED
SCALE 1/4" = 1"
NOTE
1. SHAFT SUPPORT MATERIAL ALUM. ALLOY EXTRUSION PER THOMSON IND. SR-16
2. HOLES TO ACCOMMODATE 1/4-28 SOC. HD CAP SCREWS C'SINK TOL. ±.005
FIND NO. QTY REQD PART OR IDENT NO. NOMENCLATURE OR DESCRIPTION MATERIAL OR SPECIFICATION
LIST OF MATERIALS
CENTER FOR SPACE RESEARCH
MASSACHUSETTS INSTITUTE OF TECHNOLOGY
CAMBRIDGE, MASS.
UNLESS OTHERWISE SPECIFIED CAPACITOR VALUES ARE IN μf RESISTOR VALUES ARE IN OHMS ELECTRICAL TOLERANCES = ±5%
DIMENSIONS ARE IN INCHES TOLERANCES ON FRACTIONS DECIMALS ANGLES ± 1/16 .xx ± .005 .xxx ± .002 ±
DO NOT SCALE THIS DRAWING
MATERIAL SEE NOTES
FINISH
DRAWN JCR
CHECKED
APPROVED
APPROVED
MFT APPROVED DATE
WEIGHT
NEXT ASSY USED ON APPLICATION
SIZE C CODE IDENT NO. 80230 DRAWING NO. REV
SCALE SHEET

Figure A.9

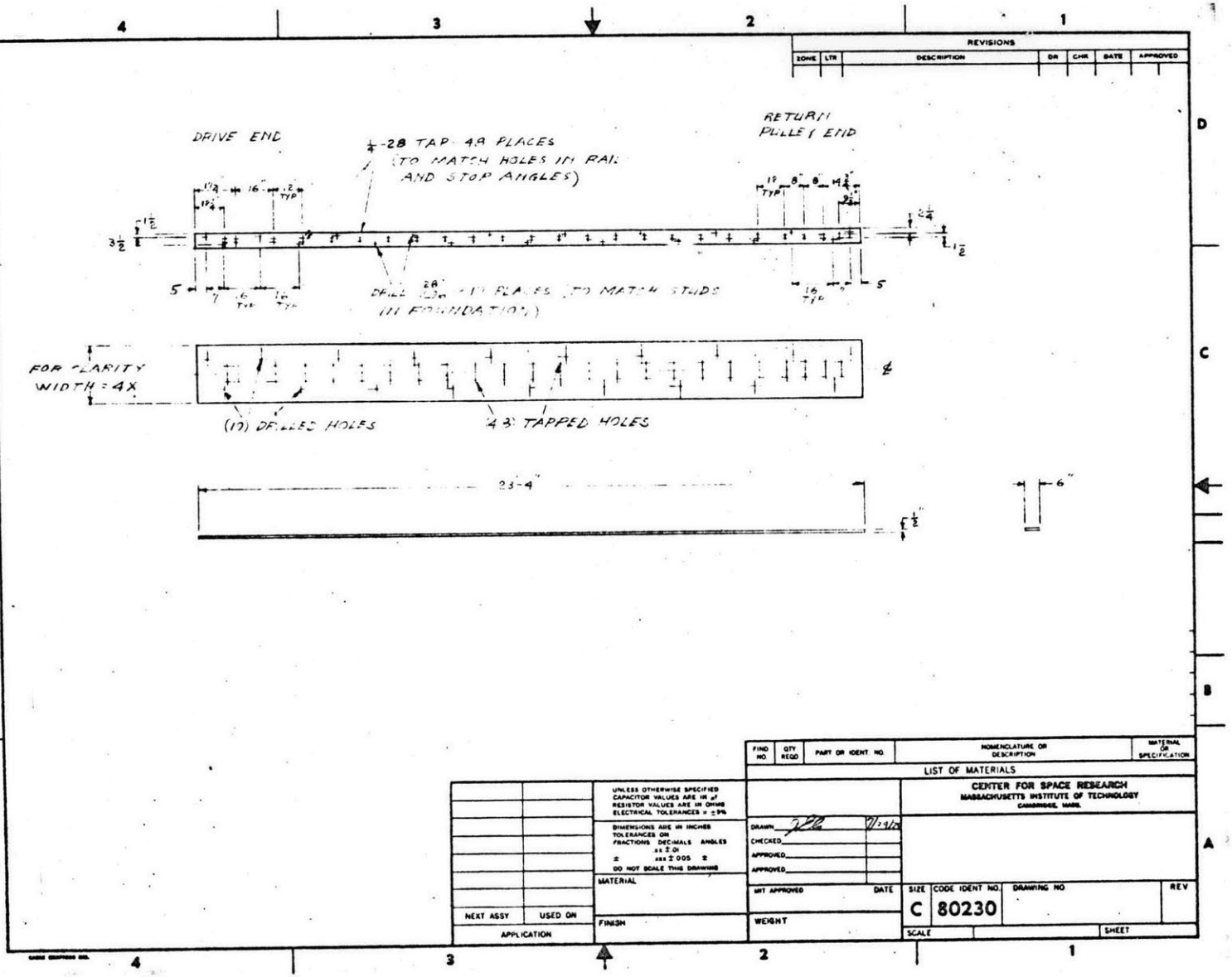
REVISIONS
ZONE LTR DESCRIPTION DR CHK DATE APPROVED
DRIVE END
RETURN PULLEY END
1/4-28 TAP 48 PLACES (TO MATCH HOLES IN RAIL AND STOP ANGLES)
DRILL 28 PLACES .53 DIA (TO MATCH STUDS IN FOUNDATION)
FOR CLARITY WIDTH = 4X
(17) DRILLED HOLES
48 TAPPED HOLES
23-4
LIST OF MATERIALS
FIND NO. QTY REQD PART OR IDENT. NO. NOMENCLATURE OR DESCRIPTION MATERIAL OR SPECIFICATION
UNLESS OTHERWISE SPECIFIED CAPACITOR VALUES ARE IN μF RESISTOR VALUES ARE IN OHMS ELECTRICAL TOLERANCES = ±5%
DIMENSIONS ARE IN INCHES TOLERANCES ON FRACTIONS DECIMALS ANGLES
DO NOT SCALE THIS DRAWING
MATERIAL
FINISH
NEXT ASSY USED ON
APPLICATION
DRAWN JCC 7/29/70
CHECKED
APPROVED
APPROVED
MIT APPROVED DATE
WEIGHT
CENTER FOR SPACE RESEARCH
MASSACHUSETTS INSTITUTE OF TECHNOLOGY
CAMBRIDGE, MASS.
SIZE C
CODE IDENT NO. 80230
DRAWING NO
REV
SCALE
SHEET

Figure A.10

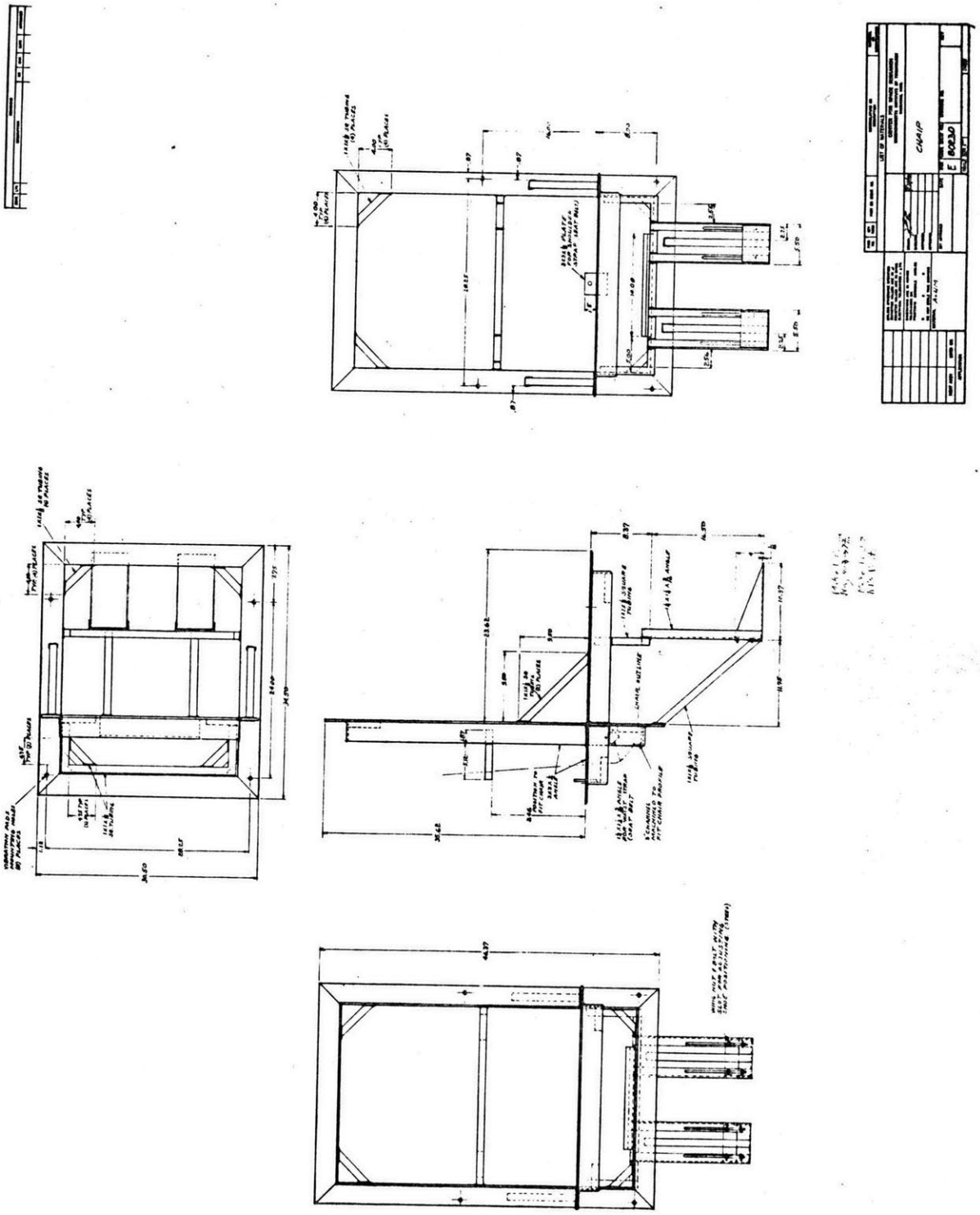

APPENDIX B

COMPUTER PROGRAM (SLDRUN)

The input to the motor controller is a velocity command. To generate the appropriate commands and monitor the operation of the cart, a computer program was written for the laboratory minicomputer (PDP 11/34). A flow chart of the program is shown in Figure B.1. This appendix will detail the computer interfaces (input and output quantities and scale factors), software capabilities, logic, and normal operating procedures. A complete printout of the program is also listed in Figure B.4.

The capacity of the computer includes 32 K words of memory, two RK05 disc drives and an LPS-11 Lab Peripheral System, including 16 multiplexed channels of 12-bit A/D and D/A. The A/D inputs have a differential pre-amplifier in the front end. The input voltage range of this system is -1 volt (0 bits) to +1 volt (4096 bits). The output D/A channels have a range of -10 volts (0 bits) to + 10 volts (4096 bits).

A complete listing of all connections to the patch board, analog and digital computers is given in Figure B-2.

B.1 Inputs, Outputs and Scale Factors

The inputs to the program are the sled position (SLPOS), sled velocity (SLVEL) and sled acceleration (SLACEL). The sled position is provided by a 10-turn precision wirewound 100 K potentiometer mounted

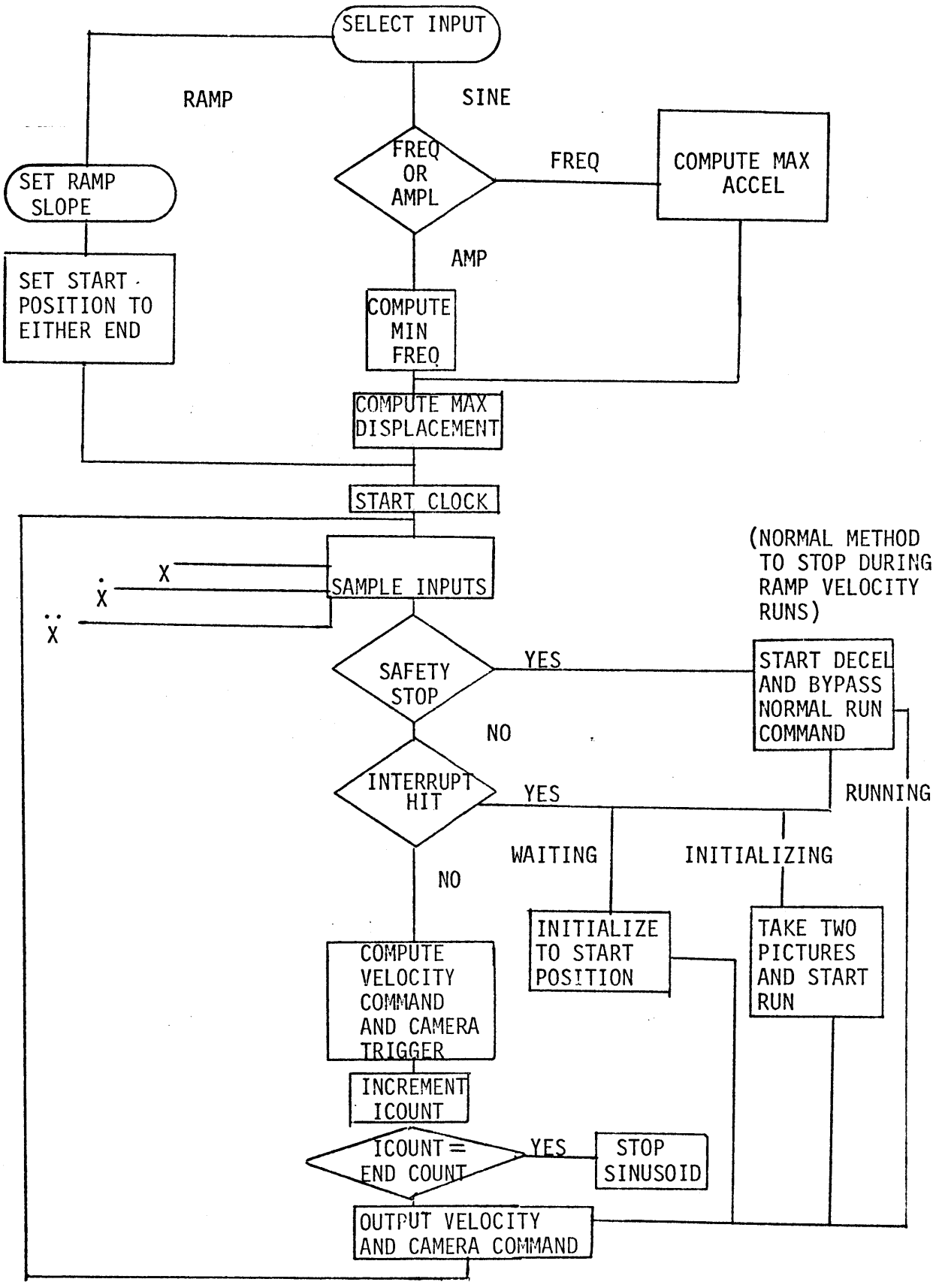

Figure B.1 SLDRUN Flowchart

on the motor shaft. This potentiometer is excited by ± 15 volts provided by the motor controller. The sled velocity is provided by the self-generating tachometer attached to the motor shaft. The cart acceleration signal is provided by a Sundstrand Q-flex servo accelerometer mounted on the sled. The polarity of the signals is such that positive position and velocity is toward the motor end of the track. Zero volts indicate the center of the track and zero velocity.

B.1.1 Sled Position

The sled position signal is fed from the potentiometer through trunk line D8 (coaxial cable) to the GPS 291T hybrid analog computer. The signal is buffered by an operational amplifier (gain of 1), then attenuated through P1 to provide a full range signal to A/D. The normal travel of the cart is ± 7.5 feet with emergency stop travel of an additional ± 2.5 feet. Therefore, 7.5 feet from the center is set at 0.75 volts output. The signal then goes through the trunk line to CH8 of the A/D on the patch board and also to channel 1 of the strip chart recorder.

Once in the computer, the bit count is transformed back into problem units (feet in this case) by the equation

$$SLPOS = (INPUT\ (BITS) - 2048)/KPOS$$

where

$$KPOS = 204.8$$

B.1.2 Sled Velocity

The sled velocity is provided by the tachometer on the motor, which has a scale factor of 18.9 volts/1000 rpm. The tachometer signal is buffered at the controller by an operational amplifier with a gain of 1.0. This signal is then fed through trunk D14 to the analog computer where it is further buffered (A16) and corrected for DC offset (0.07 volts) due to the buffer amp at the controller via potentiometer 3. The signal is attenuated through potentiometer 4, and sent to channel 9 of the A/D and channel 2 of the strip chart recorder. The input (bits) to the computer is transformed back into problem units (ft/sec) by the equation

$$SLVEL = (INPUT(BITS) - 2048)/KVEL$$

where $KVEL = 110.09.$

The value of KVEL was calculated through knowledge of the tachometer sensitivity and the measured distance that the cart travels for one revolution of the motor. The tach generates 9.45 volts/500 rpm and each revolution is 2.109 feet. The signal is then attenuated through potentiometer 4 so that the input to the digital computer falls between $\pm$ 0.945 volts.

B.1.3 Sled Acceleration

The sled acceleration is measured by a Sundstrand Q-flex linear

servo accelerometer. This accelerometer has a range of ± 15 g, a sensitivity of 0.333 volts/g and a resolution of 1 μg. The ± 15 volt excitation is provided by a bench mounted power supply (three phase 208 V AC input) in Room 37-127. This power supply also supplies power to the camera motor drive, pre-amps and low pass filter mounted on the cart. The output of the accelerometer is passed through a third order low pass filter with a break frequency of 25 Hz. This filtered signal is then pre-amplified on the sled and fed to the analog computer through the trunk line (D11) and patch board. The gain of the pre-amplifier is set so that a 1 g acceleration will produce the maximum (10 volt) input to the buffer amplifier in the analog computer. This signal is then attenuated to 10 percent of the original signal by potentiometer 23. In this manner, an emergency acceleration of 2 to 3 g will saturate the buffer amplifier (at 10 volts), rather than exceed the range of the A/D converters (± 1 volt). The sled acceleration is stored in the digital computer and on channel 4 of the strip chart recorder.

B.1.4 Other Program Inputs

The final input to the program is the interrupt signal that causes the program to initialize, run, or stop the cart. This interrupt can be generated either in the computer room or in 37-127. A switch attached to the analog control board provides 6 volts to activate electronic switch #18 which, in turn, sends 1 volt to the digital computer A/D

channel 8 on the patch board. The pushbutton switch located in 37-127, when depressed, connects 1 volt from potentiometer 15 directly to channel 8 of the A/D.

B.1.5 Velocity Command to the Sled

The primary output of the computer program is the motor velocity command. The speed scale factor on the motor controller is set so that + 10 volts (maximum output of the D/A converter) produces 500 rpm. The output velocity (VELCMD) is commanded by an equation

$$\text{OUTPUT (in bits)} = \text{VELCMD} * \text{KVOUT} + 2048$$

where

$$\text{KVOUT} = 2048 \text{ bits}/17.5 \text{ ft/sec} = 116.496 \text{ bits/ft/sec}$$

B.1.6 Other Program Outputs

The program also controls the camera motor drive and the strip chart recorder. The camera is triggered at 350 msec intervals during a run with two pictures taken before the beginning of each run to serve as control frames. The output to the camera is a 5 volt trigger signal from D/A channel 14 on the patch board through the analog to trunk line D13. This signal closes a dip relay mounted on the sled, which triggers the camera. This same signal (except amplified to 10 volts) is used to drive the strip chart event marker #1, so that camera firing and acceleration can be correlated. This camera signal is also filed on channel

4 of the data in the computer. The speed of the chart recorder is controlled by the digital computer. Channel 3 (patch board) of the D/A is used to close electronic switch #28 which supplies - 10 volts to a buffer amplifier in turn driving the speed relay in the strip chart recorder.

B.2 Software Capabilities and Program Logic

The program SLDRUN is designed to be as flexible as possible yet easy to operate. The flow chart is presented in Figure B-1. The program starts by asking for the type of input, either a ramp velocity (step acceleration), sine velocity (cosine acceleration) or pseudo-random velocity. Once the profile is selected, the desired amplitude and frequency (if a sine input) are selected. The present version has a maximum acceleration capability of 0.3 g. If a sine input is desired, the program asks for the independent variable (frequency or amplitude). Because the maximum track length is $\pm$ 7.5 feet, there are situations (low frequency) where the maximum acceleration is constrained by track length to less then 0.3 g. Conversely, if the acceleration level is high, the minimum frequency is track length limited. Therefore, the program asks for the independent variable and then responds with the minimum and maximum values of the dependent parameter. At present, the pseudorandom profile is not available; the subroutines to generate the velocity commands are available in the program LNKRUN, but need to be scaled to the sled track length and maximum acceleration. The next step of the program is to set the start position (STPOS) of the sled.

This start position for the ramp velocity input is at either end of the track. For the sinusoidal input, it is at a distance from the center of the track corresponding to the maximum displacement of the cart. To account for non-ideal behavior (i.e. slight asymmetries in the sinusoidal position profile), and the lack of continuous position feedback utilization, the actual starting point, if greater than 6.5 feet from the center, is moved one half the distance from the computed starting point to the end of the track.

The program next asks for a data filename, if the run is not a demonstration. At this point, the clock is started by the subroutine KWSET and the input data of interrupt status, sled position, velocity and acceleration are read by the A/D converter through a subroutine ATOD6. The six channels of A/D are numbered differently in the subroutine than in the patch board designation. Channel 8 on the patch board is channel 1 of the ATOD6 subroutine.[1]

The program converts the digital inputs to problem units and computes the distance between SLPOS and STPOS to be used during the initialization process. If the sled is not running, the program looks for an interrupt signal (greater than 0.75 volts) on channel 8 of the A/D. The state is set to IWAIT and the program loops to statement 10 until the interrupt is hit. To keep a constant loop cycle time, a subroutine called KWAIT is used. This routine holds up the program until the desired loop time (TMSEC) is over. If the actual time needed

[1]The subroutines KWSET, KWWAIT, ATOD6, DTOA6, and FILER are described in detail in the MVL document LNKRUN: PDP11/34 System for Control of the Link trainer, February, 1978.

to execute the steps in the loop exceeds the predetermined loop time, the program stops by setting the velocity of the sled to zero and prints out "STOP'SYNCH ERROR'". When any interrupt is triggered, the program stops the clock, restarts it and waits 500 msec for the switch contacts to stop bouncing and then restarts the clock. The state is changed from IWAIT to INITL and the sled is moved to the STPOS nearest the current SLPOS. The velocity is initially computed by a sine function with the appropriate sign determined by the SLPOS on the track and the relationship of SLPOS to STPOS. For example, if the cart is at the end of the track and is outside the STPOS (would occur after a ramp profile, if a high frequency, high g sine wave was selected), ISGN would equal -1 and ICOEFF would equal -1, so that the velocity would be positive. When the velocity is greater than the remaining distance which should happen about half way between the initial cart position and the start position, the velocity command becomes proportional to the distance remaining to the start position. When the sled position is within 0.25 feet of the desired position, the VELCMD is set to zero.

The sled is now ready to run. A second interrupt signal from the same line starts the selected velocity profile. NOTE: The sled run can be started any time during the initialization phase; no interlock is provided. When the second interrupt is detected, the state is changed to IRUN. The chart recorder is speeded up and one picture is taken. An inner loop counts 250 msec and then the first velocity command and second picture command are sent on the D/A lines. From this point on, pictures

are taken every 300 msec, with VLCMD being updated every TMSEC (currently set at 30 msec) by an increasing loop count (ICOUNT). The run can be stopped in three ways. (1) The interrupt is hit for a third time, (2) the safety interlock detects a condition of too great a velocity and too little track remaining, or (3) the time (TRUN) expires for the sinusoidal profiles. The time currently is set at 3 cycles of motion or 10 seconds, whichever is longer.

A safety interlock is built into the software to compare the current sled velocity with the remaining distance to go, knowing the deceleration. When a position is reached such that the programmed deceleration (DECEL) will use all the remaining track to stop the cart, a step deceleration is commanded (decreasing ramp velocity). This interlock, however, is not active, until the cart attains a certain velocity and is past the center of the track. For this reason, the acceleration cannot be greater than the deceleration. This safety interlock is used routinely to stop the cart during ramp velocity profiles and is also active during the sinusoidal profiles. In case a DC offset is present or the sled run starts prior to reaching the start position, the interlock will monitor the parameters and stop the cart prior to reaching the end of the track.

Because the computer is controlling a real-world device, there are certain dead bands and "slop" in the program. For instance, the velocity command during a stop is set to zero whenever the actual velocity is less than 0.41 fps. This is required because of the sampled data characteristics of the program. Also the cart should never go beyond the end of the track,

if it did, the safety interlock comparison would attempt to take the square root of a negative number and the program would stop, leaving an unknown(probably non-zero) velocity command which could cause the cart to overrun into the limit switches.

B.2.2 Communications Capability

The communications network is set up to provide two-way communication between the subject, the observer and the computer controller. A stereo amplifier, FM tuner and preamplifier are used. The two observers can always talk to each other and hear the subject. The subject can either hear the observers or a masking tone during experimental runs. The masking tone can be generated either by the FM tuner or a function generator. The switch to select the source for the subject's head set is located on the patch board in the computer room. Figure B.3 shows the current wiring of the communications system.

B.3 Normal Operating Procedures

The following section details the normal operating procedures to run the cart.

1. Remove wooden rail covers in 37-127.

2. Turn on power supply on workbench. The 208 VAC 3 phase supply must be plugged into the receptacle conduit running around the lab and the toggle switch on the small aluminum box must be turned on.

3. Turn on power to sled. Push toggle switch located on controller board down. Push start button located on the wall next to the power switch.

4. Run SLDRUN on PDP11/34.

5. Install SLD patch board and SLD analog patch board.

6. Turn on chart recorder, analog computer (compute mode) and PDP8 digital computer.

7. Select 0.05 V/div for channel 1 of recorder, normally 0.5 V/div for channel 2 and 3, and 20 μV/div with X1000 switch for channel 4, and chart speed (50 mm/sec for ramp, variable depending on the frequency of sinusoid).

8. Check proper operation and sensitivity of chart recorder, especially channel 4 by plugging ± 10 volts through potentiometer 2 into T4 on analog.

9. Set potentiometers according to Table B.1

10. Zero the outputs of A16 + A54 using potentiometer 3 and P19.

11. Remove camera and flash from locked cabinet, take to 37-127 and load film.

12. With SLDRUN operating, push toggle switch on controller up, motor should hum with very little rotation. Use the long screwdriver and adjust P2 on the rate loop PC board for zero sled velocity. P2 is on the board closest to the large transformer and is the second potentiometer in towards the winch drum. Turning the potentiometer counterclockwise makes the sled go toward the dummy pulley and vice versa.

13. Install camera on mount, plug flash into flash power supply and turn on (should see a neon glow from inside the flash. Plug camera power cord into camera.

14. Make a bite stick for the subject and inform him/her about the tests, show the subject a demonstration with the chair empty.

15. Seat subject in chair, adjust footrest, fasten lap belt, shoulder strap and head strap after adjusting head rest. Place required amount of foam padding between subject's shoulder and chair frame. Instruct subject on fixation (eye patch on other eye), keeping eye wide open, use of panic switch and communication procedures. Close and lock camera mount, focus camera, and put shroud in place.

16. Conduct communication check with subject and computer room. If okay, enter desired run parameters. Switch subject to audio masking when ready to run using the small box and switch attached to the patch board.

17. Conduct runs, change film as necessary and check focus and cart velocity drift during the runs.

18. Reverse steps 1 through 13 to shut down experiment.

Figure B.2 Connections to Trunk Lines, Patch Board, Analog and Digital Computers

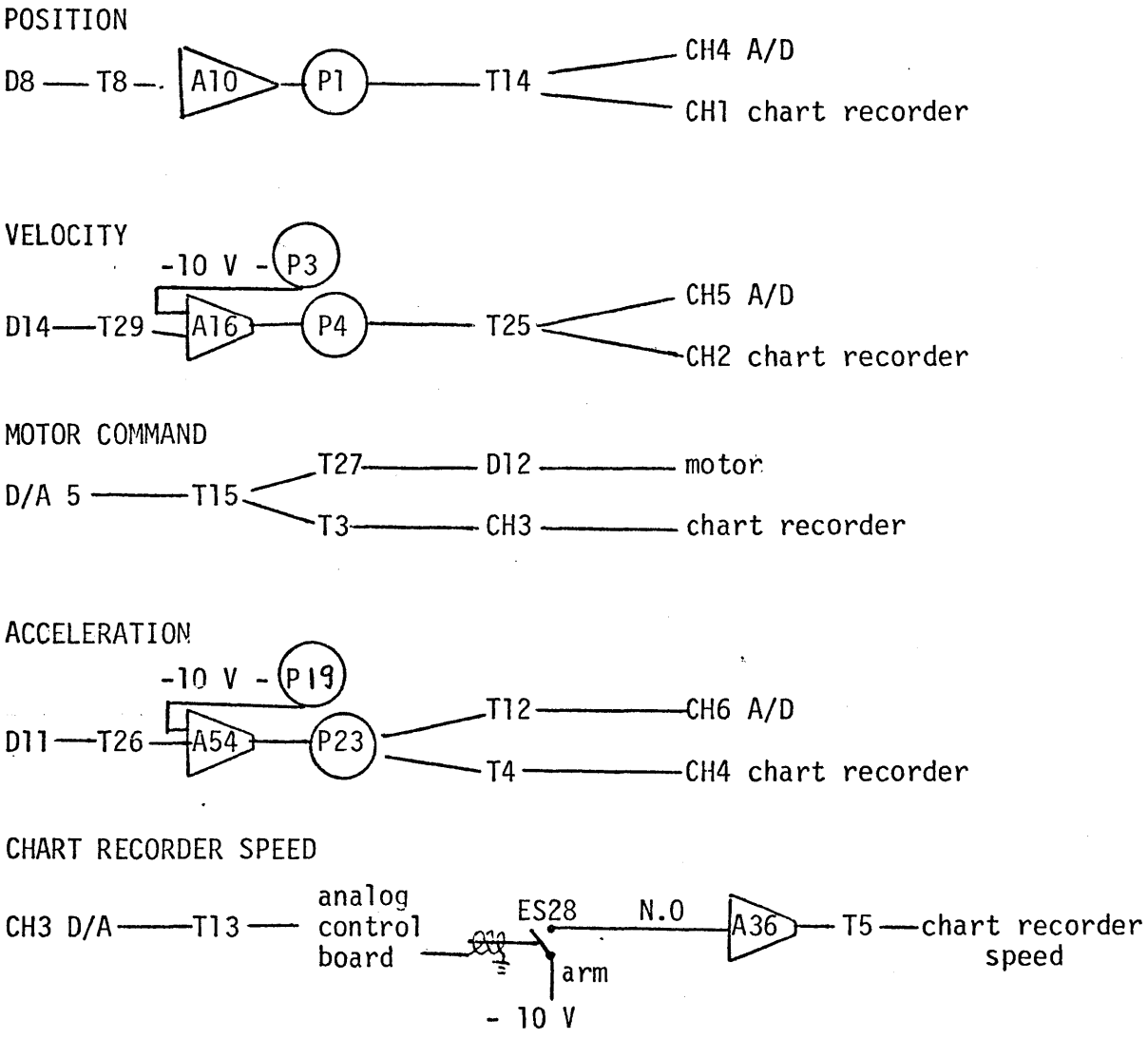

(continued)

Figure B.2 (continued)

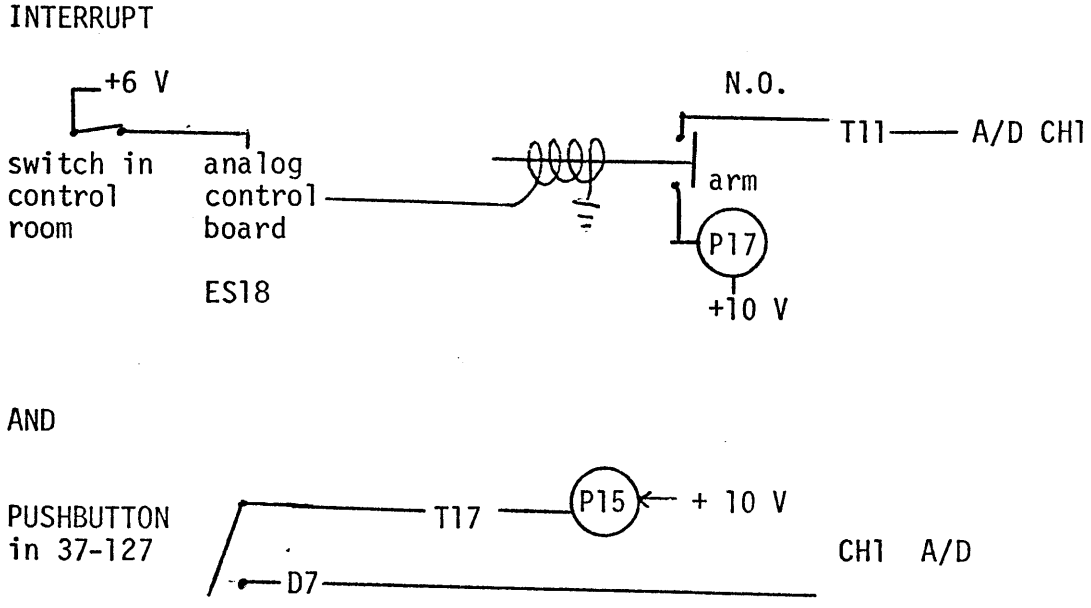

Note:	A/D Channel Number	Patch Board Channel
	1	8
	2	9
	3	10
	4	11
	5	12
	6	13

Figure B.3 COMMUNICATIONS NETWORK

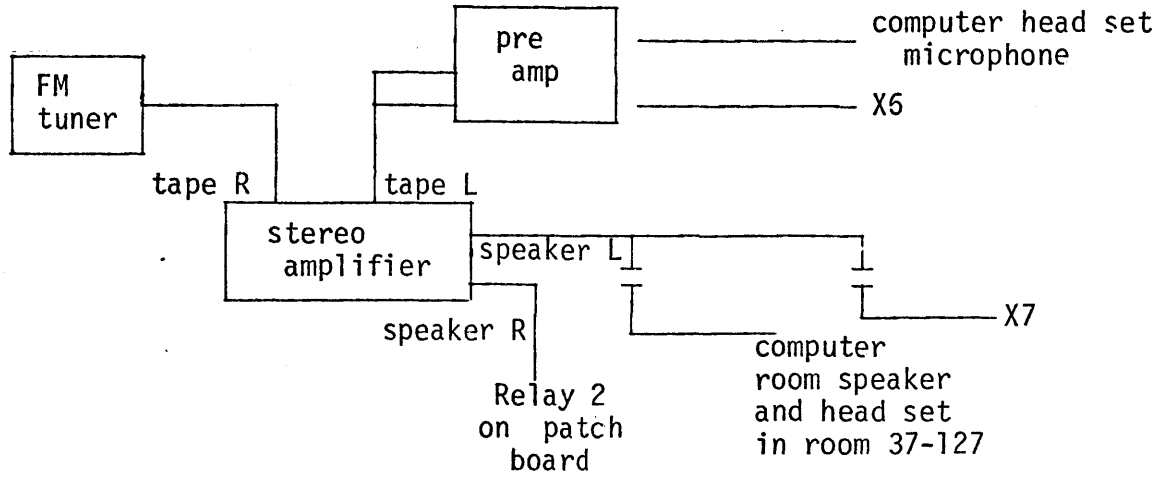

CONNECTIONS

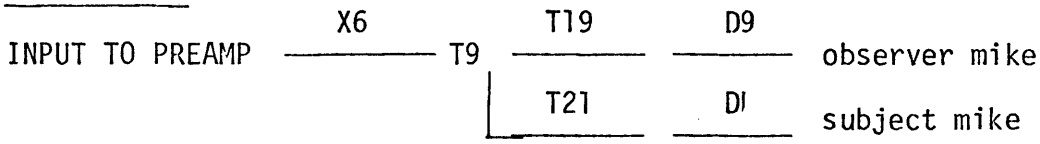

Head phones

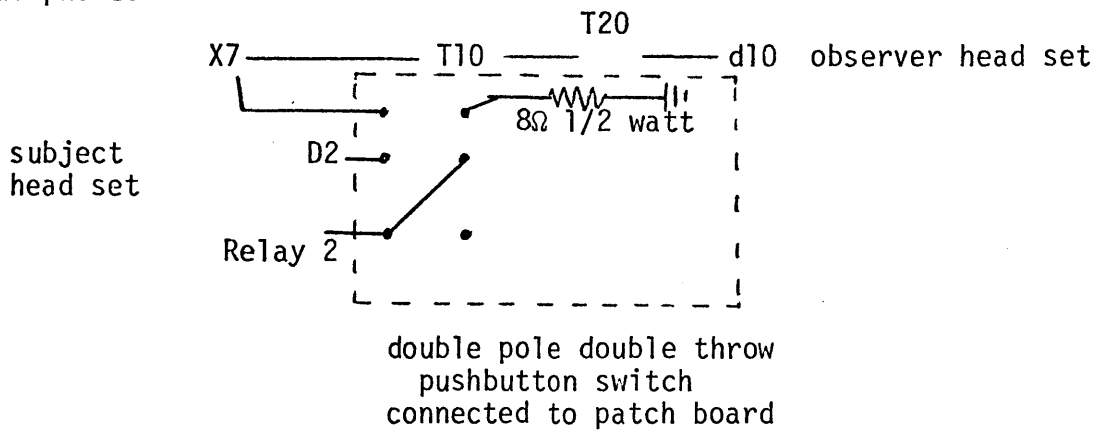

Table B.1 Analog Potentiometer Settings

P1	0.949
P2	0.2
P3	0.07*
P4	1.00
P15	0.98
P17	0.98
P19	0.109**
P23	1.04

*or as needed to zero output of A16 when SLVEL = 0

**or as needed to zero output of A54 when SLACCL = 0

B.4 Computer Printouts

```
      PROGRAM SLDRUN
      DIMENSION NULL(256),INPUT(6),IDATA(4),IZEROS(6)
      COMMON FFLAG
      EQUIVALENCE(INPUT(1),INTRPT)
      COMMON FTYPE,APOLE,RMSDT
      REAL MINVAL,MAXVAL,KVOUT
      INTEGER FFLAG,OUTPUT(6),FTYPE,SFLAG
      INTEGER PSGN,VSGN, TMSEC, TRUN, RESET,SCOUNT
      REAL KPOS,KVEL,KACCL,KCAM,NCOUNT,MCOUNT
93    CALL DTOA6 (IZEROS)
      DO 980 I=1,6
980   OUTPUT (I)=ZERO
      STPOS=0
      WRITE (7,94)
94    FORMAT (2X,'SELECT INPUT, RAMP=-1,SINE=0,RANDOM=+1: '$)
      READ (5,97) IMODE
97    FORMAT (I2)
      ICAMCY=350
      INTLCK=0
      IF (IMODE) 12, 13, 14
C
C     RAMP INPUT
C
12    WRITE (7,98)
98    FORMAT (2X,'ENTER RAMP SLOPE NOT MORE THAN 0.5G:  '$)
      READ (5,99) STAMP      ! READ RAMP SLOPE
99    FORMAT (F5.3)
      IF (STAMP  .GT. GIN) GOTO 105
      STAMP=STAMP*32.17     !CONVERT TO FT/SEC/SEC
      STPOS=TLEN-0.3
      SIFREQ=0.25           !SETS TRUN TO 15 SECS.
      GOTO 110
C
C     SINE INPUT
C
13    WRITE (7,117)
117   FORMAT (2X,'IS FREQ OR AMP THE INDEP VAR (F OR A)?: '$)
      READ (5,115) INVAR      !INDEP VARIABLE
115   FORMAT (A1)
      IF (INVAR .EQ. IFREQ) GOTO 112
116   WRITE (7,101)
101   FORMAT (2X, 'ENTER SINE AMP :'$)
      READ (5,102) SIAMP
102   FORMAT (F5.3)
      IF (SIAMP .GT. GIN) GOTO 105
      FMIN=((SIAMP*32.17/(TLEN-1.))**0.5)/6.28319  !MIN, MAX (HZ)
      FMAX=1.0
      WRITE (7,17) FMIN,FMAX
17    FORMAT (2X,'ALLOWABLE FREQ RANGE IS :',1X,F5.3,'HZ MIN,',
     1  F5.3,'HZ MAX')
112   WRITE (7,103)
103   FORMAT (2X, 'ENTER FREQ (HZ):'$)
```

```
      READ (5,104) SIFREQ
104   FORMAT (F5.3)
      W=6.28319*SIFREQ
      IF (SIFREQ .GT. 1.0) GOTO 107
      IF (INVAR .EQ. IFREQ) GOTO 18
      IF (SIFREQ .LT. FMIN) GOTO 109
23    A=SIAMP*32.17/(W**2.0)      !AMPLITUDE IN FEET
      IF (SIFREQ .LT. .25) ICAMCY=500
      IF (A .GT. 6.5) GOTO 24
      STPOS=A
      GOTO 110
24    STPOS=A+(TLEN-A)/2.
      GOTO 110
18    GMAX=((TLEN-1.5)*W**2.0)/32.17
      IF (GMAX .LE. GIN) GOTO 19
      GMAX=GIN
19    WRITE (7,21) GMAX
21    FORMAT (2X,'MAX AMPLITUDE (G)=',1X,F5.3,1X,':ENTER AMPLITUDE
     1 (G)= '$)
      READ (5,22)SIAMP
22    FORMAT (F5.3)
      IF (SIAMP .GT. GMAX) GOTO 19
      GOTO 23
C
C     PARAMETERS OUT OF LIMITS
C
105   WRITE (7,106) GIN
106   FORMAT (2X,'AMPLITUDE MUST BE NOT MORE THAN',F5.3, 'G')
      IF (IMODE) 12, 116,14
107   WRITE (7,108)
108   FORMAT (2X,'FREQUENCY MUST BE NOT MORE THAN 1.0 HZ')
      GOTO 112
109   WRITE (7,111) FMIN
111   FORMAT (2X,'FREQUENCY MUST BE GREATER THAN',1X,F5.3,1X,'HZ')
      GOTO 112
C
C     RANDOM INPUT
C
14    STOP 'NO RANDOM SUBROUTINE'
110   CONTINUE
      WRITE (7,95)
95    FORMAT (2X,'IS THIS A DEMO(Y OR N)?: '$)
      READ (5,96) IDEMO
96    FORMAT (A1)
      PFLAG=1       !FIRST PASS
5     PFLAG=2     !SECOND PASS
      IF (IDEMO .EQ. IYES) GOTO 6
      WRITE (7,100)
100   FORMAT (2X,'ENTER DATA FILENAME:'$)
      DEFINE FILE1(0,256,U,NREC)
      CALL ASSIGN (1,,-1)
      WRITE (1'1) NULL
```

```
        ICHAN=ILUN(1)
        CALL FILER (ICHAN, IDATA)
6       CONTINUE
        ID=0
        ISET=0
        IPASS=1
        ICYCL=0
        IFLAG=0
        ICOUNT=0
        IFRAME=0
        IPAUSE=500/TMSEC
        TSEC=TMSEC*0.001              !SETS RUN TIME TO 10 SEC
        TRUN=5/SIFREQ                 !OR 5 CYCLES WICHEVER
        IF (TRUN .LT. 10) TRUN=10     !GREATER
        NSTEP=(1/TSEC)*TRUN
        NCOUNT=1./(SIFREQ*TSEC)
        MCOUNT=2.*NCOUNT
        RFLAG=0
        EVENT=0
        TEMP=ZERO
        RESET=ICAMCY/TMSEC-1
        VELCMD=0
        CAMCMD=0
        ITEST=0
        PFLAG=3
        SFLAG=0
        ISIGN=1
        ISTATE=IWAIT
        CALL KWSET(0,0)      !START WAITING
        WRITE (7,114)
114     FORMAT (2X,'HIT INTRPT TO INITIAL.,2ND INTRPT STARTS SLED')
25      CALL KWSET (TMSEC,"411)     !START CLOCK
C*****************************************************************
C
10      CONTINUE                    !TOP OF LOOP
        IF (KWWAIT() .NE. 0) GOTO 845
        CALL ATOD6 (INPUT)
        SLPOS=(INPUT(4)-ZERO)/KPOS
        SLVEL=(INPUT(5)-ZERO)/KVEL
        SLACCL=(INPUT(6)-ZERO)/KACCL
        PSGN=1
        IF (SLPOS .LT. 0) PSGN=-1
301     VSGN=1
        IF (SLVEL .LT. 0) VSGN=-1
        IF (ABS(SLVEL) .LT. 0.2) GOTO 306
302     IF (ISTATE .NE. IRUN) GOTO 306
        IF (PSGN .NE. VSGN) GOTO 306
        IF (TLEN-ABS(SLPOS) .LT. 0.000001) GOTO 700
        IF (ABS(SLVEL)-(2*(TLEN-ABS(SLPOS))*
     1  32.17*DECEL)**0.5 .GT. -2.)   INTLCK=1
306     IF (INTRPT .LE. 3747) GOTO 15   !CHECK FOR INTERRUPT
        CALL KWSET (0,0)
        CALL TTYOUT ('INTERRUPT HIT')
```

```
        CALL KWSET (TMSEC,'411)
        DO 20 I=1,IPAUSE
20      CALL KWWAIT()
        CALL KWSET (0,0)
        CALL KWSET (TMSEC,'411)
        IF (INTLCK .NE. 0) SFLAG=2        !IF INTRPT HIT 4 TIMES
        IF (ISTATE) 7,38,8                !STOP CAMERA AND SLED
8       INTLCK=1
        GOTO 38
7       ISTATE=INITL
        GOTO 10
15      IF (ISTATE) 10,29,38
29      D=ABS(ABS(SLPOS)-STPOS)
        IF (IPASS .GT. 1) GOTO 33
        SGN=PSGN                          !USES SIN VEL FOR 1/8 CYCLE
        B=D                               !THEN PROPORTIONAL TO D
        COEFF=1.
        IF (ABS(SLPOS) .GT. STPOS) COEFF=-1.
33      IF (RFLAG .EQ. 1) GOTO 34
        VELCMD=(B/2.+.05)*COEFF*SGN*SIN(TSEC*IPASS)
        IF (ABS(SLVEL) .GT. D) RFLAG=1
        IF (RFLAG .EQ. 0) GOTO 35
34      VELCMD=(D+.05)*SGN*COEFF
35      IPASS=IPASS+1
        IF (ABS(D) .LT. .05) VELCMD=0.
        OUTPUT (2)=VELCMD*KVOUT+ZERO
        CALL DTOA6 (OUTPUT)
        GOTO 10
38      ISTATE=IRUN
        SPEED=6.                          !SPEED UP C.R.
        IF (IFRAME .GT. 1) GOTO 41        !WAIT AND TAKE TWO PICTURES
39      IF (ICYCL .NE. 0) GOTO 200        !AT 350MSEC THEN
        CAMCMD=5.
        OUTPUT (1)=CAMCMD*KCAM+ZERO
        OUTPUT (3)=CAMCMD*2*KCAM+ZERO
        OUTPUT (4)=SPEED*KCAM+ZERO
        CALL DTOA6(OUTPUT)                !TAKE PIC AT ICYCL=0
        GOTO 201
200     IF (ICYCL .NE. 1) GOTO 201
        CAMCMD=0.
        OUTPUT(1)=CAMCMD*KCAM+ZERO
        OUTPUT(3)=CAMCMD*2*KCAM+ZERO
        CALL DTOA6(OUTPUT)
201     ICYCL=ICYCL+1
        IF (ICYCL .LT. RESET) GOTO 10
        IFRAME=IFRAME+1
        ICYCL=0
        GOTO 10
41      ICOUNT=ICOUNT+1
        IF (IMODE .EQ. -1) GOTO 42
        IF (ICOUNT .LT. MCOUNT) GOTO 375
42      IF (ICYCL .NE. 0) GOTO 300.  !RUN STARTED, TAKE PICTURE
```

```
        CAMCMD=5                        !AND START SLED
        ICYCL=ICYCL+1
        GOTO 375
300     IF (ICYCL .NE. 1) GOTO 360
        ICYCL=ICYCL+1
        CAMCMD=0
        GOTO 370            !WAIT ICAMCY MSEC AND TAKE ANOTHER PIC
360     ICYCL=ICYCL+1
370     IF (ICYCL .LT. RESET) GOTO 375  !AFTER ICAMCY MSEC RESET TO 0
        ICYCL=0
375     CONTINUE
        IF (ICOUNT .GT. 2) GOTO 376
        ISIGN=-1*PSGN
376     IF (INTLCK .NE. 0) GOTO 700     !SAFETY LOGIC TRIPPED
        IF (SFLAG .NE. 0) GOTO 800
        IF (IMODE) 400, 500, 600        !SELECT OUTPUT
C
C
400     VELCMD=ISIGN*STAMP*ICOUNT*TSEC          !RAMP VEL. CMD
        GOTO 800
C
C
500     VELCMD=A*W*ISIGN*SIN(W*TSEC*ICOUNT)     !SINE VEL. CMD
        GOTO 800
C
C
600     STOP'NO RANDOM SUBROUTINE'
C
C
700     IF (IFLAG .NE. 0) GOTO 705      !SAFETY INTERLOCK SET
        INTLCK=1
        ISTOP=ICOUNT
        VEL=VELCMD
        IFLAG=1
705     IF (ABS(VELCMD) .GT. .41) GOTO 707
        VELCMD=0.
        GOTO 800
707     VELCMD=VEL-(VSGN*32.17*DECEL*(ICOUNT-ISTOP)*TSEC)
C
C
800     PFLAG=4
        IF (IDEMO .EQ. IYES) GOTO 45    !OUTPUT VELCMD AND FILE DATA
801     IDATA(1)=SLPOS*K
        IDATA (2)=SLVEL*K
        IDATA (3)=SLACCL*K
        IDATA(4)=CAMCMD*2*K
        CALL FILER (ICHAN,IDATA)
45      OUTPUT (1)=CAMCMD*KCAM+ZERO
        OUTPUT (2)=VELCMD*KVOUT+ZERO
        OUTPUT (3)=CAMCMD*2*KCAM+ZERO
        CALL DTOA6 (OUTPUT)
        IF (INTLCK .EQ. 1) GOTO 47
```

```
        IF (IMODE .EQ. -1) GOTO 10
        IF (ICOUNT .LT. NSTEP) GOTO 10
47      IF (ABS(SLVEL) .GT. .41) GOTO 10     !END OF LOOP
        IF (SFLAG .EQ. 2) GOTO 76
        VELCMD=0.
        IF (SFLAG .EQ. 1) GOTO 46
        SCOUNT=ICOUNT
        SFLAG=1
46      IF (ICOUNT .GT. (SCOUNT+NCOUNT)) GOTO 76
        GOTO 10
845     CALL DTOA6 (IZEROS)              !STOP FOR SYNCH ERROR
        STOP 'SYNCH ERROR IN PROGRAM'
76      CONTINUE
        CALL KWSET (0,0)        !STOP CLOCK
        CALL DTOA6(IZEROS)      !ZERO D-A LINES
        PFLAG=5
        IF (IDEMO .EQ. IYES) GOTO 909
        IDATA (1)=SLPOS*K
        IDATA (2)=SLVEL*K
        IDATA (3)=SLACCL*K
        IDATA (4)=CAMCMD*2*K
        CALL FILER (ICHAN,IDATA)
        CALL CLOSE(1)
909     WRITE (7,910)
910     FORMAT (2X,'WANT ANOTHER RUN (Y OR N)?: '$)
        READ (5,911) IREQ
911     FORMAT (A1)
        IF (IREQ .EQ. IYES) GOTO 93
        DATA NULL/256*0/,
     1  IZEROS,ZERO/6*2048,2048./,
     1  IWAIT,INITL,IRUN/-1,0,1/,
     1  TLEN,DECEL,KPOS,KVEL,KACCL/7.5,0.35,204.8,110.09,2048./,
     1  IYES,INO,IFREQ,IAMP/'Y','N','F','A'/,
     1  FTYPE,APOLE,RMSDT/2,3.14,15./,
     1  MAXVAL,MINVAL,TMSEC /32767.,-32767.,30/,
     1  KVOUT,KCAM,K/116.496,204.8,1000/,
     1  GIN/0.3/
        END
```

APPENDIX C

LNS DIGITIZER OPERATION

C.1 Vacuum System

Before turning on the machine, turn on the vacuum pump that is used to hold down the film. The controls are in the room across the hall from room 428. Switch on VAC 3, using the controls on the wall to the left of the door. The needle on the gauge labelled "Scanning Room" should drop from zero to somewhere between 20 and 30.

C.2 Power Controls and Loading Film - Hermes Senior

The power switch is in the upper right hand corner. Turn it on. To load the film, put all three operate switches down, i.e. 1, 2, and 3. Inside the door of the cabinet are three switches for the film drive motors for the three views. Put those down. Load your film. Then turn on only the drive motors and the operate switch for the view(s) you are using. Other controls:

Lamps: on

Reticle: Start by turning this knob clockwise and holding it there for a few seconds while the reticle motor speeds up.

Move-Measure: Move for moving film; Measure for measuring.

Keys and Data: The use of keys and data will be explained in the measuring procedure.

C.3 ZEROING THE MACHINE COORDINATES

The binary registers for the x and y coordinates are not zeroed when the machine power comes on. They occasionally can pick up erroneous readings during machine use due to power surges, etc. Therefore, they should be zeroed after the power is turned on and about every fifteen minutes during use. Note that the zeroing should not be done during the measurement of an event (a series of measurements terminated by the E key). The following procedure is the normal zeroing procedure. The procedure noted in Section 3.5 should be followed for OCR recording.

(1) Set the view switch to view 2. Move the film until the white spot in the dark frame above the center of the frame is centered on the reticle. While holding the CTL key down, press the Ø key. To check that the coordinates are correctly zeroed, now or at any later time, center the white spot on the reticle, push the FL key, press 1 and then 7 to set indicator to 1700, then press either data key. You should hear a beep. If no beep and/or the red error light comes on, press FL, 5,6 and the data key. This will remove the red error light. Then repeat above. If still no beep and/or a red light, call Ragnhild. If you press Fl, 1 and 7 when the spot on view 2 is not centered on the reticle, you should get the red light, unless you have zeroed the registers at the place where the film is currently positioned.

Setting FRAME Number

Press the FC key. The current frame number will be displayed. To type in a new frame number, key in the four desired digits. The digit entered by the stroke of a key will appear to the left of the dot on the indicator. For output on the typewriter, frame numbers are not printed.

C.4 LOGGING IN

In the PDP8 room, there are two teletypewriters. On the one being used for log-in, log-out, turn the line-off-local switch to line. Type LG and carriage return (CR). The teletypewriter will type:

TBL,ROLL,EXP,OP,SN,MN,SCNR,G/S. You should respond with the following information, separated by commas except after the G/S which is to be followed by a CR.

TBL - your machine number. Hermes Senior is number 9, for example. The table numbers are posted on the frame of each machine.

ROLL - Obtain a roll number from Marianne and use it regularly, since your data will be taken off the data tape, if used, by that number. Data with other roll numbers will have to be taken off in separate computer runs. Logging with the wrong table number may cause all your data to be lost.

EXP - You may assign any two digit (decimal) number to your experiment that you wish.

OP - 0 - means that your data will be put on the magnetic tape to be subsequently converted to card format data for you on

cards or tape.

1 - means that your data will be punched on paper tape. If you want this option, be sure to turn the other teletype to LINE, make sure that there is paper in the paper punch and push the "on" button on the punch.

2 - means that your data will be typed on the typewriter in the following format:

FLAG	x in microns	y in microns
	OCTAL (DECIMAL)	OCTAL (DECIMAL)
xxxx	xxxxxx (xxxxxx)	xxxxxx (xxxxxx)

The meaning of the flag will be described under measuring.

SN - Scan number; use any decimal digit

MN - Measurement number; use any decimal digit.

SCNR - Your assigned scanner number. Please get a number from Marianne and use only that number.

G/S - G means go, S means stop.

1. After G or S type CR.
2. After G, one of two messages will be typed.

   TYPE FIRST FRAME NUMBER

   or START AT FRAME NUMBER NNNNNN

   If you receive the first message, type any six digit number you wish and CR. For the second message, no response is needed.
3. After S a message will be typed.

TYPE LAST FRAME NUMBER

Type any six digit frame number you wish and then CR.

C.5 MEASURING

A. The first point

You can measure any number of points up to 88 in a series called an event. For the first point, press FL, then 7 so the indicator reads 7000. Then set the reticle on the point and press the data key.

B. Subsequent points

On subsequent points, you may set the indicator to any one of the following values as a marker. On the printed output, the flag will have a value that is uniquely, but mystifyingly, related to the value to which you set the indicator. The allowed indicator values are indicated below with the corresponding flag values.

INDICATOR	FLAG	
7000	0000	(must be used on first point of
0000	0000	event)
1000	0000	
2000	0010	
3000	0100	
5000	0200	
6000	0210	
1200	0400	
1300	1000	
1011	0000	
1111	0001	
1211	0002	
1311	0003	
1411	0004	
1511	0005	

If you use other values you may cause an error, or worse, erase the previous data in your event. DO NOT USE 7000 after the first point. Using the 7000 indicator causes all previous points to be rejected.

C. Ending a series of measurements (an event)

When you have finished a series, or measured in 88 points, press the E key.

NOTE: If you are taking your output on punched paper tape, you must warn the other users before you push E, since their machines will not respond until the tape has been completely punched.

This will advance the event number by one and start putting your output on the chosen device. You cannot start measurements again until the data are all written out. If you do, you will get a red error light. To remove the red error light, press FL, 5 and 6 and then data. You should get a beep, the red light will go out and you can try again, repeating your new first point. If your output is on paper tape or the typewriter, it will take a long time. You can listen to the machine typing to hear when it is finished. If you are not sure how many points you have measured, you can go to the log-in typewriter, switch it to LINE and type 1AAAA CR where AAAA is given below.

Table #	AAAA
6	3023
7	3623
8	4423
9	5223
10	6023

The typewriter will respond with an octal number equal to the number of points you have measured since last pushing E.

C.6 LOGGING OUT

Same as logging in except type S (stop) instead of G. If you are working alone, turn off the PDP8 following the instruction manual at the computer. If other people are working, leave your machine on. It will be turned off at the end of the shift. If no one else is using a hand-measuring machine, turn off the vacuum system.

C.7 DATA FORMATS

A. Typed: this format is described in section 2.

B. Paper tape punch:

The format is the following. The six bits per row of tape are, in pairs, the most significant six bits (0-5) and the least significant six bits (6-11) of each word of the record. The record format (12 bit) is as follows.

WORD #	
1	number of words to follow in record
2	record type (irrelevant)
3	roll number
4	scanner number (yours)
5	frame number, most significant bits
6	frame number, least significant bits
7	event number in bits 5-7
8	table number
9	scan number (2-6), measurement number (7-11)
10	scanner number (yours)
11	spare
12	spare
13	2048 + view number
14	point code, P. (1-3), generation code, G (4-6) 1 if key pushed, T. (7), ionization code, I. (9-11)
15	most significant bits of x (0-5), most significant bits of y (6-11)

WORD #

16 least significant bits of x
17 least significant bits of y

Words 14-17 are the first x-y point. Successive x-y points are formatted in 4-word blocks like 14-17, for a total of 88 points.

The relationship between the keys pushed on measuring a point and the bits that end up in word 14 are a bit confusing but the following keys are legal and produce simple results.

KEY	P	G	T	I	OCTAL
0000	0	0	0	0	0000
1000	0	0	1	0	0020
2000	0	1	1	0	0060
3000	0	2	1	0	0020
5000	0	4	1	0	0220
6000	0	5	1	0	0260
1200	1	0	1	0	0420
1300	2	0	1	0	1020
1011	0	0	0	0	0000
1111	0	0	0	1	0001
1211	0	0	0	2	0002
1311	0	0	0	3	0003
1411	0	0	0	4	0004
1511	0	0	0	5	0005

C. Magnetic tape output

Under this mode, data are written on the magnetic tape of the PDP8 and are extracted on the LNS IBM 360/65 in the following format on cards, or magnetic tape (FORTRAN format notation).

FRAME NUMBER, table number, view number, 5 measured points (c,y), card index, measurement number, event number

I4, I2, 3x, I1, 10I6, "0", I1, 6x, 2I1

This format is repeated for each set of five points. The card number is 0 for a card if more data are coming in a series, 1 if the card is the last one of a series.

APPENDIX D

Data

A complete set of OCR versus time plots for static OCR data is presented first, followed by the ramp data and finally the sinusoidal data. During the data collection, the ramp velocity data was taken before the sinusoids on each subject. The run number indicates the order within ramps or sines in which the stimuli were presented. For example, subject 7 received the static OCR stimuli first, then the ramp velocity profiles 0.05, 0.1, 0.2, 0.3 g then followed by 0.2 Hz, 0.4 Hz, and 1.0 Hz sinusoids all at 0.2 g. The labeling of plots consists of first the type of stimulus, static, ramp, or sine, second the subject number and third the acceleration level (for ramps) or frequency (for sines). All sinusoids were performed at 0.2 g except for subject 14 who underwent stimuli of 0.3 Hz, 0.1, and 0.2 and 0.3 g.

Ramp Code		Sine Code	
0	0.05 g	1	1.0 Hz
1	0.1 g	2	0.2 Hz
2	0.2 g	4	0.4 Hz
3	0.3 g		

In this manner STAT08 is the static OCR data for subject 8, ramp 72 is the ramp data for subject 7 at 0.2 g and sin 121 is sinusoidal data for subject 12 at 0.2 g, 1.0 Hz.

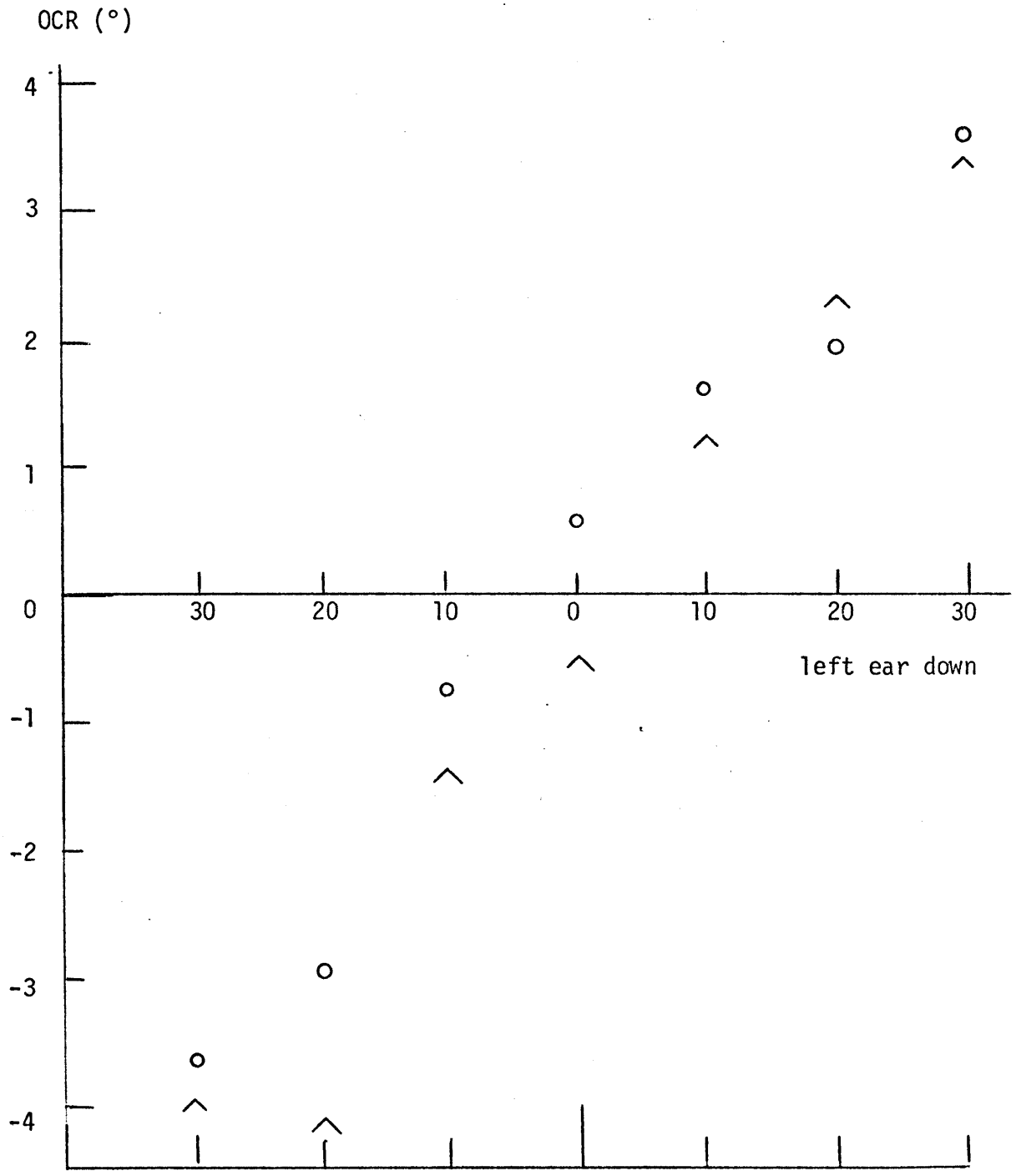

Figure D.1 Static OCR of subject O. Two symbols indicate two different pictures taken about 5 to 10 seconds apart.

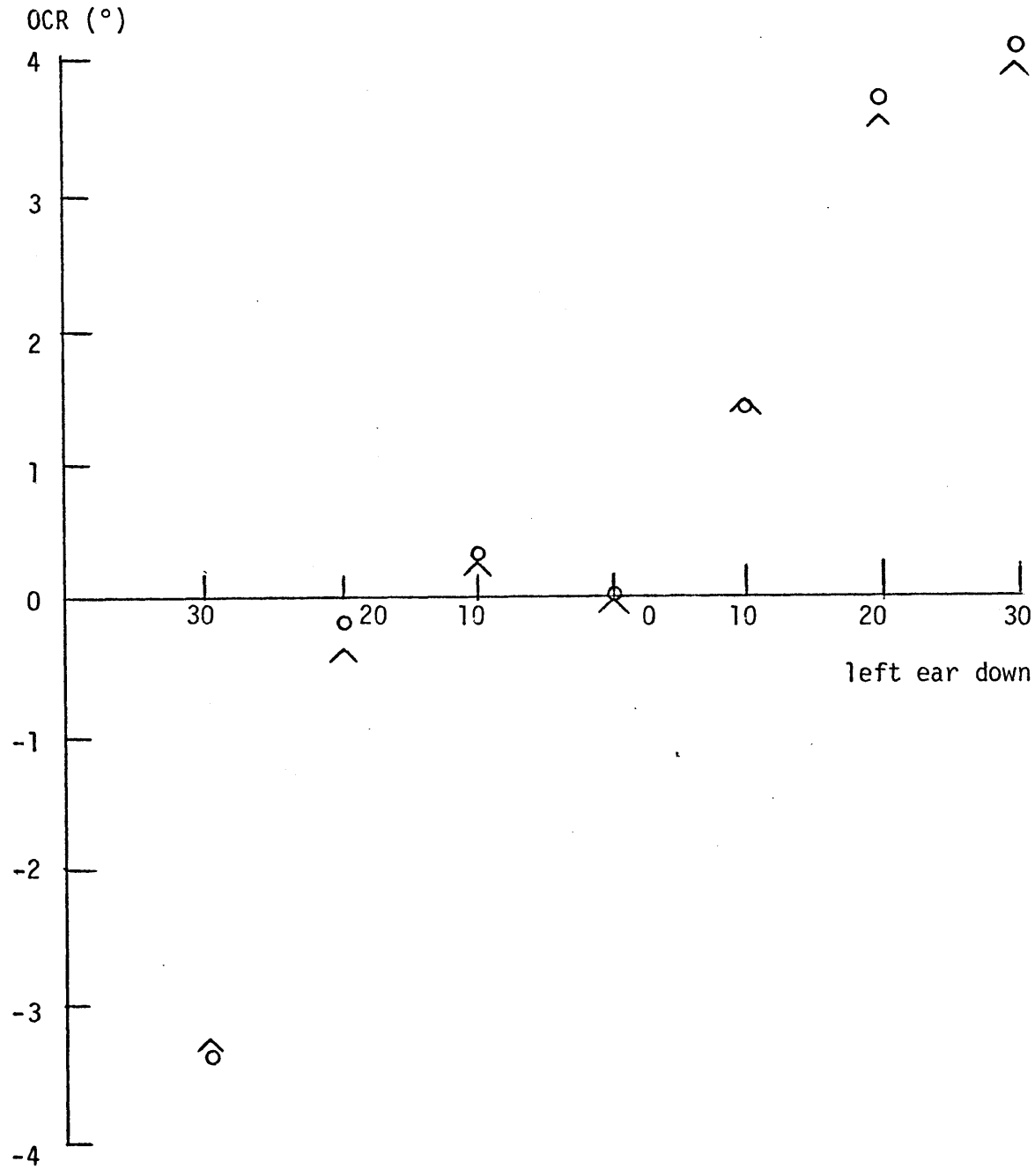

Figure D.2 Static OCR of subject 3. Two symbols indicate two different pictures taken 5 to 10 seconds apart.

Figure D.3 Static OCR of subject 6. Two symbols indicate two different pictures taken 5-10 seconds apart.

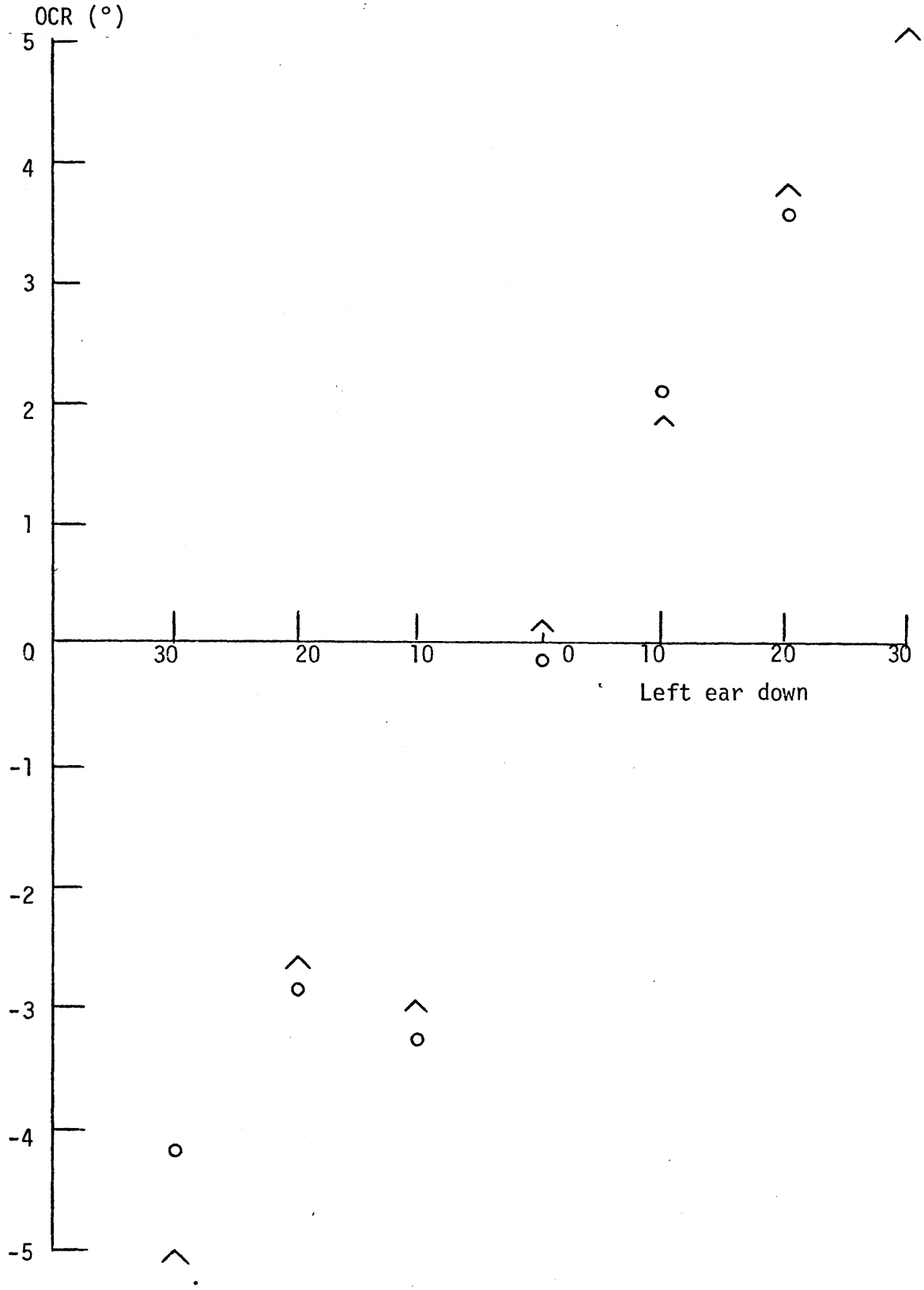

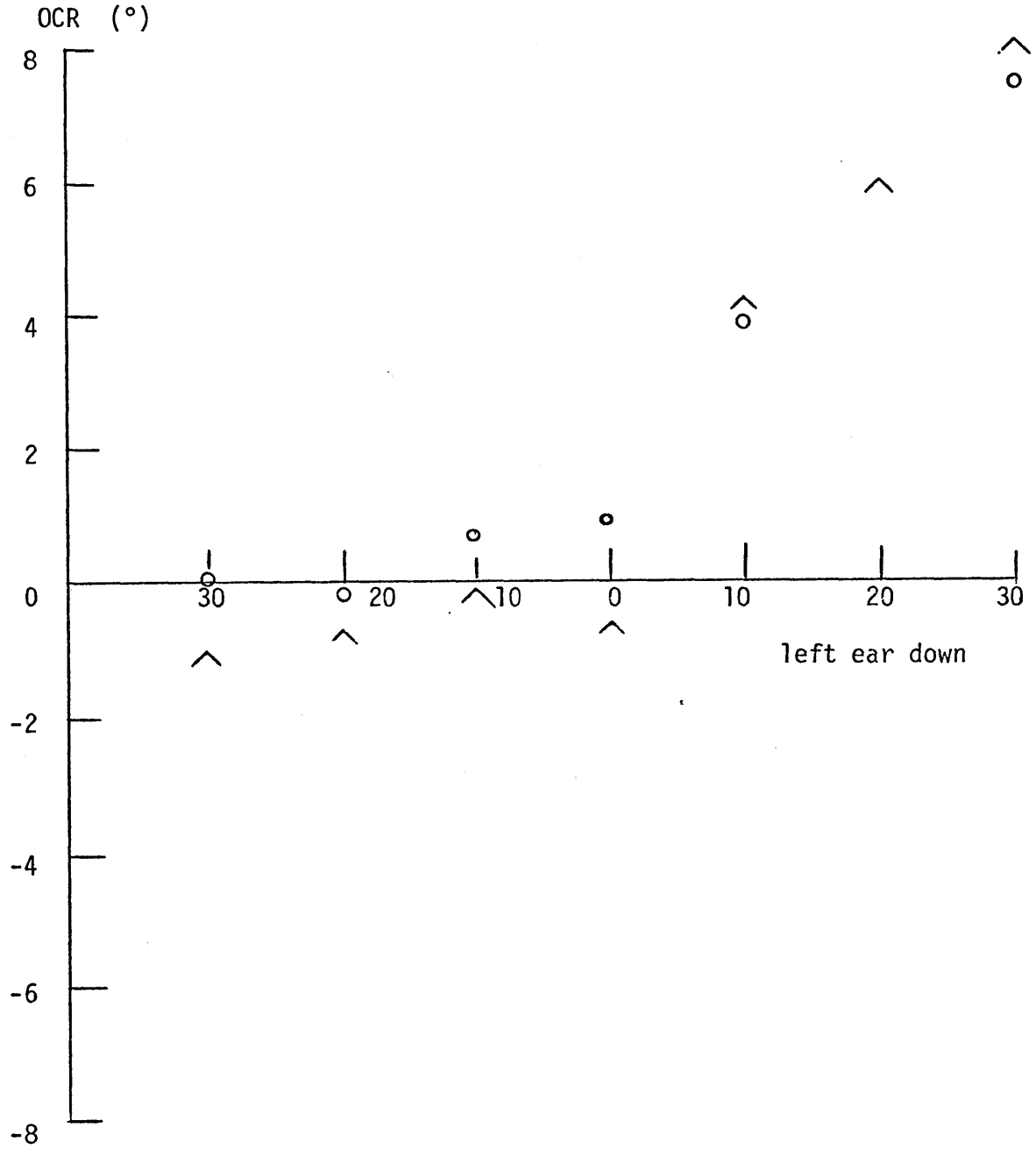

Figure D.4 Static OCR of subject 7. Two symbols indicate two different pictures taken about 5-10 seconds apart.

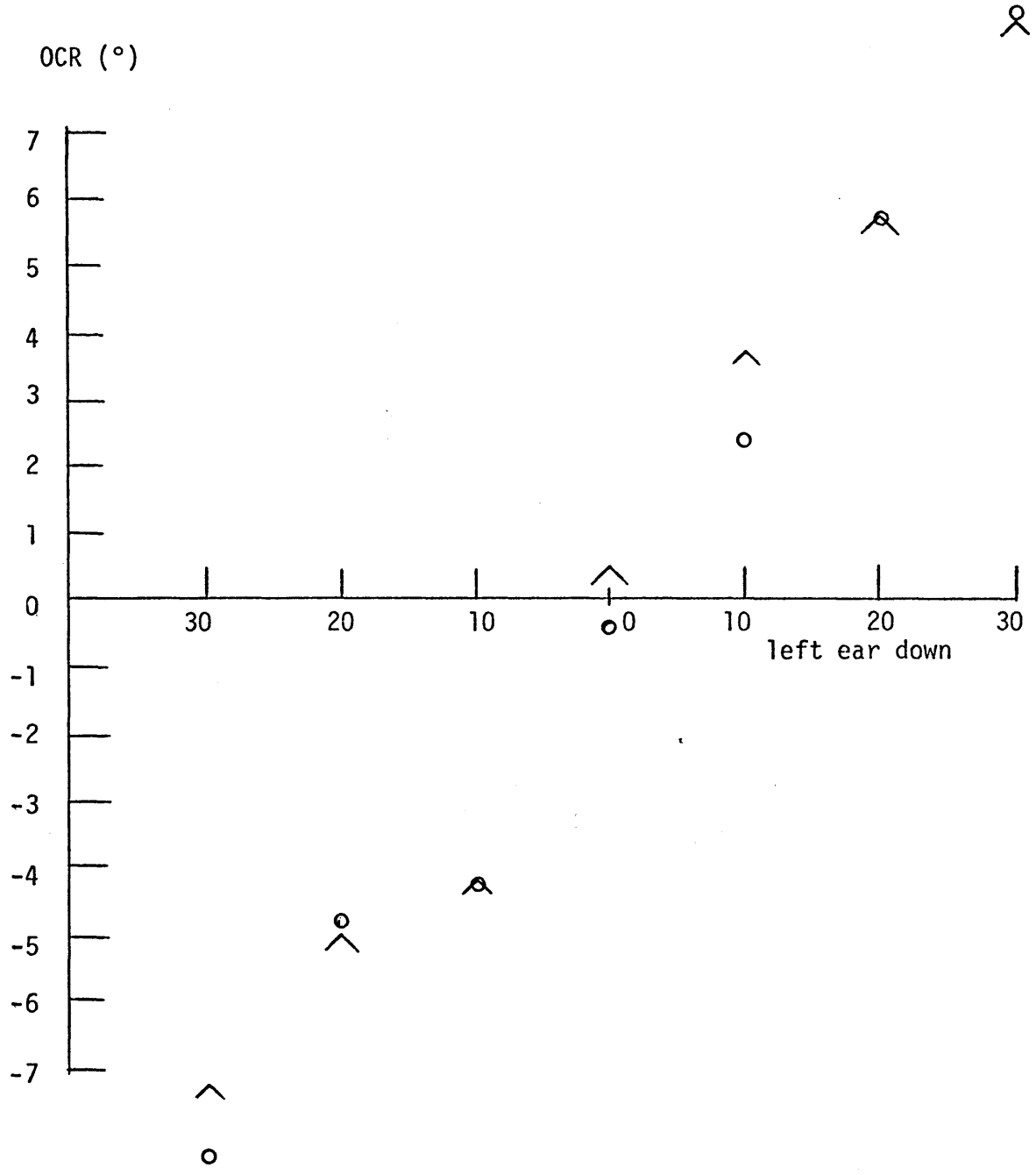

Figure D.5 Static OCR of subject 8. Two symbols indicate two different pictures taken about 5-10 seconds apart.

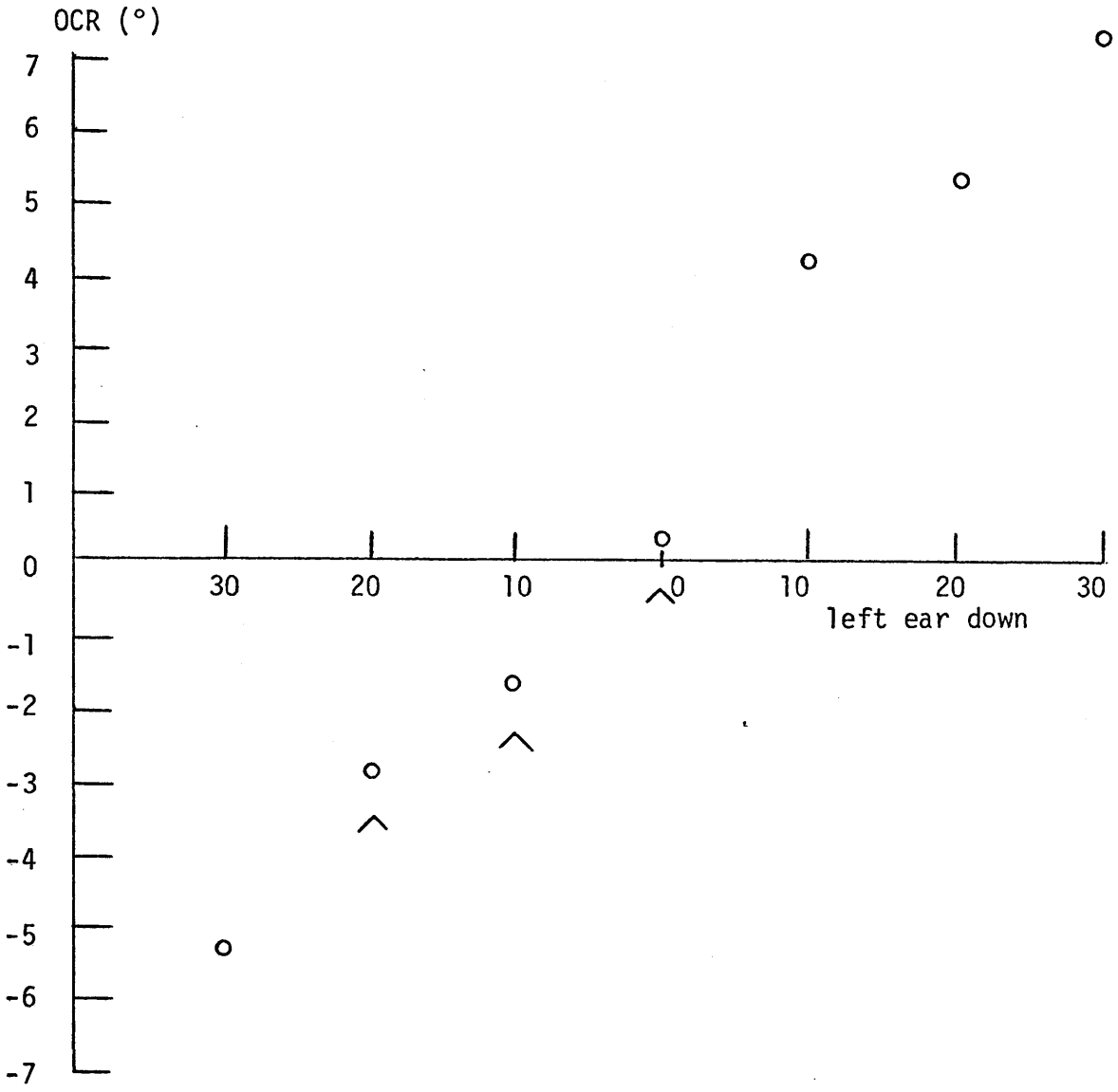

Figure D.6 Static OCR of subject 12. Two symbols indicate two different pictures taken 5 to 10 seconds apart.

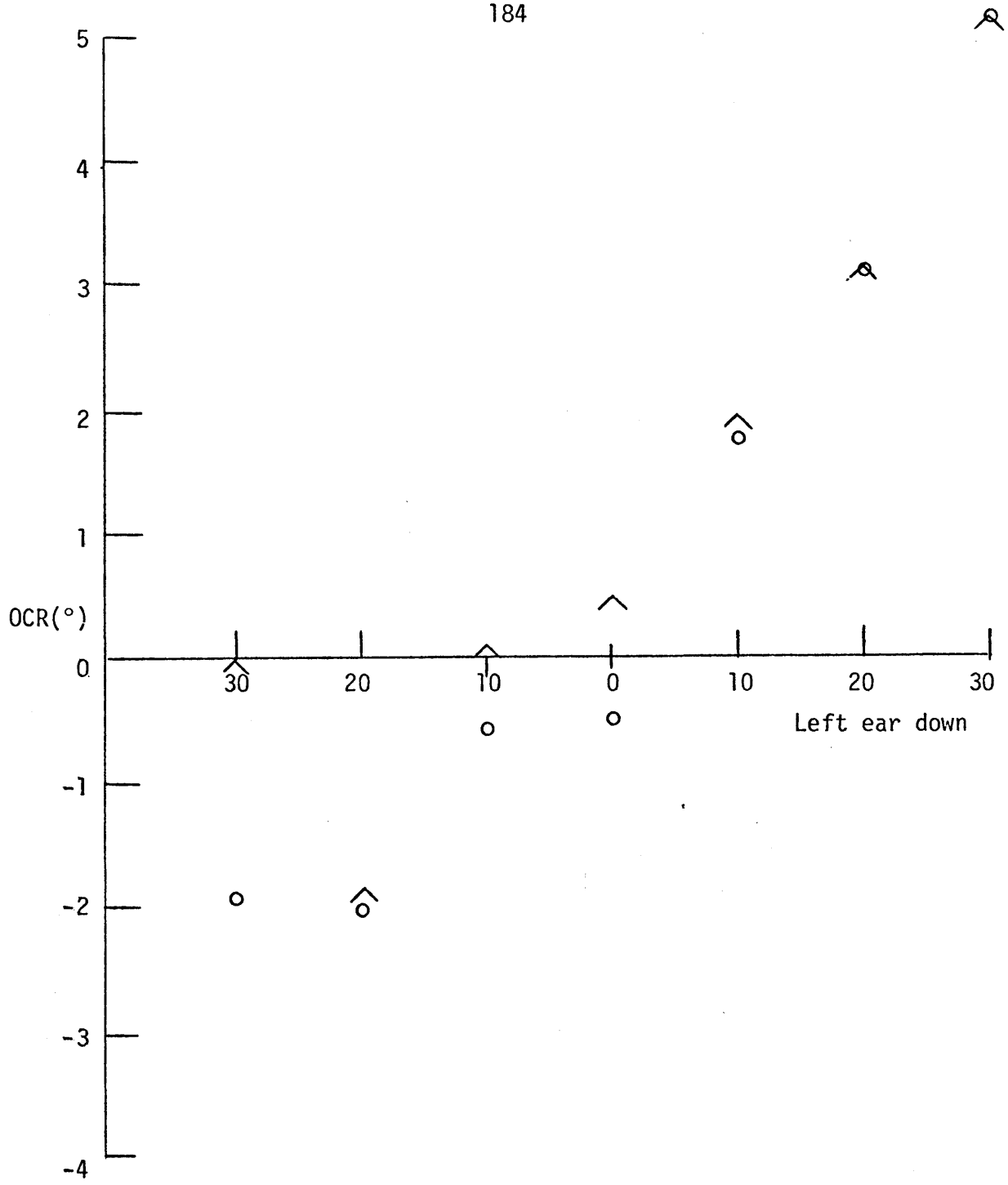

Figure D.7 Static OCR of subject 14. Two symbols indicate two different pictures taken about 5 to 10 seconds apart.

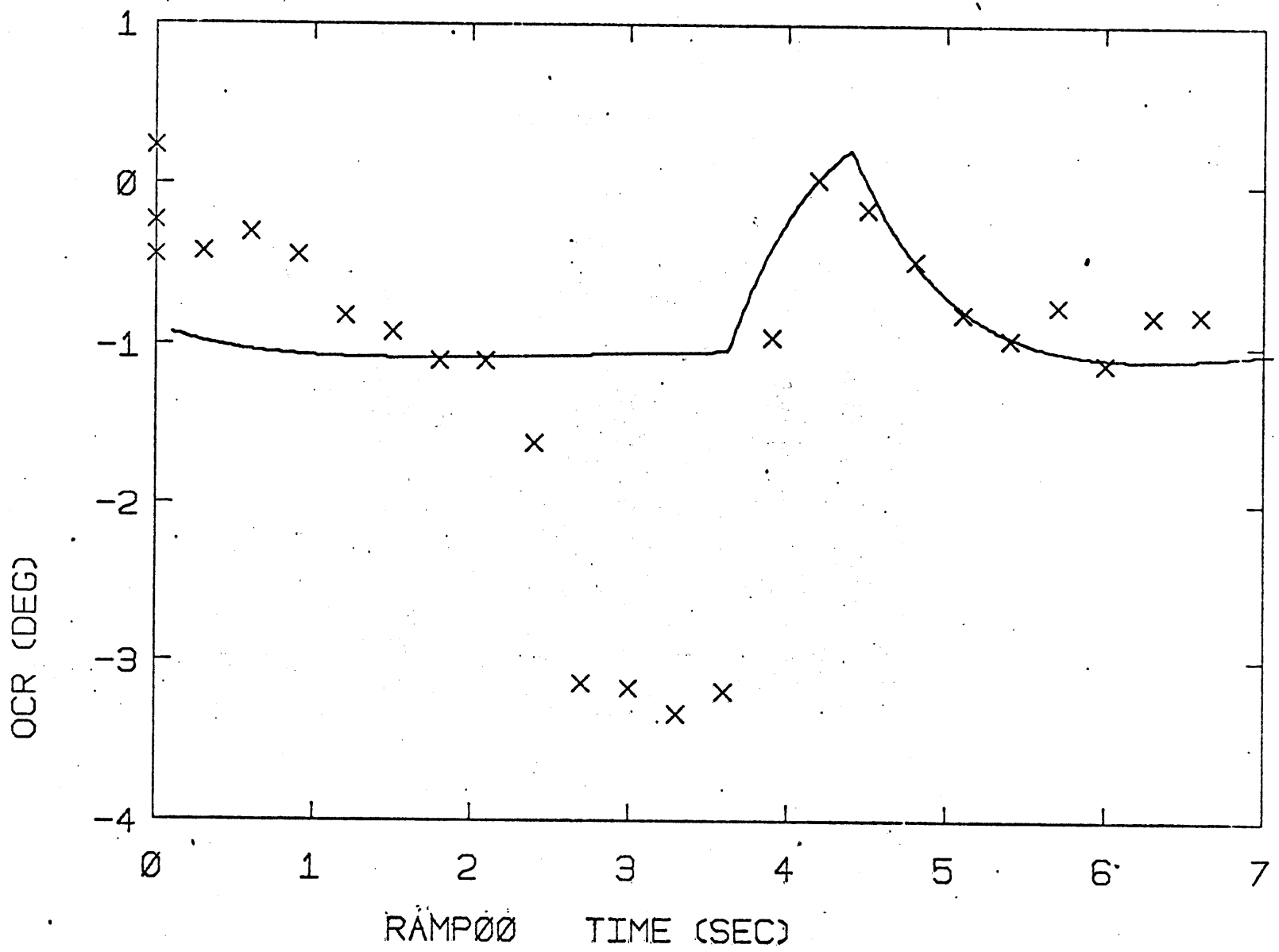
1
0
-1
-2
-3
-4
0
1
2
3
4
5
6
7
OCR (DEG)
RAMP00 TIME (SEC)

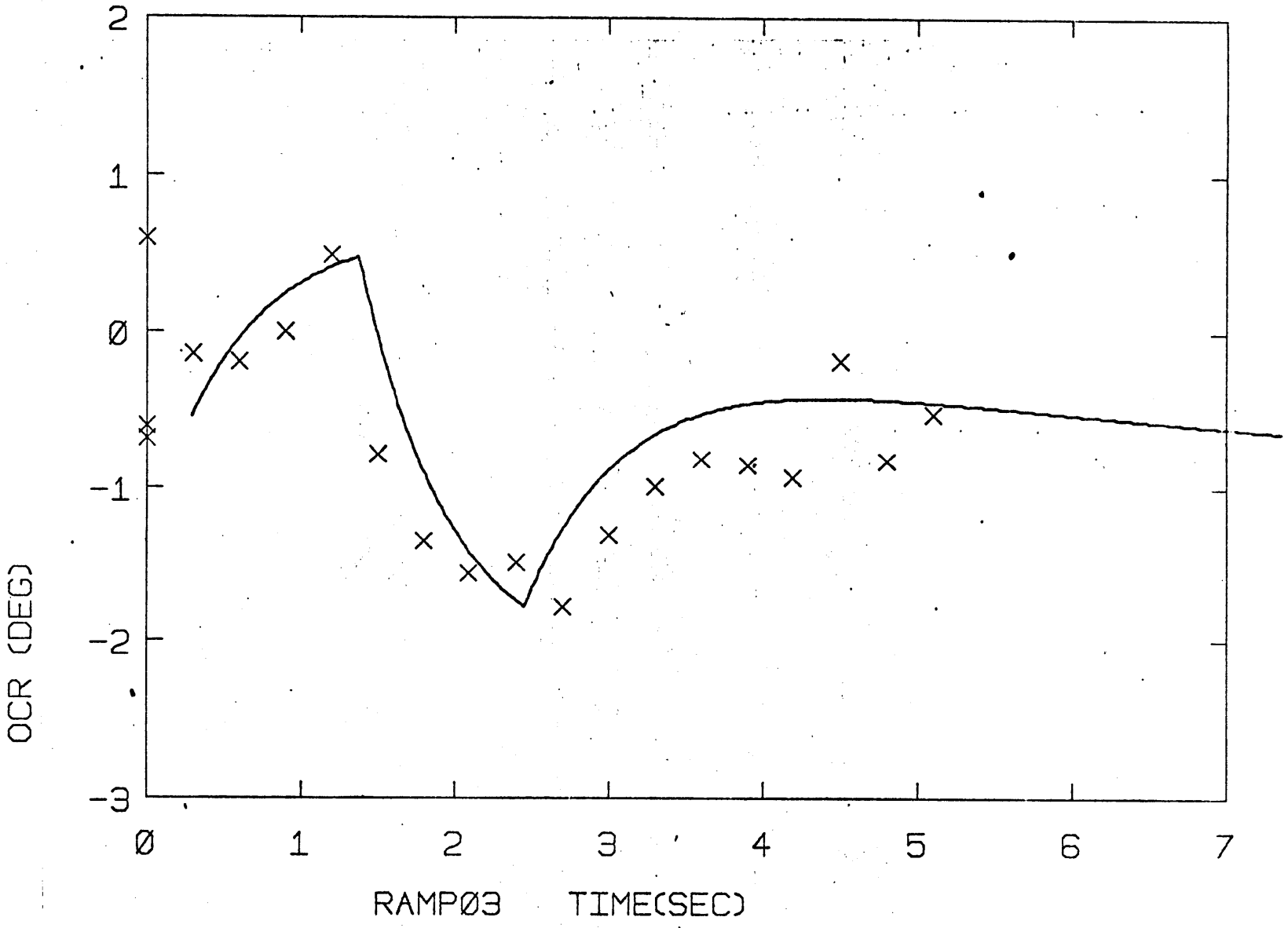
2
1
0
-1
-2
-3
0
1
2
3
4
5
6
7
OCR (DEG)
RAMP03 TIME(SEC)

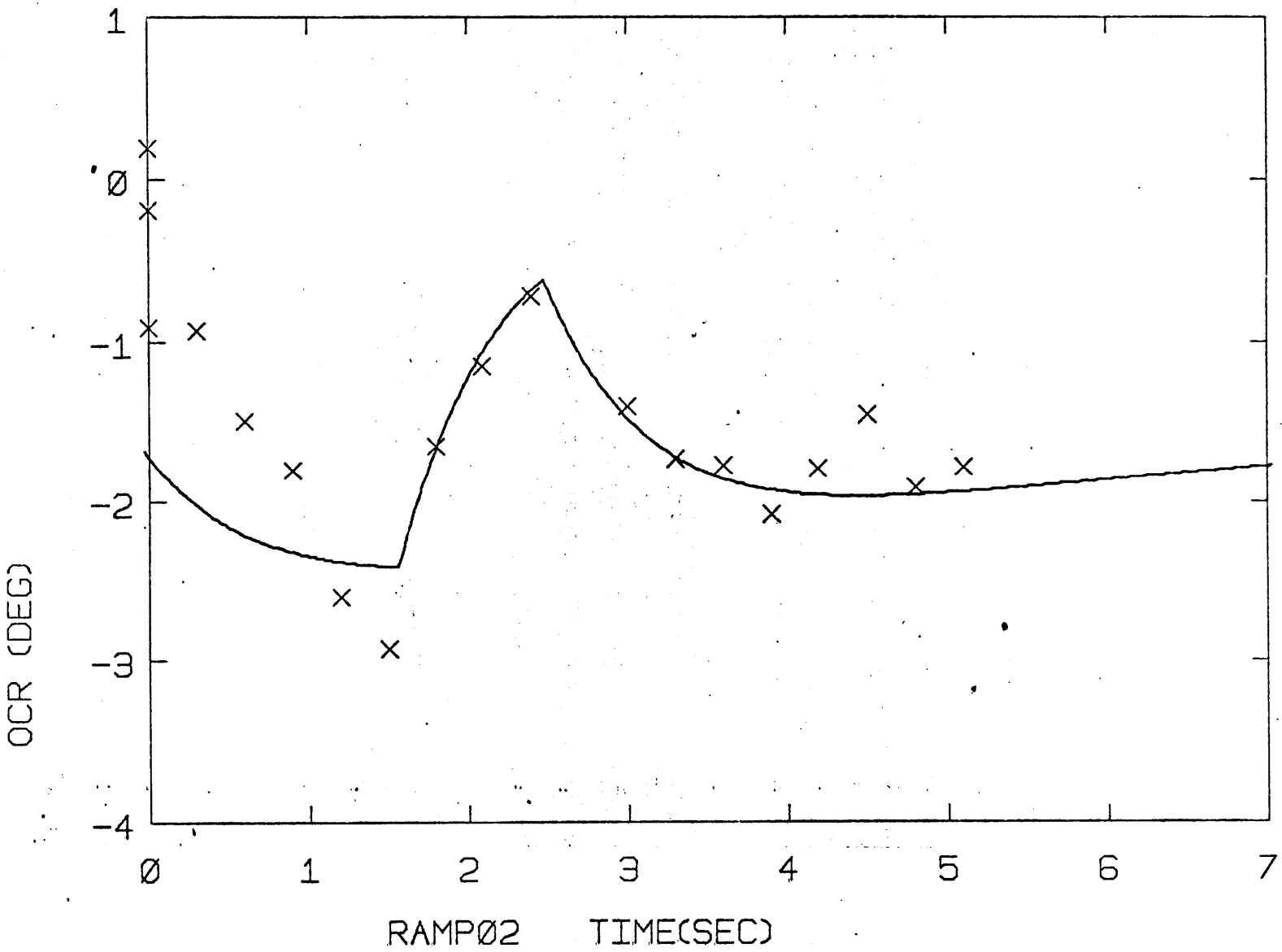
1
0
-1
-2
-3
-4
OCR (DEG)
0
1
2
3
4
5
6
7
RAMP02 TIME(SEC)

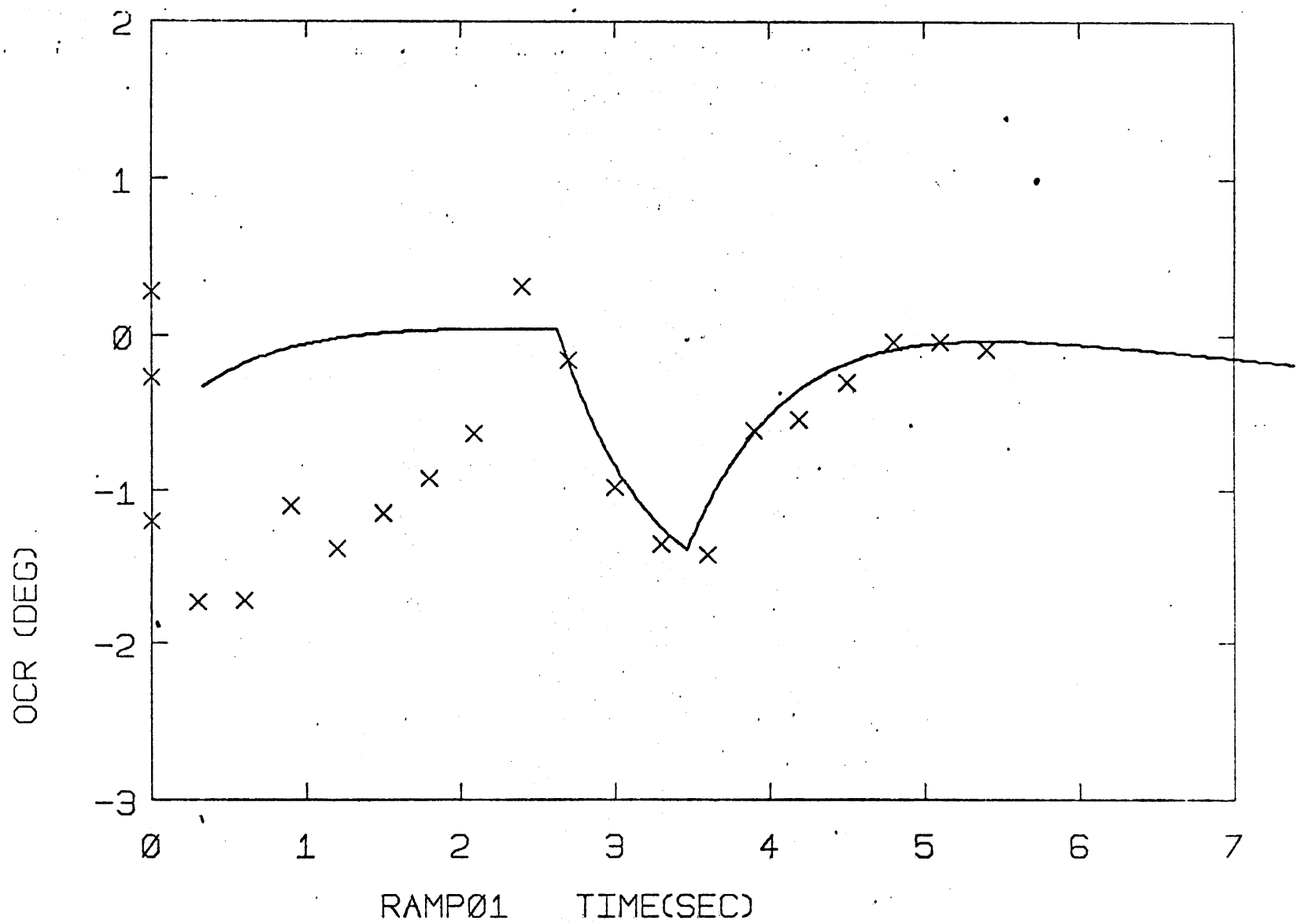
2
1
0
-1
-2
-3
0
1
2
3
4
5
6
7
OCR (DEG)
RAMP01 TIME(SEC)

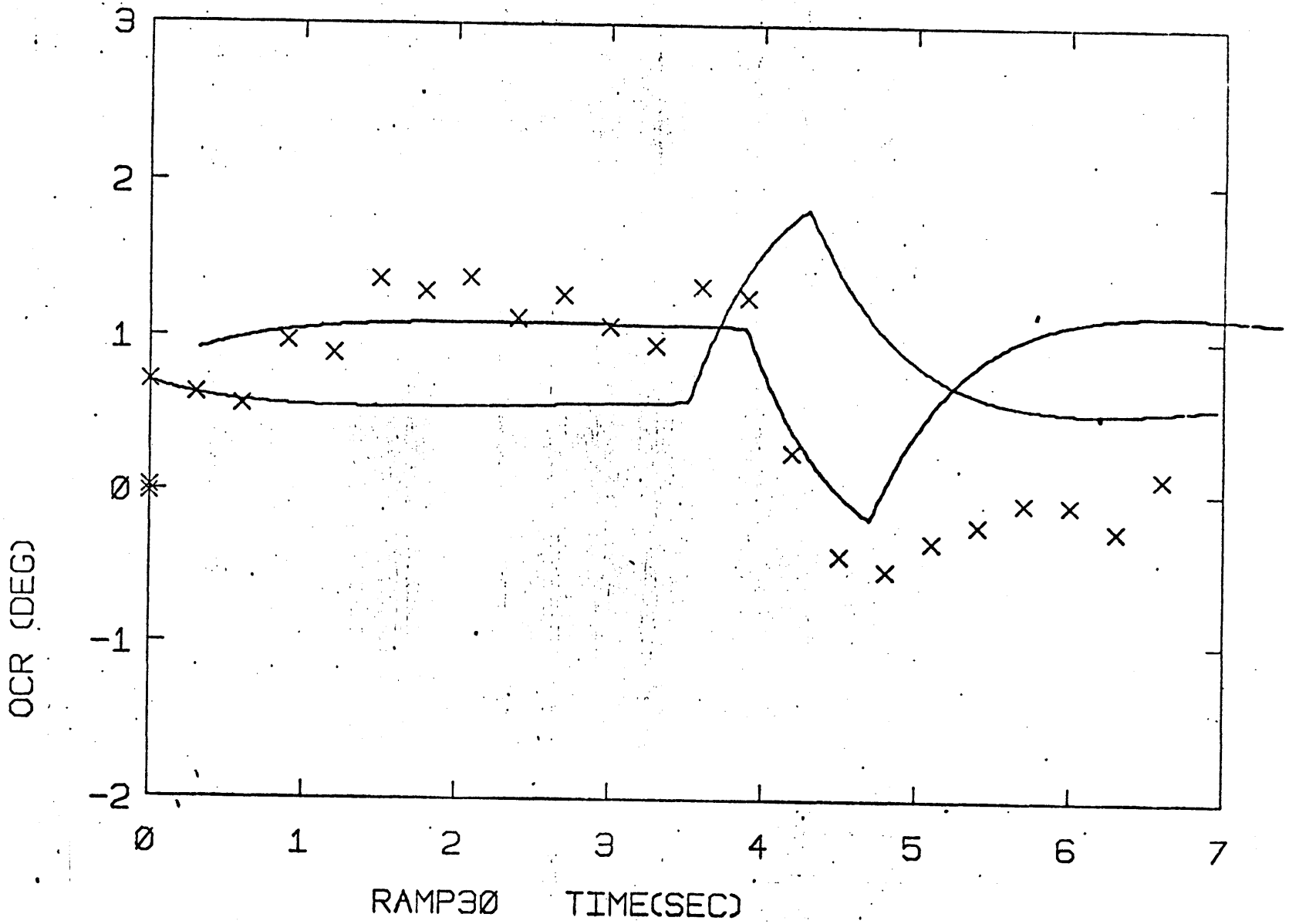
3
2
1
0
-1
-2
0
1
2
3
4
5
6
7
OCR (DEG)
RAMP30 TIME(SEC)

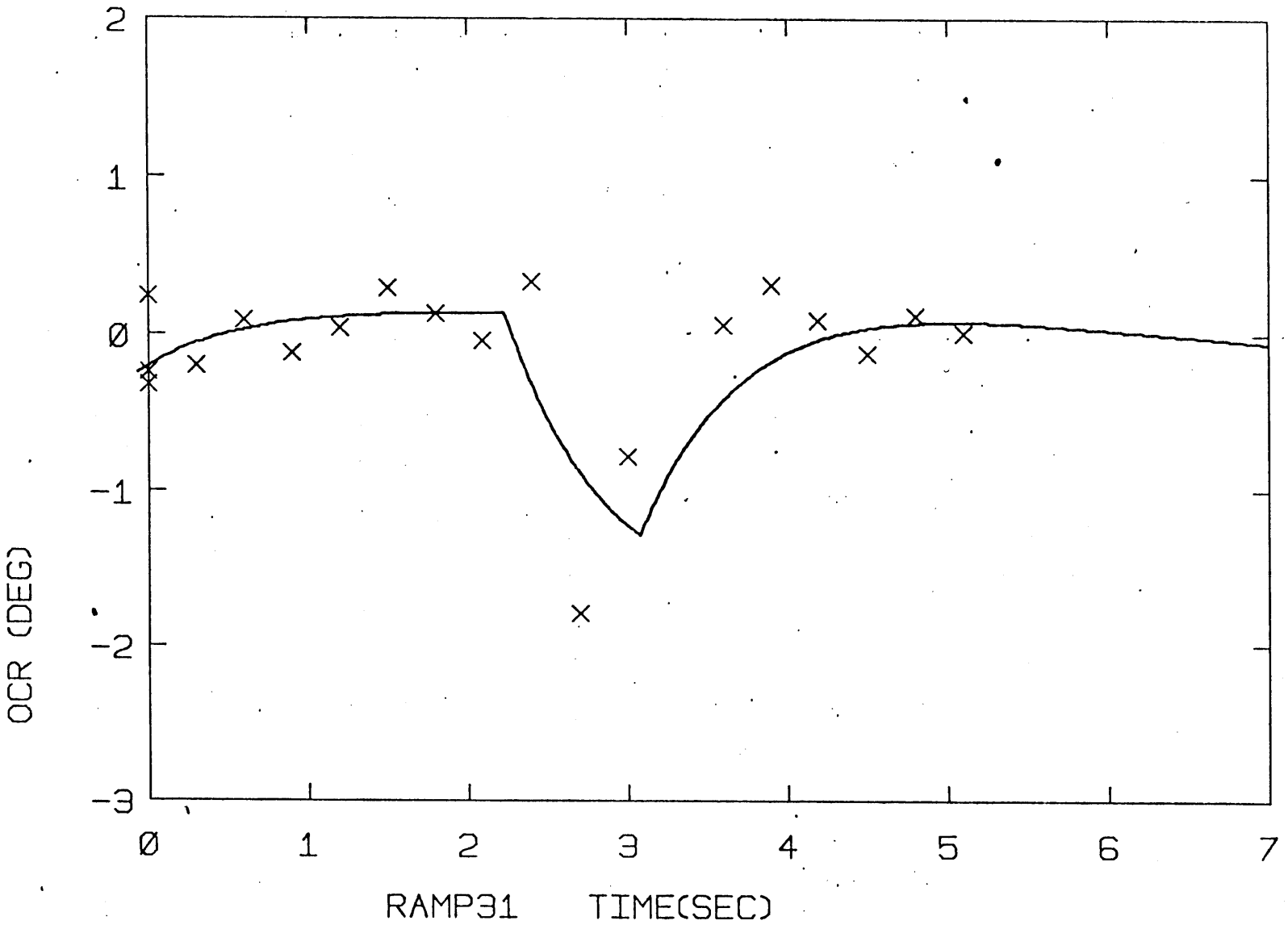
2
1
0
-1
-2
-3
0
1
2
3
4
5
6
7
OCR (DEG)
RAMP31 TIME(SEC)

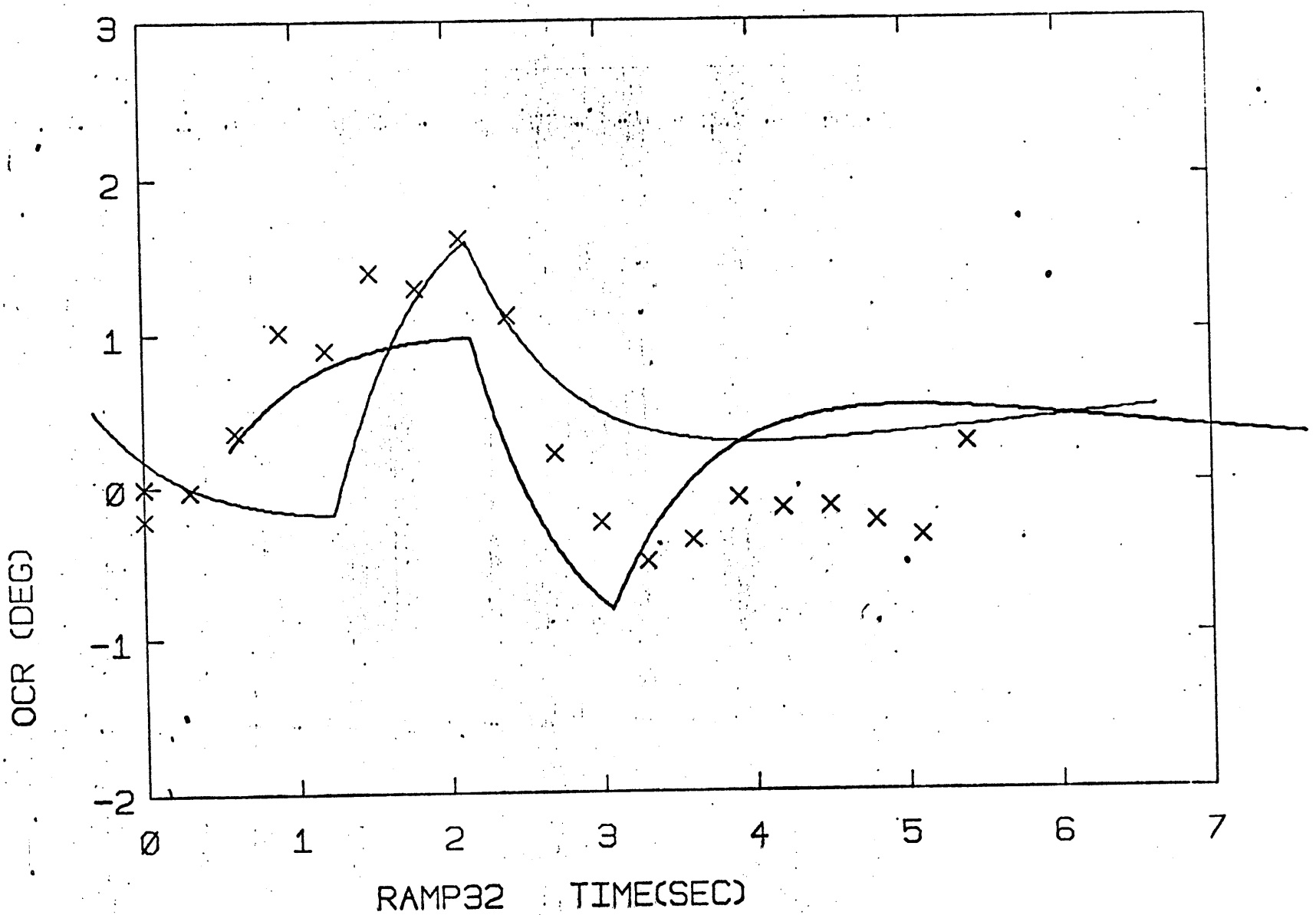
3
2
1
0
-1
-2
OCR (DEG)
0
1
2
3
4
5
6
7
RAMP32 TIME(SEC)

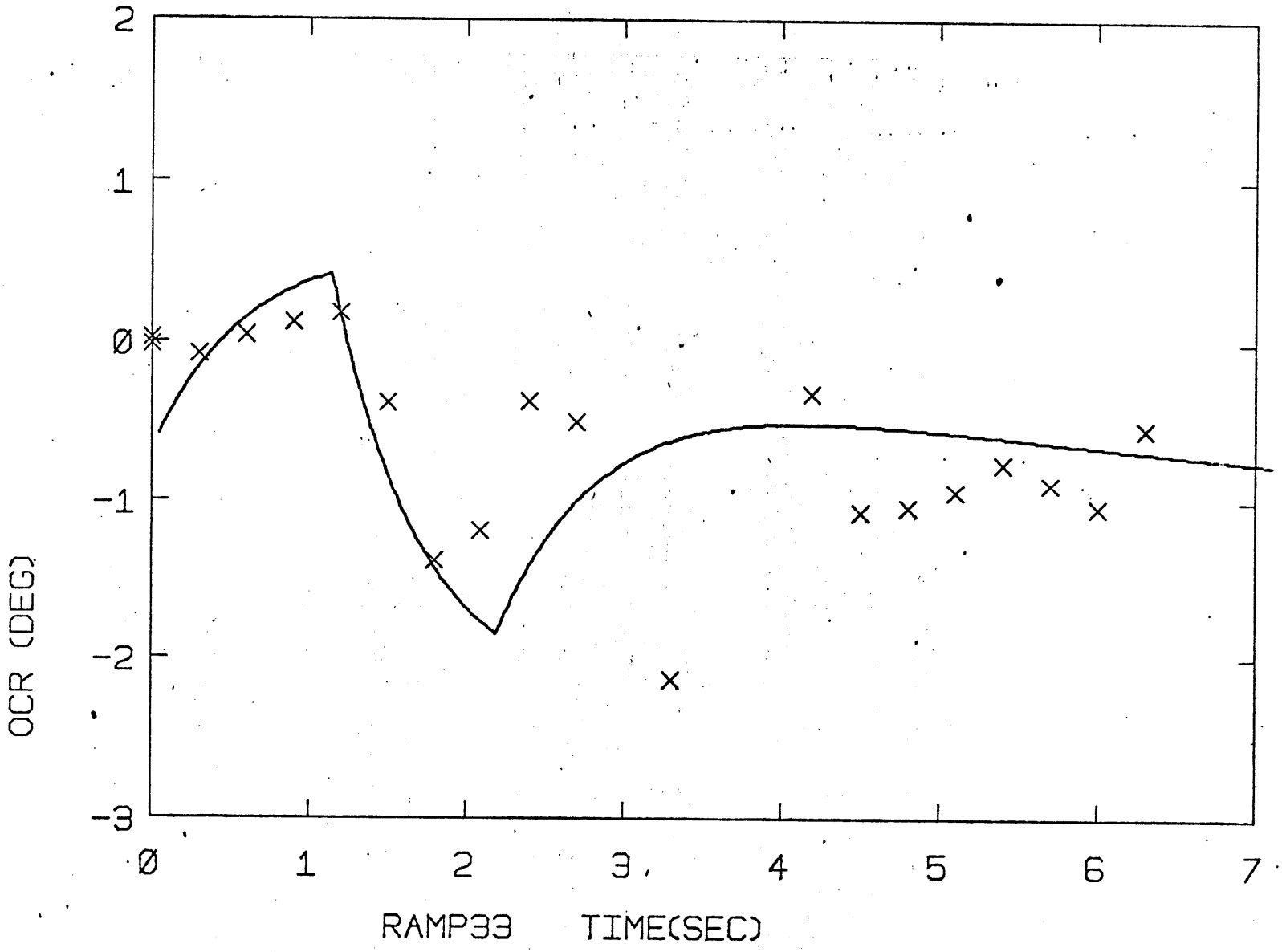
2
1
0
-1
-2
-3
OCR (DEG)
0
1
2
3
4
5
6
7
RAMP33 TIME(SEC)

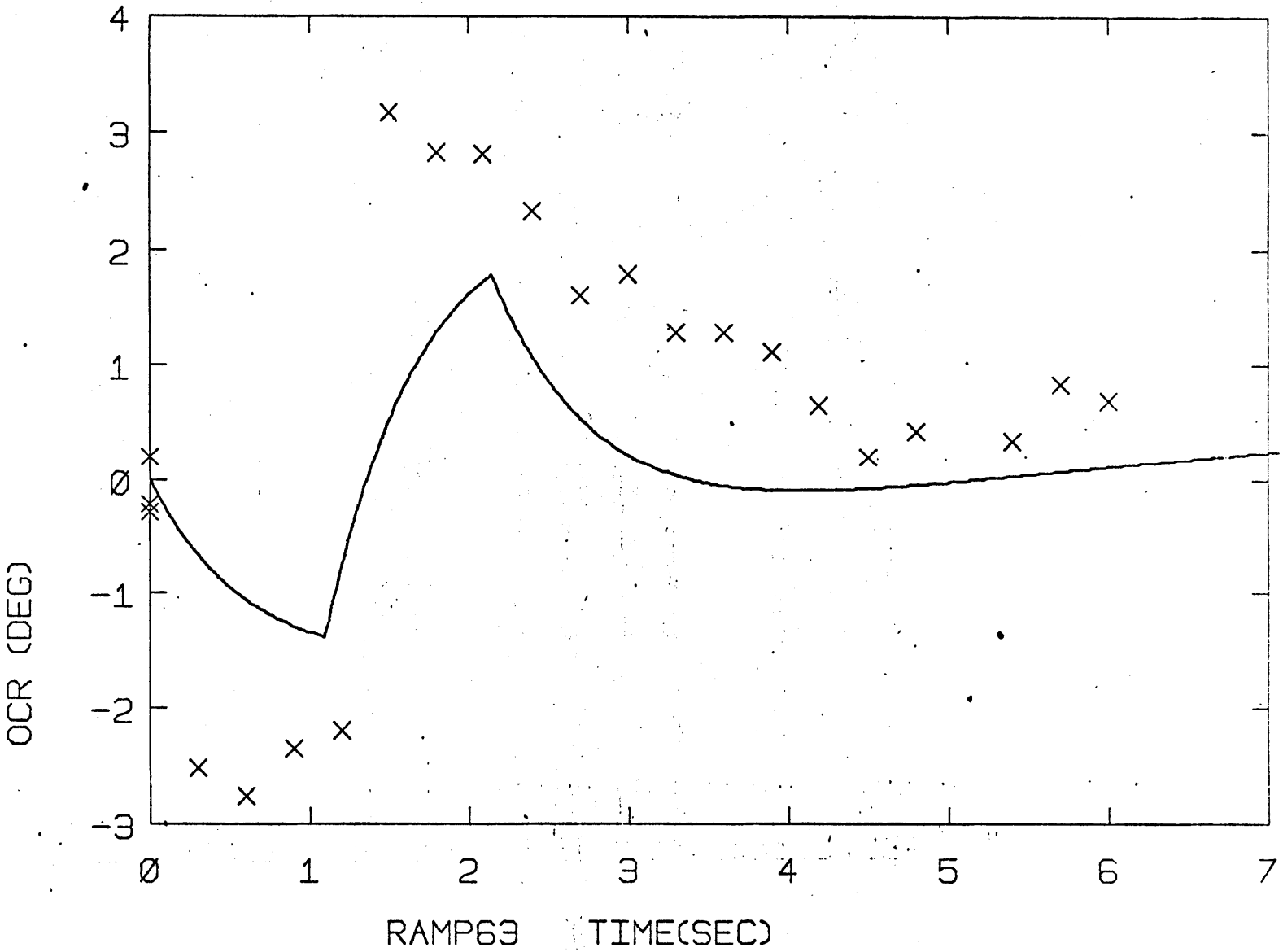
4
3
2
1
0
-1
-2
-3
OCR (DEG)
0
1
2
3
4
5
6
7
RAMP63 TIME(SEC)

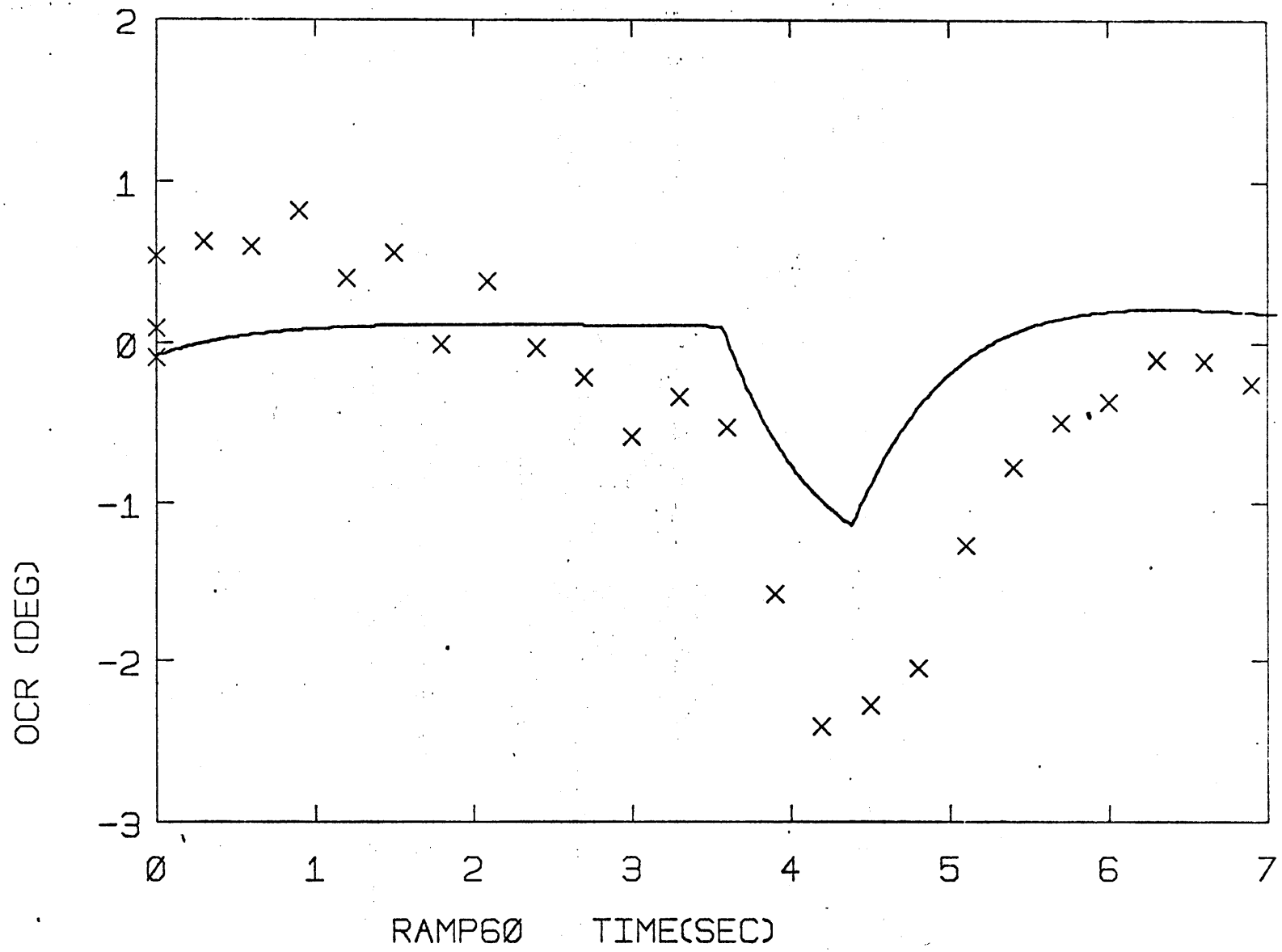
2
1
0
-1
-2
-3
OCR (DEG)
0
1
2
3
4
5
6
7
RAMP60 TIME(SEC)

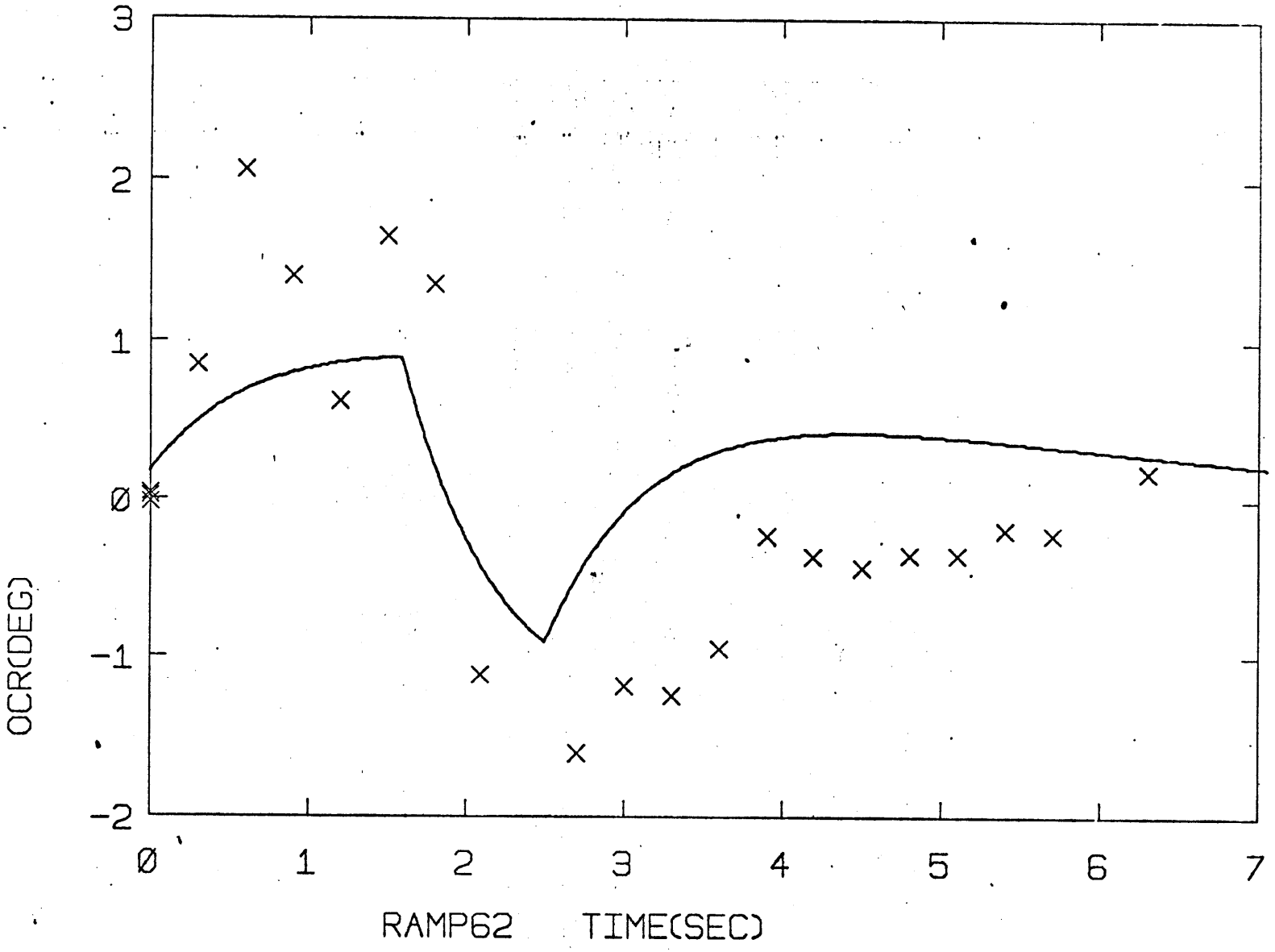
3
2
1
0
-1
-2
0
1
2
3
4
5
6
7
OCR(DEG)
RAMP62 TIME(SEC)

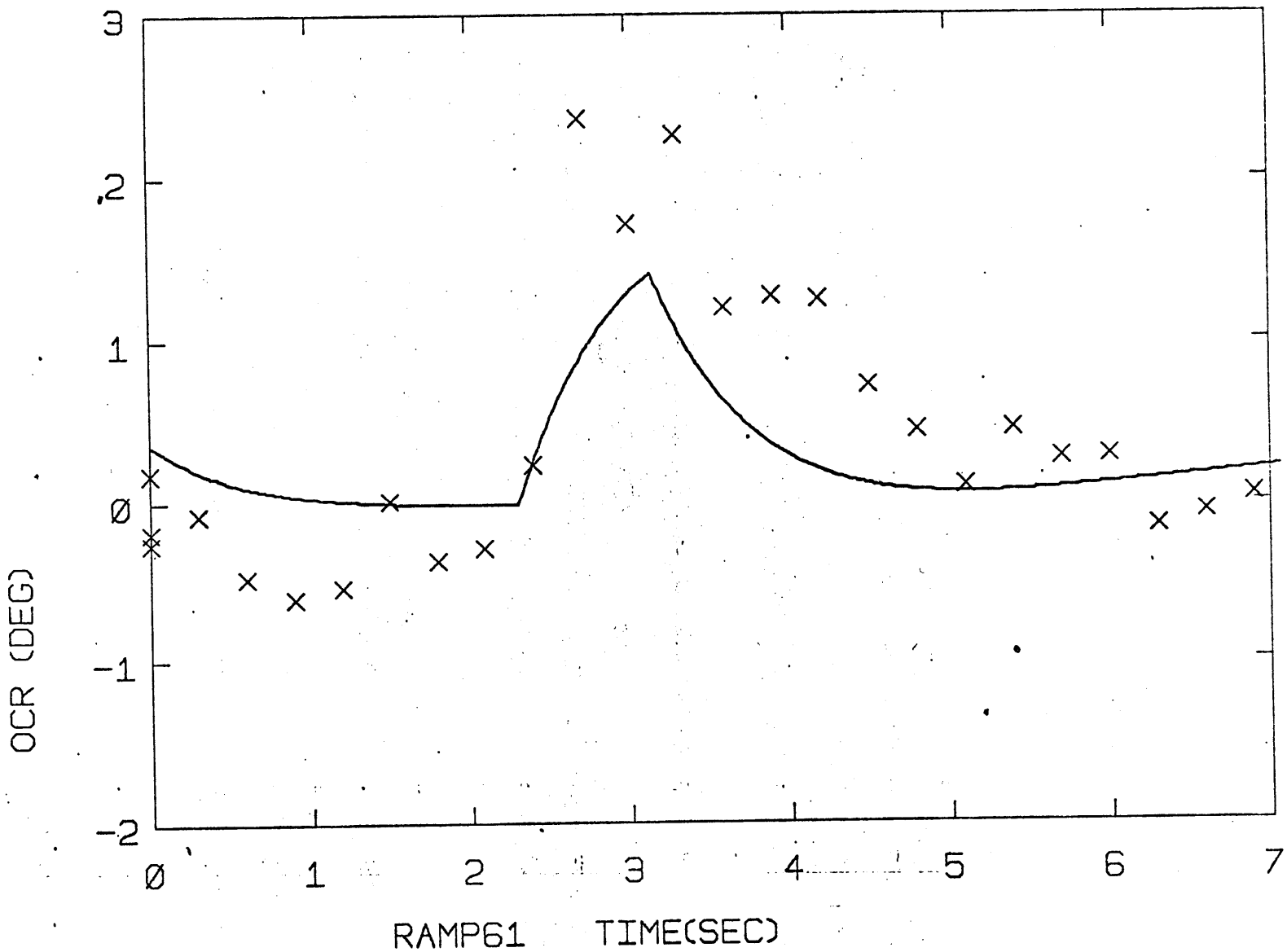
3
2
1
Ø
-1
-2
Ø
1
2
3
4
5
6
7
OCR (DEG)
RAMP61 TIME(SEC)

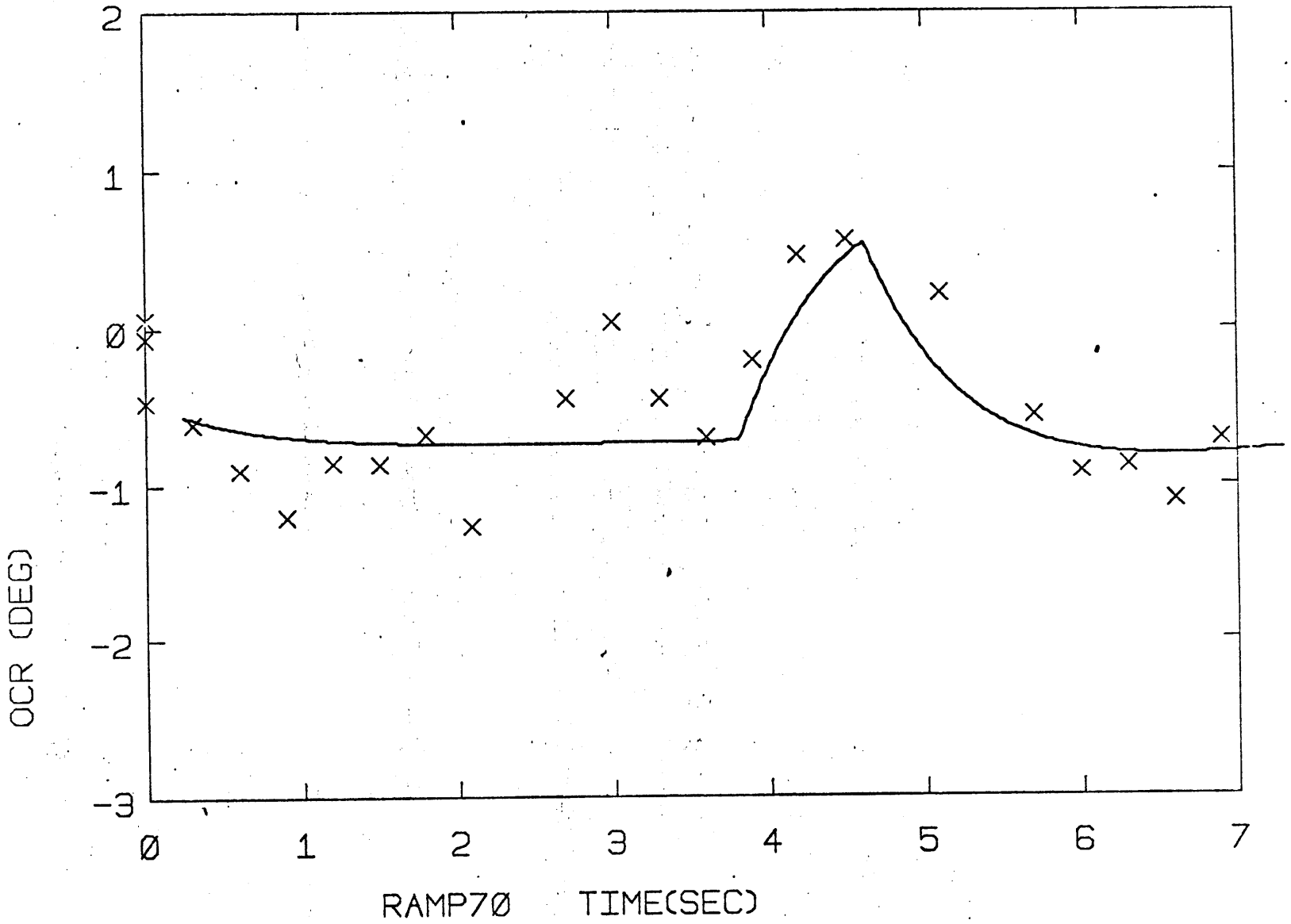
2
1
0
-1
-2
-3
0
1
2
3
4
5
6
7
OCR (DEG)
RAMP70 TIME(SEC)

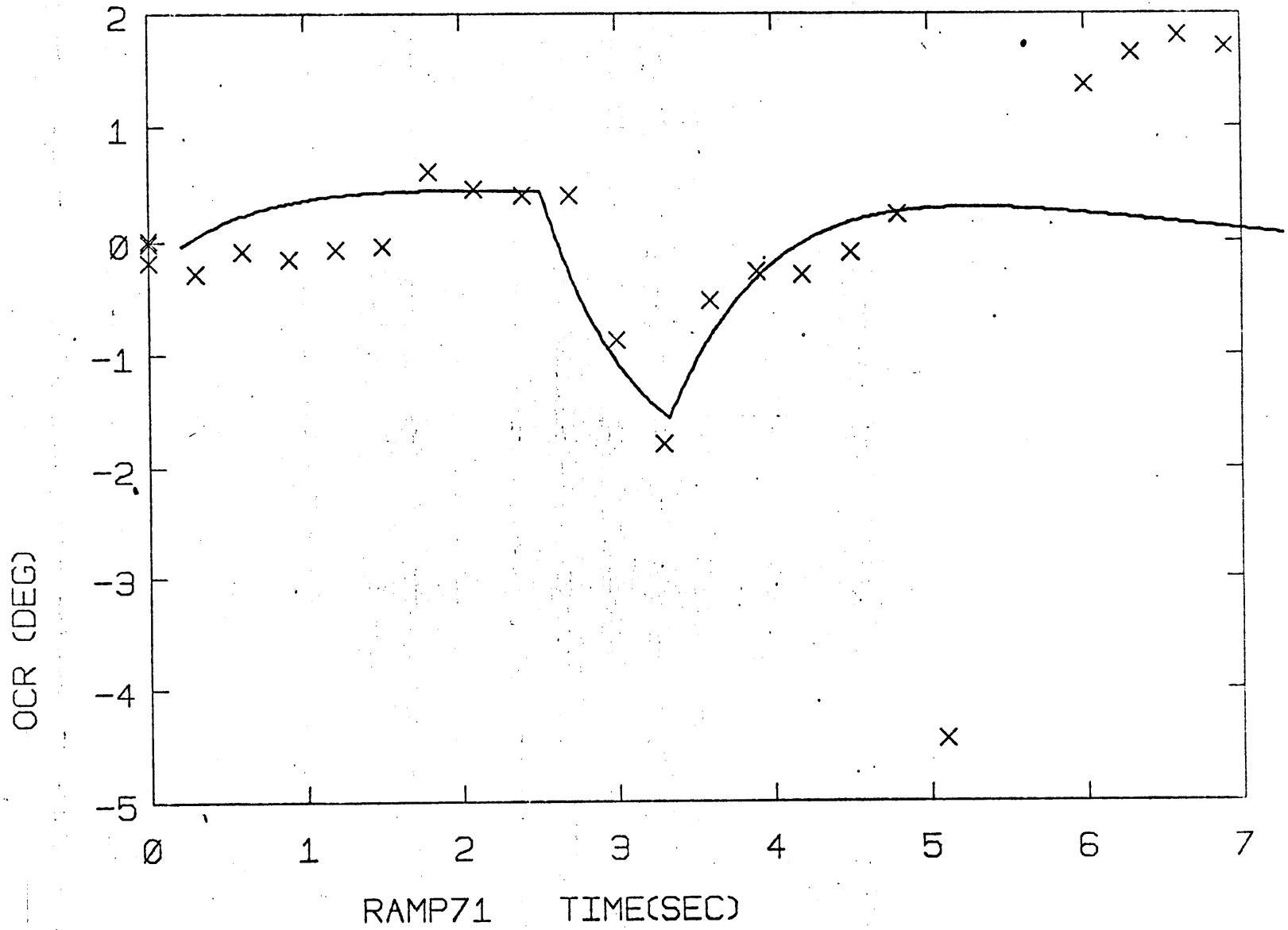
2
1
0
-1
-2
-3
-4
-5
0
1
2
3
4
5
6
7
OCR (DEG)
RAMP71 TIME(SEC)

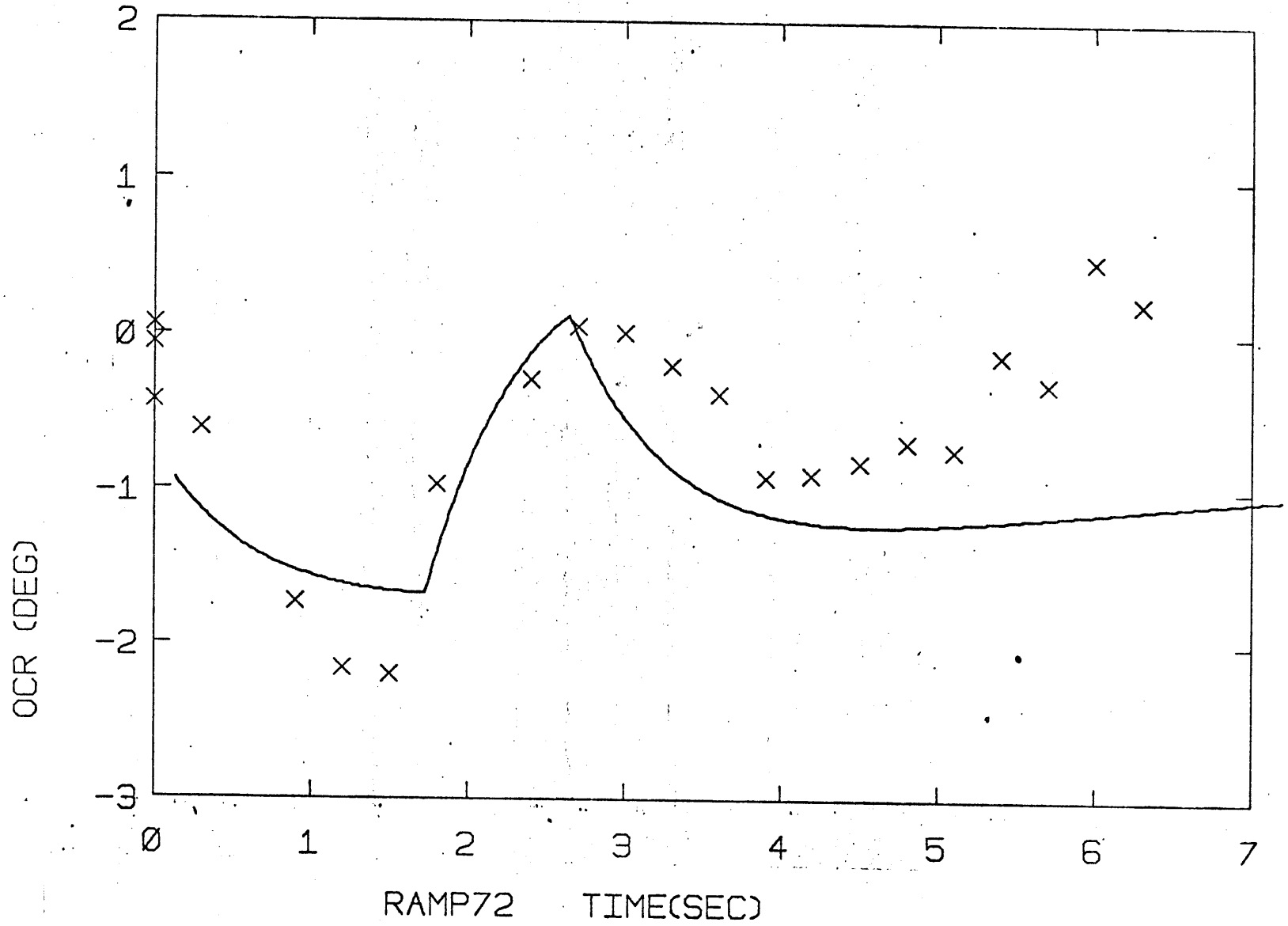
2
1
0
-1
-2
-3
0
1
2
3
4
5
6
7
OCR (DEG)
RAMP72 TIME(SEC)

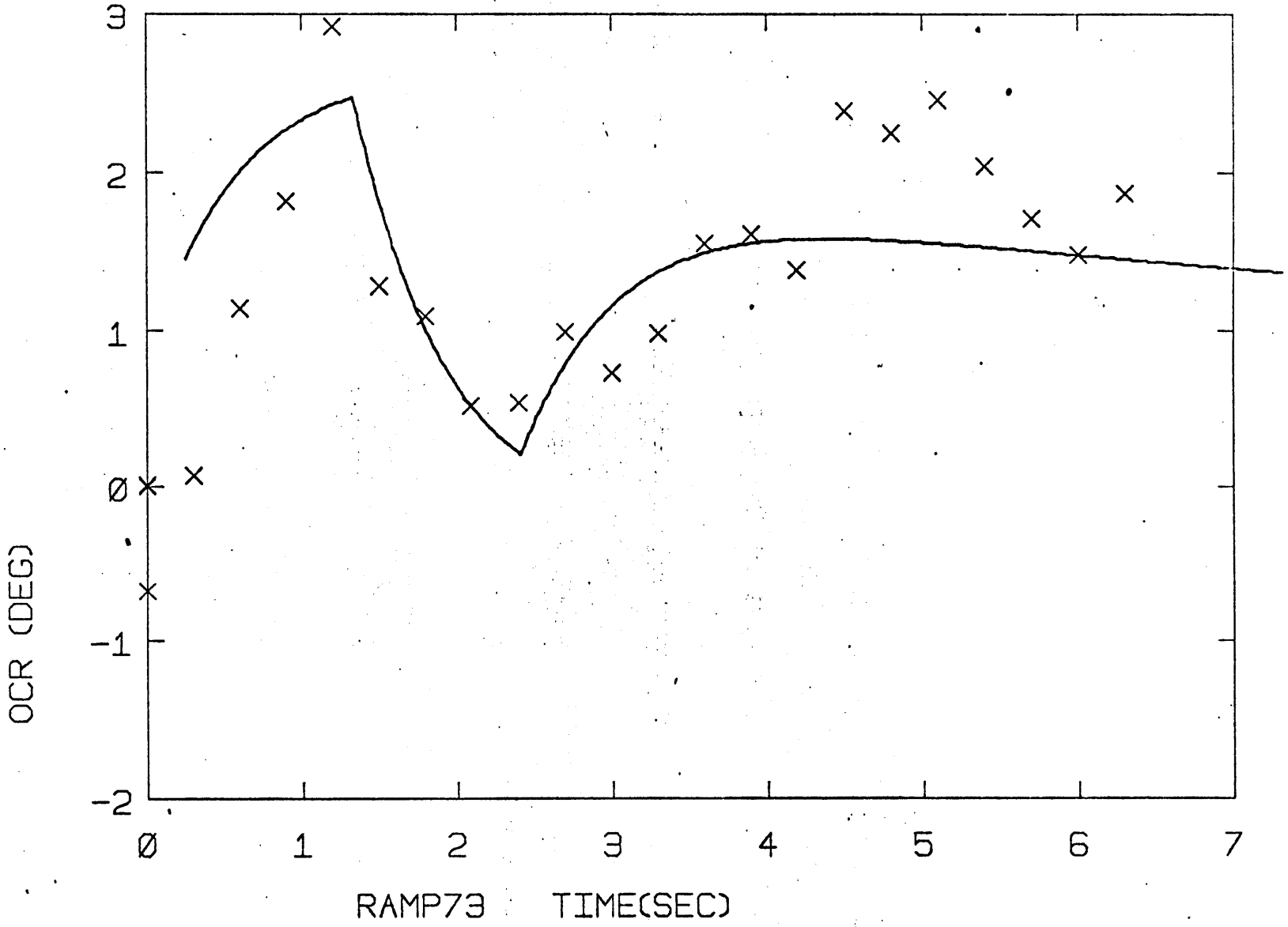
3
2
1
0
-1
-2
0
1
2
3
4
5
6
7
OCR (DEG)
RAMP73 TIME(SEC)

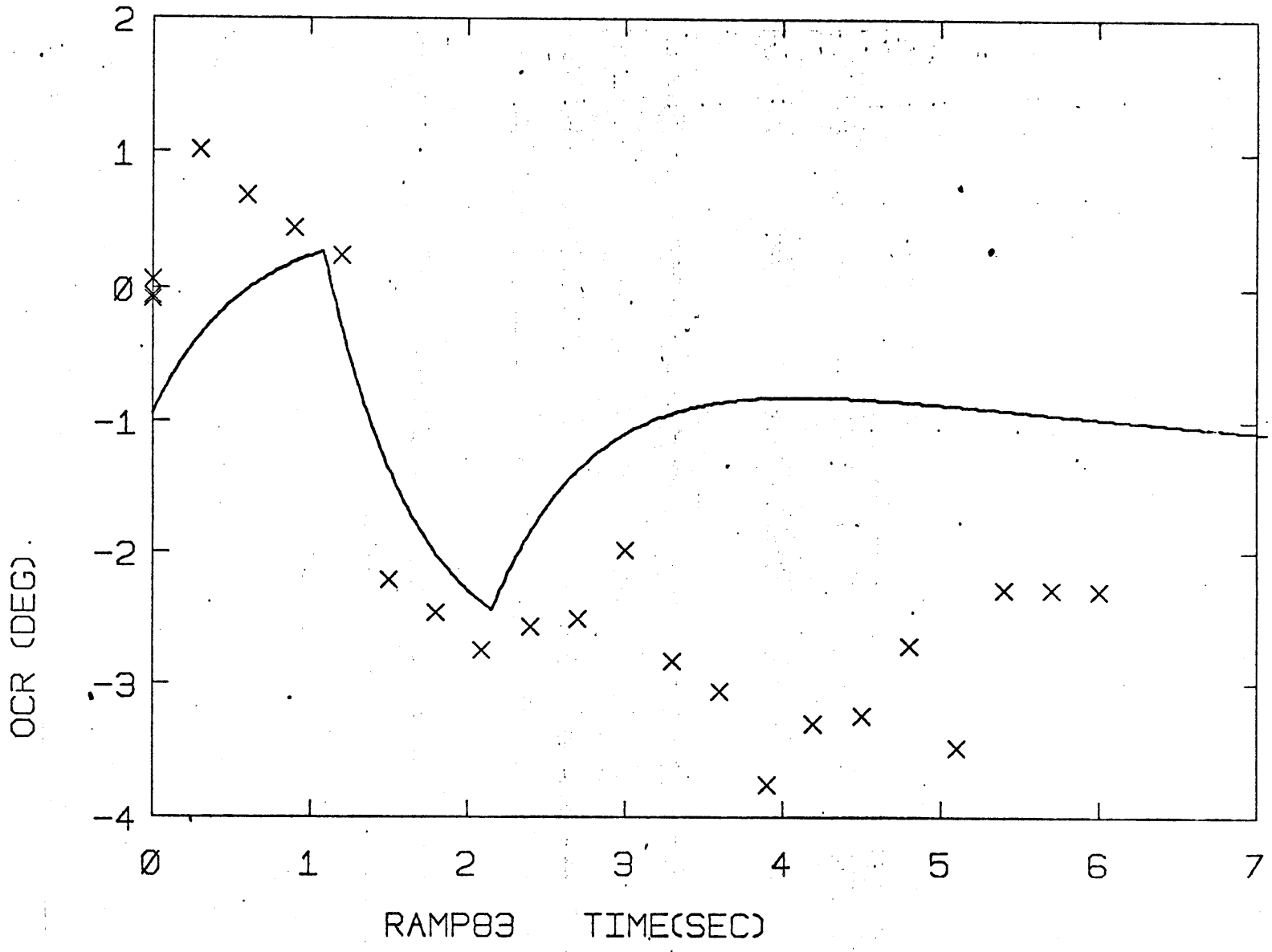
2
1
0
-1
-2
-3
-4
0
1
2
3
4
5
6
7
OCR (DEG)
RAMP83 TIME(SEC)

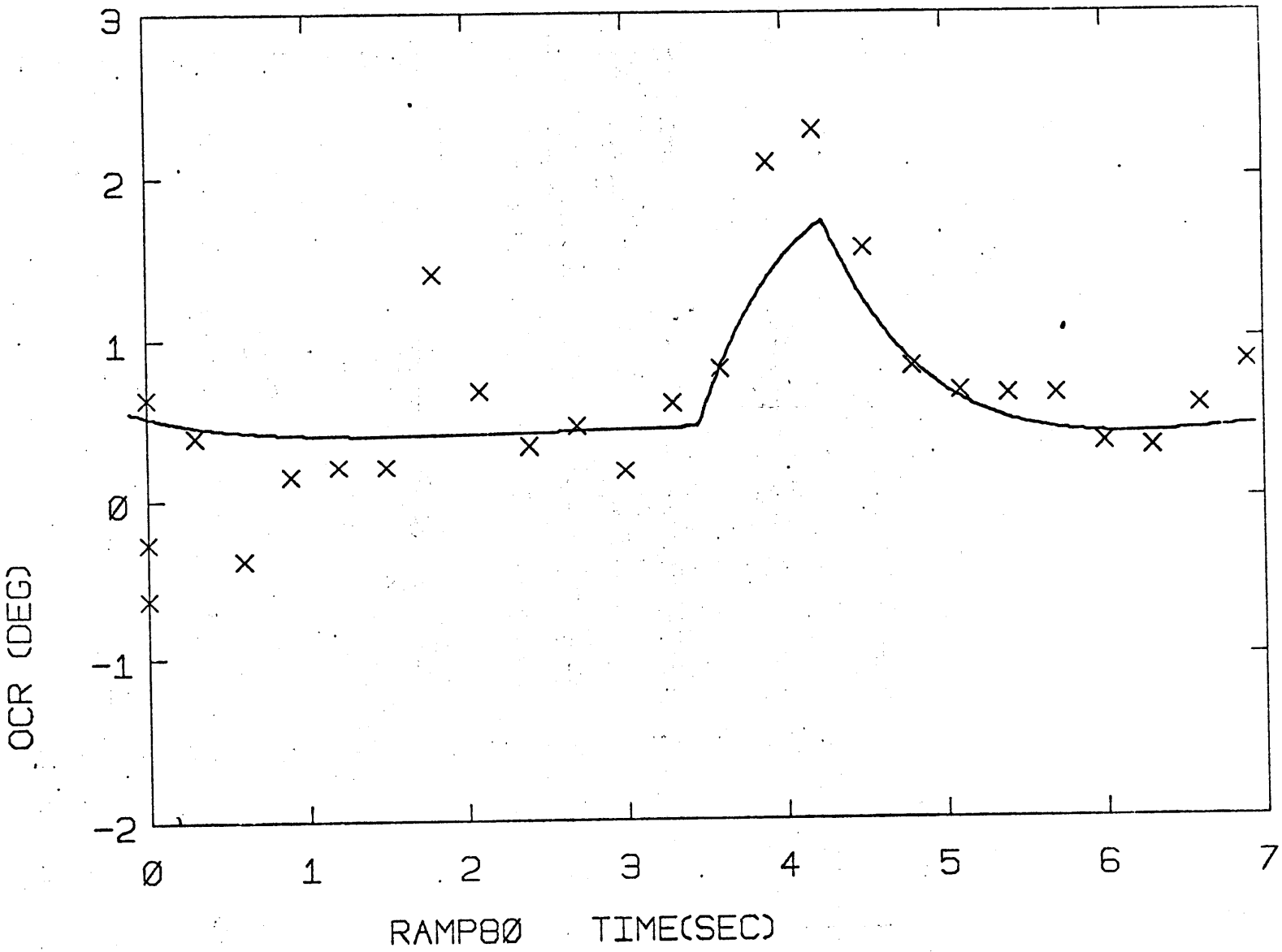
3
2
1
0
-1
-2
0
1
2
3
4
5
6
7
OCR (DEG)
RAMP80 TIME(SEC)

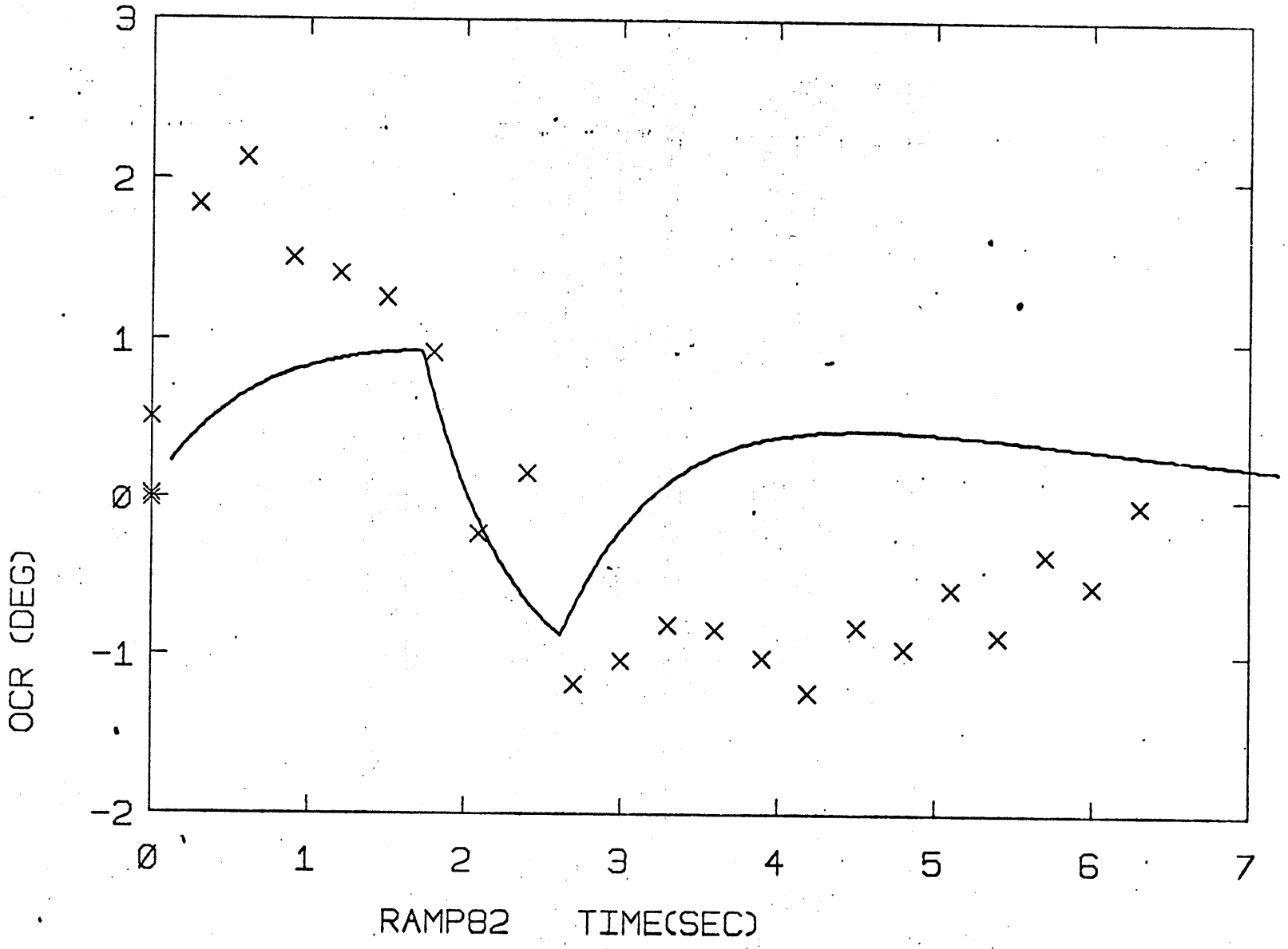
3
2
1
0
-1
-2
0
1
2
3
4
5
6
7
OCR (DEG)
RAMP82 TIME(SEC)

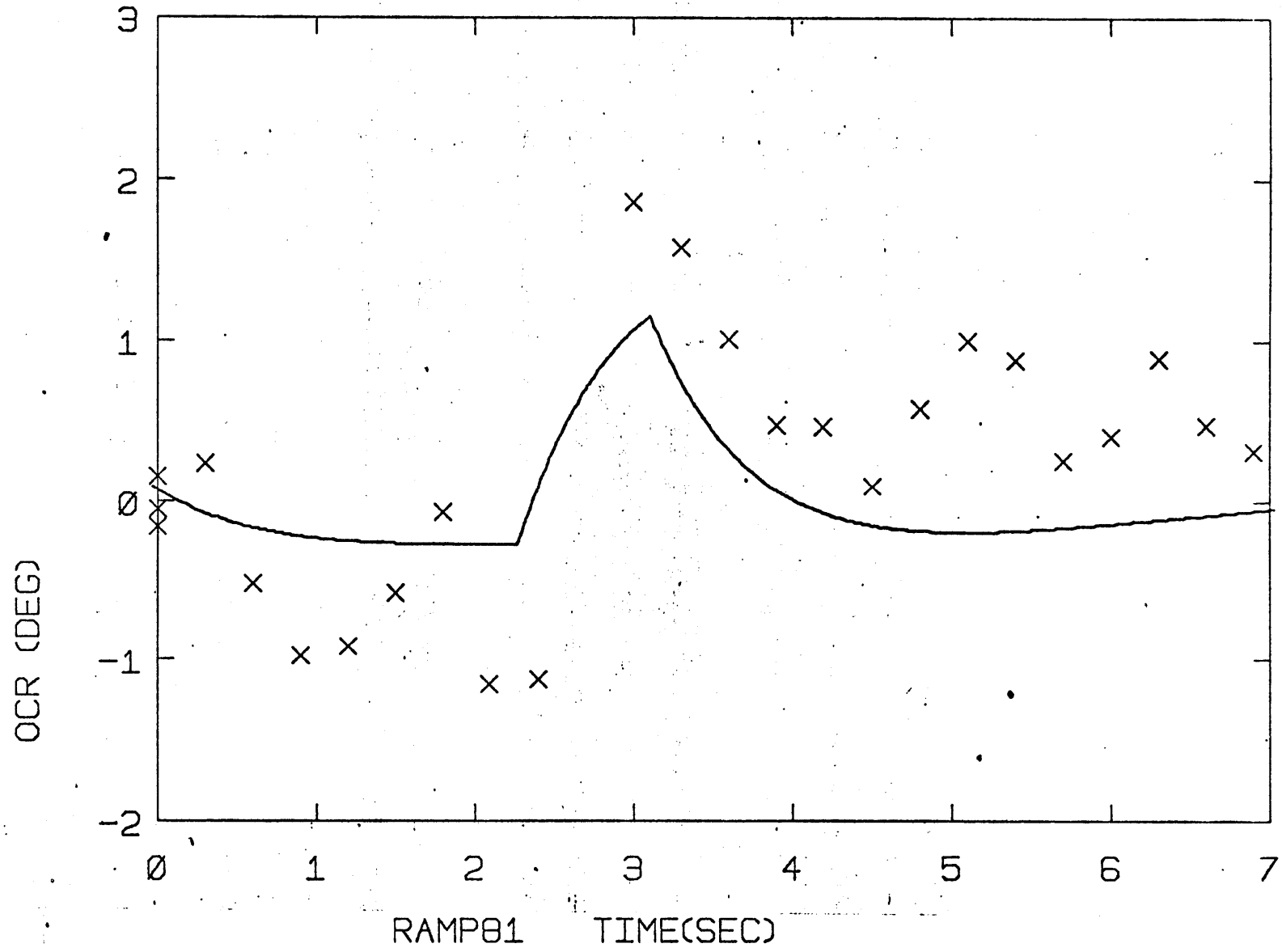
3
2
1
0
-1
-2
0
1
2
3
4
5
6
7
OCR (DEG)
RAMP81 TIME(SEC)

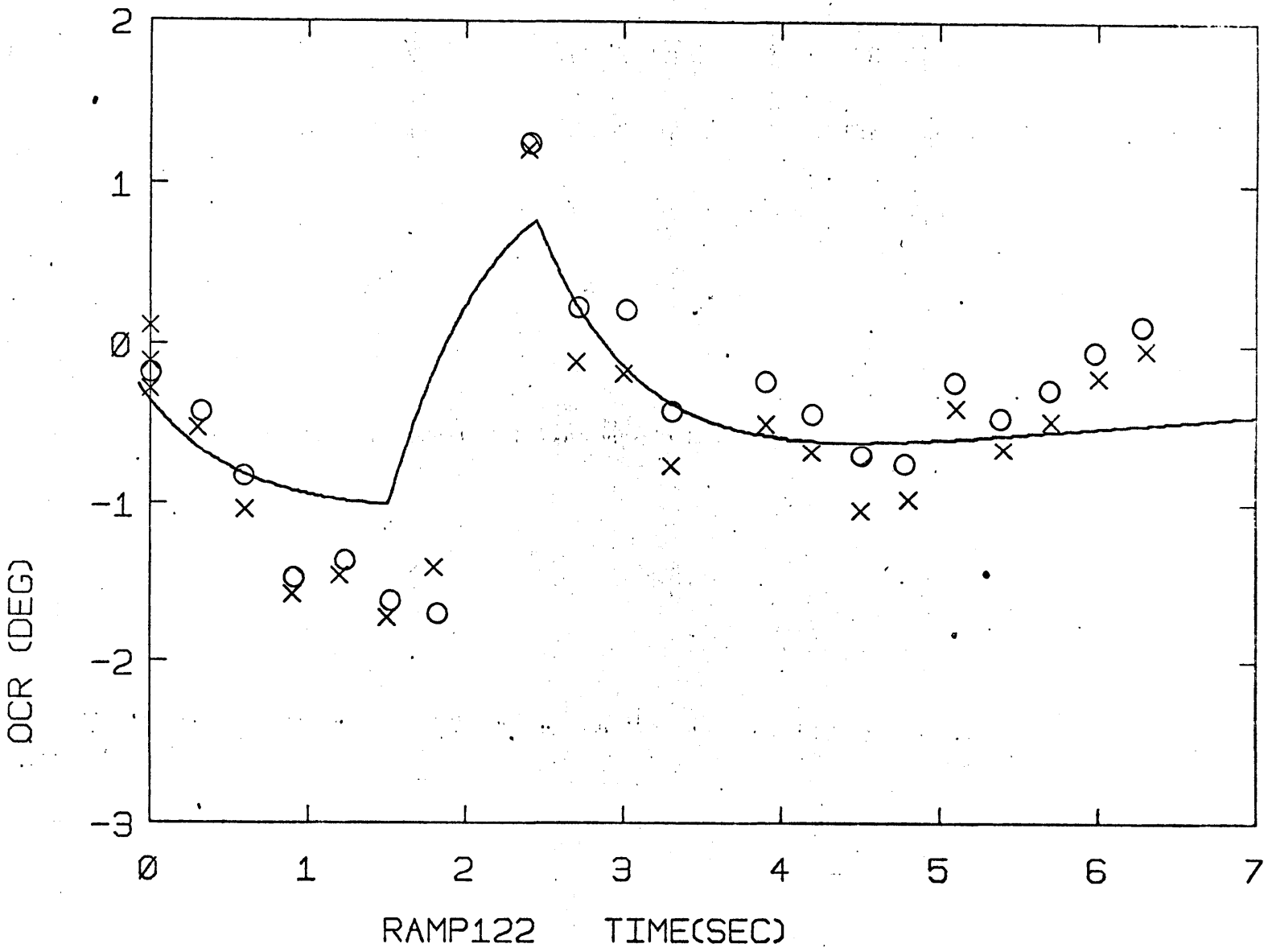
2
1
0
-1
-2
-3
0
1
2
3
4
5
6
7
QCR (DEG)
RAMP122 TIME(SEC)

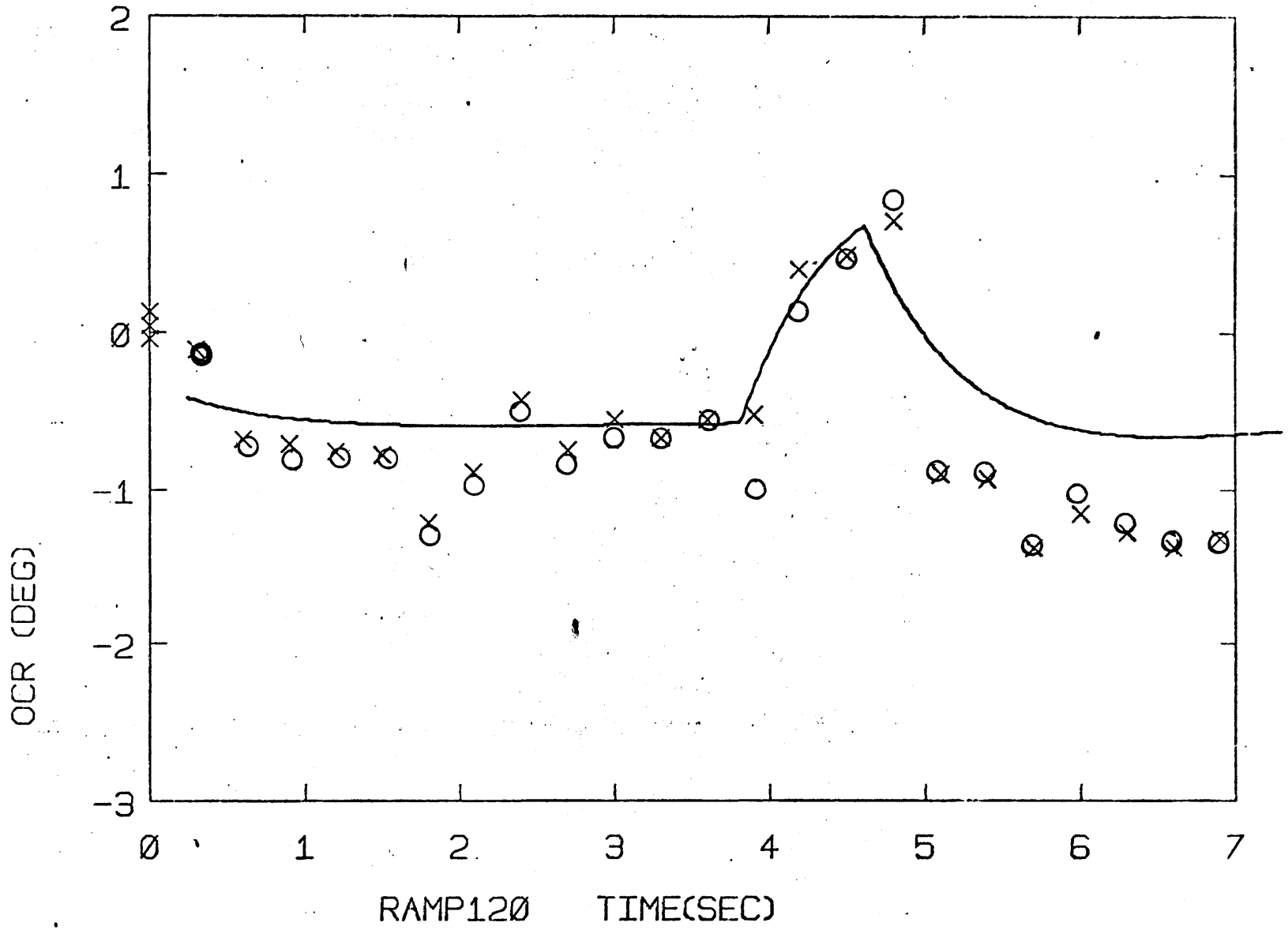
2
1
0
-1
-2
-3
0
1
2
3
4
5
6
7
OCR (DEG)
RAMP120 TIME(SEC)

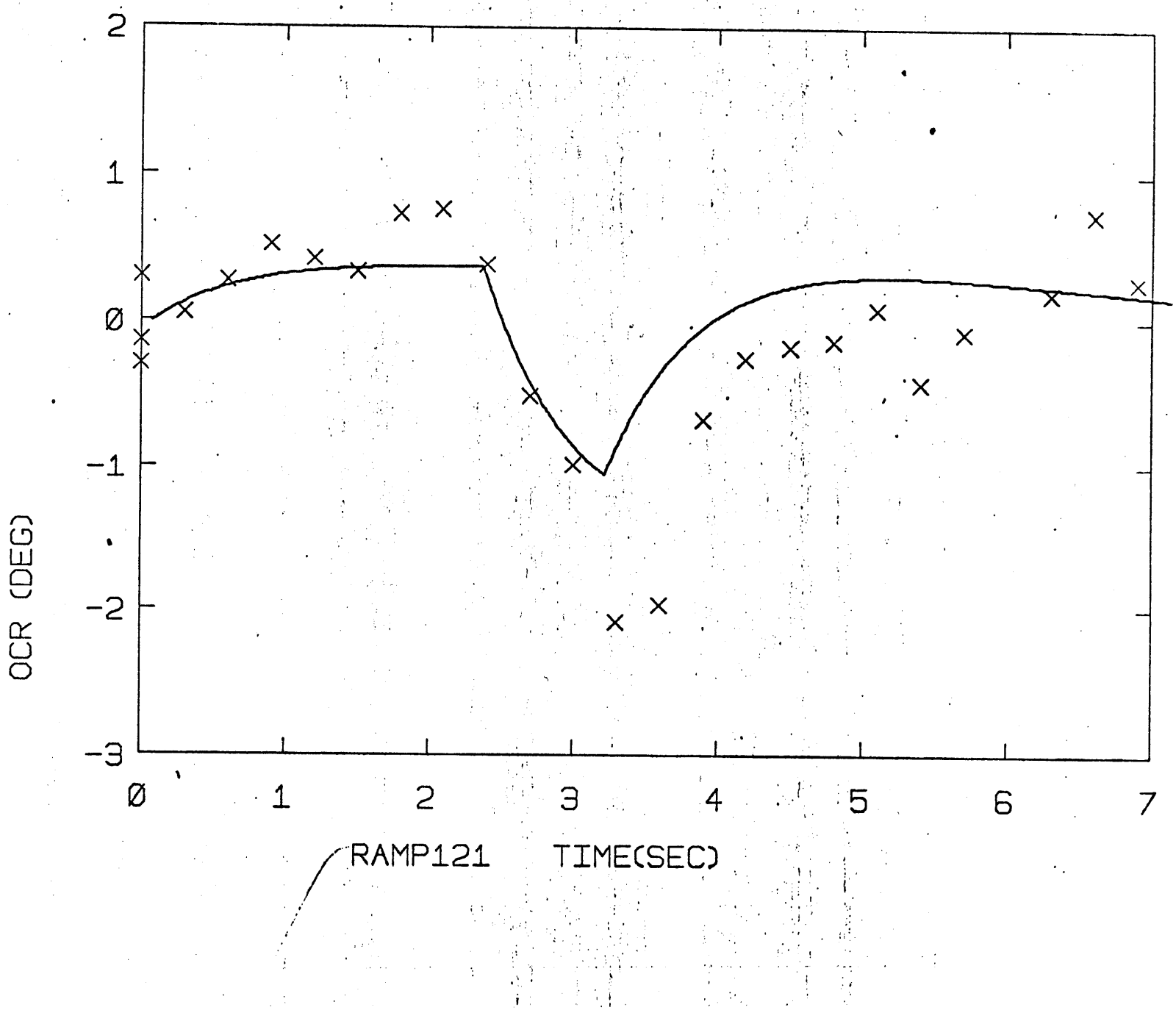
2
1
0
-1
-2
-3
0
1
2
3
4
5
6
7
OCR (DEG)
RAMP121 TIME(SEC)

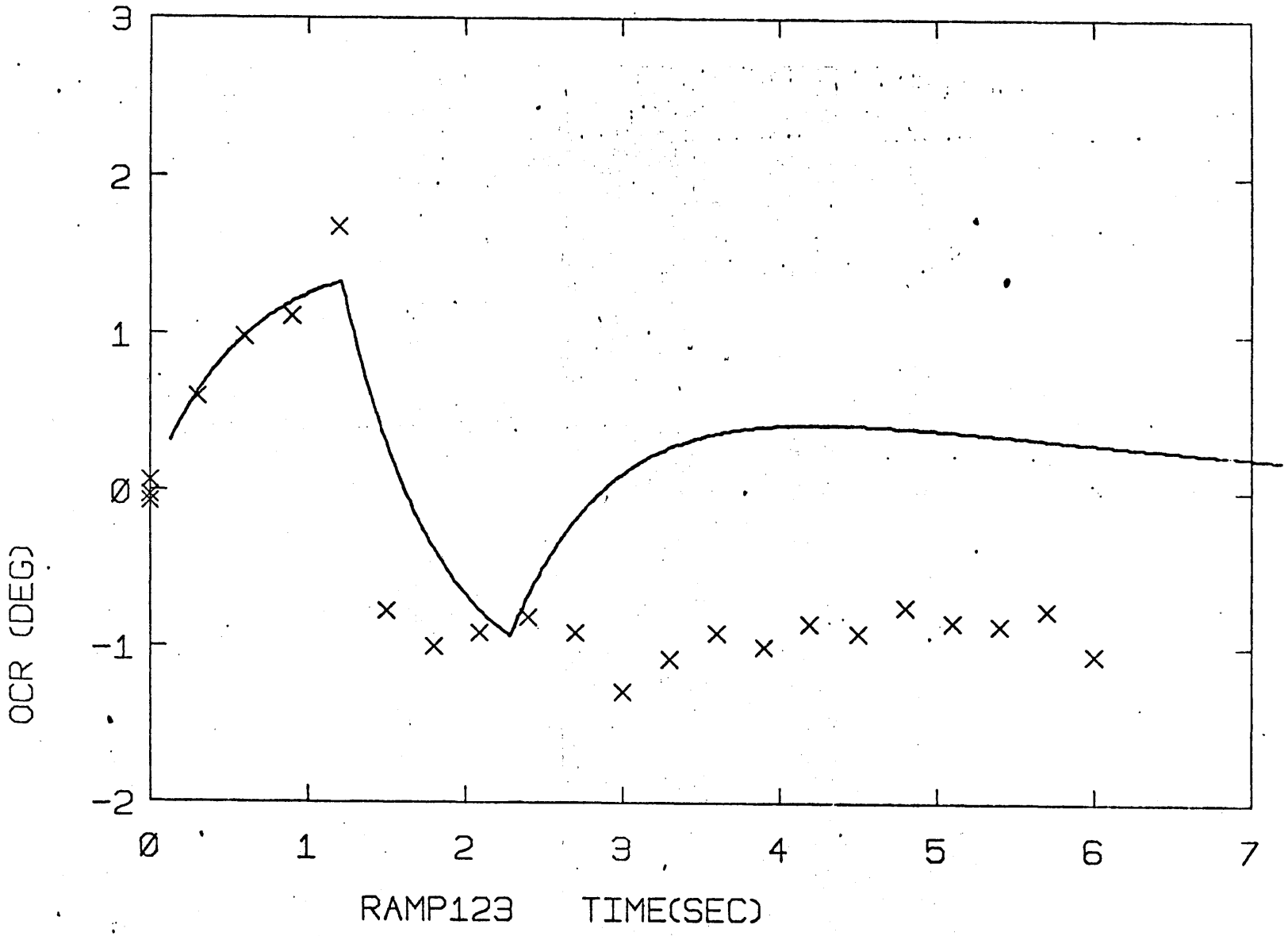
3
2
1
0
-1
-2
0
1
2
3
4
5
6
7
OCR (DEG)
RAMP123 TIME(SEC)

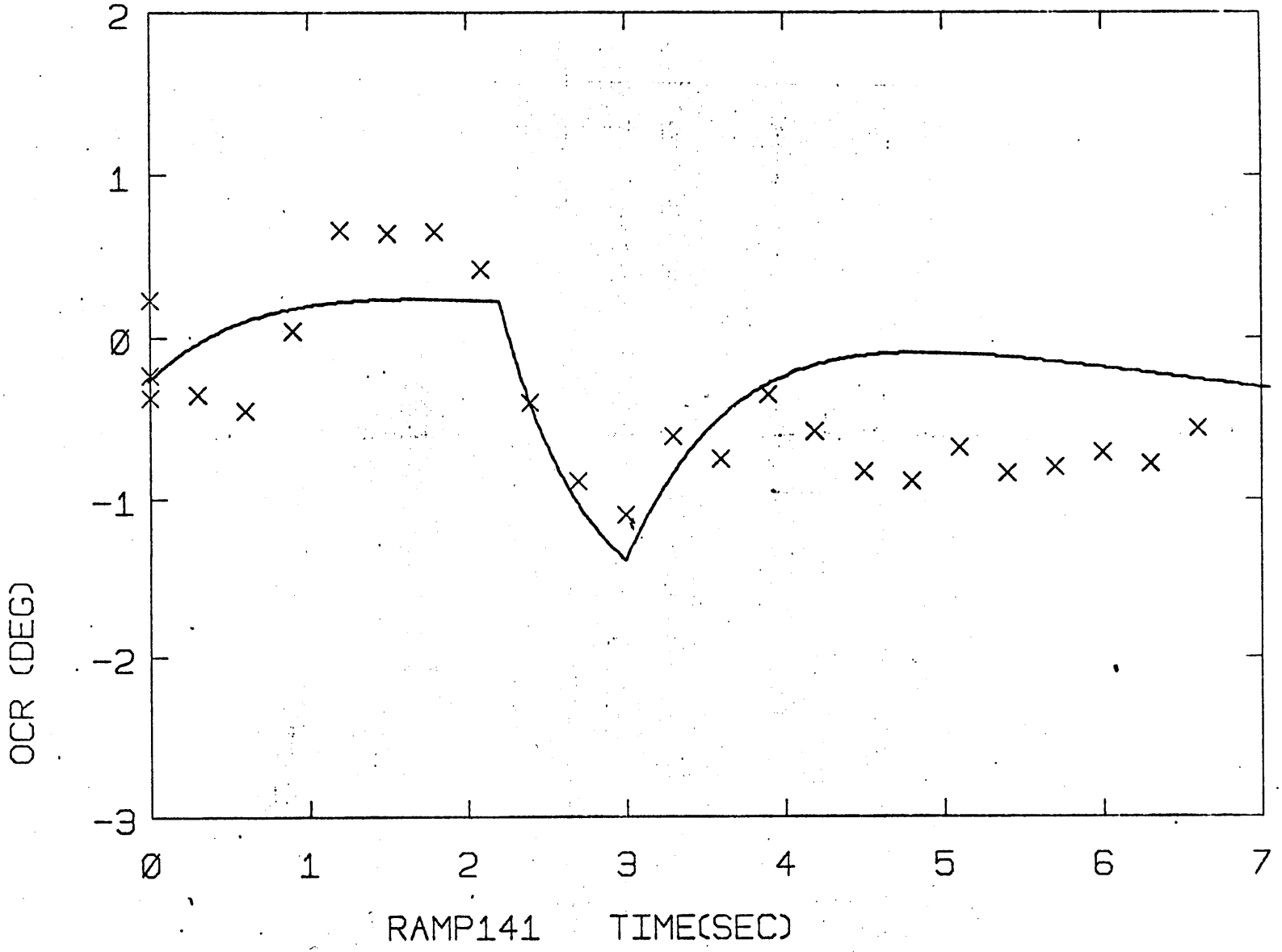
2
1
0
-1
-2
-3
0
1
2
3
4
5
6
7
OCR (DEG)
RAMP141 TIME(SEC)

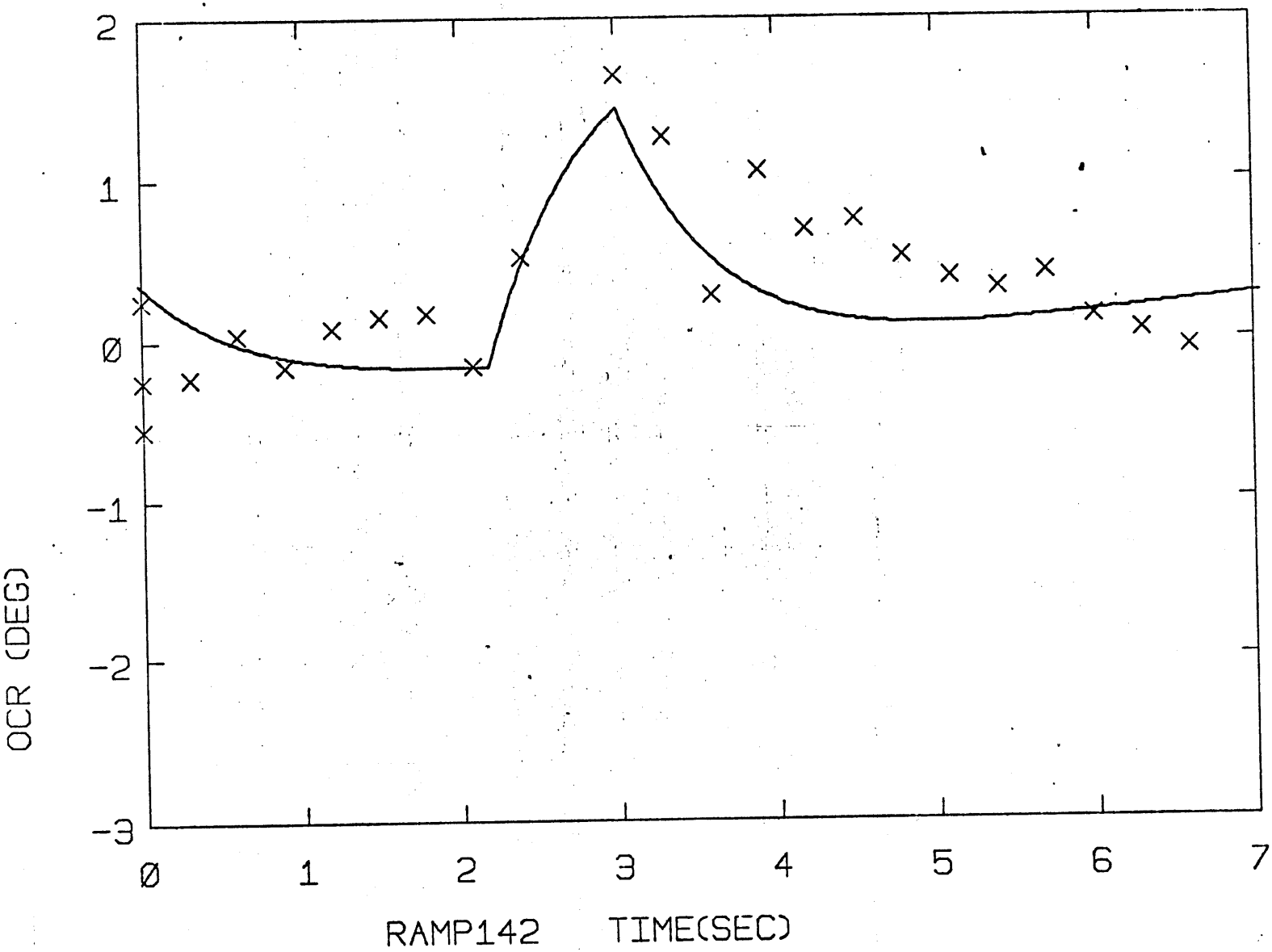
2
1
0
-1
-2
-3
0
1
2
3
4
5
6
7
OCR (DEG)
RAMP142 TIME(SEC)

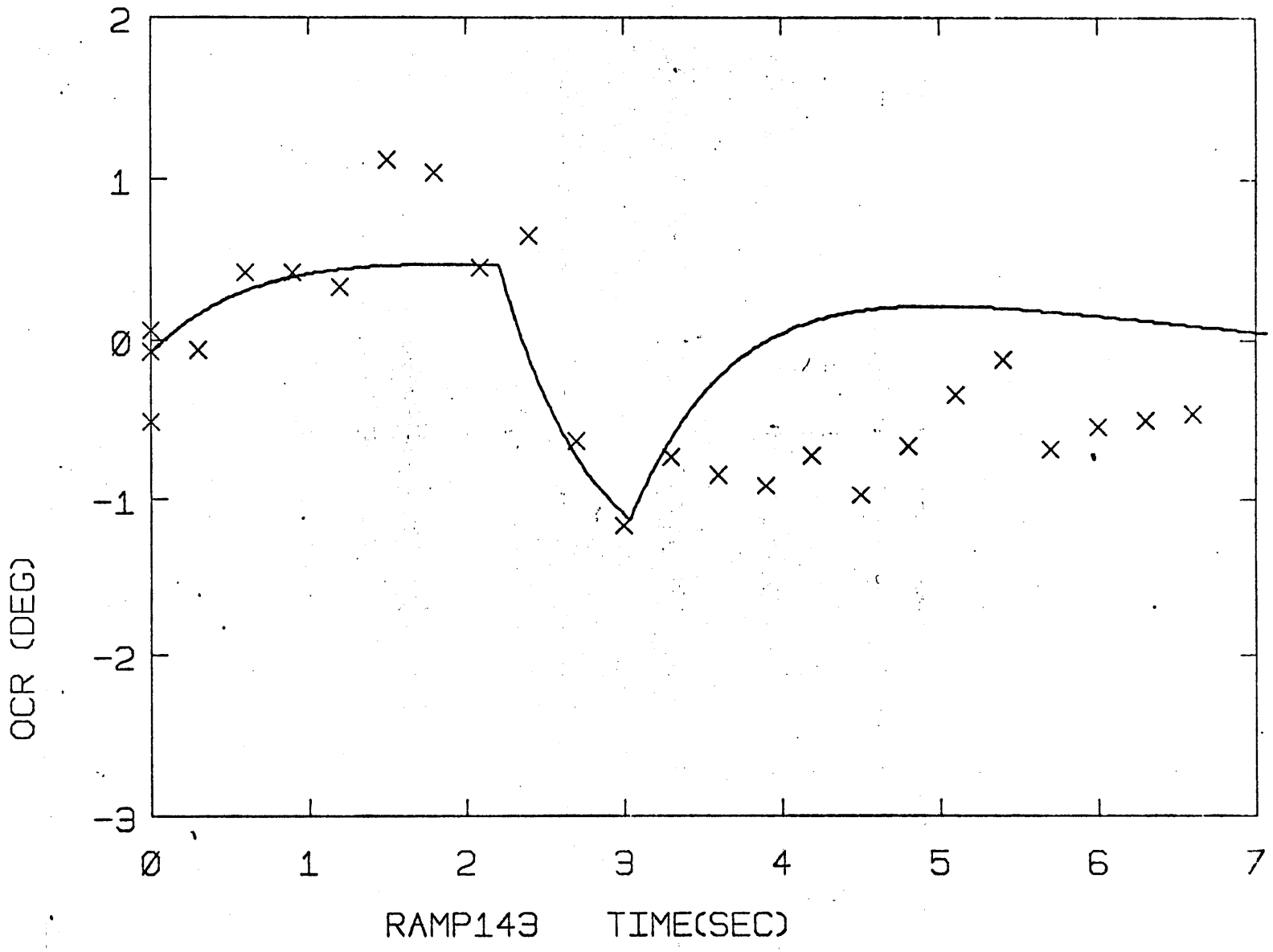
2
1
0
-1
-2
-3
0
1
2
3
4
5
6
7
OCR (DEG)
RAMP143 TIME(SEC)

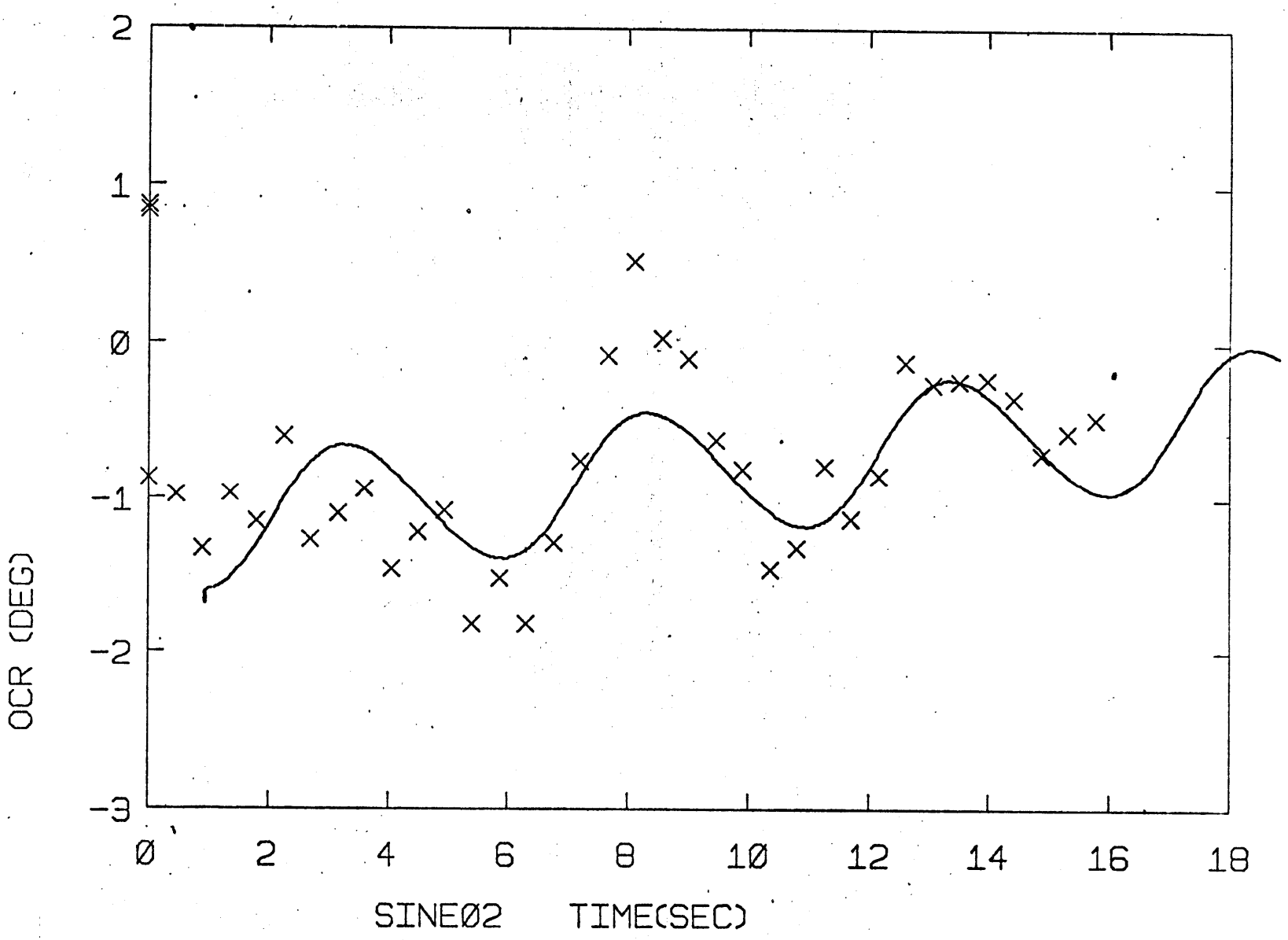
2
1
0
-1
-2
-3
0
2
4
6
8
10
12
14
16
18
OCR (DEG)
SINE02 TIME(SEC)

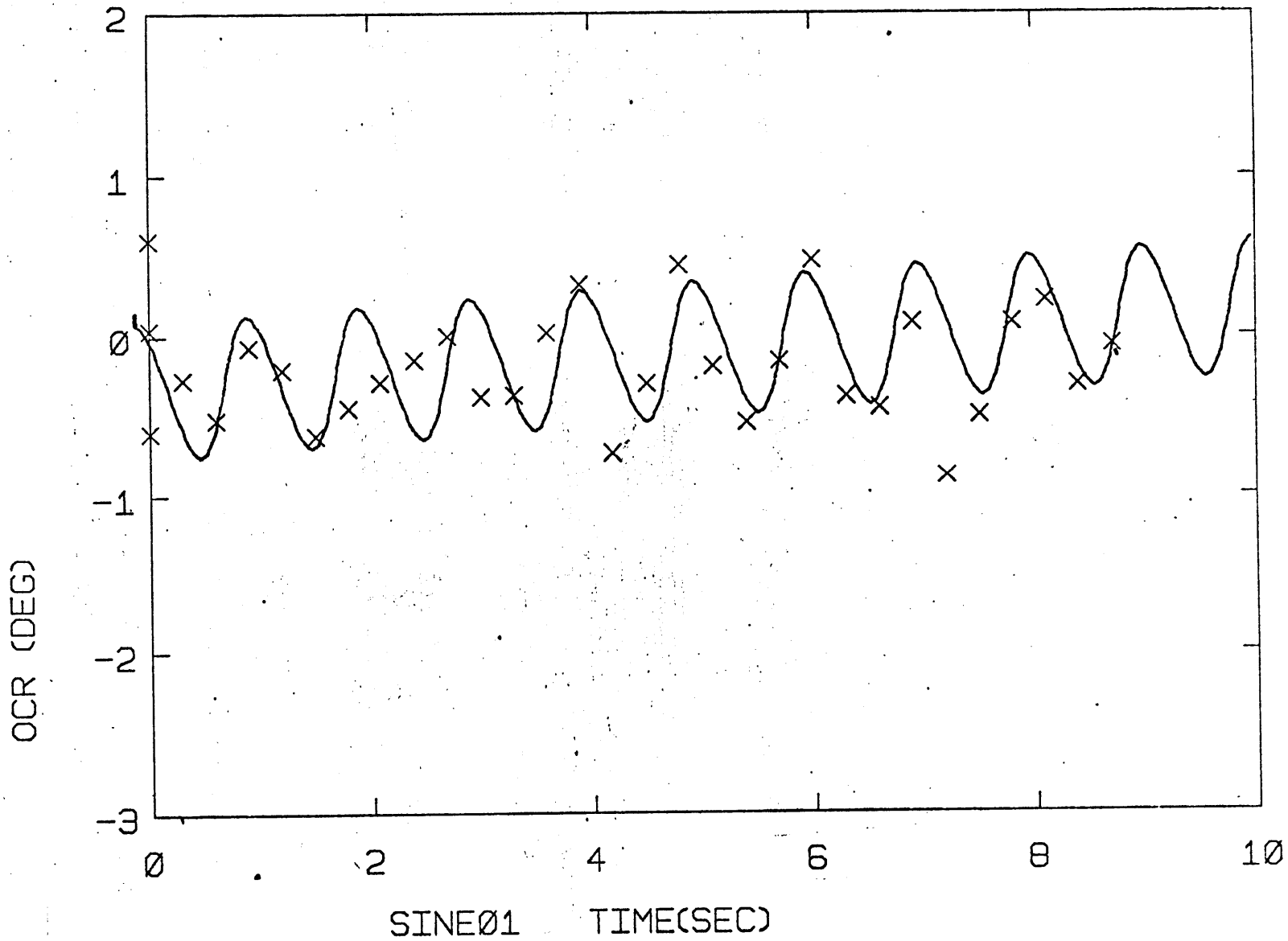
2
1
0
-1
-2
-3
0
2
4
6
8
10
OCR (DEG)
SINE01 TIME(SEC)

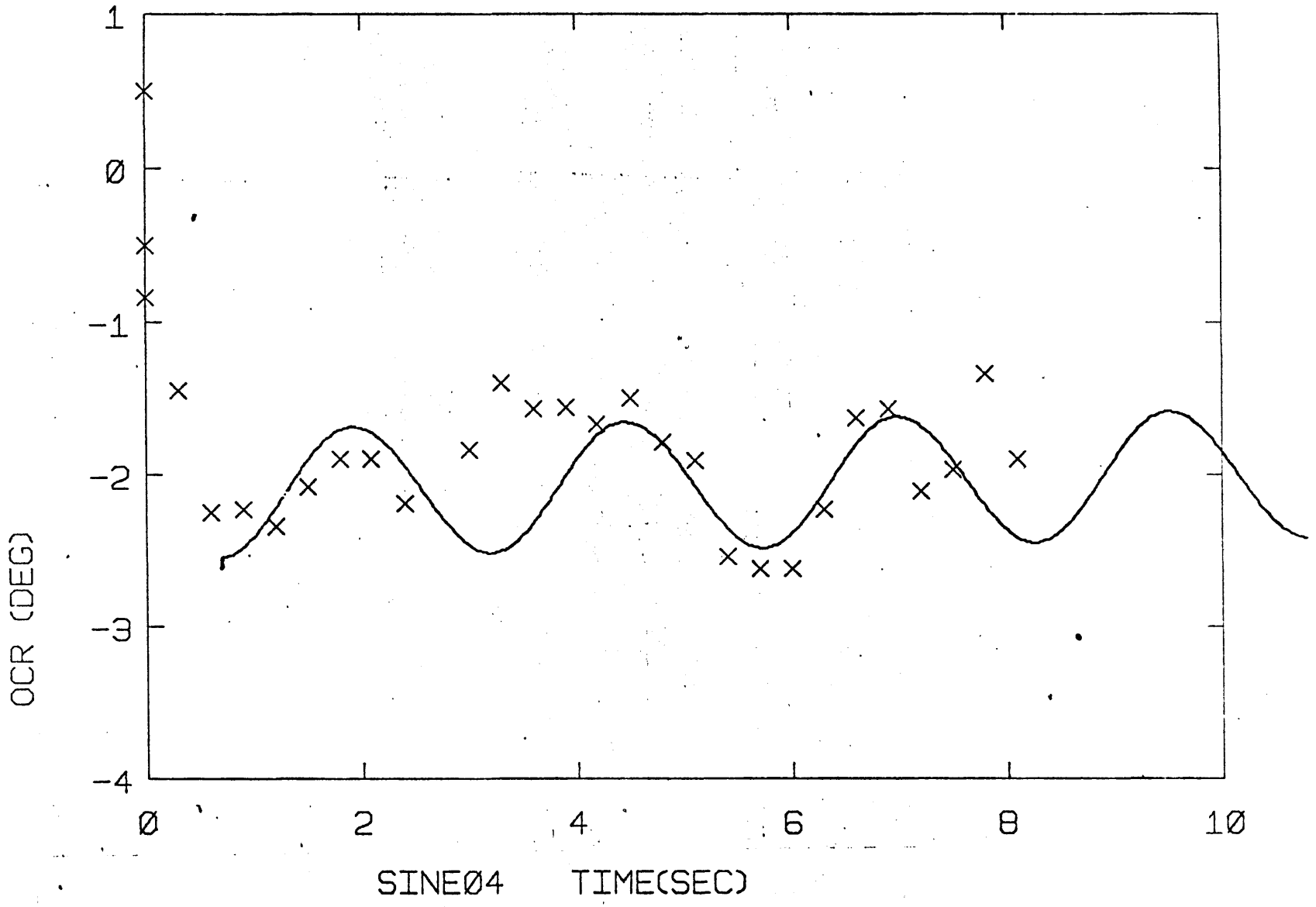
1
0
-1
-2
-3
-4
0
2
4
6
8
10
OCR (DEG)
SINE04 TIME(SEC)

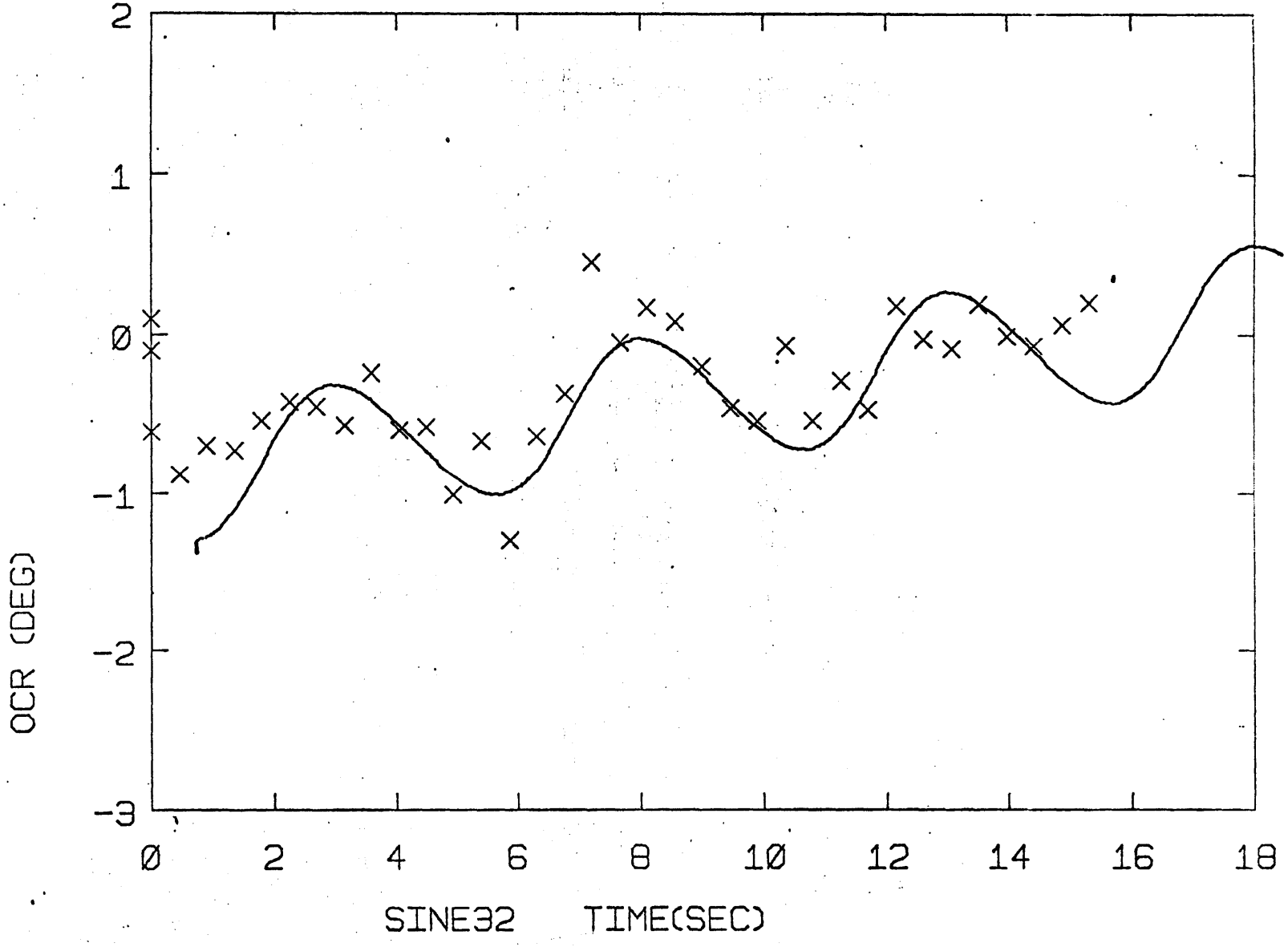
2
1
0
-1
-2
-3
0
2
4
6
8
10
12
14
16
18
OCR (DEG)
SINE32 TIME(SEC)

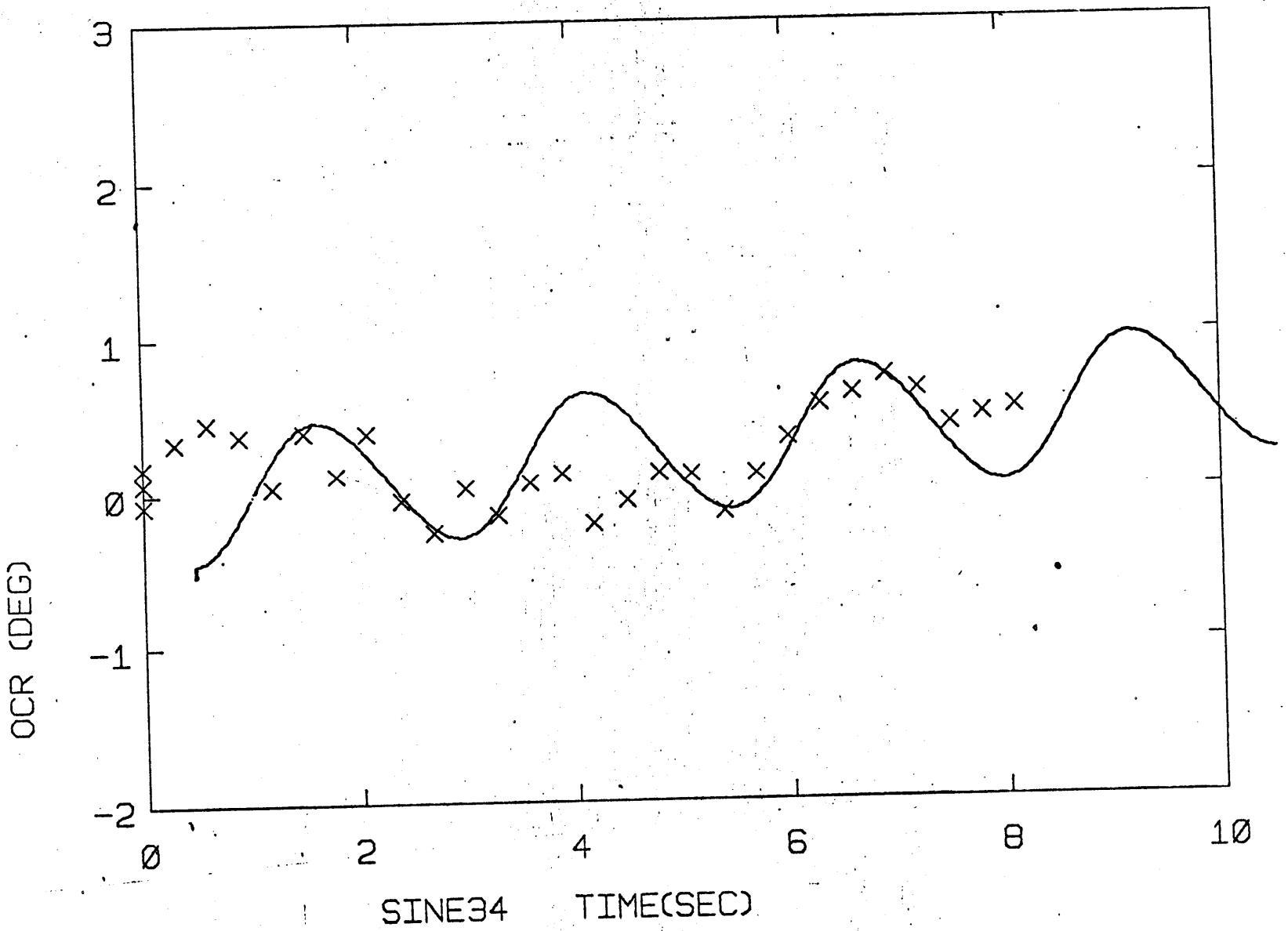
3
2
1
0
-1
-2
0
2
4
6
8
10
OCR (DEG)
SINE34 TIME(SEC)

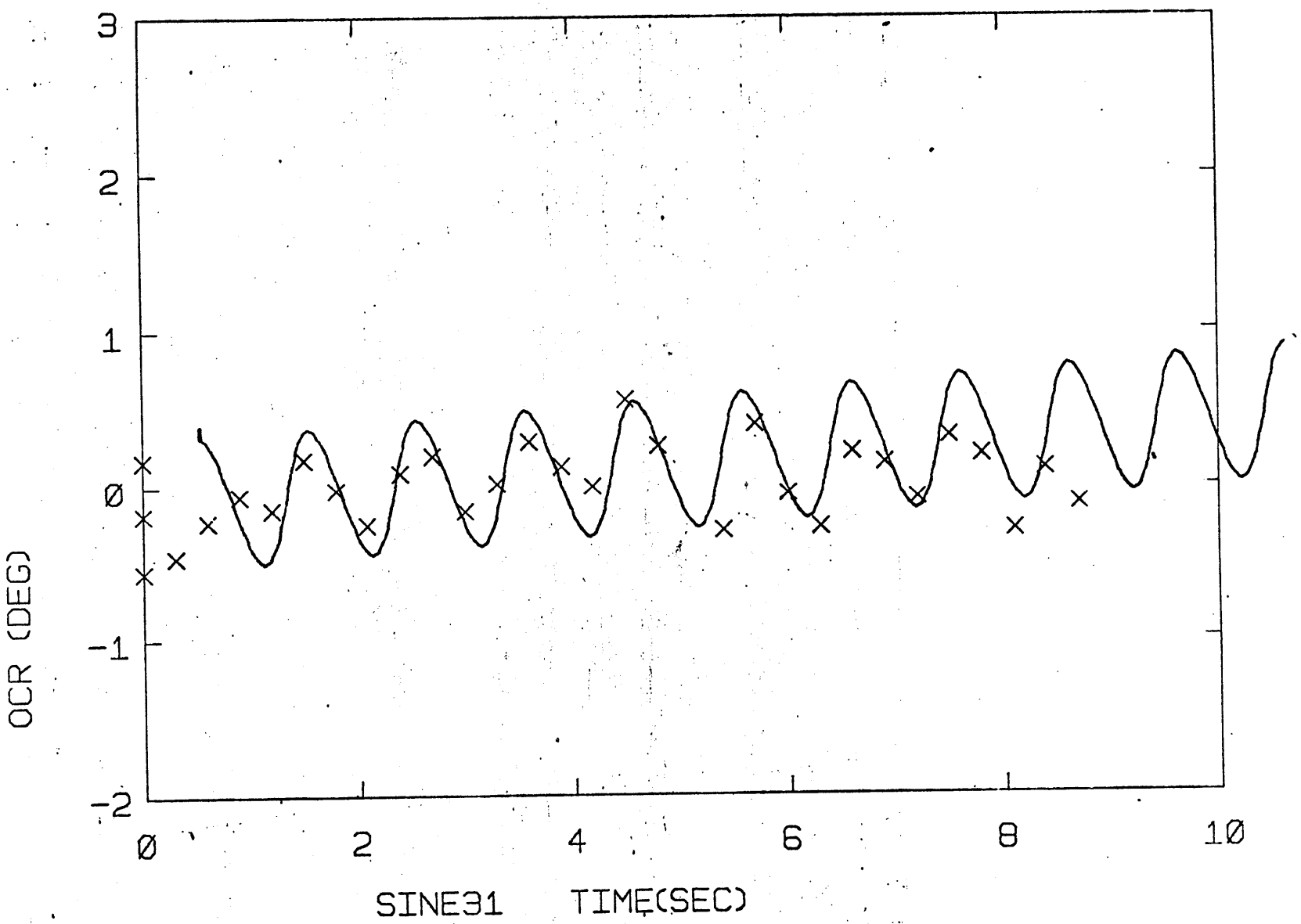
3
2
1
0
-1
-2
OCR (DEG)
0
2
4
6
8
10
SINE31 TIME(SEC)

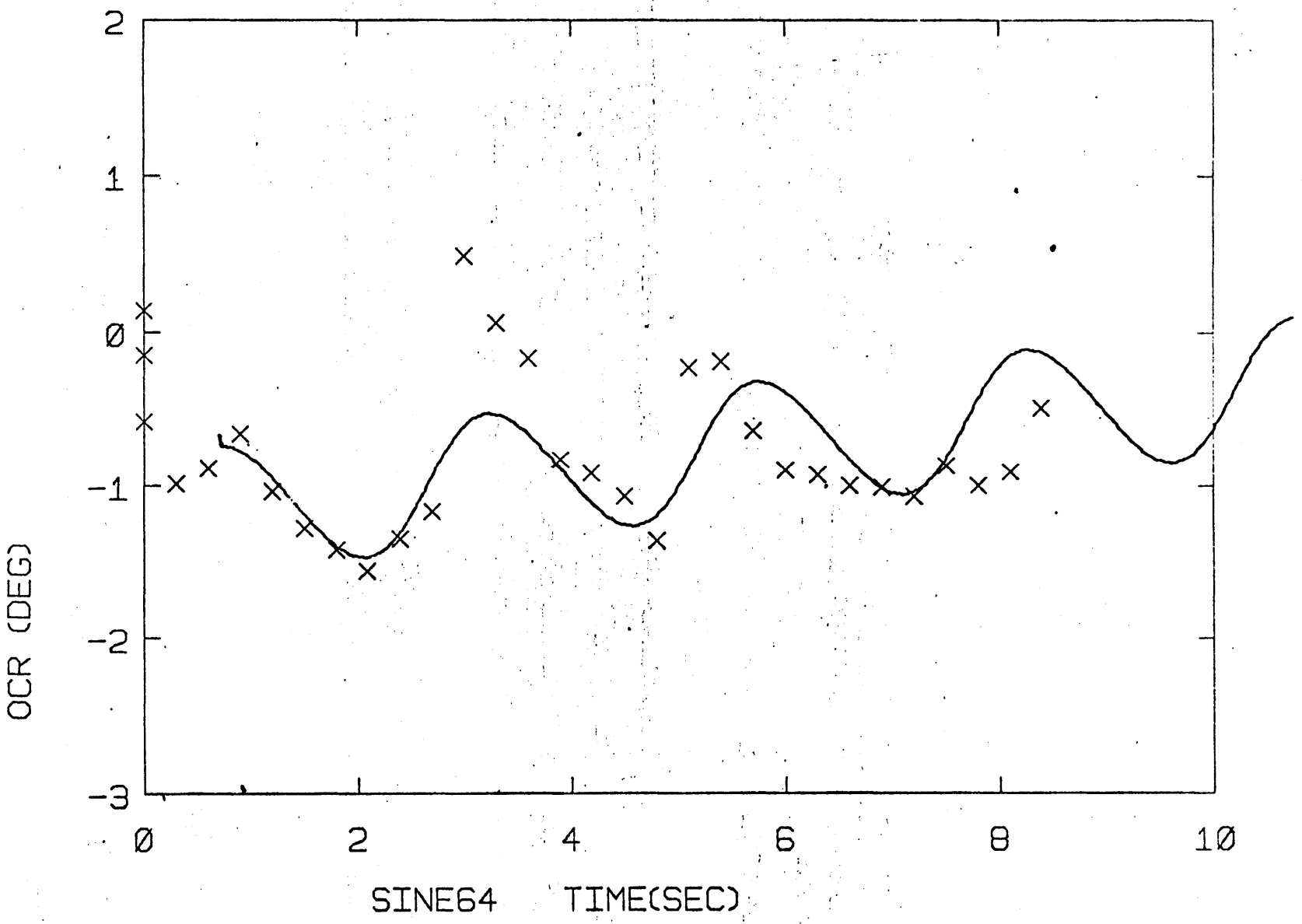
2
1
0
-1
-2
-3
0
2
4
6
8
10
OCR (DEG)
SINE64 TIME(SEC)

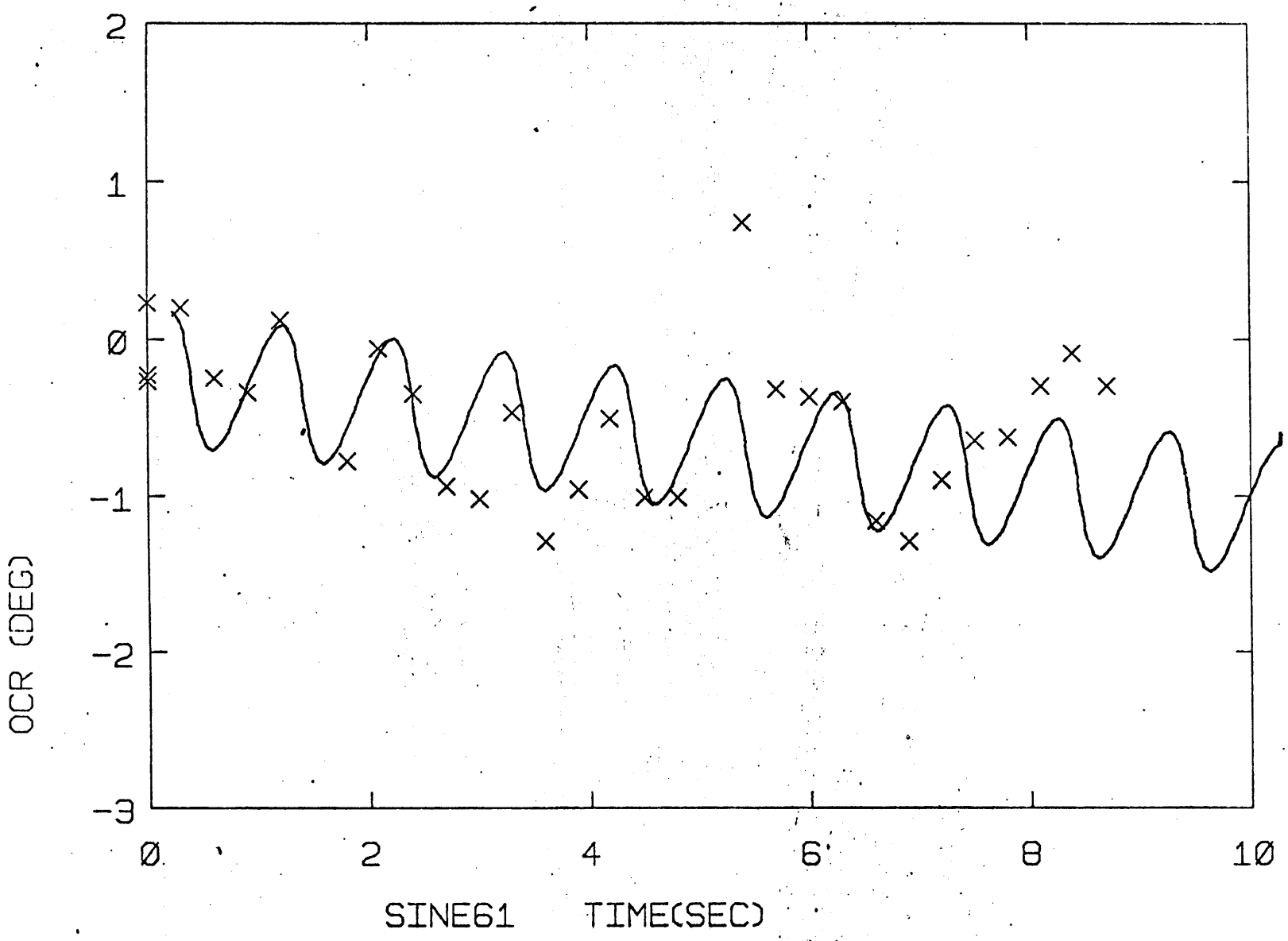
2
1
0
-1
-2
-3
0
2
4
6
8
10
OCR (DEG)
SINE61 TIME(SEC)

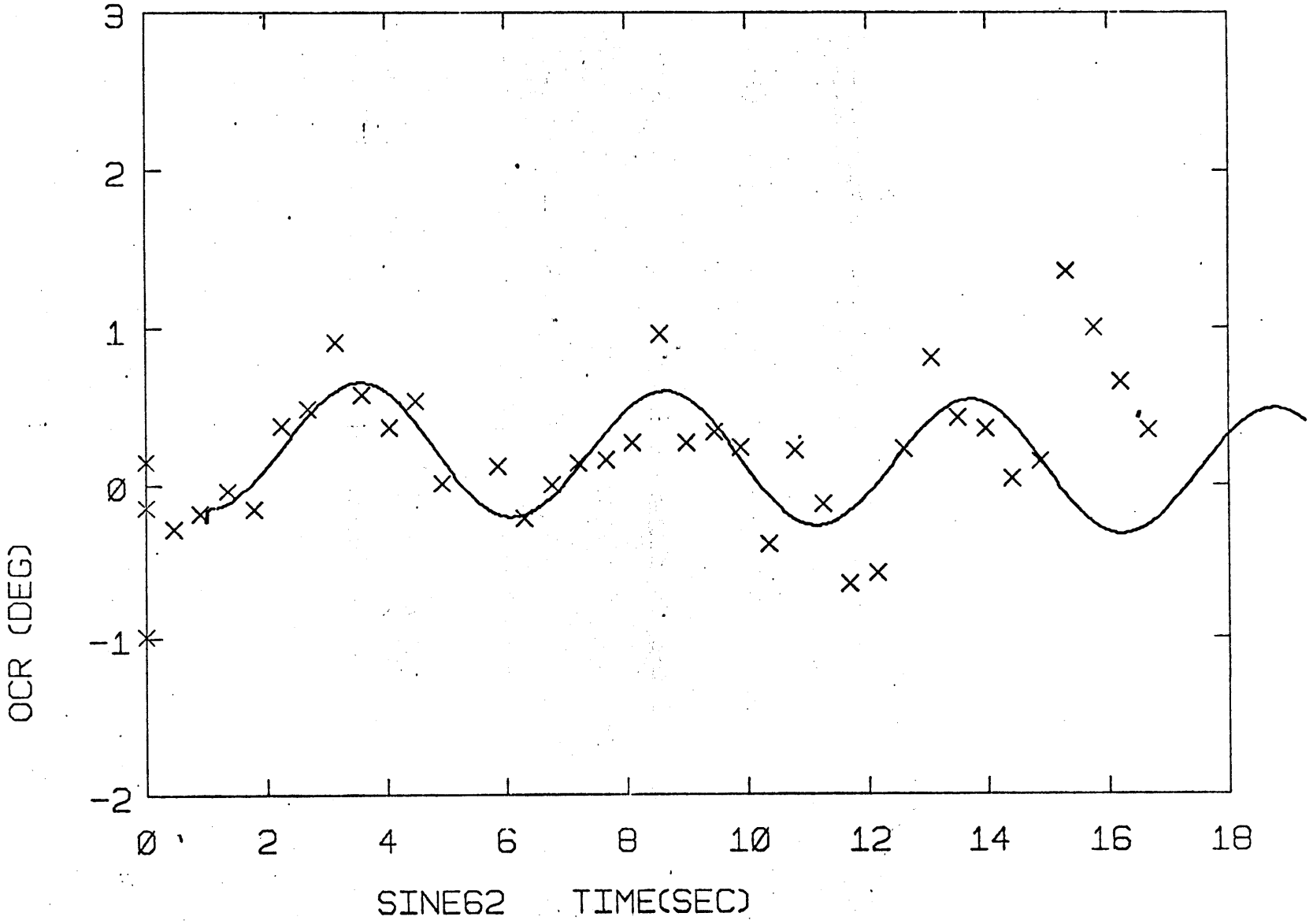
3
2
1
0
-1
-2
OCR (DEG)
0
2
4
6
8
10
12
14
16
18
SINE62 TIME(SEC)

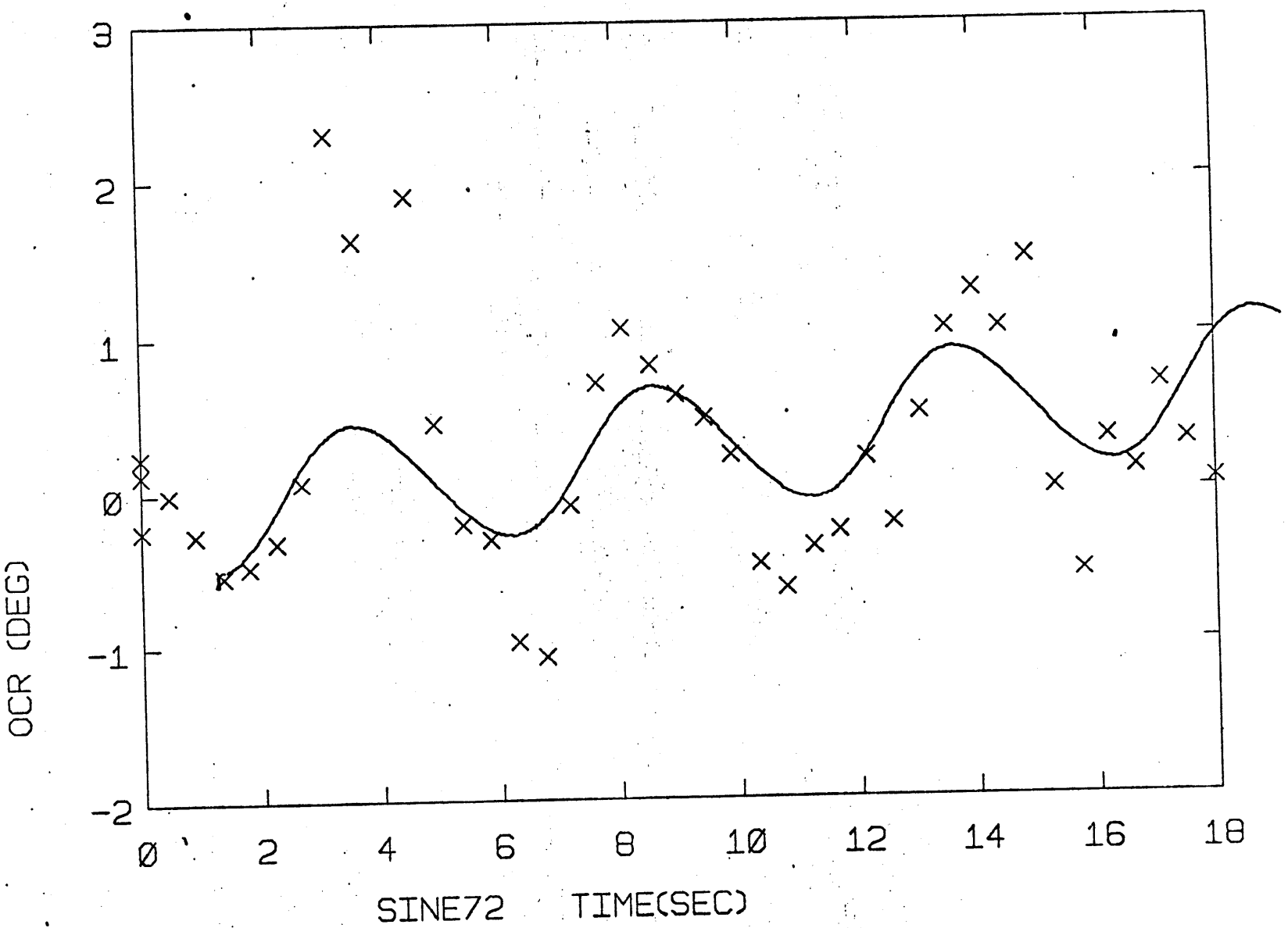
3
2
1
0
-1
-2
0
2
4
6
8
10
12
14
16
18
OCR (DEG)
SINE72 TIME(SEC)

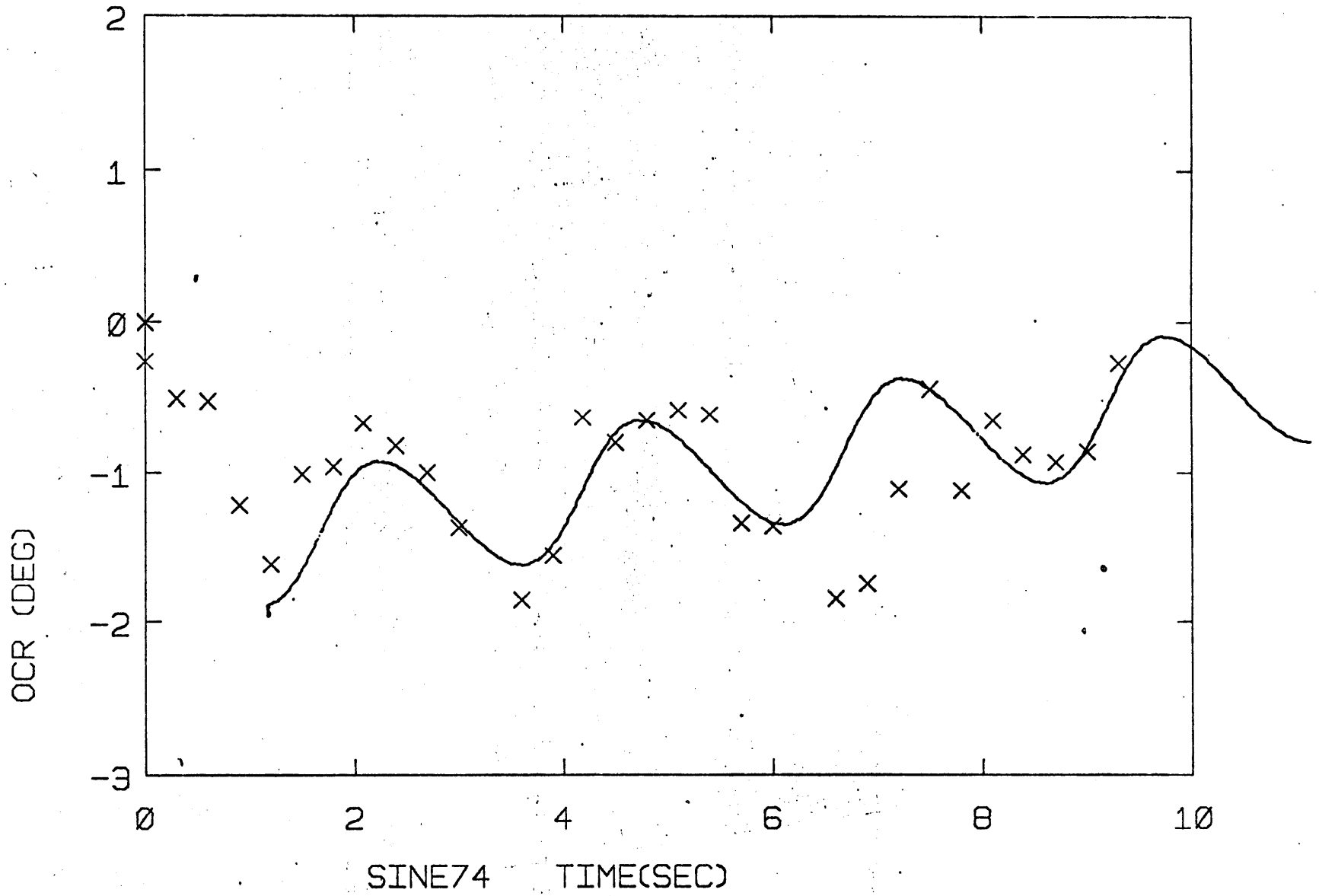
2
1
0
-1
-2
-3
0
2
4
6
8
10
OCR (DEG)
SINE74 TIME(SEC)

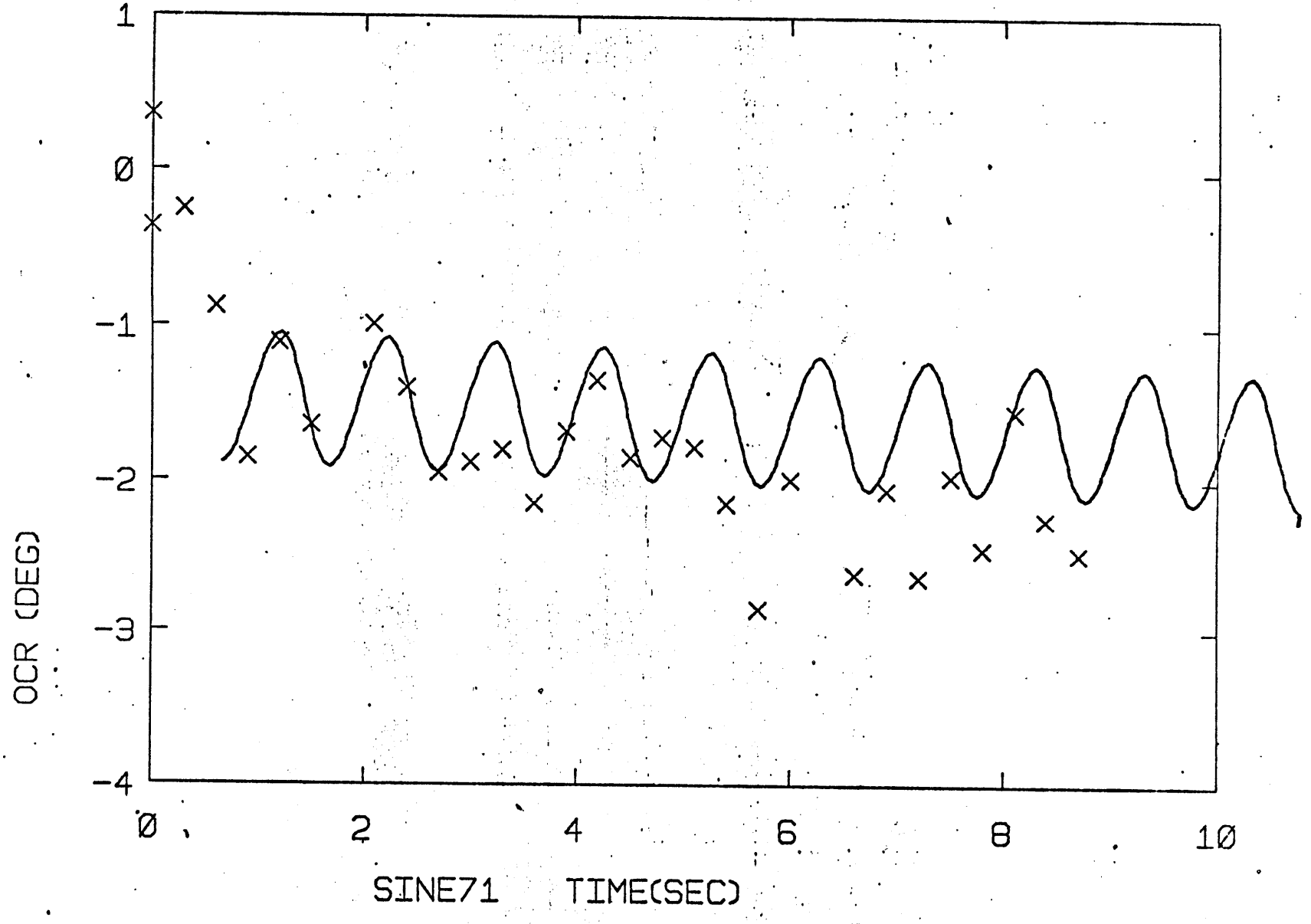
1
0
-1
-2
-3
-4
0
2
4
6
8
10
OCR (DEG)
SINE71 TIME(SEC)

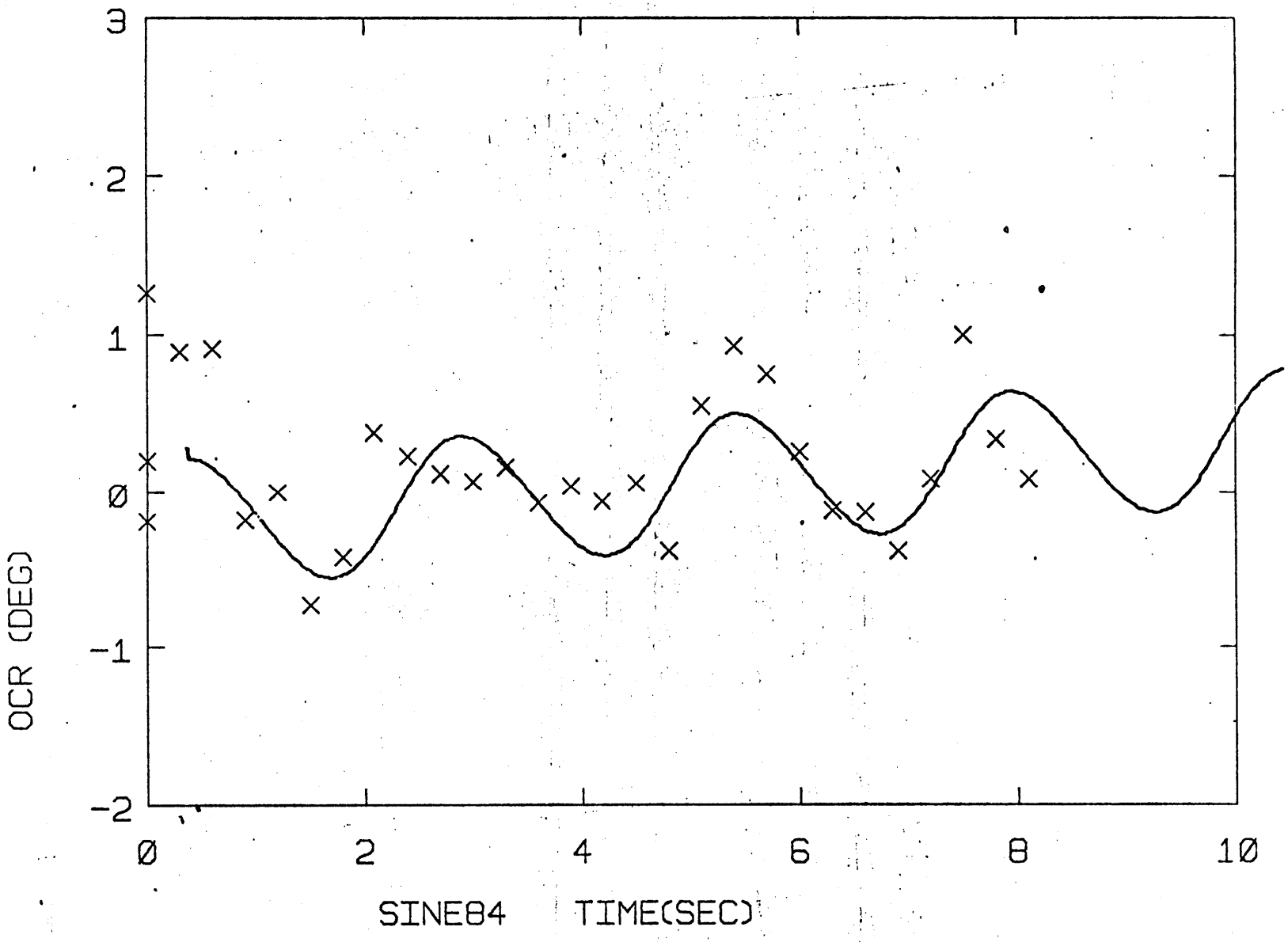
3
2
1
0
-1
-2
OCR (DEG)
0
2
4
6
8
10
SINE84 TIME(SEC)

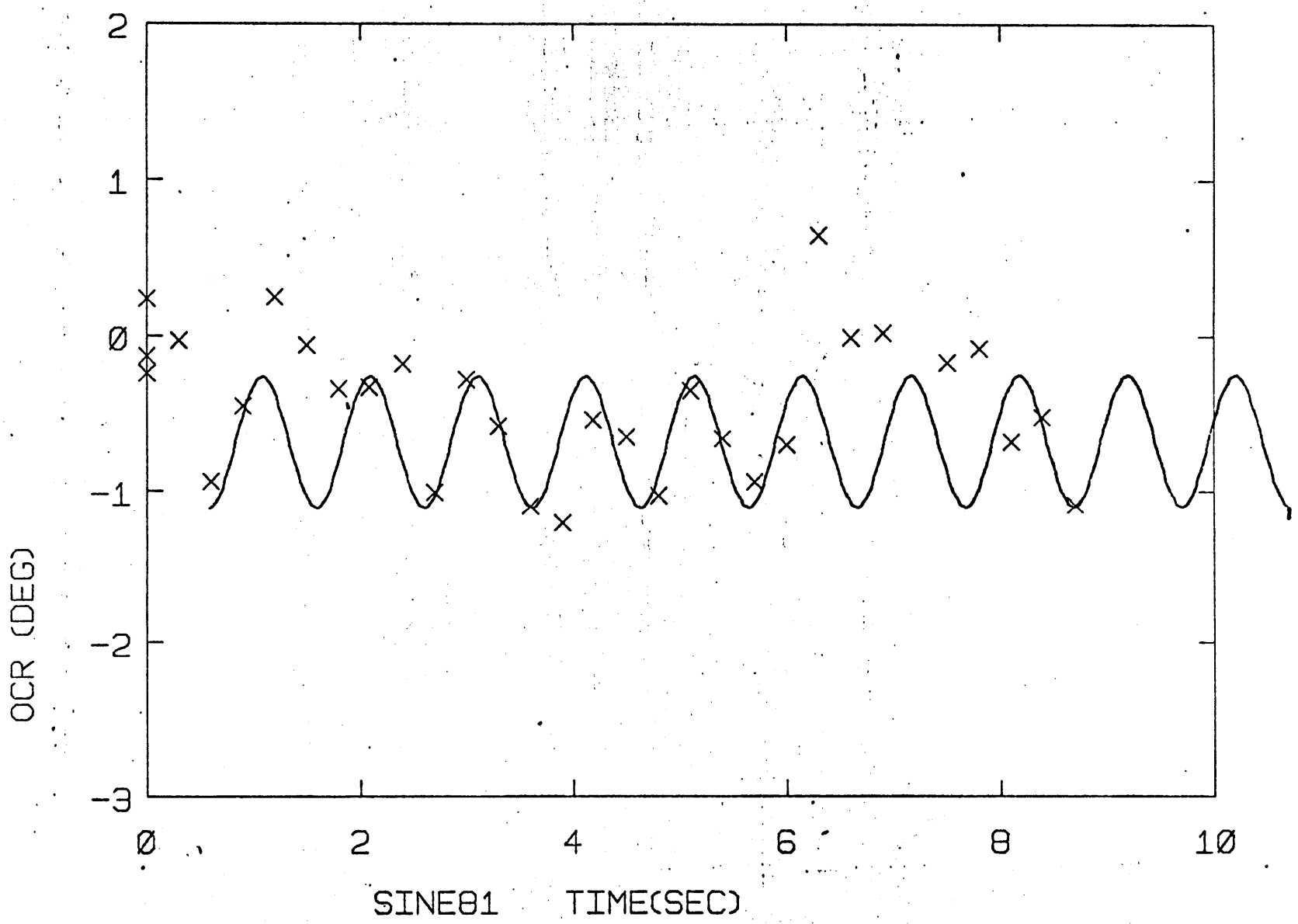
2
1
0
-1
-2
-3
0
2
4
6
8
10
OCR (DEG)
SINE81 TIME(SEC)

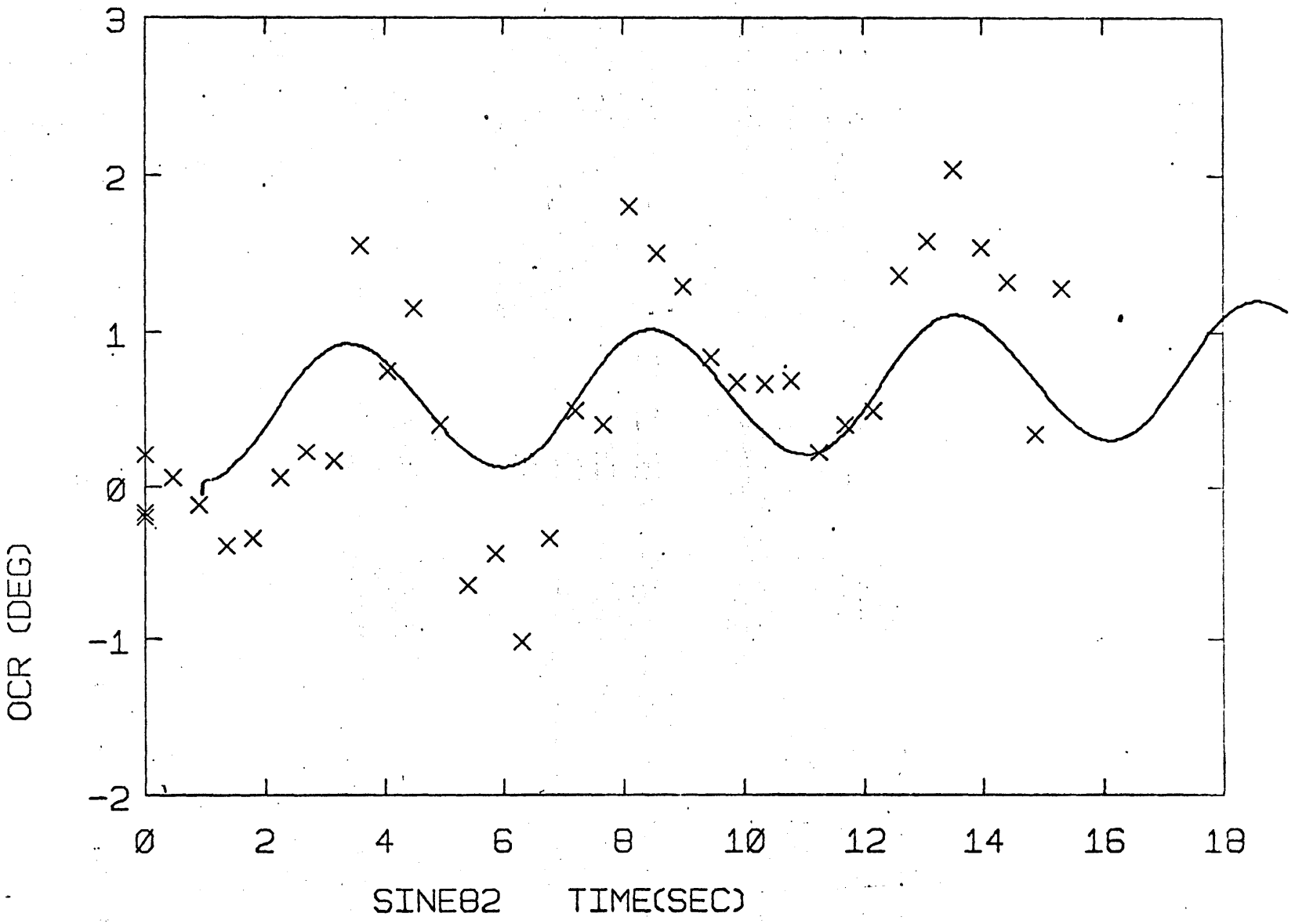
3
2
1
0
-1
-2
OCR (DEG)
0
2
4
6
8
10
12
14
16
18
SINE82 TIME(SEC)

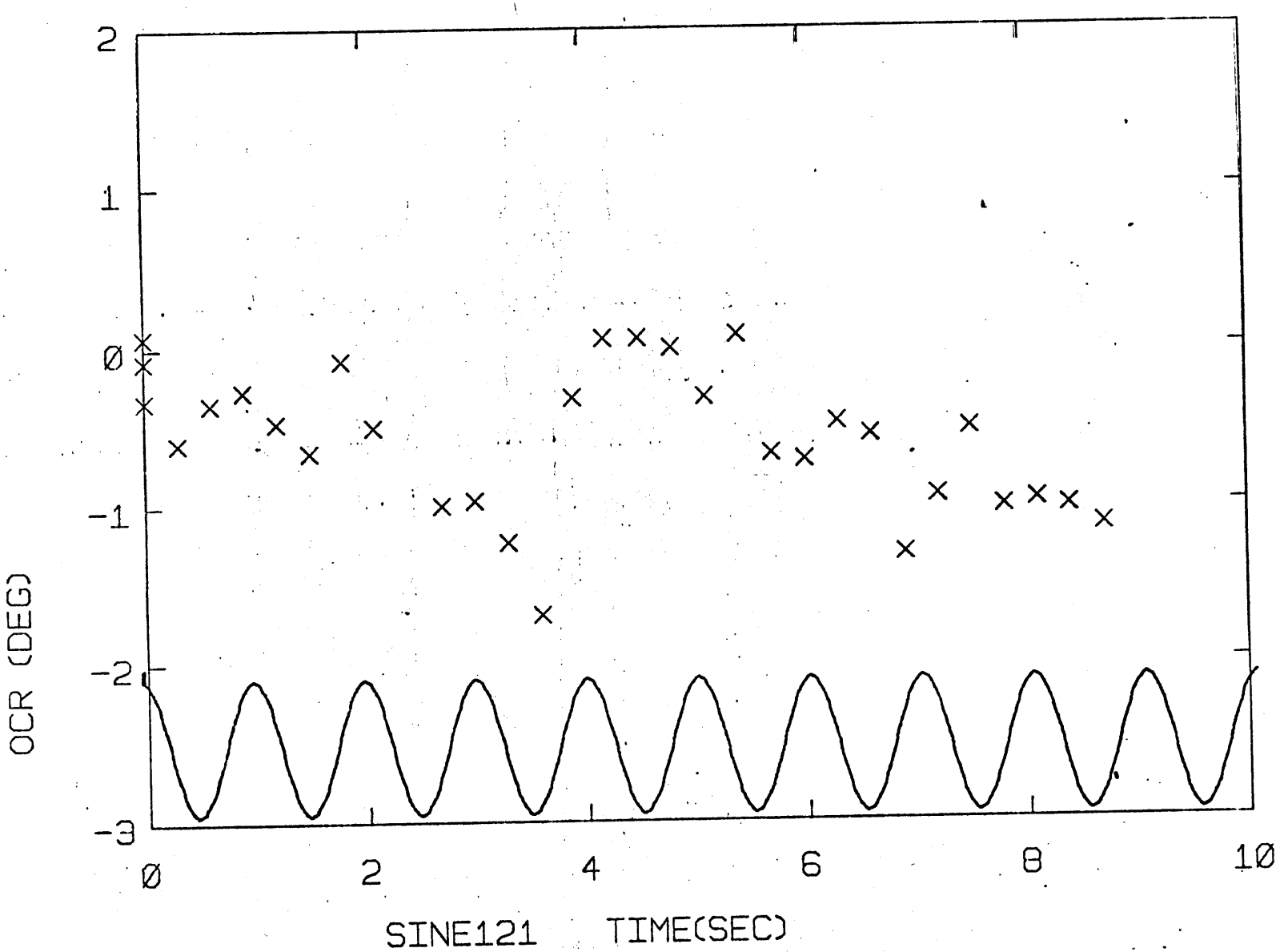
2
1
0
-1
-2
-3
0
2
4
6
8
10
OCR (DEG)
SINE121 TIME(SEC)

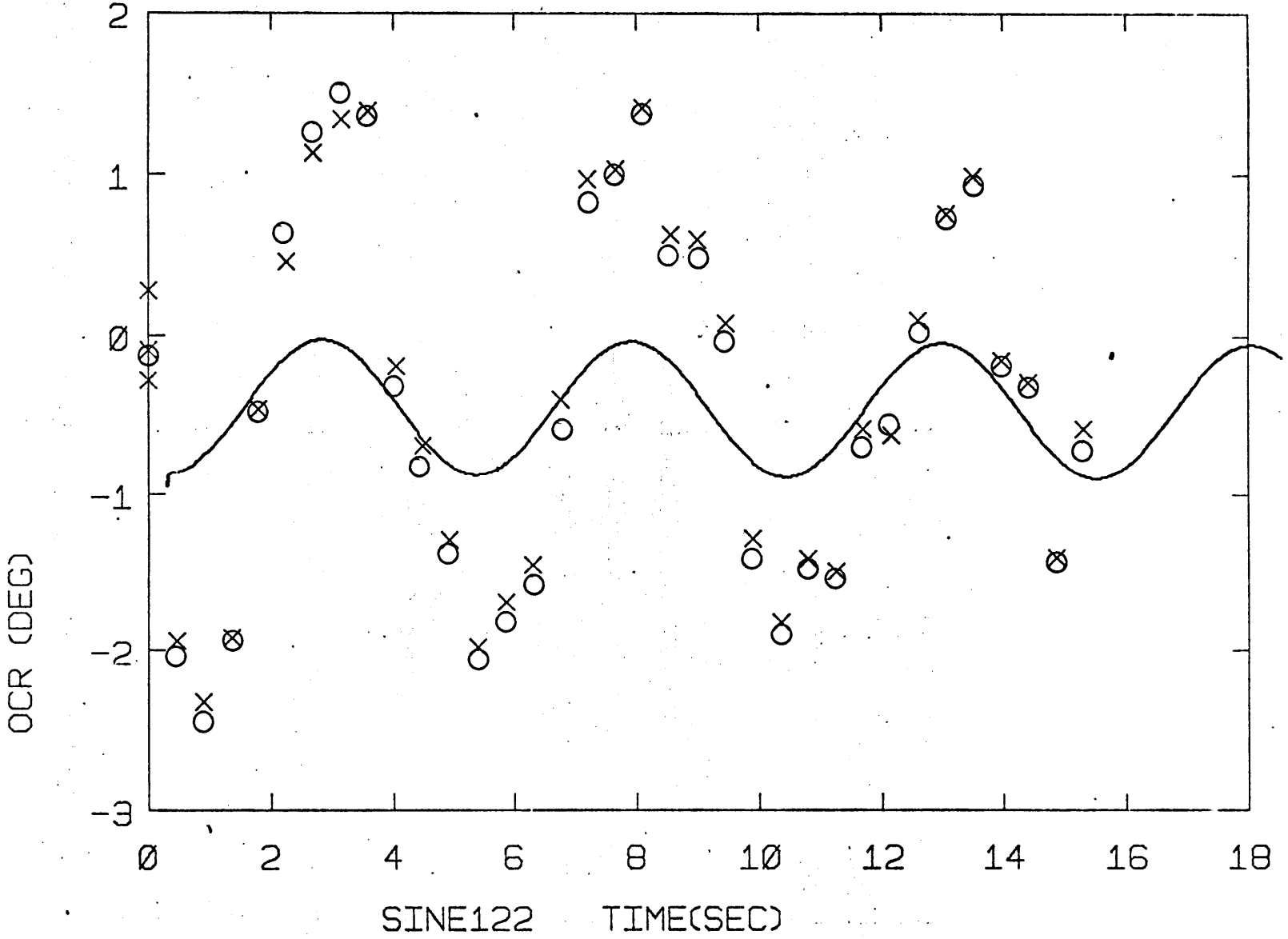
2
1
0
-1
-2
-3
0
2
4
6
8
10
12
14
16
18
OCR (DEG)
SINE122 TIME(SEC)

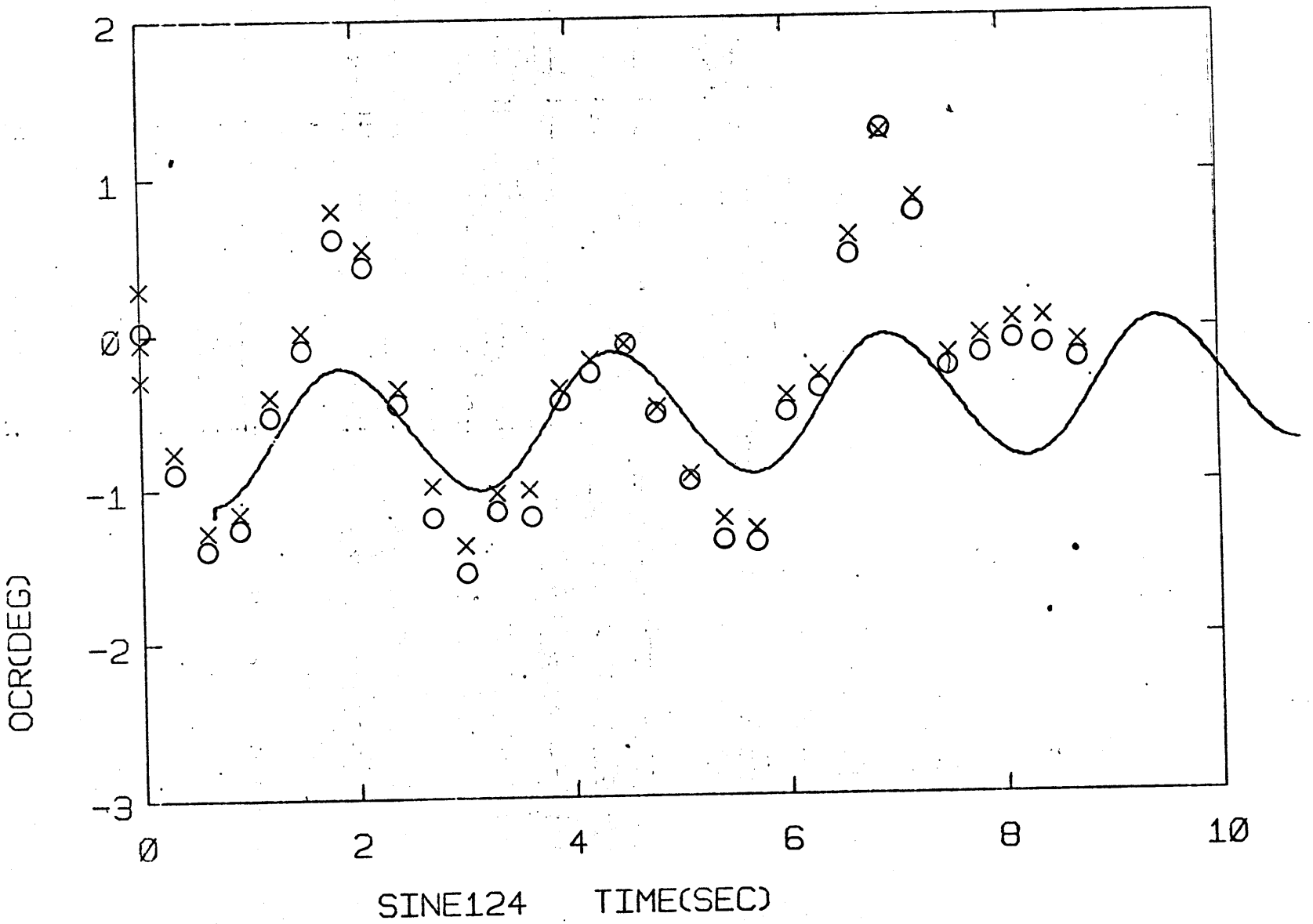
2
1
Ø
-1
-2
-3
Ø
2
4
6
8
1Ø
OCR(DEG)
SINE124 TIME(SEC)

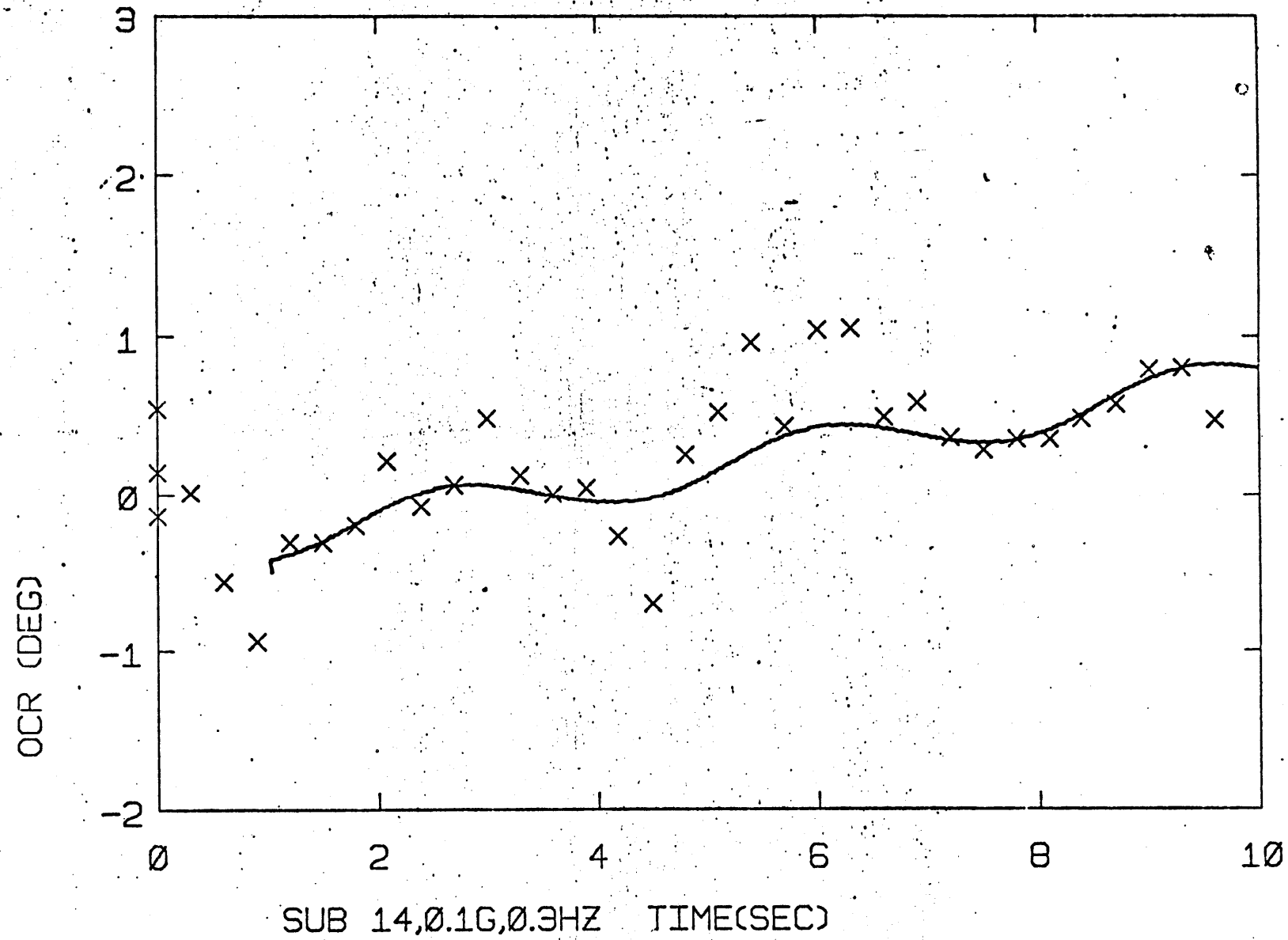
3
2
1
0
-1
-2
0
2
4
6
8
10
OCR (DEG)
SUB 14,0.1G,0.3HZ TIME(SEC)

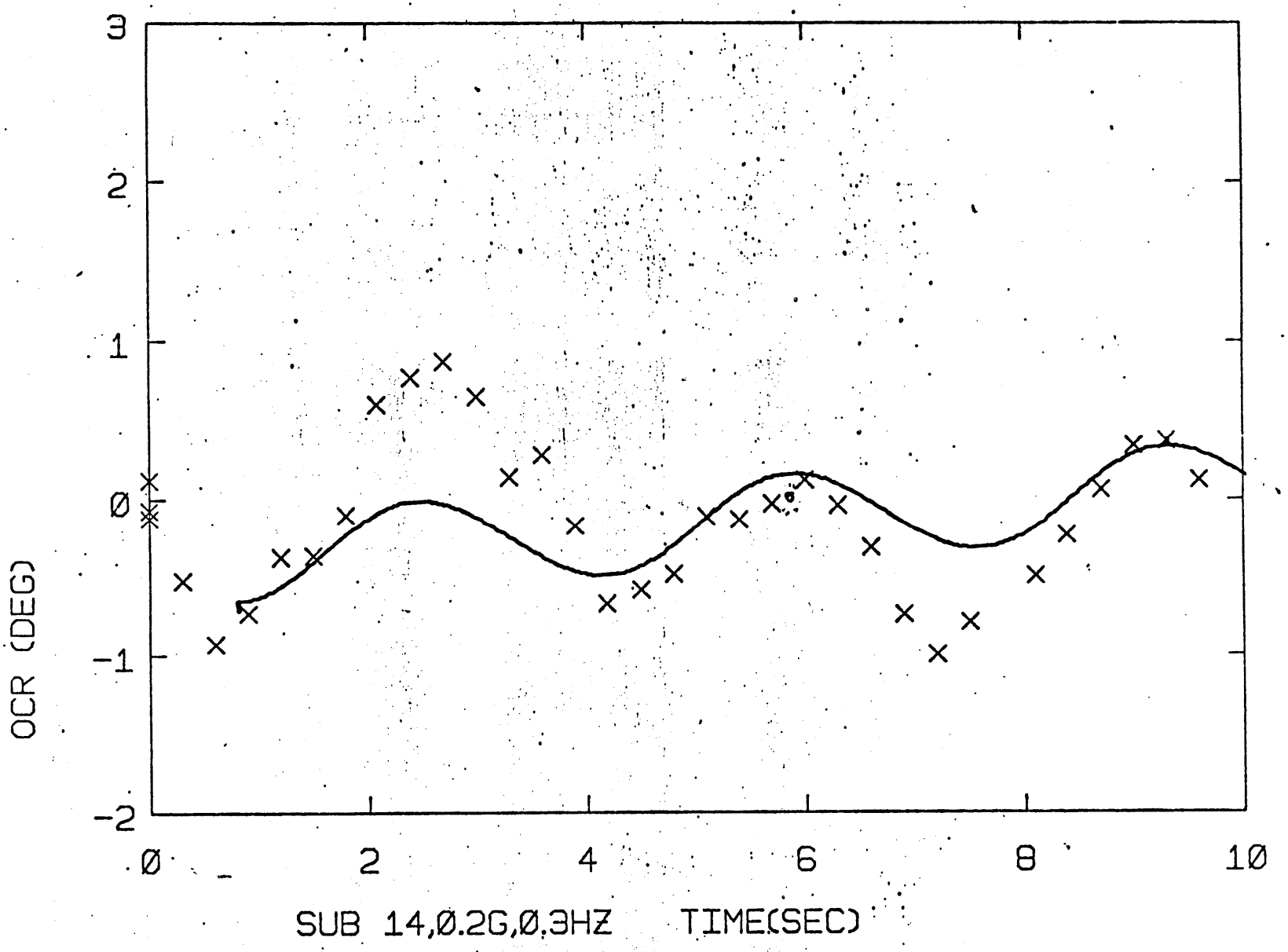
3
2
1
0
-1
-2
0
2
4
6
8
10
OCR (DEG)
SUB 14,0.2G,0.3HZ TIME(SEC)

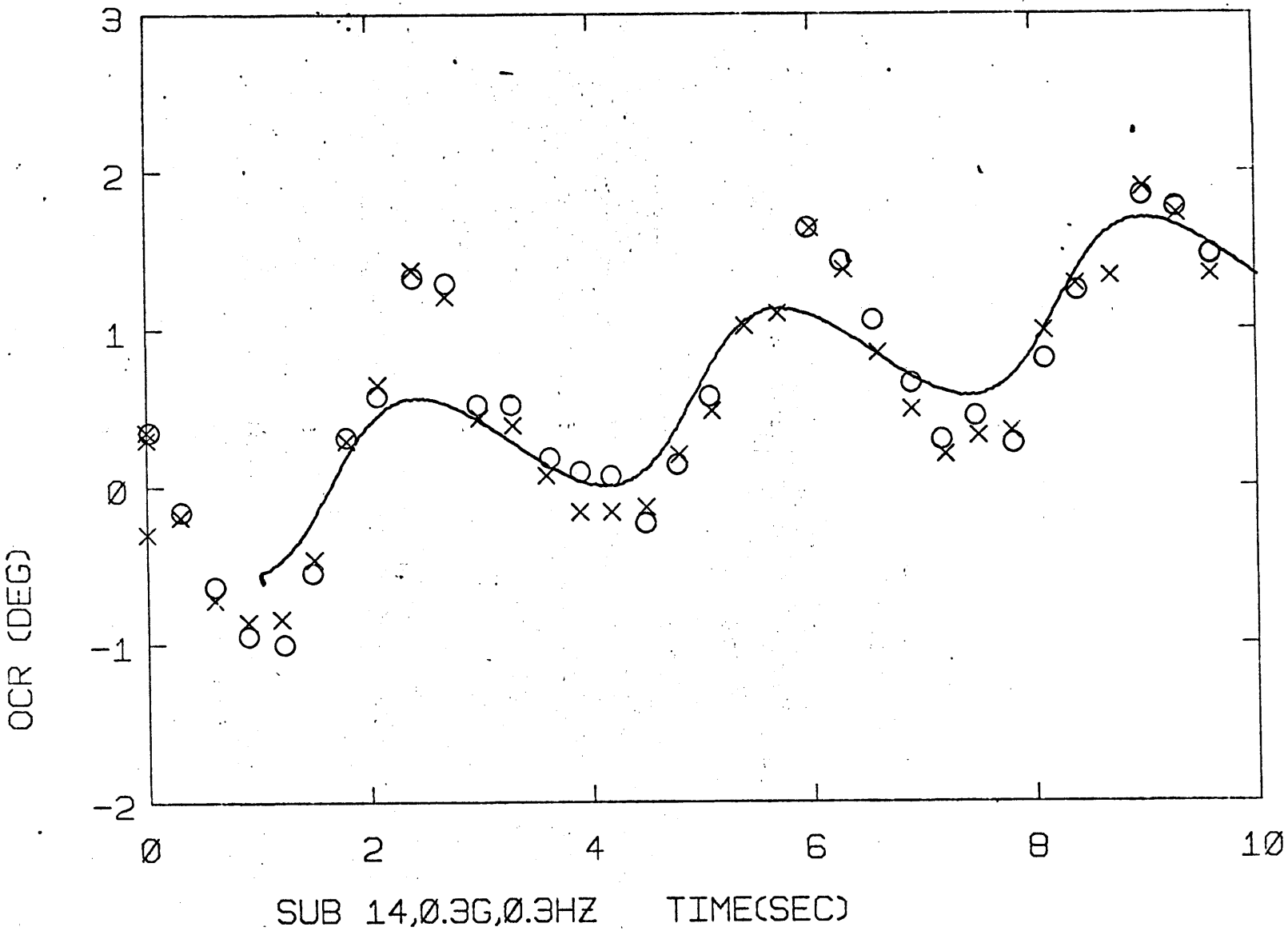
3
2
1
0
-1
-2
0
2
4
6
8
10
OCR (DEG)
SUB 14,0.3G,0.3HZ
TIME(SEC)

REFERENCES

ADRIAN, E.D., "Discharges from vestibular receptors in the cat", J. Physiol. 101:389-407, 1943.

BAARSMA, E.A. and COLLEWIJN, H., "Eye movements due to linear accelerations in the rabbit", J. Physiol. 245:227-247, 1975.

BENJAMINS, C.E. and NIENHUIS, J.H., "Die Raddrehungskurve beim Menschen", Arch Ohr-Nas-u Kehlk Heilk, 116:241-245, 1927.

BENSON, A.J. and BARNES, G.R., "Responses to rotating linear acceleration vectors considered in relation to a model of the otolith organs", in: Fifth Symposium on the Role of the Vestibular Organs in Space Exploration Washington, DC, National Aeronautics and Space Administration, SP-314, p. 221-236, 1973.

BISCHOF, N., "Optic-vestibular orientation to the vertical", in Vestibular System Part 2: Psychophysics, Applied Aspects and General Interpretations, ed. Kornhuber, H.H., Springer-Verlag, 1974, pp. 155-190.

BISCHOF, N., and SCHEERER, E., "System Analyse der optisch-vestibulären Interaction bei der Wahrnehmung der Vertikalen", Psychol. Forsch., 34:99-181, 1970.

BRACCHI, R., GUALTIEROTTI, T., MORABITO, A., and ROCCA, F., "Multiday recordings from the primary neurons of the statoreceptors of the frog labyrinth of the bullfrog", Acta Otolaryngologica Suppl. 334, 1975.

BREUER, J., "Uber die Funktion der Otolithem-aparates", Pflugers Arch ges Physiol. 48:195-306, 1891.

CHASEN, M.H., GUTHRIE, J.W., REPLOGLE, C.R., and JUNKER, A.M., Investigation of the Primate Vestibular System Function Through Analysis of the Vestibulo-ocular Reflex Response to Various Input Stimuli, AMRL-TR-71-4, 1967.

CLARK, B., "The oculogravic illusion as a test of otolith function", in: The Third Symposium on the Role of the Vestibular Organs in Space Exploration, NASA, SP-152, 1967, pp. 331-339.

COHEN, B., "Vestibulo-ocular relations" in: The Control of Eye Movements Eds: Bach-Y-Rita, P., Collins, C.C. and Hyde, J.E., Academic Press New York and London, 1971.

COHEN, B., KREJCOVA, H. and HIGHSTEIN, S., "Ocular counterrolling induced by static head tilt in the monkey", Fed. Proc. 454, 1970.

COLENBRANDER, A., "Eye and Otoliths", Aeromed. Acta, Soesterberg, 9:45-91, 1963-4.

CORREIA, M.H., HIXSON, W.C., and NIVEN, J.I., "Otolith shear and the visual perception of force direction: Discrepancies and a proposed resolution" Naval Aerospace Medical Institute, NAMI-951, 1965.

CORVERA, J., HALLPIKE, C.S., and SCHUSTER, E.H.J., "A new method for the anatomical reconstruction of the human macular planes", Acta Otolaryngologica 49:4-16, 1958.

DE VRIES, H.L., "The mechanics of the labyrinth otoliths", Acta Otolaryngologica 38:262-273, 1950.

DEKLEYN, A and MAGNUS, R, "Uber die Unabhangigkeit der Labyrinthreflex vom kleinhern und uber die Lage der Zentren fur die Labyrinthreflexe in hirnstamm", Pflugers Arch ges Physiol. 178:124-178, 1920.

DIAMOND, J.G., MARKHAM, C.H., SIMPSON, N.E., and CURTHOYS, I.S., "Binocular counterrolling in humans during dynamic rotation", Acta Otolaryngol. in press 1979.

FENDER, D.J., "Torsional motions of the eyeball", Brit. J. Ophthal. 39:65, 1955.

FERNANDEZ, C. and GOLDBERG, J.M., "Physiology of peripheral neurons innervating otolith organs of the squirrel monkey. I. Response to static tilts and long duration centrifugal force", J. Neurophysiology 39:970-984, 1976a.

FERNANDEZ, C. and GOLDBERG, J.M., "Physiology of peripheral neurons innervating otolith organ in the squirrel monkey. II. Directional selectivity and force response relations" J. Neurophysiology 39:985-995, 1976b.

FERNANDEZ, C. and Goldberg, J.M., "Peripheral neurons innervating otolith organs in the squirrel monkey. III. Response dynamics" J. Neurophysiol. 39:996-1008, 1976c.

FINKE, R.A. and HELD, R., "State reversals of optically induced tilt and torsional eye movements", Perception and Psychophysics 23:337-340, 1978.

FLOCK, A. and WERSALL, J., "A study of the orientation of the sensory hairs of the receptor cells in the lateral line organs of fish, with special reference to the function of the receptors", J. Cell Biol. 15:19, 1962.

FLUUR, E. and MELLSTROM, A., "Utricular stimulation and oculomotor reactions" Laryngoscope 80:1701-1712, 1970a.

FLUUR, E. and MELLSTROM, A., "Saccular stimulation and oculomotor reactions" Laryngoscope 80:1713-1721, 1970b..

FUJITA, Y., ROSENBERG, J. and SEGUNDO, J.P., "Activity of cells in the lateral vestibular nucleus as a function of head position", J. Physiol. 196:1-18, 1968.

GALOYAN, U.R., ZENKIN, G.M., and PETROV, A.P., "Investigation of the torsional movements of the human eyes - II. Slow phase of torsion", Biofizika 21:6, 1081-1086, 1976.

Gernandt, B.E., "Otolithic influences and extraocular and intraocular muscles" in: Fifth Symposium on the Role of the Vestibular Organs in Space Exploration, NASA SP-314, 195-201, 1973.

GOLDBERG, J.M. and FERNANDEZ, C., "Vestibular mechanisms", Ann. Rev. Physiol. 37:129-162, 1975.

GRAYBIEL, A., MILLER, E.F., II. and HOMICK, J.L., "Experiment M-131 - Human vestibular function", in: The Proceedings of the Skylab Life Sciences Symposium, Volume I, NASA TMX-58154, p. 169-212, 1974.

GUNDRY, A.J., "Thresholds of perception for periodic linear motion", ASEM 49:679-686, 1978.

HANNEN, R.A., KABRISKY, M., REPLOGLE, C.R., HARTZLER, V.L., and ROCCAFORTE, P.A., "Experimental determination of a portion of the human vestibular response through measurement of eyeball counterroll", IEEE Transactions on Biomedical Engineering BME-13:65-70, 1966.

HIEBERT, T.G. and FERNANDEZ, D., "Deitersian response to tilt" Acta Otolaryngologica 60:180-190, 1965.

HOLST, E. von, "Die Arbeitsweise des Statolithen apparates bei Fischen", Z. vergl. Physiol. 32:60-120, 1950.

HUDSPETH, A.J. and COREY, D.P., "Sensitivity, polarity and conductance changes in the response of vertebrate hair cells to controlled mechanical stimulus", Proc. Natl. Acad. Sci., 74:2407-2411, 1977.

JONGKEES, L.B.W., "On the otoliths: Their function and the way to test them" in: Third Symposium on the Role of the Vestibular Organs in Space Exploration, NASA SP-152, 1967, p. 307-330.

JONGKEES, L.B.W., "The parallel swing test", in: The Vestibular System and its Diseases, R.J. Wolfson, Ed., University of Pennsylvania Press, 218-228, 1966.

JUNKER, A.M., REPLOGLE, C.R., SMILES, K.A., BROWN, R.D., and WHEELER, R., "Analysis of the vestibulo-ocular counteroll reflex in primates" AMRL-TR-71-59, Aerospace Medical Research Laboratory, Wright-Patterson AFB, Ohio, 1971.

LINDERMAN, H.H., "Studies on the morphology of the sensory regions of the vestibular apparatus", Ergnb. Anat. Entw. Gesch. 42:1-113, 1969.

LOPEZ-ANTUNE, Z.L., Atlas of Human Anatomy, W.R. Saunders Co., Philadelphia 1971, pp. 334-335.

MACADAR, O., WOLFE, G.E., O'LEARY, D.P., and SEGUNDO, J.P., "Response of the elasmobranch utricle to maintained spatial orientation, transistions and jitter", Exp. Brain Res. 22:1-13, 1975.

MALCOLM, R. and MELVILL JONES, G., "Erroneous perception of vertical motion by humans seated in the upright position", Acta Otolaryngolica, 77: 274-283, 1974.

MATSUOKA, I., FUKUDA, N., TAKAORI, S., and MORIMOTO, M., "Responses of single neurons of the vestibular nuclei to lateral tilt and caloric stimulation in the intact and hemilabyrinthectomized cat", Acta Otolaryngologica 72:182-190, 1971.

MEIRY, J.L., The Vestibular System and Human Dynamic Orientation, Sc.D. Thesis Department of Aeronautics and Astronautics, Massachusetts Institute of Technology, 1965.

MELVILL JONES, G., "Vestibular interference with vision in flight", Proc. Roy. Soc. Med. 52:185-186, 1958.

MELVILL JONES, G. and YOUNG, L.R. "Subjective detection of vertical acceleration: A vertical dependent response?" Acta Otolaryngologica 85:1, 1978.

MILLER, E.F., II., "Counterrolling of the human eyes produced by tilt with response to gravity", Acta Otolaryngologica 54:479-501, 1962.

MILLER, E.F., II. and GRAYBIEL, A., "Otolith function as measured by ocular counterrolling", in: The Role of the Vestibular Organs in Space Exploration, NASA SP-77, 1965.

MILLER, E.F., II. and GRAYBIEL, A., "Effects of drugs on ocular counter-rolling" NAMI-1046, 1968.

MILLER, E.F., II. and GRAYBIEL, A., "Effects of gravitoinertial force on ocular counterrolling", J. Applied Phys. 31:697-700, 1971.

MILLER, E.F., II. and GRAYBIEL. A., "Ocular counterrolling measured during eight hours of sustained body tilt", NASA T-81633, 1972.

ORMSBY, C.C. Model of Human Dynamic Orientation, Ph.D. Thesis, Department of Aeronautics and Astronautics, Massachusetts Institute of Technology, 1974.

OWADA, K. and SHIZU, S., "The eye movement as a saccular function", Acta Otolaryngologica 52:63-71, 1960.

PETERSON, B.W., "Effect of tilting on neurons in the vestibular nuclei of the cat", Barin Res. 6:606-9, 1967.

PETROV, A.P. and ZENKIN, G.M., "Torsional eye movements and constancy of the visual field", Vision Res. 13:2465-77, 1973.

QUIX, F.H., "The function of the vestibular organ and the clinical examination of the otolithic apparatus", J. Laryngol. Otol. 40:425-443, 493-511, 1925.

ROBINSON, D.A., "A method of measuring eye movement using a scleral search coil in a magnetic field", IEEE Transactions BME-10:1370145, 1963.

SCHÖNE, H., "On the role of gravity in human spatial orientation" Aerospace Med. 35:764-772, 1964.

SCHOR, R.H., "Responses of cat vestibular neurons to sinusoidal roll tilt" Exp. Brain Res. 20:347-362, 1974.

SCHULTE, R.J. and VREELAND, R.E., The Design and Construction of An Acceleration Cart, M.S. Thesis, Massachusetts Institute of Technology, 1964.

SHIMAZU, H. and SMITH, C.M., "Cerebellar and labyrinthine influences on single vestibular neurons identified by natural stimuli", J. Neurophysiol. 34:493-508, 1971.

SMILES, K.A., HITE, D., HYAMS, V.J., and JUNKER, A.M., "Effects of labyrinthectomy of the dynamic vestibulo-ocular counterroll reflex in the Rhesus monkey", ASEM, 46:1017-1022, 1975.

SPOENDLIN, H., "Ultrastructure of the vestibular sense organ", in: The Vestibular System and Its Diseases, R.J. Wolfson, Ed., University of Pennsylvania Press, 1966, 39-68.

STEIN, B.M. and CARPENTER, M.B., "Central projections of portions of the vestibular ganglia innervating specific parts of the labyrinth in the Rhesus monkey", Am. J. Anat. 12:281-318, 1967.

SUZUKI, J.I., TOKUMASU, L., and GOTO, K. "Eye movements from single utricular nerve stimulation in the cat", Acta Otolaryngologica 68: 350-362, 1969.

TOKUMASU, K., GOTO, L., and COHEN, B., "Eye movements from vestibular nuclei stimulation in monkeys", Annals Oto-Rhino-Laryngology 78:1105-1118, 1969.

TRUEX, R.C. and CARPENTER, M.B. Human Neuroanatomy, Sixth Edition, William and Wilkins Company, Baltimore, MD, 1969.

VIDAL, J., JEANNEROD, M., LIFSCHITZ, W., LEVITAN, H., ROVENBERG, J., and SEGUNDO, J.P., "Static and dynamic properties of gravity-sensitive receptors in the cat vestibular system", Kybernetik 9:205-215, 1971.

VILSTRUP, G and VILSTRUP, T., "Does the utricular otolitic membrane move on postural changes of the head?" Ann. Otol. 61:189-197, 1952.

WESTHEIMER, G and BLAIR, S.M., "The ocular tilt reaction - a brainstem oculomotor routine", Invest. Ophthalmol. 14:833-839, 1975.

WOELLNER, R.C. and GRAYBIEL, A., "Counterrolling of the eyes and its dependence on the magnitude of gravitational or inertial force acting laterally on the body", J. Appl. Physiol. 14:632-634, 1959.

YOUNG, L.R. and MEIRY, J.L., "A revised dynamic otolith model", Aerospace Med. 39:606-608, 1968.

BIOGRAPHICAL SKETCH

Byron K. Lichtenberg received his Bachelor of Science degree (cum laude) from Brown University in 1969. He entered the U.S. Air Force and was a fighter pilot for four years. During this time, he had a tour in southeast Asia; he was awarded 11 air medals and 2 Distinguished Flying Crosses. Upon his return to civilian life, he entered M.I.T. in 1973 and was awarded the Master of Science degree in 1975 for his work in the neural control of prostheses. He joined the Man-Vehicle Laboratory in the Department of Aeronautics and Astronautics in 1976. When the Man Vehicle Laboratory was awarded a contract to develop a series of space experiments in the vestibular research and space sickness areas, he was nominated and finally chosen as one of two U.S. Payload Specialist Astronauts. He currently is training for Spacelab 1, the first scientific flight of the Space Shuttle.